UNIVERSITY OF CALIFORNIA
Santa Barbara

Robust Hybrid Systems for Control, Learning, and Optimization in Networked Dynamical Systems

A dissertation submitted in partial satisfaction
of the requirements for the degree

Doctor of Philosophy
in
Electrical and Computer Engineering

by

Jorge Ivan Poveda Fonseca

Committee in charge:

Professor Andrew R. Teel, Chair
Professor Joao P. Hespanha
Professor Jason R. Marden
Professor Brad E. Paden

September 2018

The Dissertation of Jorge Ivan Poveda Fonseca is approved.

Professor Joao P. Hespanha

Professor Jason R. Marden

Professor Brad E. Paden

Professor Andrew R. Teel, Committee Chair

June 2018

Robust Hybrid Systems for Control, Learning, and Optimization in Networked Dynamical Systems

Jorge Ivan Poveda Fonseca

To my mother Rosa Yolanda, and my father Jorge Alfonso.

Acknowledgements

This dissertation would not have been possible without the support, guidance, and encouragement that I have received from so many people during the last several years.

First of all, I would like to thank my advisor Prof. Andrew R. Teel for his patience, guidance, and mentorship. Specially, I want to thank him for giving me the freedom to pursue a research direction that I find fascinating, as well as for showing me how to address difficult research questions by using elegant and rigorous analytical tools. His advice on both research as well as on my career have been invaluable during all these years, and as a role model he represents a standard of personal and professional integrity and accomplishment to which I can only hope to aspire.

I would also like to thank Prof. Jason Marden for his guidance and mentorship, as well as for giving me the chance to collaborate with his group. During the last two years, Jason was essentially my co-advisor, and I am grateful for all the generous feedback, advice, and perspective that he offered to me, which had a tremendous impact in shaping my career as a researcher.

I want to thank Prof. Joao Hespanha and Prof. Brad Paden for their constructive comments, suggestions, and inputs, as well as for being on my dissertation committee. I am also grateful to Dr. Mouhacine Benosman for giving me the opportunity to further develop some of my research ideas at the Mitsubishi Electric Research Laboratories in Cambridge, MA.

I am indebted to all my coauthors, who generously took some of their time to read and revise my drafts, as well as to share their ideas with me. In particular, I would like to thank Dragan Nešić, Kyriakos Vamvoudakis, Ricardo Sanfelice, Corrado Possieri, Chris Manzie, Ronny Kutadinata, Julian Barreiro, and German Obando. I would also like to thank Prof. Nicanor Quijano for showing me the path to a world of endless

possibilities, and for all these years of friendship and persistent encouragement.

My time at UCSB was enriched by multiple technical and non-technical discussions that I deeply enjoyed. The CCDC is a very inspiring and diverse group, and I truly enjoyed the different conversations that I had with professors Francesco Bullo, Bassam Bamieh, Mahnoosh Alizadeh, and Ramtin Pedarsani, as well as with the current and former CCDC members Anantharaman Subbaraman, Matthew Hartman, Sven Bruggemann, Herbert Cai, Nihar Talele, Arjun Muralidharan, Justin Pearson, David Copp, Hari Sivakumar, Hector Rios, Tom Strizic, Scott Erwin, Sharad Shankar, Elizabeth Huang, Emily Jensen, Guosong Yang, Masashi Wakaiki, Kunihisa Okano, Murat Erdal, Raphael Chinchilla, Philip Brown, David Grimsman, Rahul Chandan, Nate Tucker, Daniel Lazar, Ahmadreza Moradipari, and Matina Baradaran. A special thanks is reserved for Henrique Ferraz for his friendship and generosity during the last five years.

The smooth development of this dissertation would not have been possible without the efficient support from the CCDC and ECE Staff Kallie Hill and Valerie De Veyra, as well as the support provided by the Air Force Office of Scientific Research and by the National Science Foundation.

Last, and most importantly, I want to thank my family for its unconditional support. Everything that I have accomplished is a credit to them (except the mistakes, which have been my own). To Cata and Simon, for making me feel at home in a foreign land; to Ana, for her unbounded generosity, kindness, and continuous belief in me; and to my parents, Yolanda and Alfonso, for their selfless love and support. I dedicate this dissertation to them.

Curriculum Vitæ

Jorge Ivan Poveda Fonseca

Education

2015	M.Sc. in Electrical Engineering, University of California, Santa Barbara.
2013	M.Sc. in Electrical Engineering, University of Los Andes, Colombia.
2012	B.S. in Electronics Engineering, University of Los Andes, Colombia.
2012	B.S. in Mechanical Engineering, University of Los Andes, Colombia.

Experience

2014 - 2018	Graduate Student Researcher, University of California, Santa Barbara.
2017	Research Intern, Mitsubishi Electric Research Laboratories, Cambridge, MA.
2016	Research Intern, Mitsubishi Electric Research Laboratories, Cambridge, MA.
2012 - 2013	Graduate Student Researcher, University of Los Andes, Bogota, Colombia.

Selected Publications

1. J. I. Poveda and A. R. Teel, "Hybrid Mechanisms for Robust Synchronization and Coordination of Networked Multi-Agent Sampled-Data Systems", *Automatica*, 2018, to appear.
2. J. I. Poveda, M. Benosman, and A. R. Teel, "Hybrid Online Learning Control in Networked Multi-Agent Systems: A Survey", *International Journal of Adaptive Control and Signal Processing*, 1-34, 2018.
3. J. I. Poveda and A. R. Teel, "A Robust Event-Triggered Approach for Fast Sampled-Data Extremization and Learning", *IEEE Transactions on Automatic Control*, Volume 62, Number 10, 2017, pp. 4949-4964.
4. J. I. Poveda and A. R. Teel, "A Framework for a Class of Hybrid Extremum Seeking Controllers with Dynamic Inclusions", *Automatica*, Volume 76, 2017, pp. 113-126.
5. J. I. Poveda and N. Quijano, "Shahshahani gradient-like extremum seeking", *Automatica*, Volume 58, 2015, pp. 51-59.

6. G. Obando, J. I. Poveda, and N. Quijano, "Replicator dynamics under perturbations and time-delays", *Mathematics of Controls, Signals and Systems*, Volume 28, Issue 3, 2016, pp. 1-32.
7. J. I. Poveda, M. Benosman, A. R. Teel, and R. G. Sanfelice, "Coordinated Hybrid Source Seeking with Robust Obstacle Avoidance in Multivehicle Autonomous Systems", to be submitted, 2018.
8. J. I. Poveda, J. Barreiro-Gomez, J. R. Marden, A. R. Teel, N. Quijano, "Data-Driven Hybrid Dynamics for Initialization-Free Optimization and Learning in Multiagent Systems", to be submitted, 2018.
9. J. I. Poveda, A. Subbaraman, and A. R. Teel "Lyapunov Characterization of Stochastic Difference Inclusions with Persistent Disturbances", to be submitted, 2018.
10. J. I. Poveda, A. R. Teel and D. Nešić, "Stochastic Learning in Sampled-Data Games Under Attacks: The Role of Non-Causal Selections", to be submitted, 2018.
11. J. I. Poveda, R. Kutadinata, C. Manzie, D. Nesic, A. R. Teel, C. Liao, "Hybrid Extremum Seeking for Black-Box Optimization in Hybrid Plants: An Analytical Framework", *57th IEEE Conference on Decision and Control*, Miami, FL, 2018.
12. M. Baradaran, J. I. Poveda, A. R. Teel, "Stochastic Hybrid Inclusions Applied to Non-Convex Optimization and Distributed Learning", *57th IEEE Conference on Decision and Control*, Miami, FL, 2018.
13. J. I. Poveda, M. Benosman, A. R. Teel, and R. G. Sanfelice, "A Hybrid Adaptive Feedback Law for Robust Obstacle Avoidance and Coordination in Multiple Vehicle Systems", *American Control Conference*, Milwaukee, MI, 2018.
14. J. I. Poveda, P. N. Brown, J. R. Marden and A. R. Teel, "A Class of Distributed Adaptive Pricing Mechanisms for Societal Systems with Limited Information", *56th IEEE Conference on Decision and Control*, Melbourne, Australia, 2017, pp. 1490-1495.
15. T. Strizic, J. I. Poveda, and A. R. Teel, "Hybrid Gradient Descent for Robust Global Optimization on the Circle", *56th IEEE Conference on Decision and Control*, Melbourne, Australia, 2017, pp. 2985-2990.
16. J. I. Poveda, M. Benosman, and A. R. Teel, "Distributed Extremum Seeking in Multi-Agent Systems with Arbitrary Switching Graphs", *IFAC World Congress*, Toulouse, France, 2017, pp. 758-763.
17. J. I. Poveda, K. G. Vamvoudakis, M. Benosman, "A Neuro-Adaptive Architecture for Extremum Seeking Control Using Hybrid Learning Dynamics", *American Control Conference*, Seattle, WA, 2017, pp. 542-547.
18. J. I. Poveda and A. R. Teel, "Distributed Robust Stochastic Learning in Asynchronous Networks of Sampled-Data Systems", *55th IEEE Conference on Decision and Control*, Las Vegas, NV, 2016, pp. 401-406.

19. S. Bruggemann, C. Possieri, J. I. Poveda, and A. R. Teel, "Robust Constrained Model Predictive Control with Persistent Model Adaptation", *55th IEEE Conference on Decision and Control*, Las Vegas, NV, 2016, pp. 2364-2369.

20. J. I. Poveda and A. R. Teel, "A Hybrid Systems Approach for Distributed Nonsmooth Optimization in Asynchronous Multi-Agent Sampled-Data Systems", *10th IFAC Symposium on Nonlinear Control Systems*, Monterrey, CA, 2016, pp. 152-157.

21. J. I. Poveda and A. R. Teel, "Event-Triggered Based On-Line Optimization for a Class of Nonlinear Systems", *54th IEEE Conference on Decision and Control*, Osaka, Japan, 2015, pp. 5474 - 5479.

22. A. R. Teel and J. I. Poveda, "A Hybrid Systems Approach to Global Synchronization and Coordination of Multi-Agent Sampled-Data Systems", *5th Conference on Analysis and Design of Hybrid Systems*, Atlanta, GA, 2015, pp. 123-128.

23. J. I. Poveda, A. R. Teel and D. Nesic, "Flexible Nash seeking using stochastic difference inclusions", *American Control Conference*, Chicago, USA, 2015, pp. 2236-2241.

24. J. I. Poveda and A. R. Teel, "A hybrid seeking approach for robust learning in multi-agent systems", *53rd IEEE Conference on Decision and Control*, Los Angeles, USA, 2014, pp. 3463-3468.

25. J. Poveda and N. Quijano, "Extremum seeking for multi-population games", *52nd IEEE Conference on Decision and Control*, Florence, Italy, 2013, pp. 409 - 414.

26. J. Poveda and N. Quijano, "Distributed extremum seeking for real-time resource allocation", *American Control Conference*, Washington D.C., USA, 2013, pp. 2772 - 2777.

27. J. Poveda and N. Quijano, "Dynamic bandwidth allocation in wireless networks using a Shahshahani gradient based extremum seeking control", *International Conference on Network Games, Control and Optimization*, Avignon, France, 2012, pp. 44-50.

28. J. Poveda and N. Quijano, "A Shahshahani Gradient Based Extremum Seeking Scheme", *51st IEEE Conference on Decision and Control*, Maui, HI, 2012, pp. 5104-5109.

29. J. Poveda, N. Ochoa-Lleras, and C. F. Rodriguez, "Guidance of an Autonomous Glider Based on Proportional Navigation and Virtual Targets: A Hybrid Dynamical Systems Approach", AIAA Guidance, Navigation, and Control Conference, Minneapolis, MN, 2012.

Abstract

Robust Hybrid Systems for Control, Learning, and Optimization in Networked Dynamical Systems

by

Jorge Ivan Poveda Fonseca

The deployment of advanced real-time control and optimization strategies in socially-integrated engineering systems could significantly improve our quality of life while creating jobs and economic opportunity. However, in cyber-physical systems such as smart grids, transportation networks, healthcare, and robotic systems, there still exist several challenges that prevent the implementation of intelligent control strategies. These challenges include the existence of limited communication networks, dynamic and stochastic environments, multiple decision makers interacting with the system, and complex hybrid dynamics emerging from the feedback interconnection of physical processes and computational devices.

In this dissertation, we study the problem of designing robust control and optimization algorithms for cyber-physical systems using the framework of hybrid dynamical systems. We propose different theoretical frameworks for the design and analysis of feedback mechanisms that optimize the performance of dynamical systems without requiring an explicit characterization of their mathematical model, i.e., in a model-free way. The closed-loop system that emerges of the interconnection of the plant with the feedback mechanism describes, in general, a set-valued hybrid dynamical system. These types of systems combine continuous-time and discrete-time dynamics, and they usually lack the uniqueness of solutions property. The framework of set-valued hybrid dynamical systems allows us to study many complex dynamical systems that emerge in different engineering applications, such as networked multi-agent systems with switch-

ing graphs, non-smooth mechanical systems, dynamic pricing mechanisms in transportation systems, autonomous robots with logic-based controllers, etc. We propose a step-by-step approach to the design of different types of discrete-time, continuous-time, hybrid, and stochastic controllers for different types of applications, extending and generalizing different results in the literature in the area of extremum seeking control, sampled-data extremization, robust synchronization, and stochastic learning in networked systems. Our theoretical results are illustrated via different simulations and numerical examples.

List of Symbols

Notation

- The set of (positive) integers is denoted as ($\mathbb{Z}_{>0}$) $\mathbb{Z}$.
- The set of (nonnegative) real numbers is denoted as ($\mathbb{R}_{\geq 0}$) $\mathbb{R}$.
- The cartesian product of $n \in \mathbb{Z}_{>0}$ identical sets M is denoted by M^n.
- $\mathbb{S}^1$ denotes the unit circle in $\mathbb{R}^2$.
- Given a compact set $\mathcal{A} \subset \mathbb{R}^n$, and a column vector $x \in \mathbb{R}^n$, we define $|x|_{\mathcal{A}} := \min_{y \in \mathcal{A}} |x - y|$.
- $\mathbb{B}$ denotes a closed unit ball of appropriate dimension, $\rho\mathbb{B}$ denotes a closed ball of radius $\rho > 0$, and $\mathcal{X} + \rho\mathbb{B}$ denotes the union of all sets obtained by taking a closed ball of radius ρ around each point in the set $\mathcal{X}$.
- A set-valued mapping $M : \mathbb{R}^m \rightrightarrows \mathbb{R}^n$ is outer semi-continuous (OSC) at $x \in \mathbb{R}^m$ if for all sequences $x_i \to x$ and $y_i \in M(x_i)$ such that $y_i \to y$ we have that $y \in M(x)$.
- A set-valued mapping $M : \mathbb{R}^m \rightrightarrows \mathbb{R}^n$ is locally bounded (LB) at $x \in \mathbb{R}^m$ if there exists a neighborhood U_x of x such that $M(U_x) \subset \mathbb{R}^n$ is bounded.
- Given a set $\mathcal{X} \subset \mathbb{R}^m$ the mapping M is said to be OSC and LB relative to $\mathcal{X}$ if the set-valued mapping from $\mathbb{R}^m$ to $\mathbb{R}^n$ defined by $M(x)$ for $x \in \mathcal{X}$ and $\emptyset$ for $x \notin \mathcal{X}$ is OSC and LB at each $x \in \mathcal{X}$.
- $\overline{\text{co}}\ \mathcal{X}$ denotes the closed convex hull of $\mathcal{X}$, $\overline{\mathcal{X}}$ denotes its closure, $\text{int}(\mathcal{X})$ denotes its interior, and $\text{bd}(\mathcal{X})$ denotes its boundary. If $\mathcal{X}$ is finite we use $\text{card}(\mathcal{X})$ to denote its cardinality.
- A function $\sigma_L : \mathbb{R}_{\geq 0} \to \mathbb{R}_{\geq 0}$ is of class $\mathcal{L}$, i.e., $\sigma_L \in \mathcal{L}$, if: (i) it is continuous, (ii) non-increasing, and (iii) converging to zero as its argument grows unbounded.
- A function $\alpha : \mathbb{R}_{\geq 0} \to \mathbb{R}_{\geq 0}$ is of class $\mathcal{K}$, i.e., $\alpha \in \mathcal{K}$, if: (i) it is continuous, (ii) zero at zero, and (iii) strictly increasing.

- A function $\tilde{\alpha} : \mathbb{R}_{\geq 0} \to \mathbb{R}_{\geq 0}$ is of class $\mathcal{K}_\infty$, i.e., $\tilde{\alpha} \in \mathcal{K}_\infty$, if $\tilde{\alpha} \in \mathcal{K}$ and $\tilde{\alpha}$ grows unbounded as its argument grows unbounded.
- A function $\beta : \mathbb{R}_{\geq 0} \times \mathbb{R}_{\geq 0} \to \mathbb{R}_{\geq 0}$ is said to be of class $\mathcal{KL}$, i.e., $\beta \in \mathcal{KL}$ if: (i) it is of class $\mathcal{K}$ in its first argument; (ii) it is of class $\mathcal{L}$ in its second argument.
- For a couple of sets Q' and $Q \subset \mathbb{Z}$ we define the indicator function $\mathbb{I}_{Q'} : Q \to \{0, 1\}$ to be nonempty only on Q, and to satisfy $\mathbb{I}_{Q'}(q) = 1$ if $q \in Q'$, and $\mathbb{I}_{Q'}(q) = 0$ if $q \notin Q'$.

Contents

Chapter 1

Introduction

The development of feedback controllers that are able to achieve adaption and learning by using information from the environment has been motivated by the uncertain and complex nature of real-life engineering systems deployed in unpredictable and dynamic environments where external disturbances, aging of components, and time-varying operating conditions may significantly deteriorate the performance of the system. In such situations, control systems that are able to adjust their behavior under changes in the environment emerge as a suitable control methodology to maintain a good performance of the system. During the last 60 years, the concepts of learning and adaptation have played a key role in the area of feedback control systems. Classic textbooks on control systems that incorporate adaptation and learning include [1], [2], [3], [4], [5], [6], [7], [8], [9], [10], [11], [12] and [13] for example. A recent survey on adaptive control for multivariable systems was presented in [14].

One of the fields where control systems with learning and adaptation have recently seen increased attention is in the area of networked multi-agent systems (MAS) [15], [16], that is, systems comprised of multiple *interacting* subsystems, each subsystem having individual dynamics and computational capabilities, as well as limited sensing,

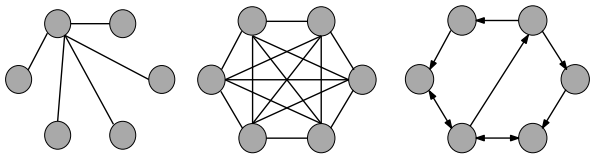

Figure 1.1: Networked Multi-Agent System with a centralized agent (left), full information (center), and local information (right).

communication, and actuation. Depending on the structure of the underlying communication graph between the agents of the system, MAS can be centralized or decentralized. In a centralized MAS there exists one central agent who has access to the state information of all other agents, and who is able to compute the control action for all agents of the network. On the other hand, in a decentralized or distributed MAS, agents individually compute their own control signals, which are shared with a subset of the other agents characterized by a communication graph. Figure 1.1 illustrates three MAS with different communication graphs. Centralized MAS are typically not scalable, and they possess the disadvantage of having a single point of failure that could potentially shut down the complete system [15]. Decentralized and distributed systems, on the other hand, are scalable, more robust, and in non-stationary environments they allow for adaptation and self-organization of the system [17]. Recent technological advances in communication and computation have made MAS ubiquitous, and today they can be found in several engineering and societal systems such as in power generation and distribution systems [18], [19], [20], groups of robots [21],[22],[23], water-distribution systems [24], [25], urban traffic networks [26], [27], [28], swarms of UAVs [29], [30], networks of sensors [31],[32],[33], and social networks [34],[35].

In this dissertation, we study robust learning and adaptive feedback mechanisms for complex multi-agent dynamical systems. In particular, we study control algorithms that improve the performance of dynamical systems in real time, without requiring an accurate model of the plant under control, and with provable convergence, stability,

and robustness properties. Feedback mechanisms of this kind have been historically studied in the context of iterative learning control [36] , [37], extremum seeking control [38], [39], [40], [41], [42], [43], [44], [45], [46], [47], model predictive control with learning [48], [49], neuroadaptive control [50], [51], [52], [53], [54], [55], robust adaptive dynamic programming [56], adaptive control with reinforcement learning [57], [58], [59], adaptive control with policy iteration [60], [56], fuzzy-based control [61], [58], and virtual reference and iterative feedback tuning [62], [63], [64]. However, although these types of control systems have been studied since almost 70 years ago, it is only recently that they have received significant attention in the context of MAS. This interest has been motivated mainly by three facts: a) large amounts of data are now available in engineering and societal systems, as well as advanced sensing algorithms, communication technologies, and cheap massive computational power, b) distributed coordination techniques for consensus [65], [66], synchronization [67], [68], formation control [69],[70], and flocking [71], [72] have reached a certain level of maturity that has lead to well established analysis and design tools based on graph theory [73], and c) in MAS each agent can use information from the other agents to achieve cooperative learning. This strategic interaction between agents has also motivated the study of game-theoretic models and algorithms in multi-agent dynamical systems, e.g, [74], [75], [76].

In the literature, learning control methods are also usually classified as "intelligent control" systems [77], in which standard continuous-time feedback mechanisms interact with discrete-event systems, automata mechanisms, supervisory control, etc. The complex interactions between continuous-time dynamics and discrete-time dynamics that emerge in these intelligent control systems generate a class of systems called *hybrid dynamical systems* [78, 79, 80]. Indeed, as noted in [77] and [81], hybrid dynamical systems (HDS) offer a powerful framework to model and analyze the qualitative proper-

ties of learning and intelligent control mechanisms [82]. Nevertheless, although several theoretical results for modeling and stability analysis of HDS have been obtained during the last years, e.g., [78, 79, 80], their application to the development of intelligent learning control methods with provable stability and robustness guarantees is still at its infancy stage, especially in the multi-agent setting.

1.1 Hybrid Dynamical Systems

In this thesis we consider dynamical systems that incorporate continuous-time dynamics and discrete-time dynamics. These systems are called hybrid dynamical systems. While usually continuous-time dynamical systems are modeled as ordinary differential and difference equations of the form

$$\dot{x} = f(x) \quad \text{and} \quad x^+ = g(x), \tag{1.1}$$

we will also consider set-valued dynamical systems of the form

$$\dot{x} \in F(x) \quad \text{and} \quad x^+ \in G(x), \tag{1.2}$$

where the mappings $F(\cdot)$ and $G(\cdot)$ are set-valued. Working with systems of the form 1.2 allows us to consider (1.1) as a particular case, as well as to analyze the robustness properties of dynamical systems with possible discontinuous mappings $f(\cdot)$ and $g(\cdot)$. In order to characterize the points in the space where the hybrid system is allowed to evolve according to the differential or difference inclusion (1.2), we introduce the flow

set C and the jump set D. The complete hybrid system can then be written as

$$\dot{x} \in F(x), \quad x \in C \tag{1.3a}$$

$$x^+ \in G(x), \quad x \in D. \tag{1.3b}$$

A precise mathematical characterization of the properties of system (1.3), including definitions of solutions, stability notions, and generic robustness principles, is presented in Appendix A. This modeling framework will be used throughout this dissertation to model and analyze the convergence and robustness properties induced by the feedback mechanisms that we consider in this work.

1.2 Hybrid Extremum Seeking Control

The second chapter of this thesis introduces the paradigm of hybrid extremum seeking control in hybrid dynamical systems. Extremum seeking control (ESC) is a type of feedback adaptive control designed to achieve real-time optimization of dynamical systems that have a well-defined steady state input-to-output mapping, also called *response map*, which is only accessible by measurements. This type of feedback control for black-box optimization of dynamical systems has been considered since the early 1920's [83], and further developed in the 1950's and 1960s in [84], [85]. Different types of ESCs have been designed during the last years [86], [45], [87], being the periodic perturbation approach presented in [88] one of the most populars due to its simplicity and adaptability to different types of applications. The analysis of this periodic perturbation approach relies on averaging and singular perturbation theory for Lipschitz differential equations [89], which allowed the authors in [88] to establish a local exponential stability result for the optimal point of the closed-loop system. This

result was later extended in [90] to obtain a semi-global practical stability result, whose foundation exploits the "two-time scale averaging" setting analyzed in [91]. In general, these methods of analysis have proven to be instrumental for the design of several different extremum seeking controllers during the last years, e.g., [92], [93], [94], [95], [96], [97], [98], [99], [100], [101], [102], with applications in ABS break control [103], formation flight optimization, [104], learning in non-cooperative games [105], [106], dynamic resource allocation [107], [108], [109], robot source seeking [110], optimization of wind turbines [111], and human exercise machine control [112], for example.

Deterministic ESCs have been historically designed and analyzed based on dynamical systems theory for ordinary differential equations (ODEs) or difference equations (i.e., recursions). However, the study of ESCs in systems with hybrid dynamics in the plant and in the feedback loop remains unexplored. This type of hybrid dynamics emerge frequently in real-world control and optimization algorithms that have the form of switched systems, logic and event-based controllers, continuous-time systems with weakly jumping parameters, supervisory-based control systems, multi-agent systems with switching communication topologies, etc. Moreover, the standard ESCs developed for continuous-time systems preclude the implementation of discontinuous dynamics commonly used in optimization to achieve finite-time convergence, as well as *set-valued* optimization dynamics that arise in some learning and parametric optimization problems.

Motivated by this background, we study in Chapter 2 a new class of ESCs that allows us to implement continuous-time and discrete-time dynamics during the learning process, guaranteeing a robust convergence to a neighborhood of the optimal solution of the extremum seeking problem. We study ESCs based on averaging theory, as well as some recent neuro-adaptive architectures that implement neural networks in the feedback loop. In both cases, we developed a comprehensive theoretical framework for

the design and analysis of ESCs, as well a representative examples and applications where hybrid or/and non-smooth dynamics emerge in a natural way.

1.3 Online Learning for Dynamic Pricing in Societal Systems

Many of today's engineered systems are tightly interconnected with their users, and in many cases system performance depends greatly on user behavior [113]. Because of this, game theory is playing a bigger a role in the analysis and design of many engineering systems that interact with a large population of users making decisions in real time. This type of socially integrated engineering systems, also called societal systems, appear in a variety of contexts in theory and practice; transportation networks [114], ride-sharing applications [115], supply-chain management [116], water distribution networks [117], and electric power grids [117] are immediate examples. Since the performance of societal systems depends heavily on the behavior of the users, a social planner interested in optimizing the performance of the overall system will need to consider methods to influence the behavior of the users in order to induce a positive change on aggregate system performance [113]. Because of this, the problem of designing "smart" pricing mechanisms for societal systems has been extensively studied in the literature during the last years [118], [114], [119], [120], [113]. In [118] and [121] the authors presented a class of marginal-based pricing mechanisms corresponding to a static mapping that is implemented for a class of social dynamics. In these works, it was shown via Lyapunov arguments that if the population dynamics satisfy a positive correlation property, convergence towards the socially optimal Nash flow is obtained. Flow-varying tolls were also considered in [122] and [123]. However, even though flow-

varying tolls based on marginal cost can successfully influence the population towards the socially optimal Nash equilibrium, some limitations prevent their application in practical environments. In particular, as noted in [114], in practical applications users dislike fast-changing tolls, and would prefer prior information of the tolls before making a decision. Because of this, fixed tolls that stay constant for a fixed number of days were considered in [114], and some interaction between a class of social dynamics and the toll mechanism was allowed. It is well known that fixed tolls can be designed to incentivize any feasible Nash equilibria in congestion games [124], [125].

One of the challenges of designing real-time pricing mechanisms for tolls in societal systems comes from the complex nature of large-scale interconnected systems operating under uncertain time-varying conditions. Because of this, social planners are also faced with the challenge of characterizing or learning the model of the system by using real-time data [126]. For instance, in transportation systems, where the delay associated to a path or road may depend heavily on external factors such as time and weather conditions, it is in general difficult to have a precise characterization of the gradient of the cost function representing the delay. Nevertheless, the delay experienced by drivers using a particular road can actually be measured by current technology [114]. This suggest that designing distributed data-driven pricing mechanisms that are agnostic with respect to the exact mathematical model of the game is a desirable objective. This idea has been studied in some settings where one is interested in achieving a particular target *known* equilibria [123]. Nevertheless, the case where one is interested in converging to the set of unknown tolls that induce a socially optimal Nash equilibrium in congestion games seems to be mostly unexplored.

Motivated by this background, we presented in Chapter 3 a novel class of algorithms that achieve model-free distributed pricing in a class of societal systems describing congestion games with affine cost functions and a finite number of available resources.

The distributed dynamic pricing mechanisms are based on the observation that welfare-gradient dynamics in affine congestion games with full utilization of resources can be seen as a type of full-information linear Laplacian flow with respect to a vector of induced cost functions with marginal tolls. We consider the case when the dynamics of the society are instantaneous, as well as the case where the social dynamics cannot be omitted by the pricing mechanism. Using some of the analytical tools developed in Chapter 2 we establish a convergence result for the complete closed-loop system involving the dynamic society and the dynamic pricing mechanism.

1.4 Event-Triggered Sampled-Data Extremization

The concept of event-triggered control [127], [128], has emerged as an interesting control paradigm that can significantly improve the efficiency of a closed-loop system by mitigating unnecessary waste of communication, computational, or *physical* resources. In an event-triggered setting, the control algorithm is not periodically updated based on a fixed sampling-time or step size, but rather based on the occurrence of an event. One of the areas where event-triggered control methods have recently received significant attention is in the area of learning and optimization in dynamical systems. Applications of event-triggered methods in learning and optimization have been presented in the context of distributed optimization of static maps [129], model-free learning in optimal control settings [130], self-triggered learning in games [131], and event-triggered control with neural networks [132], for example.

On the other hand, extremum seeking architectures that use discrete-time optimization algorithms have historically been studied using a periodic sampled-data approach, e.g., [133], [134], [135], [136]. In this sampled-data setting, a stable multiple-input-single-output (MISO) nonlinear plant, having an unknown model, is interconnected

with a discrete-time optimizer by means of a sampler/zero-order hold with a fixed *large* sampling period T. Using a sequence of dither signals the plant is sequentially perturbed at a given operational point, such that, by designing T to be sufficiently large, a corresponding sequence of measurements of the output can be collected at an approximated quasi-steady state condition. By using this sequence of measurements the optimizer generates the new input signal, and the process is then repeated. This approach was studied from a Lyapunov perspective in [133] and [87], and from a trajectory based perspective in [135, Sect. 5]. Related works have been pursued in [134], [137], and [138].

One of the major drawbacks of existing sampled-data approaches is that although a fixed large sampling time T simplifies the stability analysis of the closed-loop system by decoupling the dynamics of the plant and the controller, it also imposes a direct limitation on the convergence rate of the closed-loop system. This limitation has been extensively documented and discussed in [133, Chap. 2], [134, Remark 10], and [135, Sec. 6.3]. In particular [134, Remark 10] shows that the rate of convergence of the output of the plant to a neighborhood of its optimal value is proportional to T. In fact, since the plant under control is assumed to be a black box, the selection of such T must be performed based on a *worst-case* scenario, guaranteeing a quasi-steady state condition of the plant for *all times* that a measurement of the output y is gathered, and for *all solutions* generated by the closed-loop system from a given compact set of initial conditions. Naturally, in most of the cases, for *each given* solution generated by the closed-loop system, a worst-case selection of T leads to a sampling period that, during most of the learning process, overestimates the waiting time required by the plant to settle to a neighborhood of its steady-state condition. This overestimation is particularly noticeable as the input signal approaches the optimal operational value, and generates smaller variations in the states of the plant, which generally translates

into smaller settling times for the continuous-time dynamics.

On the other hand, for a given continuous-time dynamical system, the *worst-case* waiting time T generated by *two* different solutions with the same initial conditions can significantly differ. This observation is important since systems generating non-unique solutions include those with a right-hand side that is continuous but not Lipschitz continuous, discontinuous systems whose analysis is based on a related differential inclusion, systems arbitrarily switching between a finite number of vector fields, and plants with parameters that are known to only lie on compact and convex sets, for example. In this case, in order to apply existing results in sampled-data based optimization and extremum seeking, a fixed sampling time T would need to be selected as the *largest* waiting time among all the *worst-case* waiting times generated by all solutions of the plant from a given compact set of initial conditions, a selection that would clearly further deteriorate the convergence time of the closed-loop system, *irrespective* of the discrete-time controller or optimization algorithm being used.

Motivated by these challenges, Chapter 4 presents a theoretical framework to design and analyze a class of novel *efficient* and model-free *event-triggered* sampled-data based controllers for set-valued nonlinear systems with well-defined response maps. The type of systems presented in this chapter have three main features: First, in contrast to existing approaches, the update frequency of the discrete-time control dynamics is not constant, but ruled by the occurrence of an event, namely the detection of a quasi-steady state condition in a monitored triggering signal. Second, by introducing the concept of *target optimizing dynamical system* (TODS) we reformulate and characterize the class of well-posed *set-valued discrete-time learning dynamics* that can be used to solve the model-free extremization problem. Third and finally, in contrast to existing results in the literature, the class of controllers presented in this chapter is not restricted to solve only standard smooth and nonsmooth maximization problems, but

also learning problems in game-theoretic settings. We provide a complete stability and robustness characterization of the closed-loop even-triggered system, and we illustrate the fast convergence properties of the algorithm via simulations.

1.5 Robust Coordination of Sampled-Data Systems

The development of analytical tools for the coordination and control of networked cyber-physical systems (CPS) has received significant attention during the last years [139], [140], [141]. This interest has been motivated by a dramatic increase in computational power and information exchange in large scale networked systems. In CPS, the complex interactions between physical dynamics and digital dynamics require the implementation of additional protocols and coordination mechanisms that guarantee a desirable performance of the system. An example of this, emerges in the context of networked multi-agent sampled-data systems, where decentralized digital controllers are designed to coordinate a large number of plants. These plants may represent industrial processes [142], autonomous vehicles [143], [144], or biological systems [145], for example. For a recent survey in the area of networked multi-agent hybrid systems see [146].

Analytical and constructive tools for networked sampled-data systems have been studied in [147], [148], [149], and [150], for example. For this type of systems, a popular approach to design control mechanisms is the so called *emulation* approach, where the control architecture is first assumed to be designed for an ideal simplified nominal system that ignores delays, quantization, asynchrony, etc, and where the controller is later modified to cope with the nonideal nature of the original system. While this approach is well established for networked systems with a unique sampling mechanism that grants access to the network, the case where multi-agents implement multiple

asynchronous sampling mechanisms needs to be treated with care. In particular, as noted in [141, Remarks 5 and 7], when multiple clocks trigger the control dynamics of the MAS, arbitrarily small perturbations can dramatically change the sampling and updating times in the closed-loop system, leading to potentially unstable behaviors. This situation does not emerge in settings such as those considered in [151], [152], [149], where a minimum inter-event time is guaranteed between samplings. However, in MAS with local triggering mechanisms, it is possible to have situations where multiple finite samplings and updates occur simultaneously in the network. For the case when the control dynamics are designed to emulate a nominal stable system, the simultaneous updates in the MAS may induce closed-loop systems that have zero margins of robustness under arbitrarily small perturbations.

Motivated by this background, we present in Chapter 5 a novel framework to design robust decentralized feedback mechanisms for networked multi-agent CPS, where each agent corresponds to a sampled-data system with individual sampling mechanisms and set-valued periodic nonlinear dynamics, and where the goal is to stabilize a pre-defined compact set. In order to achieve this goal, we study the robustness issues that emerge in multi-agent sampled-data systems with sampling mechanisms triggered by individual agent's clocks. To address the potentially unstable behavior that emerges due to sequential updates in the MAS, and inspired by [140], we introduce the idea of "pre-jump sampling control", which allows agents to coordinate their sampling and update times, such that the emergent behavior in the asynchronous networked system emulates the behavior of a synchronous networked nominal MAS designed a priori. Unlike existing results for networked sampled-data systems with single triggering mechanisms [147], [148], [149], and multiple triggering mechanisms [141], [140], [139], we developed our results for well-posed sampled-data systems with general plants characterized by difference inclusions, and general controllers characterized by periodic difference in-

clusions parameterized by logic states. This allows us to cover the special cases of plants modeled by differential equations and controllers modeled by non-periodic difference equations. Moreover, control systems with integer or logic states are common in switched control systems with hysteresis [153], coordinated learning mechanisms in games [154], event-triggered control [155], robust moving horizon controllers [156], and discrete-time periodic systems [142], for example. In fact, as shown in [157], logic states are indeed necessary to achieve *global* and *robust* asymptotic stability in dynamical systems under some topological or discontinuous obstructions.

The idea of pre-jump sampling control requires the implementation of synchronized clocks in the networked system. Therefore, the second main contribution of this chapter corresponds to a novel decentralized robust synchronization algorithm for a network of periodic resetting clocks and logic states. Unlike existing results in the literature of clock synchronization and pulse-coupled oscillators [158], [159], [160], our results guarantee *global* and *robust* synchronization, i.e., there is no problematic set of measure zero of initial conditions from which synchronization cannot be achieved. To achieve this, we use a set-valued resetting rule that implements a small individual parameter $r_i \in (0, N^{-1})$, where N is the number of agents in the network. The complete closed-loop system is studied using the formalism of HDS presented in [78]. This allows us to employ Lyapunov tools, invariance principles, and robustness corollaries for HDS, such that a semi-global practical asymptotic stability result can be established for the closed-loop system. For the clock synchronization problem we formulate our results for general directed time-varying graphs that are strongly connected only "sufficiently often". The results of this chapter are instrumental for the design and coordination of classic stabilizing controllers in multi-agent sampled-data systems, as well as distributed learning algorithms for sampled-data systems [154], multi-agent sampled-data extremum seeking controllers [161], decentralized estimation algorithms

[162], and in general multi-agent discrete-time systems with local clocks designed under the assumption of a single clock.

1.6 Stochastic Learning in Sampled-Data Systems

Chapter 6 studies the problem of robust Nash seeking in sampled-data Nash games, which are non-cooperative games where the players correspond to sampled-data systems sharing information via a directed communication graph, and who aim to selfishly maximize their own individual payoff function by controlling their own action. This type of games models some applications in engineering and networked control systems where different agents with conflicting interests interact [163], [164], [165], [166], [167]. One of the main challenges for the implementation of classic learning dynamics in practical applications comes from the model-based nature of most of the existing algorithms. In this way, assuming a full communication structure between players, full knowledge of their mathematical models, as well as a synchronous behavior may not be realistic in many scenarios [168], [107]. In fact, in practical settings where a perfect model of the system is not available, it may be necessary to implement learning dynamics that do not explicitly depend on the mathematical model of the agents, and which still can guarantee convergence to the Nash equilibrium of the game. Motivated by the undesirable predictable behavior of deterministic systems, stochastic learning dynamics for discrete-time systems were considered in [169] and [170]. Stochastic continuous-time learning dynamics were also recently studied in [171].

On the other hand, the area of security has been one of the most active research areas in the control community during the last years [172], [173], [174], [175]. Indeed, given the increasing size and exposure of automated systems, it is desirable to design control and optimization algorithms that are robust under multiple types of adversarial

attacks. In the setting of sampled-data systems, this problem has been studied in [176], [177], and [178], for example. However, in the setting of model-free stochastic learning dynamics under persistent attacks in sampled-data systems, few results have been developed in the literature.

Motivated by this background, we developed in Chapter 6 a class of model-free stochastic learning dynamics for sampled-data Nash games, where each player is a sampled-data system with a periodic sampler/zero-order hold mechanism, and set-valued continuous-time dynamics that are assumed to be unknown for the agents. For this system, we first show that convergence towards a neighborhood of the Nash equilibrium of the game can be achieved, even though the control systems of the agents are subject to attacks that persistently deactivate the control dynamics. This result is established by characterizing an upper bound on the amount of attacks that the control systems can withstand during a given period of time, and by imposing a causality condition on the nature of the attacks. Namely, in order to preserve the stability conditions of the system, the attacker must not be able to anticipate the value of the random variables used by the stochastic control system. Once a stability result has been established for the network of sampled-data systems under persistent attacks, we consider the case when a subset of the agents have control systems that have been permanently incapacitated, i.e., agents that are not able to learn. For MAS with *stubborn* agents, we characterize the stability properties of the closed-loop system in terms of input-to-state stability notions in the mean-square sense. We finish by illustrating how non-causal attacks can systematically induce false Nash equilibria in the game by interfering the learning of the gradient of the response map associated to each agent.

Chapter 2

Hybrid Extremum Seeking Control

In this chapter, we will present a general framework to design and analyze a class of time-invariant set-valued *hybrid extremum seeking controllers* (HESCs) with continuous and discrete-time dynamics expressed as dynamic inclusions, and with states constrained to evolve on specific closed sets characterizing potential constraints on the optimization problem. These HESCs are suitable to control/optimize not only plants described by differential equations with a Lipschitz right-hand side, but also plants described by well-posed differential inclusions or/and hybrid systems, commonly used to analyze discontinuous and switched systems. Since dynamical systems described by set-valued mappings usually lack of the uniqueness of solutions property, we do not insist on it, but rather we analyze all the possible solutions that may emerge from a given compact set of initial conditions. We consider two types of HESCs: Averaging-based HESC, which are analyzed based on averaging theory for hybrid systems; and neuro-adaptive HESCs, which rely on the approximation properties of neural networks. In both scenarios we establish a semi-global practical result for the emerging closed-loop system. Different applications of our theoretical results are presented for single-agent and multi-agent systems .

2.1 Averaging-Based Hybrid Extremum Seeking for Differential Inclusions

We start this chapter by considering averaging-based HESCs applied to plants described by differential inclusions.

2.1.1 Model of the Plant

Consider a dynamical system with state $\theta \in \mathbb{R}^m$, input $u \in \mathbb{R}^n$, and output $y \in \mathbb{R}$, modeled by the constrained differential inclusion

$$\dot{\theta} \in P(\theta, u), \qquad (\theta, u) \in \Lambda_\theta \times \mathbb{U}, \qquad y = \varphi(\theta, u), \tag{2.1}$$

where $P : \mathbb{R}^m \times \mathbb{R}^n \rightrightarrows \mathbb{R}^m$ is a set-valued mapping, $\varphi : \mathbb{R}^m \times \mathbb{R}^n \to \mathbb{R}$ is an output function, θ evolves in the compact set $\Lambda_\theta := \lambda_\theta \mathbb{B} \subset \mathbb{R}^m$, $\lambda_\theta \in \mathbb{R}_{>0}$, and u evolves in the closed set $\mathbb{U} := \hat{\mathbb{U}} + \mathbb{B}$, where $\hat{\mathbb{U}} \subset \mathbb{R}^n$. Systems of the form (2.1) with θ evolving on $\mathbb{R}^m$ can be considered by taking λ_θ to be sufficiently large to encompass all complete solutions of practical interest. The unitary inflation on $\hat{\mathbb{U}}$ is motivated by the fact that we will design the control system such that the state u will satisfy $u(t, j) \in \hat{\mathbb{U}} + a\mathbb{B} \subset \mathbb{U}$ for all (t, j) in the domain of the solutions, where $a \in (0, 1)$ is a tunable parameter. We make the following regularity assumption on system (2.1).

Assumption 1 *The set $\hat{\mathbb{U}}$ is closed. The set-valued mapping $P(\cdot, \cdot)$ is OSC, LB, and convex-valued relative to $\mathbb{R}^m \times \mathbb{U}$, and the mapping $\varphi(\cdot, \cdot)$ is continuous.*

Remark 1 *The mathematical model given by (2.1) is quite general in the sense that it captures differential equations with a continuous right-hand side, as well as discontinuous plants modeled by their corresponding Krasovskii regularizations [78, Def. 4.13].*

In the former case, a differential equation with a continuous right-hand side $p(\theta, u)$ can be represented as (2.1) by means of the set-valued mapping

$$P(\theta, u) := \begin{cases} p(\theta, u) & (\theta, u) \in \Lambda_\theta \times \mathbb{U} \\ \emptyset & (\theta, u) \notin \Lambda_\theta \times \mathbb{U}, \end{cases}$$

which satisfies Assumption 1, while in the later case the Krasovskii regularization of a discontinuous vector field $p(\theta, u)$, which is defined as

$$P(\theta, u) := \bigcap_{\delta > 0} \overline{co}\; p\big((\theta + \delta\mathbb{B}) \cap \Lambda_\theta, (u + \delta\mathbb{B}) \cap \mathbb{U}\big), \tag{2.2}$$

also satisfies Assumption 1, see [78, Lemma 5.16].

Common examples of plants with a discontinuous right-hand side include mechanical systems with Coulomb friction [179, Chapter 12], systems arbitrarily switching between a finite number of continuous vector fields [78, Example 2.14], and plants with uncertain models and internal discontinuous feedback controllers [89].

The differential inclusion (2.1), together with the auxiliary dynamics $\dot{u} = 0$, can be modeled as an open-loop HDS (1.3) with state (x, u) and with no jumps, i.e., with $D := \emptyset$ and $G := \emptyset$, given by $\mathcal{H}_P := \{\Lambda_\theta \times \mathbb{U}, P \times \{0\}, \emptyset, \emptyset\}$. We make the following assumption on this HDS.

Assumption 2 *There exists a set-valued mapping $H : \mathbb{R}^n \rightrightarrows \mathbb{R}^m$ that is OSC and LB relative to $\mathbb{U}$, such that for each $\rho > 0$ the compact set $\mathbb{M}_\rho := \{(\theta, u) : \ \theta \in H(u), u \in \mathbb{U} \cap \rho\mathbb{B}\}$ is UGAS for the restricted HDS $\mathcal{H}_{P_\rho} := \{\Lambda_\theta \times (\mathbb{U} \cap \rho\mathbb{B}), P \times \{0\}, \emptyset, \emptyset\}$ with state $[\theta^\top, u^\top]^\top$.*

Assumption 2 generalizes the classic assumptions made for ESC, e.g., [90, Assumptions 1 and 2], for the case that the plant under control is given by a constrained set-valued

dynamical system. Note that we do not assume that $H(u) \subset \Lambda_\theta$ for all $u \in \mathbb{U}$, since for the closed-loop system we will always restrict u to lie on a compact set that can be selected arbitrarily large to encompass all complete solutions of interest. Once u has been restricted to a compact set, the constant λ_θ can be selected large enough to guarantee the containment $H(u) \subset \Lambda_\theta$.

Example 1 *Consider a simple harmonic oscillator with Coulomb friction and controllable velocity offset, given in open-loop by the discontinuous dynamics*

$$\epsilon\dot{\theta}_1 = \theta_2 - u, \qquad \epsilon\dot{\theta}_2 = -\frac{B}{M}sgn(\theta_2 - u) - \frac{K}{M}\theta_1, \qquad \dot{u} = 0, \tag{2.3}$$

with $\Lambda_\theta = \lambda_\theta\mathbb{B} \subset \mathbb{R}^2$, $\mathbb{U} = \mathbb{R}$, $(\epsilon, B, K, M) \in \mathbb{R}^4_{>0}$, *and* $\lambda_\theta > \frac{B}{K} > 0$ *selected sufficiently large to characterize all the complete solutions of interest. The Krasovskii regularization of this system affects only the dynamics of* θ_2, *and is given by*

$$\dot{\theta}_2 \in P_2(\theta, u) = \begin{cases} -\frac{B}{M} - \frac{K}{M}\theta_1 & \text{if } \theta_2 > u \\ \left[-\frac{B}{M}, \frac{B}{M}\right] - \frac{K}{M}\theta_1 & \text{if } \theta_2 = u \\ \frac{B}{M} - \frac{K}{M}\theta_1 & \text{if } \theta_2 < u. \end{cases} \tag{2.4}$$

In this case, for each $\rho > 0$ *the constrained system* $\mathcal{H}_{P_\rho}$ *renders the set* $\mathbb{M}_\rho := \{(\theta, u) : \theta \in [-\frac{B}{K}, \frac{B}{K}] \times \{u\}, u \in \mathbb{R} \cap \rho\mathbb{B}\}$ *UGAS [180, Section 3], thus satisfying Assumption 2.*

Example 2 *Consider an open-loop switched linear system given by* $\epsilon\dot{\theta} = p_q(\theta, u) := A_q\theta + B_q u$, $\dot{u} = 0$, $\mathbb{U} := \mathbb{R}$, $(\epsilon, \lambda_\theta) \in \mathbb{R}^2_{>0}$, *with matrices*

$$A_q = \begin{bmatrix} -1 & \frac{3}{2} - \frac{5}{4}q \\ -\frac{9}{4} + \frac{5}{4}q & -1 \end{bmatrix}, \; B_q = \begin{bmatrix} 1 \\ \frac{9}{4} - \frac{5}{4}q \end{bmatrix}, \tag{2.5}$$

where $q \in \{1, 2\}$. *Under arbitrary switching this system is conveniently modeled by*

the differential inclusion $\epsilon\dot{\theta} \in \{\alpha p_1(\theta,u) + (1-\alpha)p_2(\theta,u), \alpha \in [0,1]\}$, $\dot{u} = 0$, *which satisfies Assumption 1. Moreover, for each* $\rho > 0$ *the system* $\mathcal{H}_{P_\rho}$ *renders the set* $\mathbb{M}_\rho := \{(\theta,u) : \theta \in \{u\} \times \{0\}, u \in \mathbb{R} \cap \rho\mathbb{B}\}$ *UGAS. This can be established by using the common Lyapunov function* $V = (\theta_1 - u)^2 + \theta_2^2$, *thus satisfying Assumption 2.*

To guarantee a well defined extremum seeking problem in set-valued dynamical systems of the form (2.1), the following assumption is needed.

Assumption 3 *For each* $u \in \mathbb{U}$ *and each pair* $\theta, \theta' \in H(u)$ *we have that* $\varphi(\theta,u) = \varphi(\theta',u)$.

Note that for Example 1 any output function $\varphi(\cdot,\cdot)$ whose first argument depends only on θ_2 will satisfy Assumption 3. On the other hand, for Example 2 we have that Assumption 3 holds for any output function depending on the overall state θ.

2.1.2 Problem Statement

Based on Assumptions 1, 2, and 3, the steady-state input-to-output mapping associated to the dynamical system (2.1), also known as the *response map*, is well-defined in $\mathbb{U}$, and given by

$$J(u) := \{\varphi(\theta,u) : \ \theta \in H(u)\}. \tag{2.6}$$

The main goal in an extremum seeking problem is to control in real-time the input u of system (2.1) by using only measurements of the output y, i.e., in a data-driven way, such that an *application-dependent* optimization problem of the form

$$\text{optimize} \ \ f(J(u)), \quad \text{s.t.} \ \ u \in \hat{\mathbb{U}}, \tag{2.7}$$

is solved. In equation (2.7), the mapping $f(\cdot)$ captures the control objective associated to the plant (2.1). In general, this objective is formulated based on the particular

application. We make the following assumption on (2.7).

Assumption 4 *The response map $J : \mathbb{R}^n \to \mathbb{R}$ is smooth, and the set of solutions of problem (2.7), denoted by $\mathcal{O} \subset \mathbb{R}^n$, is nonempty and compact.*

Remark 2 *Systems of the form (2.1) can also be used to study networked systems, i.e., multi-agent systems (MAS) with individual outputs φ_i, for all $i \in \{1, \ldots, N\}$, being N the number of subsystems. In this case, Assumptions 3 and 4 should be satisfied for each response map $J_i(u) := \{\varphi_i(\theta, u) : \theta \in H(u)\}$ associated to each subsystem $i \in \{1, \ldots, N\}$, where the characterization of the set $\mathcal{O}$ will depend on the particular application, and where the response map of each subsystem may depend only on the actions of a subset of the other subsystems. This case is relevant for distributed optimization problems in multi-agent systems, as well as for Nash equilibrium seeking problems in game theoretic scenarios where the set $\mathcal{O}$ corresponds to the set of Nash equilibria. See for instance [105], [106], [169], and [101], for different examples of Lipschitz continuous ESCs studied in these settings.*

2.1.3 Extremum Seeking Controllers with Hybrid Learning Dynamics

We now consider a class of time-invariant gradient-based HESCs comprised by a dynamic gradient estimator with states $(\xi, \mu) \in \mathbb{R}^n \times \mathbb{R}^{2n}$, and a hybrid learning mechanism with overall state $x_{u,z} := (\hat{u}, \hat{z}) \in \mathbb{R}^n \times \mathbb{R}^r$. Together, the gradient estimator and the learning mechanism regulate the input of the plant (2.1) towards the optimal set $\mathcal{O}$ by using only measurements of the output of the plant (2.1). This idea is illustrated in the conceptual scheme presented in Figure 2.1.

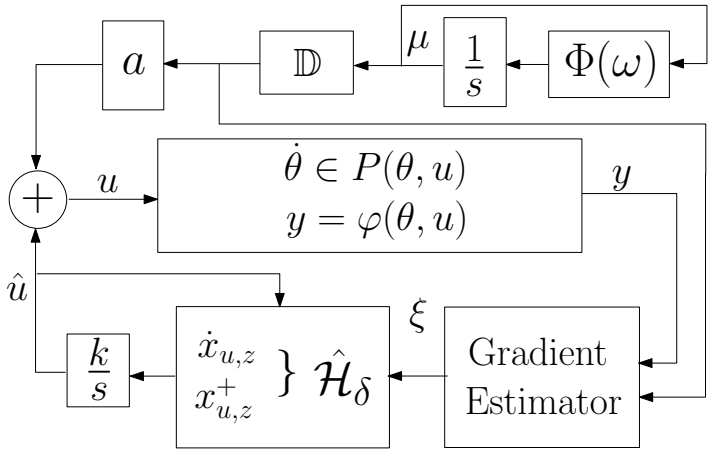

Figure 2.1: Conceptual Scheme of HESC for set-valued plants.

Continuous-Time Gradient Estimator

The gradient estimator for the response map J is characterized by a system with states $(\xi, \mu) \in \mathbb{R}^n \times \mathbb{R}^{2n}$, input y given by the output of (2.1), and continuous-time dynamics

$$\begin{pmatrix} \dot{\xi} \\ \dot{\mu} \end{pmatrix} = \begin{pmatrix} -\omega_L \cdot \left(\xi - \frac{2}{a} y \cdot \mathbb{D}\ \mu\right) \\ \Phi(\omega)\ \mu \end{pmatrix}, \ (\xi, \mu) \in \Lambda_\xi \times \mathbb{S}^n, \tag{2.8}$$

where $\mu := [\mu_1, \ldots, \mu_n]^\top \in \mathbb{S}^n$, $\mu_i = (\mu_{i,1}, \mu_{i,2})^\top \in \mathbb{S}^1$, for all $i \in \{1, \ldots, n\}$, ξ evolves in a compact set $\Lambda_\xi := \lambda_\xi \mathbb{B} \subset \mathbb{R}^n$, where $\lambda_\xi \in \mathbb{R}_{>0}$ is selected sufficiently large to encompass all the complete solutions of interest, $\mathbb{D} := [e_1, \mathbf{0}, e_2, \mathbf{0}, \ldots, e_i, \ldots, \mathbf{0}, e_n, \mathbf{0}]$ is a block matrix where $\mathbf{0} \in \mathbb{R}^n$ corresponds to a column vector of zeros, and $e_i \in \mathbb{R}^n$ corresponds to the unitary vector with the i^{th} entry equal to 1. The ω-parameterized

block matrix $\Phi_\omega : \mathbb{R}^{2n} \to \mathbb{R}^{2n}$ is given by

$$\Phi_\omega := \begin{bmatrix} \Omega_{\omega_1} & \mathbf{0} & \dots & \mathbf{0} \\ \mathbf{0} & \Omega_{\omega_2} & \dots & \mathbf{0} \\ \vdots & \vdots & \ddots & \vdots \\ \mathbf{0} & \mathbf{0} & \dots & \Omega_{\omega_n} \end{bmatrix}, \tag{2.9}$$

where the block components Ω_{ω_i} are given by

$$\Omega_{\omega_i} := \begin{bmatrix} 0 & \omega_i \\ -\omega_i & 0 \end{bmatrix}, \quad \forall\, i \in \{1, \dots, n\}, \tag{2.10}$$

$\omega = [\omega_1, \dots, \omega_n]^\top$, $\omega_i = \epsilon\kappa_i$, $\omega_L = \epsilon\overline{\omega}$, $(\epsilon, \bar{\omega}) \in \mathbb{R}^2_{>0}$, κ_i is a rational number that satisfies $\kappa_i \neq \kappa_j$ for $i \neq j$ and $(i, j) \in \{1, \dots, n\}$, $u = \hat{u} + a\ \mathbb{D}\mu$, where $a \in (0, 1)$ is a small tunable parameter, and $\hat{u} \in \mathbb{R}^n$ is an auxiliary state with dynamics that will be characterized in the next section. The continuous-time dynamics associated to the linear oscillator $\dot{\mu} = \Phi(\omega)\mu$ in (2.8) generates a vector of periodic signals with odd components given by $\mu_{i,1}(t) = \cos(\omega_i t)\mu_{2i-1}(0) + \sin(\omega_i t)\mu_{2i}(0)$, for each $i \in \{1, \dots, n\}$. These signals can then be injected into the closed-loop system in order to estimate, on average, the derivatives of J.

Remark 3 *A linear oscillator of the form (2.9) is not the only dynamical system that can be used to generate the dither signals μ. For example, well-posed nonlinear systems having an asymptotically stable limit cycle could also be used to generate the dither signals.*

Apart from the compactness assumption on the set Λ_ξ, system (2.8) essentially mirrors the behavior generated by the standard gradient estimators used in Lipschitz continuous extremum seeking controllers for standard optimization [96], [95], and for

learning in games [106], [101]. However, constraining the state ξ to lie in a compact set is required in our case in order to apply averaging and singular perturbation results for hybrid systems.

Remark 4 *Dynamic Hessian estimators for the implementation of Newton-based algorithms could also be considered in (2.8). This is a relevant case since switching between gradient and Newton-based algorithms is a common approach to improve the convergence rate during the optimization process. However, since we pursue non-local stability results, we restrict our attention to gradient-based learning dynamics.*

Remark 5 *In the multi-agent systems case (see also Remark 2), the output y in (2.8) will correspond to a vector with entries given by the outputs of each of the individual subsystems, and the product $y \cdot \mathbb{D}\mu$ will correspond to the Hadamard product. In this case every agent will implement its own individual oscillator with matrix (2.10).*

Hybrid Learning/Optimization Dynamics

The hybrid learning dynamics are characterized by an auxiliary state $x_{u,z} := [\hat{u}^\top, \hat{z}^\top]^\top \in \mathbb{R}^\ell$, where $z \in \mathbb{R}^r$ can be used to model states that act as timers, monitors, logic modes, etc, $r \in \mathbb{Z}_{\geq 0}$, and $n + r = \ell$. The evolution of the hybrid learning dynamics is characterized by a HDS $\hat{\mathcal{H}}_\delta := \left\{C_u \times C_z, \hat{F}_\delta, D_u \times D_z, \hat{G}_\delta\right\}$, with $C_u, D_u \subset \mathbb{R}^n$, $C_z, D_z \subset \mathbb{R}^r$, and where $\delta \in \mathbb{R}_{>0}$ is a small tunable parameter that gives additional flexibility for the design of $\hat{\mathcal{H}}_\delta$. In the closed-loop system the hybrid learning dynamics $\hat{\mathcal{H}}_\delta$ receive as input the state ξ generated by the dynamics (2.8), and the evolution of the state $x_{u,z}$ is ruled by the equations

$$\dot{x}_{u,z} \in \hat{F}_\delta\big(x_{u,z}, \xi\big), \qquad x_{u,z} \in C_u \times C_z, \tag{2.11a}$$

$$x_{u,z}^+ \in \hat{G}_\delta\big(x_{u,z}\big), \qquad x_{u,z} \in D_u \times D_z, \tag{2.11b}$$

where $\hat{F}_\delta : \mathbb{R}^\ell \times \mathbb{R}^n \rightrightarrows \mathbb{R}^\ell$ and $\hat{G}_\delta : \mathbb{R}^\ell \rightrightarrows \mathbb{R}^\ell$ are set-valued mappings. In order to design the data of system $\hat{\mathcal{H}}_\delta$ we assume that $\xi := \nabla J(\hat{u})$, being $\nabla J : \mathbb{R}^n \to \mathbb{R}^n$ the gradient of the response map J. The following regularity and stability assumptions characterize the data (2.11) of $\hat{\mathcal{H}}_\delta$.

Assumption 5 *There exists a $\delta^* \in \mathbb{R}_{>0}$ such that for all $\delta \in (0, \delta^*]$ the following holds:*

(a) $C_u \times C_z$ and $D_u \times D_z$ are closed.

(b) $\hat{F}_\delta(\cdot,\cdot)$ is OSC, LB, and convex-valued relative to $(C_u \times C_z) \times \mathbb{R}^n$, and $\hat{G}_\delta(\cdot)$ is OSC and LB relative to $D_u \times D_z$.

(c) For each compact set $K \subset (C_u \times C_z) \cup (D_u \times D_z)$ there exists $\epsilon^* \in \mathbb{R}_{>0}$ such that for each $x_{u,z}(0,0) \in K$ and measurable $e(\cdot)$ with unbounded time domain and $\sup_{t\geq 0} |e(t)| \leq \epsilon^*$, the HDS (2.11) with perturbed flow map $\hat{F}_\delta(x_{u,z}, \nabla J(\hat{u}) + e)$ generates at least one complete solution.

Assumption 6 *The sets C_u and D_u satisfy $C_u \cup D_u = \hat{\mathbb{U}}$, and there exists a compact set $\Psi \subset C_z \times D_z$, such that the set $\mathcal{A} := \mathcal{O} \times \Psi$ is semiglobally practically asymptotically stable[1] (SGP-AS) as $\delta \to 0^+$ for the HDS (2.11) with $\xi := \nabla J(\hat{u})$, where $\mathcal{O}$ is given by Assumption 4.*

Items (a) and (b) in Assumption 5 are needed in order to obtain a well-posed closed-loop HDS with good robustness properties. Item (c), on the other hand, is mainly needed to guarantee that arbitrarily small perturbations on ∇J do not preclude the existence of complete solutions for system (2.11). This last property is relevant to achieve constrained extremum seeking on bounded sets.

[1]See Definition 9 in Appendix A.

Remark 6 *For gradient-based Nash seeking schemes for MAS, Assumptions 5-6 must hold replacing* ∇J *by the vector of individual partial derivatives* $\left[\frac{\partial J_1(\hat{u})}{\partial \hat{u}_1}, \ldots, \frac{\partial J_N(\hat{u})}{\partial \hat{u}_N}\right]^\top$.

The class of learning dynamics described by the HDS (2.11) is quite general in the sense that it requires only a well-posed HDS rendering the optimal compact set $\mathcal{A}$ SGP-AS with respect to a tunable parameter δ. In the case that the mappings $\hat{F}_\delta$ and $\hat{G}_\delta$ do not depend on any parameter δ, Assumption 6 is just a UGAS requirement on $\mathcal{A}$. If, additionally, the dynamics (2.11) do not depend on any auxiliary state $\hat{z} \in \mathbb{R}^r$, the sets Ψ, C_z, and D_z, can be neglected. We will use the convention $r = 0$ to specify this case. Finally, note that if in addition we have that $D_u = \emptyset$, $C_u = \mathbb{R}^n$, and $\hat{F}_\delta$ is a Lipchitz continuous function, Assumptions 5 and 6 reduce to the classic standing assumptions for purely continuous-time unconstrained extremum seeking controllers found in the literature.

Different examples of hybrid learning dynamics that can be modeled as (2.11) will be presented in Sections 2.1.4 and 2.1.5.

Closed-loop System

The complete closed-loop HESC is obtained by interconnecting the plant (2.1), the gradient estimator dynamics (2.8), and the hybrid learning dynamics (2.11), leading to a system with overall state $x := [x_{u,z}^\top, \xi^\top, \mu^\top, \theta^\top]^\top \in \mathbb{R}^{\ell+3n+m}$. This system is a HDS

represented by $\mathcal{H} := \{C, F, D, G\}$, with data given by

$$C := (C_u \times C_z) \times \Lambda_\xi \times \mathbb{S}^n \times \Lambda_\theta, \tag{2.12a}$$

$$\dot{x} \in F(x) := \begin{pmatrix} k\ \hat{F}_\delta(x_{u,z}, \xi) \\ -\omega_L\ \left(\xi - \frac{2}{a}\varphi(\theta, u) \cdot \mathbb{D}\ \mu\right) \\ \Phi(\omega)\ \mu \\ P(\theta,\ \hat{u} + a\ \mathbb{D}\ \mu) \end{pmatrix}, \tag{2.12b}$$

$$D := (D_u \times D_z) \times \Lambda_\xi \times \mathbb{S}^n \times \Lambda_\theta, \tag{2.12c}$$

$$x^+ \in G(x) := \begin{pmatrix} \hat{G}_\delta(x_{u,z}) \\ \xi \\ \mu \\ \theta \end{pmatrix}, \tag{2.12d}$$

where $k = \omega_L \sigma$, and $\sigma \in \mathbb{R}_{>0}$. The following theorem characterizes the stability and convergence properties of the closed-loop HDS (2.12). The proof is presented in the Appendix.

Theorem 1 *Suppose that Assumptions 1-6 hold. Then for each compact set $\tilde{K}$ satisfying $\mathcal{O} \times \Psi \subset int\ (\tilde{K})$ and each $\varepsilon > 0$, there exists a pair $(\lambda_\xi^*, \lambda_\theta^*) \in \mathbb{R}_{>0}^2$ such that for each $\lambda_\xi \geq \lambda_\xi^*$ and each $\lambda_\theta \geq \lambda_\theta^*$ there exists $\delta^* \in \mathbb{R}_{>0}$ such that for each $\delta \in (0, \delta^*)$ there exists $a^* \in \mathbb{R}_{>0}$ such that for each $a \in (0, a^*)$ there exists $\sigma^* \in \mathbb{R}_{>0}$ such that for each $\sigma \in (0, \sigma^*)$ there exists $\bar{\omega}^* \in \mathbb{R}_{>0}$ such that for each $\bar{\omega} \in (0, \bar{\omega}^*)$ there exists ϵ^* such that for each $\epsilon \in (0, \epsilon^*)$ there exists a compact set $\mathcal{A}_\varepsilon$ satisfying*

$$\mathcal{A}_\varepsilon \subset ((\mathcal{O} \times \Psi) + \varepsilon\mathbb{B}) \times \lambda_\xi \mathbb{B} \times \mathbb{S}^n \times \lambda_\theta \mathbb{B}, \tag{2.13}$$

which is UGAS for the closed-loop system (2.12) with restricted flow set $\hat{C} \cap \tilde{K} \times \lambda_\xi \mathbb{B} \times$

$\mathbb{S}^n \times \lambda_\theta \mathbb{B}$ *and restricted jump set* $\hat{D} \cap \tilde{K} \times \lambda_\xi \mathbb{B} \times \mathbb{S}^n \times \lambda_\theta \mathbb{B}$.

The next corollary is a direct consequence of Theorem 1 and Remark 31.

Corollary 1 *Consider the HDS (2.12) and suppose that Assumptions 1-6 hold. Suppose also that the sets* C_u, D_u, C_z *and* D_z *are bounded. Then, the result of Theorem 1 holds with the original flow and jump set given by* (2.12a) *and* (2.12c).

Theorem 2.12a is a type of "semi-global" practical stability result, similar in spirit to those in [90], [95], [96], for purely continuous-time systems. However, some subtle differences emerge for the hybrid case. In particular, for the case that the hybrid extremum seeking is performed in unbounded sets, e.g., when $C_u = D_u = \mathbb{R}^n$, Theorem 2.12a establishes GP-AS of the optimal set $\mathcal{A}$ for initial conditions and trajectories of the state component $x_{u,z}$ defined in the set $(\mathbb{R}^n \times (C_z \cup D_z)) \cap \tilde{K}$, where the compact set $\tilde{K}$ can be selected arbitrarily large. Note that although this implies that certain solutions of the system might not be complete, they will always be bounded, and the existence of complete solutions will always be guaranteed by selecting λ_ξ and λ_θ sufficiently large. Indeed, any solution of interest of system (2.12) can be guaranteed to be complete by taking the compact sets $\tilde{K}$, Λ_ξ, and Λ_θ sufficiently large, or alternatively, by defining these sets as the positively invariant level sets of Lyapunov functions obtained via converse Lyapunov theorems [181]. Note that Theorem 1 does not explicitly relate in any way the rate of convergence of the learning dynamics (2.11) with the rate of convergence of the closed-loop system, i.e., in general, the $\mathcal{KL}$ function characterizing the convergence towards the set $\mathcal{A}_\varepsilon$ depends on the parameters of the controller.

Similarly, Corollary 1 says that if the hybrid extremum seeking is performed on bounded sets, i.e., if C_u, D_u, C_z, and D_z are compact, the stability result holds for system (2.12) with the original flow and jump sets given by (2.12a) and (2.12c). Note that

Theorem 1 does not specify the type of hybrid time domains related to the solutions of system (2.12), which means that the hybrid system could generate solutions that are purely continuous, eventually continuous, eventually discrete, etc. However, since the mapping $\hat{G}_\delta$ is independent of J and ∇J, systems generating purely or eventually discrete solutions will most likely be ruled out by Assumption 6.

Remark 7 *When $D_u := \emptyset$, no solutions with jumps exist, and the HESC reduces to a constrained continuous-time set-valued extremum seeking control. If additionally $\hat{F}_\delta$ is a Lipschitz continuous function, and $C_u = \mathbb{R}^n$, we recover the standard gradient-based extremum seeking control for black-box optimization of [90], [95], or [96].*

For the HESC (2.12) no prominent role is given to the discrete-time dynamics of the states (ξ, μ, θ) in (2.12d). HESCs with active jumps in the plant, dither signal, filter, and optimizer, require a different set of analytical tools, and will be considered later in Section 2.2.

2.1.4 Examples of Hybrid Learning Dynamics

We now present some simple examples of classes of hybrid learning dynamics that satisfy Assumptions 5 and 6, and that emerge frequently in optimization, learning, and adaptive control. These dynamics are related to the hybrid system

$$\dot{\hat{u}} \in f_q\left(\hat{u}, \nabla J(\hat{u})\right), \quad \dot{q} = 0, \quad (\hat{u}, q) \in \hat{\mathbb{U}} \times Q, \tag{2.14a}$$

$$\hat{u}^+ = \hat{u}, \quad q^+ \in Q, \quad (\hat{u}, q) \in \hat{\mathbb{U}} \times Q, \tag{2.14b}$$

where $f_q : \mathbb{R}^n \times \mathbb{R}^n \rightrightarrows \mathbb{R}^n$ is OSC, LB, and convex-valued relative to $\hat{\mathbb{U}} \times \mathbb{R}^n$, $q \in \mathbb{R}$, $C_u = D_u = \hat{\mathbb{U}} \subset \mathbb{R}^n$ is a closed set, and $Q \subset \mathbb{R}$ is a compact set.

Arbitrary Switching Learning Differential Inclusions with a Common Lyapunov Function

Let $Q := \{1, \ldots, q_{\max}\}$, where $q_{\max} \in \mathbb{Z}_{\geq 1}$ and consider a collection of learning modes f_q with state $\hat{u} \in \mathbb{R}^n$, and dynamics given by (2.14a). For this dynamics the state q represents a switching signal jumping according to (2.14b), indicating which learning mode $q \in Q$ is active at every time t. The following proposition is a simple consequence of the fact that a continuous common Lyapunov function for a set of finite well-posed differential inclusions is also a Lyapunov function for the closure of their convex combination.

Proposition 1 *Suppose that for each $q \in Q$ the mapping f_q in (2.14a) satisfies item (c) in Assumption 5. Suppose also that there exists $\alpha_1, \alpha_2 \in \mathcal{K}_\infty$, a continuous positive definite function $W : \mathbb{R}_{\geq 0} \to \mathbb{R}_{\geq 0}$, and a continuous function $V : dom(V) \to \mathbb{R}_{\geq 0}$, with $\hat{\mathbb{U}} \subset dom(V)$ that is continuously differentiable on an open neighborhood of $\hat{\mathbb{U}}$ and satisfies: a) $\alpha_1(|\hat{u}|_{\mathcal{O}}) \leq V(\hat{u}) \leq \alpha_2(|\hat{u}|_{\mathcal{O}})$, and b) $\langle \nabla V(\hat{u}), \tilde{f} \rangle \leq -W(|\hat{u}|_{\mathcal{O}})$, for all $\hat{u} \in \hat{\mathbb{U}}$, $\tilde{f} \in f_q$, and $q \in Q$. Then, the system*

$$\dot{\hat{u}} \in \hat{F} := \overline{co} \bigcup_{q \in Q} f_q(\hat{u}, \nabla J(u)), \quad \hat{u} \in \hat{\mathbb{U}}, \tag{2.15}$$

has the structure of (2.11) with state $x_{uz} = \hat{u}$, $r = 0$, $\xi = \nabla J$, and sets $C_u = \hat{\mathbb{U}}$, $D_u = \emptyset$, $C_z = D_z = \Psi = \hat{G}_\delta = \emptyset$. Moreover, system (2.15) satisfies Assumptions 5 and 6, and for each ($\hat{u}$,q) that is a solution of the switching system (2.14), $\hat{u}$ is also a solution of (2.15).

Common Lyapunov functions satisfying the conditions of Proposition 1 emerge frequently in optimization algorithms since the same payoff function J is generally used to construct a candidate Lyapunov function. For example, this is the case in the

standard gradient ascent and Newton methods, as well as related discontinuous dynamics such as the *Newton variable structure algorithm* or the *continuous Jacobian matrix transpose algorithm*, for quadratic cost functions (see [182, Ch. 2]). A common Lyapunov function also emerges frequently in algorithms for distributed optimization, and learning in multi-agent systems with switching communication topologies [65]. It also emerges frequently in many learning dynamics for unconstrained and constrained *potential games* [183, Ch. 7.1].

Switched Learning Differential Inclusions with Dwell-time and Average Dwell-time Constraints

A common Lyapunov function may not exist for some classes of seeking dynamics. This applies, for instance, to some learning dynamics in game theoretic problems where a *potential* function does not exist [183, Chapter 7.2]. Since it is well known that switched systems do not necessarily inherit the stability properties of the individual dynamics, a standard approach consists on regulating the jumps of $q \in Q := \{1, \ldots, q_{\max}\}$ in system (2.14), aiming to satisfy a dwell-time or an average dwell-time constraint. These types of constraints on the jumps can be induced by using an automaton with state $\tau_1 \in \mathbb{R}_{\geq 0}$, and hybrid dynamics given by

$$\dot{\tau}_1 \in [0, \eta_1], \quad \tau_1 \in [0, N_0], \tag{2.16a}$$

$$\tau_1^+ = \tau_1 - 1, \quad \tau_1 \in [1, N_0], \tag{2.16b}$$

where $\eta_1 \in \mathbb{R}_{>0}$ and $N_0 \in \mathbb{R}_{\geq 1}$. It is well known [181, Proposition 1.1] that for each solution of the HDS (2.16) corresponds a hybrid time domain E such that, for each of its elements $(s, i), (t, j) \in E$ with $s+i \leq t+j$, and signal $q : E \mapsto Q$, the average dwell-time constraint $N(t, s) := j - i \leq \eta_1(t-s) + N_0$ holds, where $N(t, s)$ denotes the number

of switching times in the interval $[s,t]$ [184]. In fact, each hybrid time domain E with elements $(s,i),(t,j) \in E$, $s+i \leq t+j$, satisfying this average dwell-time constraint can be generated by system (2.16). When $N_0 = 1$ the switching times generated by system (2.16) satisfy a standard dwell-time constraint [185]. The following proposition is a direct consequence of [78, Corollary 7.28].

Proposition 2 *Suppose that for each $q \in Q$ the mapping f_q in (2.14a) satisfies item (c) in Assumption 5, and renders the set $\mathcal{O}$ UGAS. Then, the HDS generated by Equations (2.14) and (2.16) has the structure of (2.11) with $r = 2$, $\delta = \eta_1$, $\hat{z} := [q,\tau]^\top$, $C_z := Q \times [0,N_0]$, $D_z := Q \times [1,N_0]$, $\Psi := Q \times [0,N_0]$, $\hat{F}_\delta := f_q \times \{0\} \times [0,\eta_1]$, and $\hat{G}_\delta := \{\hat{u}\} \times Q \times \{\tau_1 - 1\}$. Moreover, this HDS satisfies Assumptions 5 and 6.*

Switched Learning Inclusions with Unstable Modes.

A HDS can be use to model the evolution of learning dynamics under persistent failures in communication or sensing, jamming signals, adversarial agents, and, in general, different adversarial scenarios that may cause instability in the closed-loop system. To address this case, the compact set $Q := \{1,\ldots,q_{\max}\}$ is partitioned as $Q = Q_u \cup Q_s$, where the modes $q \in Q_s$ characterize the stable dynamics, while the modes $q \in Q_u$ characterize the unstable dynamics. For this type of systems, good behavior of the solutions can be guaranteed as long as the amount of activation time of the unstable modes Q_u is bounded by a time-ratio constraint [186], [187], which usually has the form $T(s,t) \leq T_0 + \eta_2(t-s)$, where $\eta_2 \in [0,1)$, $T_0 \in \mathbb{R}_{\geq 0}$, and where $T(s,t)$ denotes the total activation time of modes $q_u \in Q_u$ between times s and t. This type of time-ratio constraint can be induced by using a time-ratio monitor with an auxiliary

state $\tau_2 \in \mathbb{R}_{\geq 0}$ evolving according to the hybrid dynamics

$$\dot{\tau}_2 \in [0, \eta_2] - \mathbb{I}_{Q_u}(q), \qquad \tau_2 \in [0, T_0], \tag{2.17a}$$

$$\tau_2^+ = \tau_2, \qquad \tau_2 \in [0, T_0], \tag{2.17b}$$

where $\mathbb{I}_{Q_u}(\cdot)$ corresponds to the indicator function. The following Lemma shows that for each solution of the HDS (2.17), corresponds a hybrid time domain E, such that for each of its elements $(s,i),(t,j) \in E$ with $s+i \leq t+j$ and signal $q : E \to Q$ we have that the time-ratio constraint holds. In fact, each hybrid time domain E with elements $(s,i),(t,j) \in E$ with $s+i \leq t+j$, satisfying the time-ratio constraint can be generated by system (2.17).

Lemma 1 *For each solution of the HDS (2.17), corresponds a hybrid time domain E, such that for each of its elements $(s,i),(t,j) \in E$ with $s+i \leq t+j$ and signal $q : E \to Q$, with $Q_u \subset Q$, we have that*

$$T(s,t) := \int_s^t \mathbb{I}_{Q_u}(q(r, j(r)))dr \leq T_0 + \eta_2(t-s), \tag{2.18}$$

where $T(s,t)$ denotes the total activation time of modes $q \in Q_u$ between times (s,t), and where $j(r)$ is the minimum j such that $(r,j) \in E$. Moreover, each hybrid time domain E with elements $(s,i),(t,j) \in E$ with $s+i \leq t+j$ satisfying the bound (2.18), can be generated by (2.17).

The following proposition is a straightforward extension of the results in [186, Theorem 2] and [187, Theorem 1], for well-posed differential inclusions without inputs.

Proposition 3 *Suppose that for each $q \in Q$ the mapping f_q in (2.14a) satisfies item (c) in Assumption 5. Consider the HDS composed by equations (2.14), (2.16), and*

(2.17). Suppose also that there exist $\mu \in \mathbb{R}_{\geq 1}$, $\alpha_{1,q}, \alpha_{2,q} \in \mathcal{K}_\infty$, $\lambda_s \in \mathbb{R}_{>0}$, $\lambda_u \in \mathbb{R}_{>0}$, *and continuously differentiable functions* $V_q : \hat{\mathbb{U}} \to \mathbb{R}_{\geq 0}$, *such that*

$$\alpha_{1,q}(|\hat{u}|_{\mathcal{O}}) \leq V_q(\hat{u}) \leq \alpha_{2,q}(|\hat{u}|_{\mathcal{O}}), \qquad \forall\ (q, \hat{u}) \in Q \times \hat{\mathbb{U}}, \tag{2.19a}$$

$$\langle \nabla V_{q_s}, \tilde{f} \rangle \leq -\lambda_s V_{q_s}(\hat{u}), \qquad \forall\ (q_s, \hat{u}, f) \in Q_s \times \hat{\mathbb{U}} \times f_q, \tag{2.19b}$$

$$\langle \nabla V_{q_u}, \tilde{f} \rangle \leq \lambda_u V_{q_u}(\hat{u}), \qquad \forall\ (q_u, \hat{u}, f) \in Q_u \times \hat{\mathbb{U}} \times f_q. \tag{2.19c}$$

$$V_p(\hat{u}) \leq \mu V_q(\hat{u}), \qquad \forall\ (q, p), \hat{u} \in Q \times \hat{\mathbb{U}}. \tag{2.19d}$$

Then, if $\lambda_s > \eta_1 \log(\mu) + \eta_2(\lambda_s + \lambda_u)$, *the HDS composed by equations (2.14), (2.16), and (2.17), has the structure of (2.11) with* $r = 3$ $z := [q, \tau_1, \tau_2]^\top$, $C_u = D_u = \hat{\mathbb{U}}$, $C_z = Q \times [0, N_0] \times [0, T_0]$, $D_z = Q \times [1, N_0] \times [0, T_0]$, *and* $\Psi := Q \times [0, N_0] \times [0, T_0]$. *Moreover, this HDS satisfies Assumptions 5 and 6.*

Remark 8 *The continuous differentiability of* V *in Propositions 1 and 3, can be relaxed to Lipschitz continuity by making use of generalized gradients and invariance principles for HDS, see [188] for further details.*

The verification of the assumptions in Proposition 3 is straightforward for *some* classes of learning dynamics, specially linear dynamics that arise when the response map J is quadratic. This is possible even if the parameters of the response map are unknown. In fact, conditions (2.19a) and (2.19b) simply ask for UGAS of $\mathcal{O}$ for each mode f_q, where $q \in Q_s$. Similarly, condition (2.19c) simply asks that solutions of the differential inclusions associated to the unstable modes $q \in Q_u$ have no finite escape times. Additionally, condition (2.19d) is easily satisfied if the Lyapunov functions are quadratic. In this case conservative estimates of the parameters λ_s, λ_u, and μ, can be used to design the parameters η_1 and η_2.

Learning Inclusions with Time-varying Parameters

In some learning and optimization problems the parameters associated to the system vary slowly in time. For example, this is the case when the amplitude of the dither signals decays in time, or when the response map J has slow-varying weakly-jumping parameters. This situation can be studied by taking Q as a compact but not necessarily finite set, and by allowing the flow dynamics in the HDS (2.14) to depend explicitly on the parameter q as $\dot{\hat{u}} \in f(\hat{u}, \nabla J(\hat{u}), q)$. The slow-varying weakly-jumping dynamics of q are modeled as

$$\dot{q} \in \eta_3 \mathbb{B}, \quad q^+ \in q + \eta_3 \mathbb{B}, \quad q \in Q, \quad \eta_3 \in \mathbb{R}_{>0}, \tag{2.20}$$

which replaces the q-dynamics in (2.14). For this scenario we assume that for each $q \in Q$ there exists an optimal compact set $\mathcal{O}_q \subset \hat{\mathbb{U}}$, and we use a simple average dwell-time automaton of the form (2.16) to eliminate purely discrete-time solutions. The following proposition is a direct consequence of [78, Corollary 7.27].

Proposition 4 *Let $\mathcal{O}_q \subset \hat{\mathbb{U}}$ satisfy Assumption 4 for each $q \in Q$. Suppose that for each $q \in Q$ the mapping f_q in (2.14a) satisfies item (c) in Assumption 5 with flow map given by $f(\hat{u}, \nabla J(\hat{u}), q)$, and q-dynamics given by (2.14). Suppose also that for each $q \in Q$ the dynamics $\dot{\hat{u}} \in f(\hat{u}, \nabla J(\hat{u}), q)$ render the set $\mathcal{O}_q$ UGAS. Then, this HDS combined with the dynamics (2.16) has the structure of (2.11) with $r = 2$, $\delta = \eta_3$, $z := [q, \tau_1]^\top$, $C_u = D_u = \hat{\mathbb{U}}$, $C_z = Q \times [0, N_0]$, $D_z := Q \times [1, N_0]$, $\mathcal{O} := \{(\hat{u}, q) : \hat{u} \in \mathcal{O}_q, q \in Q\}$, and $\Psi := Q \times [0, N_0]$. Moreover, this HDS satisfies Assumptions 5 and 6.*

Hybrid Systems for Learning on Smooth Manifolds

Since any smooth compact manifold without boundary is not contractible [189, Def. B.13. and Lemma 2.1.9], and since the basin of attraction of an asymptotically stable equilibrium point of any differential equation with a continuous right-hand side is contractible [189, Thm. 2.1.8], it is impossible to achieve global asymptotic stability of an equilibrium in compact manifolds without boundary using smooth feedback. A natural example where this situation emerges is in the solution of learning and optimization problems on manifolds like the unit circle $\mathbb{S}^1$. In fact, let $\hat{u} \in \mathbb{S}^1$ be a state evolving according to the dynamics

$$\dot{\hat{u}} = \alpha S \hat{u}, \quad \text{where} \quad S = \begin{bmatrix} 0 & -1 \\ 1 & 0 \end{bmatrix}, \tag{2.21}$$

which describes the evolution of a point $\hat{u}$ on the unit circle. Let $J : \mathbb{S}^1 \to [a, b]$ be a smooth and surjective function having exactly two critical points in $\mathbb{S}^1$, given by $\hat{u}^*$ and $\hat{u}'$, which satisfy the conditions

$$\langle \nabla J(\hat{u}^*), S\hat{u}^* \rangle = 0, \quad \langle \nabla J(\hat{u}'), S\hat{u}' \rangle = 0, \quad J(\hat{u}^*) = a, \quad J(\hat{u}') = b. \tag{2.22}$$

where $\langle \cdot, \cdot \rangle$ is the standard inner product. Then, by defining α in (2.21) as a feedback function of the form

$$\alpha := \kappa(\hat{u}) = -\langle \nabla J(\hat{u}), S\hat{u} \rangle, \tag{2.23}$$

it follows that

$$\dot{J} = \nabla J(\hat{u})^\top \dot{\hat{u}} = -\nabla J(\hat{u})^\top \left(\langle \nabla J(\hat{u}), S\hat{u} \rangle \right) S\hat{u} = -\langle \nabla J(\hat{u}), S\hat{u} \rangle^2 \leq 0, \ \forall \ \hat{u} \in \mathbb{S}^1,$$

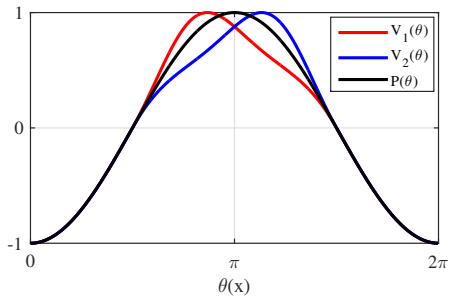

Figure 2.2: Objective function $J(\hat{u}) = -\hat{u}_1$, and skewed potentials $V_1(\theta_1), V_2(\theta_2)$ with the position $\hat{u} \in \mathbb{S}^1$ expressed as the angle $\theta(\hat{u}) \in [0, 2\pi)$.

and $\dot{J} = 0$ if and only if $\langle \nabla J(\hat{u}), S\hat{u} \rangle = 0$, which, by construction, can only happen at the critical points. Therefore, with α defined as in (2.23), we obtain that system (2.21) is a gradient descent system on $\mathbb{S}^1$ with respect to the function J, rendering *locally* asymptotically stable the point $\hat{u}^*$, with basin of attraction $\mathbb{S}^1 \backslash \{\hat{u}'\}$.

In order to be able to obtain a global asymptotic stability result instead of a local result, we can implement a hybrid learning mechanism that switches between two different potential functions generated from J by means of a couple of diffeomorphisms $\mathcal{T}_q : \mathbb{S}^1 \to \mathbb{S}^1$, $q \in \{1, 2\}$. These diffeomorphisms shift the points $\hat{u} \in \mathbb{S}^1$, except $\hat{u}^*$, such that when the potential function J is evaluated at the shifted points, we end up with two different potentials V_1 and V_2 with a common minimum point, but different peaks. Figure 2.2 illustrates this idea. Using these two potential functions, one can design a V_q-gradient-based descent mechanism that switches to the function V_q whenever the point $\hat{u}$ is too close to the maximizer of V_{3-q}. This idea can be implemented by means

of the hybrid learning dynamics

$$\left.\begin{aligned}\dot{\hat{u}} &= \kappa_{\mathcal{T}_q}(\hat{u})S\hat{u}\\ \dot{q} &= 0\end{aligned}\right\},\ (\hat{u},q)\in C_{u,q}:=\left\{(\hat{u},q)\in\mathbb{S}^1\times\{1,2\}:\min_{q\in\{1,2\}}V_q(\hat{u})-V_q(\hat{u})\geq-\delta\right\} \tag{2.24a}$$

$$\left.\begin{aligned}\hat{u}^+ &= \hat{u}\\ q^+ &\in Q(\hat{u},q)\end{aligned}\right\},\qquad (\hat{u},q)\in D_{u,q}:=\left\{(\hat{u},q)\in\mathbb{S}^1\times\{1,2\}:\min_{q\in\{1,2\}}V_q(\hat{u})-V_q(\hat{u})\leq-\delta\right\}, \tag{2.24b}$$

where the mapping $Q(\hat{u},q)$ is defined as

$$Q(\hat{u},q):=\left\{q\in\{1,2\}:V_q(\hat{u})=\min_{q\in\{1,2\}}V_q(\hat{u})\right\},$$

and the feedback law $\alpha=\kappa_{\mathcal{T}_q}(\cdot)$ is defined as

$$\kappa_{\mathcal{T}_q}(\hat{u})=\frac{\kappa(\mathcal{T}_q(\hat{u}))}{\ell_q(\hat{u})},\quad \ell_q(\hat{u}):=\begin{cases}1 & \text{if } J(\hat{u})\leq\gamma\\ 1+k_q(J(\hat{u})-\gamma)\langle\nabla J(\hat{u}),S\hat{u}\rangle, & \text{if } J(\hat{u})\geq\gamma\end{cases},$$

where the gain k_q must be selected sufficiently small, and the constant γ satisfies $\gamma\in[a,b)$ and it is assumed to be known, i.e., it is assumed that we know that the smallest value of J in $\mathbb{S}$ is smaller than γ, and its biggest value in $\mathbb{S}$ is bigger than γ. When the state $(\hat{u},q)$ is in the flow set $C_{u,q}$, the control dynamics guides the state to the minimum of the warped potential function $V_q(x)$. Because the warping process produces maximum separation between the values of the warped functions at their respective peaks, the jump set $D_{u,q}$ is designed to trigger jumps whenever the function in use has a significantly higher value than its counterpart. Continuity ensures that the jump set extends to a neighborhood around each peak, creating hysteresis

in switching that confers robustness. In fact, under an appropriate construction of the family of diffeomorphisms required by the learning dynamics (2.24), the closed-loop system guarantees robust UGAS of the point $\hat{u}^*$ that minimizes J, satisfying Assumption 5. In order to construct the family of diffeomorphisms required by the hybrid system (2.24), we define the mappings $\exp(\omega(\cdot))$ and $\Phi_{k_q}(\cdot)$ as

$$\exp(\omega S) := \begin{bmatrix} \cos(\omega), & -\sin(\omega) \\ \sin(\omega), & \cos(\omega) \end{bmatrix}, \tag{2.25}$$

$$\Phi_{k_q}(\hat{u}) := \begin{cases} I, & J(\hat{u}) \leq \gamma \\ \exp(0.5k_q(J(\hat{u}) - \gamma)S)^2, & J(\hat{u}) > \gamma. \end{cases} \tag{2.26}$$

Then, we define $\mathcal{T}_q : \mathbb{S}^1 \to \mathbb{S}^1$ as

$$\mathcal{T}_{k_q}(\hat{u}) := \Phi_{k_q}(\hat{u})\hat{u}. \tag{2.27}$$

If the parameter k_q satisfies the bound

$$|k_q| < \frac{1}{\max\{|\alpha'(J-\gamma)\langle \nabla J, S\hat{u}\rangle| : \hat{u} \in \mathbb{S}^1, J > \gamma\}}, \tag{2.28}$$

for all $q \in \{1, 2\}$, we have that (2.27) is a valid diffeomorphism that leaves unchanged the minimum point $\hat{u}^*$, see [190] for details. Then, it is easy to see that system (2.24) has the form of (2.14).

Hybrid Learning Dynamics for Non-Convex Optimization

In general, constrained optimization problems of the form 2.7 cannot be robustly solved by a standard gradient descent dynamical system of the form

$$\dot{\hat{u}} = -\nabla J(\hat{u}), \tag{2.29}$$

even when barrier functions are added to J to "push" the state away from the boundary of the feasible set. For instance, consider the scenario in $\mathbb{R}^2$ presented in Figure 2.3, where the state space has been divided in three sets $\mathcal{M}_1$, $\mathcal{M}_2$, and $\mathcal{K}$, and where the feasible set corresponds to $\mathbb{R}^2 \backslash \mathcal{N}$, being $\mathcal{N}$ an "obstacle" that needs to be avoided by the trajectories of the system. Consider an optimization algorithm given by a dynamical system with state $\tilde{z}$, dynamics $\dot{\tilde{z}} = f(\tilde{z})$, and initial condition $\tilde{z}(0) = z_0$, where $f(\cdot)$ is assumed to be locally bounded, and where it is assumed that for all $z_0 \in \mathbb{R}^2$ there exists at least one Carathéodory complete solution[2]. Due to the topological structure of the problem, there exists a boundary $\mathcal{M}$ such that for initial conditions on each side of $\mathcal{M}$, i.e., $\mathcal{M}_1$ and $\mathcal{M}_2$, the trajectories of the system approach the set $\mathcal{K}$ either from above the set $\mathcal{N}$ or from below. Because of this, it is possible to find arbitrarily small signals $e(t)$ acting on the states of the system (or on the vector field), such that some of the solutions of the dynamical system will remain in a neighborhood of the line $\mathcal{M}$, and will not converge to the set $\mathcal{K}$, where the minimizer of J is located. The following assumption and proposition, corresponding to [191, Assump 6.4 and Thm. 6.5], establish this fact.

Assumption 7 *There exists a $T > 0$ such that for each $\tilde{z}_0 \in \mathcal{M}$ and each $\rho > 0$ there exist points $\tilde{z}_1(0), \tilde{z}_2(0) \in \{\tilde{z}_0\} + \rho\mathbb{B}$, for which there exist (Carathéodory) solutions $\tilde{z}_1$*

[2] A Caratheodory solution to the system $\dot{\tilde{z}} = f(\tilde{z})$ on an interval $I \subset \mathbb{R}_{\geq 0}$ is an absolutely continuous function $\tilde{z} : I \to \mathbb{R}^n$ that satisfies $\dot{\tilde{z}}(t) = f(\tilde{z}(t))$ almost everywhere on I. A Carathéodory solution is complete if $I = [0, \infty)$.

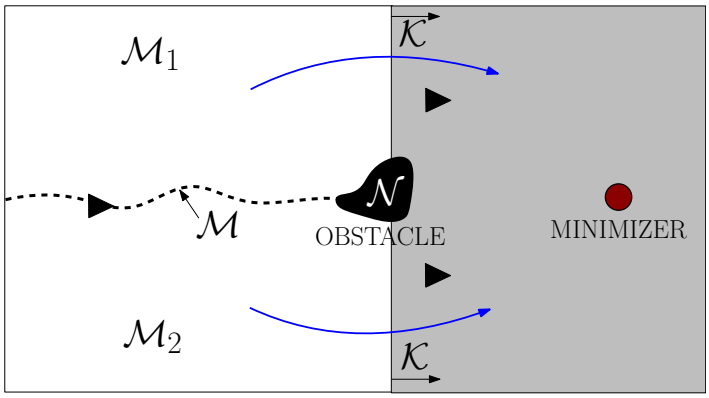

Figure 2.3: Feasible set, obstacle $\mathcal{N}$, and minimizer of J.

and $\tilde{z}_2$*, respectively, satisfying* $\tilde{z}_1(t) \in \mathcal{M}_1 \backslash \mathcal{M}$ *and* $\tilde{z}_2(t) \in \mathcal{M}_2 \backslash \mathcal{M}$ *for all* $t \in [0, T]$. □

Proposition 5 *[191, Thm 6.5] Suppose that Assumption 7 holds. Then for every positive constants* ε, ρ', ρ'', *and every* $\tilde{z}_0 \in \mathcal{M} + \varepsilon\mathbb{B}$ *such that* $\tilde{z}_0 + \rho'\mathbb{B} \subset \mathbb{R}^2 \backslash \mathcal{N}$ *and* $\tilde{z}_0 + \rho''\mathbb{B} \subset (\mathcal{M}_1 \cup \mathcal{M}_2)$ *there exist a piecewise constant function* $e : dom(e) \to \varepsilon\mathbb{B}$ *and a (Carathéodory) solution* $z : dom(z) \to \mathbb{R}^2 \backslash \mathcal{N}$ *to* $\dot{\tilde{z}} = f(\tilde{z} + e(t))$ *such that* $\tilde{z}(t) \in (\mathcal{M} + \varepsilon\mathbb{B}) \cap (\mathcal{M}_1 \cup \mathcal{M}_2) \cap (z_0 + \rho'\mathbb{B})$ *for all* $t \in [0, T')$ *for some* $T' \in (T^*, \infty]$, *where* $dom\, \tilde{z} = dom\, \tilde{e}$, $T^* = \min\{\rho', \rho''\} m^{-1}$, *and* $m = \sup\{1 + |f(\eta)| : \eta \in z_0 + \max\{\rho', \rho''\}\mathbb{B}\}$.

In order to avoid that the stability properties of the optimization dynamics are lost under arbitrarily small adversarial signals $e(t)$ acting on (2.29), we can instead implement a hybrid gradient mechanism. Following the ideas of [192], we can divided the feasible set in two parts. The division is indexed by a logic state $q \in \{1, 2\}$, which generates two different partitions for the control system. The resulting dynamical system is a switched system based on a *mode-dependent localization function* J_q defined as

$$J_q(\hat{u}) := -J(\hat{u}) + B\left(d_q(\hat{u})\right), \tag{2.30}$$

where $d_q(\hat{u}) = \left|\hat{u}\right|^2_{\mathbb{R}^2 \backslash \mathcal{O}_q}$. The function $|\cdot|^2_{\mathbb{R}^2 \backslash \mathcal{O}_q}$ maps a position $\hat{u} \in \mathbb{R}^2$ to the squared valued of its distance to the set $\mathbb{R}^2 \backslash \mathcal{O}_q$, and $B(\cdot)$ is a barrier function defined as follows

$$B(z) = \begin{cases} (z-\rho)^2 \log\left(\frac{1}{z}\right), & \text{if } z \in [0,\rho] \\ 0, & \text{if } z > \rho, \end{cases} \tag{2.31}$$

with $\rho \in (0,1]$ being a tunable parameter to be selected sufficiently small. The sets $\mathcal{O}_1$ and $\mathcal{O}_2$ are constructed as shown in Figures 2.4 and 2.5. Namely, we construct a box centered around the obstacle $\mathcal{N}$, with tunable height h, and we project the adjacent sides of the box to divide the space in two parts. Note that $\mathcal{O}_1 \cup \mathcal{O}_2$ covers $\mathbb{R}^2$ except for the box that includes the obstacle. Also, note that under this construction the function (2.30) is smooth for each q.

To define the flow and jump sets, let $\mu > 1$, and $\lambda \in (0, \mu-1)$. Using the localization function J_q (2.30), we define the sets

$$C_{u,q} := \left\{(\hat{u}, q) \in \mathbb{R}^2 \times \{1,2\} : J_q(\hat{u}) \leq \mu J_{3-q}(\hat{u})\right\}, \tag{2.32a}$$

$$D_{u,q} := \left\{(\hat{u}, q) \in \mathbb{R}^2 \times \{1,2\} : J_q(\hat{u}) \geq (\mu-\lambda) J_{3-q}(\hat{u})\right\}. \tag{2.32b}$$

The blue line and blue arrows in Figures 2.4 and 2.5 indicate the points in $\mathcal{O}_q$ that also belong to the flow set $C_{u,q}$, while the red line and the red arrows indicate the points in $\mathcal{O}_q$ that also belong to the jump set $D_{u,q}$. Note that since $(\mu - \lambda) > 1$ the sets $C_{u,q}$ and $D_{u,q}$ always overlap. The switching rule for q is then given by the mapping

$$q^+ = Q(q) := 3 - q, \qquad (\hat{u}, q) \in D_{u,q}, \tag{2.33}$$

and the learning dynamics of $\hat{u}$ are given by,

$$\dot{\hat{u}} = -\nabla J_q(\hat{u}), \qquad (\hat{u}, q) \in C_{u,q}, \tag{2.34}$$

By [192, Thm. 4.4], this hybrid learning mechanism guarantees robust global conver-

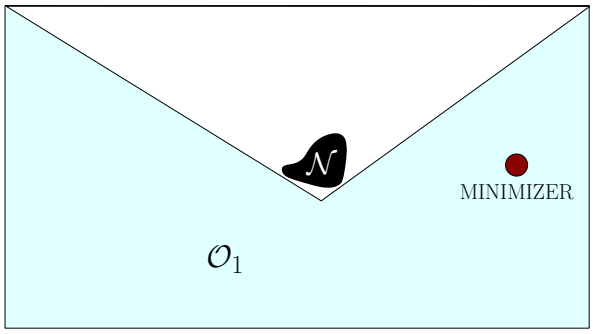

Figure 2.4: Partition of the feasible set, corresponding to $q = 1$.

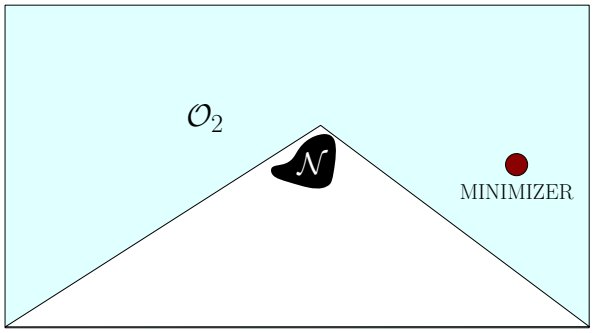

Figure 2.5: Partition of the feasible set, corresponding to $q = 2$.

gence to the minimizer of J, provided J_q is continuously differentiable on $\mathcal{O}_q$, positive definite with respect to the minimizer u^*, and radially unbounded in $\mathcal{O}_q$. Therefore, the learning dynamics (2.33)-(2.34) satisfy Assumption 5.

2.1.5 Numerical Examples of Averaging-Based HESC

We now present some numerical examples illustrating the application of the hybrid extremum seeking controllers described in the previous section.

"Finite-time"-constant rate ESC

Consider a simple SISO system with internal dynamics given by (2.3) in Example 1, with $\epsilon = 0.1$, $B = K = M = 1$, and output function given by $\varphi := -(\theta_2 - 5)^2$. This plant generates a response map given by $J = -(u_2 - 5)^2$. For this system consider an

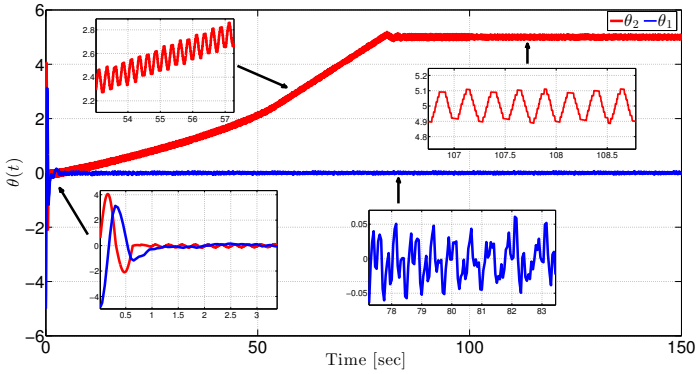

Figure 2.6: Evolution of θ using discontinuous ESC.

unconstrained HESC of the form (2.12), with learning dynamics (2.11) given by

$$\dot{\hat{u}} \in \hat{F}(\xi) := \begin{cases} k & \text{if } \xi > 0 \\ [-k, k] & \text{if } \xi = 0 \\ -k & \text{if } \xi < 0, \end{cases} \tag{2.35}$$

which corresponds to the Krasovskii regularization (2.2) of the discontinuous system $\dot{\hat{u}} = k \operatorname{sgn}(\xi)$. In this case we select $\lambda_\theta = \lambda_\xi = 50$. It is easy to see that this dynamics satisfy Assumption 5 with $r = 0$, $D_u = C_z = D_z = \emptyset$, and $C_u = \mathbb{R}^n$. Moreover, it was shown in [193, Proposition 7] that this learning dynamics satisfy Assumption 6 for the given type of J. Figures 2.6 and 2.7 show the evolution in time of the states θ and $\hat{u}$ converging to a neighborhood of the optimal operation point $\hat{u}^* = 5$. It is worth noting that in this case the notion of "finite-time" convergence is redundant, since the definition of practical asymptotic stability is *per se* a notion of finite-time stability. Nevertheless, it can be seen that the trajectories of $\hat{u}$ approximately inherit the constant evolution rate of the original discontinuous learning dynamics (2.35). The parameters in (2.12) are selected as $k = 0.1$, $a = 0.1$, $\omega_L = 0.5$, and $\omega = 25$.

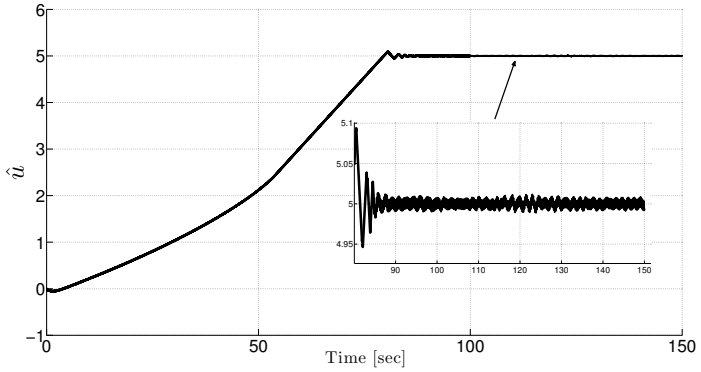

Figure 2.7: Evolution of $\hat{u}$.

ESC for Non-Strictly Contractive Games

Consider a MAS with 3 agents having simple first-order linear dynamics given by $\epsilon\dot{\theta}_i = -\theta_i + u_i$, with $\epsilon = 0.1$ for all $i \in \{1, 2, 3\}$, aiming to maximize their individual output functions given by $\varphi_1 = \theta_1(-\theta_2 + \theta_3)$, $\varphi_2 = \theta_2(-\theta_1+\theta_3)$, $\varphi_3 = \theta_3(-\theta_1 + \theta_2)$, subject to the constraint that their actions belong to an $O(a)$-inflation of the compact set $\hat{\mathbb{U}} := \{u \in \mathbb{R}^n_{\geq 0}, u^\top \mathbf{1} = 1\}$ for *all* time. The output functions φ_i are available only by measurements. This problem corresponds to the one discussed in Remarks 2, 5, and 6, and it can be characterized based on the vector of partial derivatives of the response maps J_i as a contractive (also called stable) anti-potential rock-paper-scissors game [183, Chapter 3], with unique Nash equilibrium given by $u^* = [1/3,\ 1/3,\ 1/3]^\top$. Since the game characterized by the vector $[\frac{\partial J_1}{\partial u_1}, \frac{\partial J_2}{\partial u_2}, \frac{\partial J_3}{\partial u_3}]^\top$ is not *strictly* contractive [183, Def. 3.3.1], existing gradient-based ESCs, such as those in [101], cannot guarantee convergence to u^* subject to the constraints of $\hat{\mathbb{U}}$. To solve this Nash seeking problem consider a HESC of the form (2.12), with $D_u = D_z = C_z = \emptyset$, $C_u = \hat{\mathbb{U}}$, and set-valued learning dynamics given by

$$\dot{\hat{u}} \in -\hat{u} + \left\{ w \in C_u : w^\top \xi = \min_{\hat{u} \in C_u} \hat{u}^\top \xi \right\}, \tag{2.36}$$

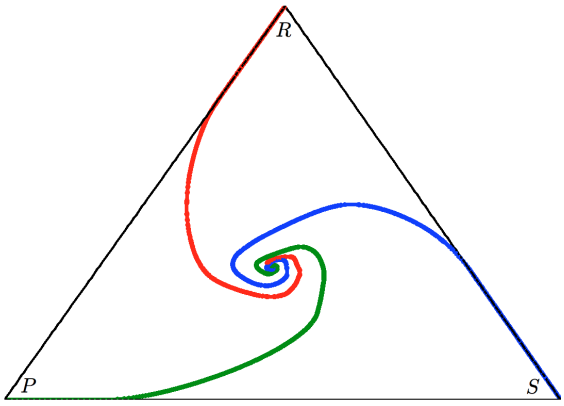

Figure 2.8: Three different solutions of the Best-response ESC from different initial conditions on the vertices of C_u.

which correspond to the well-known *best response dynamics* [183]. Since C_u is nonempty, convex, and compact, the set-valued mapping (2.36) is LB, OSC, and convex for each $(\hat{u}, \xi) \in C_u \times \mathbb{R}^n$, satisfying Assumption 5. Moreover, using the Lyapunov function $V(\hat{u}) = \max_{i\in\{1,2,3\}} \xi_i - \hat{u}^\top \xi$ it was shown in [183, Theorem 7.2.7], that if $\xi = [\frac{\partial J_1}{\partial u_1}, \frac{\partial J_2}{\partial u_2}, \frac{\partial J_3}{\partial u_3}]^\top$, this dynamics render the point u^* UGAS in C_u, thus satisfying Assumption 6. Figure 2.8 shows the evolution of three different trajectories of the state $\hat{u}$ generated by system (2.12), evolving on C_u, with initial conditions located in each of the three vertices of the simplex, and converging to a neighborhood of u^*. The parameters were selected as $k = 5 \times 10^{-4}$, $a = 0.1$, $\omega_L = 0.5$, $\omega = 25$. In this case it was used $\lambda_\theta = \lambda_\xi := 250$.

Nash Seeking with Adversarial Agents

Consider two switched linear dynamical systems of the form (2.5), with states $\theta_1 := [\theta_{1,1}, \theta_{1,2}]^\top$, $\theta_2 := [\theta_{2,1}, \theta_{2,2}]^\top$, and individual inputs $[u_1, u_2] \in \mathbb{R}^2$. Each agent i seeks to maximize its individual output $y_i = \varphi_i(\theta_{1,1}, \theta_{2,1})$ at steady-state, for all $i \in \{1, 2\}$, by controlling its own individual action u_i, using only measurements of y_i. Since the action of each agent affects the payoff function of the other agent, this

problem describes a standard noncooperative game. The output functions of the players are given by $\varphi_i = [\theta_{1,1}, \theta_{2,1}]Q_i[\theta_{1,1}, \theta_{2,1}]^\top + [\theta_{1,1}, \theta_{2,1}]B_i + C_i$, with $C_1 := 600$, $C_2 := 0$, and matrices $Q_1 := [-1,\ 0.5; 0.5, 0]$, $Q_2 := [0, 0.5; 0.5, -1]$, $B_1 := [50, -30]^\top$, $B_2 := [-30, 30]^\top$, which correspond to the quadratic cost functions presented in the duopoly market example considered in [105, Section 2]. At steady state the switching plant (2.5) generates the condition $\theta_{i,1} = u_i$, such that the response maps are described by quadratic payoffs with unique Nash equilibrium $u^* = [130/3, 110/3]^\top$. To achieve convergence to a neighborhood of u^* each player implements a Nash seeking scheme, similar as the one considered in [105], where the learning dynamics (2.11) are given by $\dot{\hat{u}}_i = q_i \frac{\partial J_i(\hat{u})}{\partial \hat{u}_i}$, which for the case that $q_i = 1$ guarantees global convergence to u^* under strict concavity-convexity assumptions on J_i [194, Theorem 9]. However, we assume that during the learning process each player can also behave in an adversarial unstable way with $q_i = -1$, where this adversarial behavior may emerge either by an individual decision, or induced by an external action, jamming signal, or hardware failure. Then, the behavior of each player is modeled by a state $q_i \in \{-1, 1\}$, where $q_i = -1$ (resp. $q_i = 1$) corresponds to the player i being (resp. not being) adversarial, for $i \in \{1, 2\}$. Since q_i is an individual decision state, its update rule is modeled by the difference inclusion $q_i^+ \in \{-1, 1\}$, for all $i \in \{1, 2\}$. Therefore, the hybrid learning dynamics have the form of (2.14), with continuous map $f_q := \left[q_1 \frac{\partial J_1(\hat{u})}{\partial \hat{u}_1}, q_2 \frac{\partial J_2(\hat{u})}{\partial \hat{u}_2}\right]^\top$, and sets $\hat{\mathbb{U}} = \mathbb{R}^2$, and $Q = \bigcup_{i=1}^4 M_i$, where $M_1 := \{1\}^2$ (no adversarial players); $M_2 := \{-1\} \times \{1\}$ (player 1 adversarial); $M_3 := \{1\} \times \{-1\}$ (player 2 adversarial); $M_4 := \{-1\}^2$ (both players adversarial). To guarantee convergence to u^* we rely on a HESC of the form (2.12), and Proposition 3, where a dwell-time automaton and a time-ratio monitor are used to bound the frequency and the activation time of the adversarial modes $Q_u := M_2 \cup M_3 \cup M_4$, guaranteeing a good behavior of the system via the stable mode $Q_s := M_1$. The conditions of Proposition 3 can be easily verified by defining $\tilde{u} = \hat{u} - \hat{u}^*$,

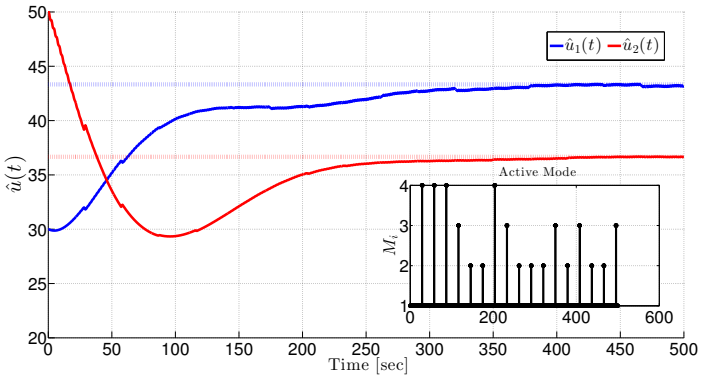

Figure 2.9: Trajectories of $\hat{u}$, and active modes.

and considering the Lyapunov function $V = \tilde{u}^\top A \tilde{u}$, with matrix $A = [1, -0.5; -0.5, 1]$, which satisfies (2.19a) with $\alpha_1(s) = \frac{1}{2}s^2$, and $\alpha_2(s) = \frac{3}{2}s^2$. Condition (2.19b) is satisfied for all $\lambda_s \in (0, \frac{2}{3}]$, condition (2.19b) is satisfied with $\lambda_u = 18$, and condition (2.19d) is satisfied with $\mu = 1$. Then, Proposition 3 is satisfied with $\eta_1 = 1$ and $\eta_2 = 0.03$. Figure 2.9 shows a simulation of $\hat{u}$, converging to the Nash equilibrium u^*. We used $T_0 = N_0 = 1$ and simulated a solution that during mode 1 (no adversarial actions) evolves at constant rate $\dot{\eta}_2 = \dot{\eta}_1 = 0.03$ until τ_1 and τ_2 hit 1, time at which a jamming mode, selected randomly, turns active, and the timer τ_1 is reset to 0. During a jamming mode the states (τ_1, τ_2) flow with the dynamics $\dot{\tau}_2 = -0.97$ and $\dot{\tau}_1 = 0.97$, until τ_1 hits 1 and τ_2 hits 0, time at which τ_1 is reset to zero and mode 1 turns active again. The internal linear switched dynamics (2.5) switch periodically every 0.1 seconds. The inset shows which of the modes M_i is active at every time. Figure 2.10, on the other hand, shows the behavior generated by selecting the parameter $\eta_2 = 0.6$, violating the conditions of Proposition 3, and using only M_4 as adversarial mode. In this case, by not constraining enough the time that players can be adversarial, instability in the system emerges. The other parameters are selected as $a = 0.2$, $k = 1.5$, $\omega_L = 0.03$, $\omega_1 = 3.4$, $\omega_2 = 3$.

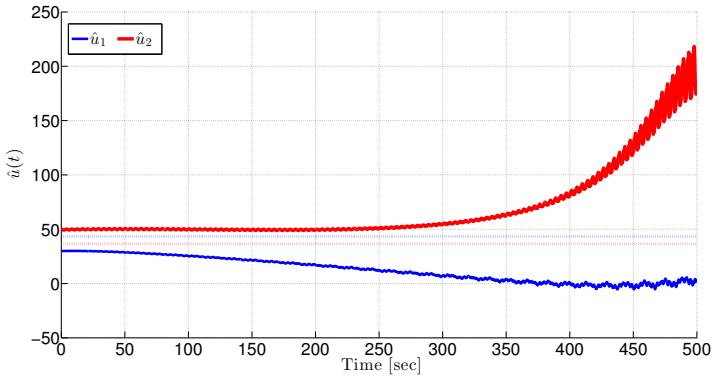

Figure 2.10: Instability generated by persistent adversarial actions.

Real-Time Optimization on the Unit Circle $\mathbb{S}^1$

Consider the $\mathcal{C}^1$ function $J : \mathbb{R}^2 \to \mathbb{R}$, defined as

$$J(\hat{u}) = -\hat{u}_1, \tag{2.37}$$

where $\hat{u} := [\hat{u}_1, \hat{u}_2]^\top$. Restricted to $\mathbb{S}^1$, this function is surjective, and its critical points in $\mathbb{S}^1$ occur at $\hat{u}^* = [1, 0]$ and $\hat{u}' = [-1, 0]$. In order to minimize J in $\mathbb{S}^1$ we make use of the learning dynamics presented in Section 2.1.4. A couple of valid picewise diffeomorphisms for this function can be obtained by selecting $\alpha^* = t^2$, $\gamma^* = 0$, $k_1 = -k_2 = 0.5$. Fig. 2.11 shows the implementation of the HESC using the hybrid learning dynamics 2.24. The amplitude of the dither is selected as $a = 0.01$, which induces small excursions in a neighborhood of $\mathbb{S}^1$. We also used $\omega_L = 1$, and $\omega = 40$. Note that the hybrid extremum seeker emulates the behavior of the nominal hybrid system, this time obtaining convergence to a neighborhood of $\hat{u}^*$.

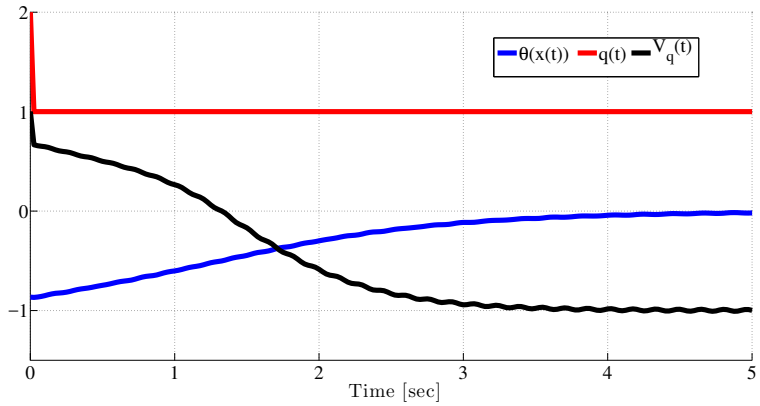

Figure 2.11: Global optimization on $\mathbb{S}^1$ using HESC.

Robust Source Seeking with Obstacle Avoidance

Consider a group of 6 autonomous vehicles aiming to locate the source of a signal J while simultaneously they achieve a particular formation. We assume that only one of the vehicles, termed the leader vehicle, can sense the intensity of the signal J, which is maximal at the location of the source. Agents should also avoid a small obstacle located at the point $[1, 0]^\top$. For the purpose of simulation we assume that this signal has a quadratic form $J = \frac{1}{2}(x_1 - 3)^2 + \frac{1}{2}y_1^2$. We emulate the situation where the 6 vehicles are initially located at the entrance of a room, and where the source of the signal J is only know to be located at the other side of the room, with the obstacle $\mathcal{N}$ located between the entrance of the room and the source of the signal J. The dynamics of the vehicles are assumed to be of the form

$$\dot{\hat{u}}_{x,i} = v_{x,i} \tag{2.38a}$$

$$\dot{\hat{u}}_{y,i} = v_{y,i} \tag{2.38b}$$

where $\hat{u}_{x,i}$ and $\hat{u}_{y,i}$ are the positions in the x-coordinate and y-coordinate, respectively, of the i^{th} vehicle. Without loss of generality we assume that the leader vehicle is characterized by the index $i = 1$. The other vehicles, characterized by the indices

$i \in \{2,3,4,5,6\}$, are followers that can sense only the position of the leader vehicle and the position of neighboring vehicles defined in terms of a communication graph $\mathcal{G}$.

In order to achieve robust source seeking with obstacle avoidance, the leader vehicle can implement a HESC with learning dynamics given by (2.32)-(2.34), which implement a switched learning mechanism based on the localization function (2.30). Nevertheless, since the dynamics of the position of the vehicles are given by (2.38), and it is possible to control only the velocities $v_{x,i}$ and $v_{y,i}$, we cannot directly implement the switched gradient descent dynamics (2.34). Therefore, inspired by the ideas of [195], we consider a modified HESC where the velocities $v_{x,1}$ and $v_{y,2}$ of the leader are defined as

$$v_{x,1} = a\omega\mu_2 - k\xi_x \tag{2.39a}$$

$$v_{y,2} = -aw\mu_1 - k\xi_y, \tag{2.39b}$$

and where the signals $\mu(t) = [\mu_1(t), \mu_2(t)]^\top$ are generated by the oscillator $\dot{\mu}_1 = \omega\mu_2$, $\dot{\mu}_2 = -\omega\mu_1$, with $\mu(0)$ constrained to $\mathbb{S}^1$. The signals ξ_x and ξ_y are generated by the dynamics

$$\dot{\xi}_x = -\bar{\omega}(\xi_x - 2a^{-1}J_q(\hat{u}_1)\mu_1) \tag{2.40a}$$

$$\dot{\xi}_y = -\bar{\omega}(\xi_y - 2a^{-1}J_q(\hat{u}_1)\mu_2). \tag{2.40b}$$

Using the change of variables $\tilde{u}_{x,1} = \hat{u}_{x,1} - a\mu_1$ and $\tilde{u}_{y,1} = \hat{u}_{y,1} - a\mu_2$, it can be shown (see [196] for details) that the feedback law (2.39) applied to (2.38) generates dynamics of the form

$$\dot{\tilde{u}}_{x,i} = k\xi_x, \tag{2.41a}$$

$$\dot{\tilde{u}}_{y,i} = k\xi_y \tag{2.41b}$$

and

$$\dot{\xi}_x = -\bar{\omega}(\xi_x - 2a^{-1}J_q(\tilde{u}_1 + a\mu_1)\mu_1) \tag{2.42a}$$

$$\dot{\xi}_y = -\bar{\omega}(\xi_y - 2a^{-1}J_q(\tilde{u}_1 + a\mu_2)\mu_2), \tag{2.42b}$$

which have the form of (2.12b). To control the position of the followers we consider cooperative feedback laws of the form

$$v_{x,i} = -\beta \sum_{j\mathcal{N}_i} (\hat{u}_{x,i} - \hat{u}_{x,j} - \hat{u}^f_{x,i} + \hat{u}^f_{x,j}) \tag{2.43}$$

$$v_{y,i} = -\beta \sum_{j\mathcal{N}_i} (\hat{u}_{y,i} - \hat{u}_{y,j} - \hat{u}^f_{y,i} + \hat{u}^f_{y,j}), \tag{2.44}$$

where $\beta > 0$ is a tunable parameter. Assuming that the leader vehicle is a globally reachable node for the communication graph $\mathcal{G}$ with fixed position $(\hat{u}_{1,x}, \hat{u}_{1,y})$, if the followers implement the feedback law (2.43), their positions will converge to the point $p^*_x = \hat{u}^f_x + \mathbf{1}_N(\hat{u}_{1,x}(0) - \hat{u}^f)$, $p^*_y = \hat{u}^f_y + \mathbf{1}_N(\hat{u}_1(0) - \hat{u}^f_1)$. Thus, as long as the leader moves sufficiently slow compared to the followers, the formation will be maintained. The parameters of the controller are selected as $h = 0.5$, $\rho = 0.4$, $\lambda = 0.09$, $\mu = 1.1$, $a = 0.01$, $\bar{\omega} = 1$, $k = 1$, and $\beta = 4$. The desired formation is characterized by the pairs $(\hat{u}_{x,i}, \hat{u}_{y,i})$ in set $\Xi = \{(-2, 0.5), (-2, -0.5), (-1.13, 0), (0, 0), (-2.86, 1), (-1.13, -1)\}$, which assigns translationally invariant coordinates to the vehicles, fixing a formation. Using the hybrid extremum seeking control we obtain Figure 2.12 which shows the position of the vehicles at 7 different time instants, over the virtual level sets of J_q, for $q \in \{1, 2\}$. After approximately 5 seconds the follower agents have achieved the desired formation behind the leader agent (represented by the black dot). The leader implements the hybrid feedback law using $q(0) = 2$, and at approximately 9 seconds the leader enters the jump set and updates its logic state as $q^+ = 1$, flowing now -on

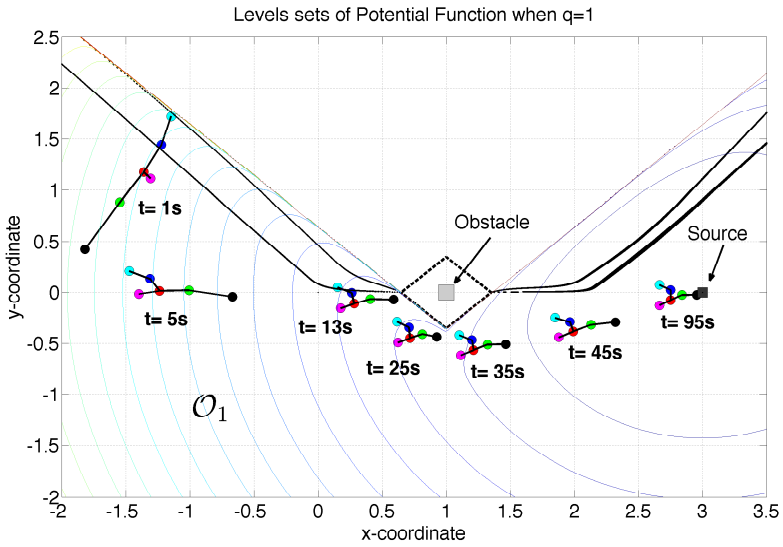

Figure 2.12: Evolution of the vehicles over the level sets of J_1.

average- over the level sets shown in Figure 2.12, until convergence to the source of the signal is achieved. Since the box around the obstacle is constructed sufficiently large compared to the size of the formation, the followers also avoid the obstacle by achieving the formation around the leader in a faster time scale and by maintaining the required formation while the leader slowly moves toward the unknown source of the signal.

Distributed Optimization of HVAC Systems with Switching Communication Graphs

Consider a multi-agent networked system characterizing an electricity market where 5 users share information and control their own individual loads in order to cooperatively optimize the energy consumption of the network. This problem is similar to the one considered in [197, Section VII]. However, in contrast to the results of [197, Section VII], we consider the case where the communication graph of the network is not time invariant, but rather characterized by a time-varying undirected graph $\mathcal{G}(t)$ that can

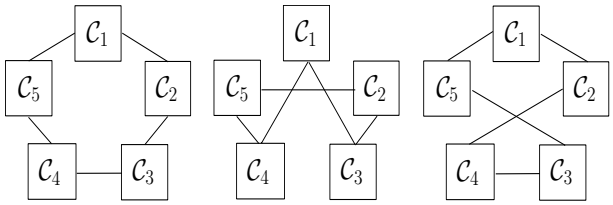

Figure 2.13: Three communication graphs for the users of the network.

take any of the three configurations shown in Figure 2.13. For simplicity, we consider that the users have no internal physical dynamics, such that the response maps J_i are static maps defined as

$$J_i(u_i) := \rho_i(u_{ii} - \bar{u}_{ii})^2 + u_i \left(\frac{1}{2} \left(\sum_{j=1}^{n} u_{ij} - 640 \right) + 10 \right), \tag{2.45}$$

which is accessible only to the i^{th} agent via measurements, and where the parameters $\bar{u}_{ii}$ are defined as $\bar{u} := [120, 140, 160, 180, 200]^\top$, and $\rho := [5.2,\ 5.4,\ 5.6,\ 5.8,\ 6]^\top$. We refer the reader to [198] for a justification of the structure and parameter values of the cost functions (2.45). By using the communication graph $\mathcal{G}_{\mathcal{C}}(t)$, and measuring their individual cost function (2.45), the agents aim to cooperatively find the optimal energy consumption $u^* \in \mathbb{R}^n$ that minimizes the social cost $J = \sum_{i=1}^{N} J_i$, i.e., agents aim to agree in a common optimal point u^* such that $u_i^* = u_{1i} = u_{2i} = \ldots = u_{Ni}$, for all $i \in \{1, \ldots, n\}$. If one had knowledge of the mathematical form of (2.45) one has that the theoretical optimal solution to this problem is

$$u^* = [82.23,\ 103.63,\ 124.93,\ 146.14,\ 167.27]^\top.$$

However, in order to converge to u^* in a model-free way, we consider a HESC of the

form (2.12), where the learning dynamics of the i^{th} agent are defined as

$$\dot{\hat{u}} \in \hat{F}_{\delta,i}(\hat{u}, \xi_i) := \frac{1}{\delta} \cdot \sum_{j \in \mathcal{N}_{\mathcal{C},i}(t)} \overline{\text{sign}}(\hat{u}_j - \hat{u}_i) - \gamma \cdot \nabla J_i(\hat{u}), \tag{2.46}$$

which is based on the optimization dynamics presented in [199], and where $\overline{\text{sign}} : \mathbb{R}^n \rightrightarrows \mathbb{R}^n$ maps each entry $z_i \in \mathbb{R}$ of a vector $z \in \mathbb{R}^n$ to a set $\overline{\text{sign}}(z_i) \subset \mathbb{R}$ defined as

$$\overline{\text{sign}}(z_i) := \begin{cases} \{1\}, & \text{if } \ z_i > 0 \\ [-1, 1], & \text{if } \ z_i = 0 \\ \{-1\}, & \text{if } \ z_i < 0 \end{cases}, \tag{2.47}$$

which again corresponds to the Krasovskii regularization of the standard scalar function $\text{sign}(\cdot)$. To analyze the learning dynamics (2.46) under time-varying graphs, we denote by $Q = \{1, 2, \ldots, \bar{q}\}$ the set of indices characterizing every possible connected and undirected communication graph realizable with n nodes, and by $c : \mathbb{R}_{\geq 0} \to Q$ as the switching signal that characterizes the current configuration of the graph. Then, the solutions of (2.46) are also solutions of the time-invariant differential inclusion

$$\dot{\hat{u}} \in \hat{F}_\delta(\hat{u}, \xi) := \overline{\text{co}} \bigcup_{c \in Q} \hat{F}^c_\delta(\hat{u}, \xi), \quad \hat{u} \in \mathbb{R}^{nN}, \tag{2.48}$$

where $\hat{F}^c_\delta := \hat{F}^c_{\delta,1} \times \ldots \times \hat{F}^c_{\delta,N}$, $\hat{u} = [\hat{u}_1, \ldots, \hat{u}_N]^\top$, and $\xi := [\xi_1, \ldots, \xi_N]^\top$. Since, by [199, Thm. 1], for $\delta > 0$ sufficiently small there exists a common Lyapunov function for the switched system (2.46), this Lyapunov function is also valid for system (2.48), thus establishing UGAS for the dynamics (2.48) and (2.46) [200]. Hence, Assumption 5 is satisfied.

Figures 2.14-2.19 show the evolution in time of each component j of the state $\hat{u}_{ij}$ of each agent i, where it can be seen that the estimate of each agent of the optimal

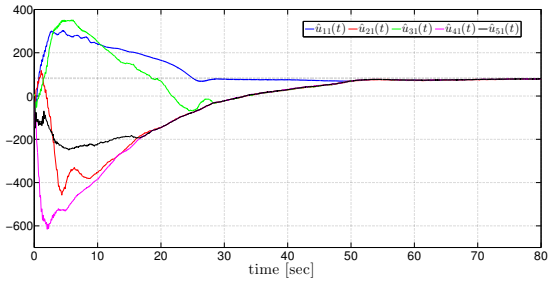

Figure 2.14: Evolution in time of $\hat{u}_1$ for each agent $i \in \mathcal{V}$.

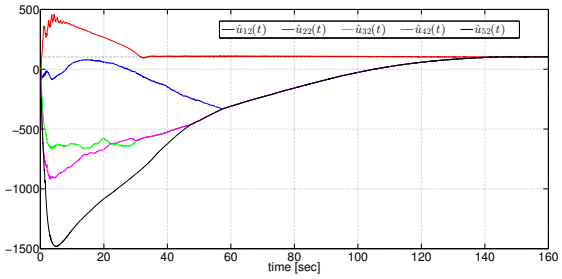

Figure 2.15: Evolution in time of $\hat{u}_2$ for each agent $i \in \mathcal{V}$.

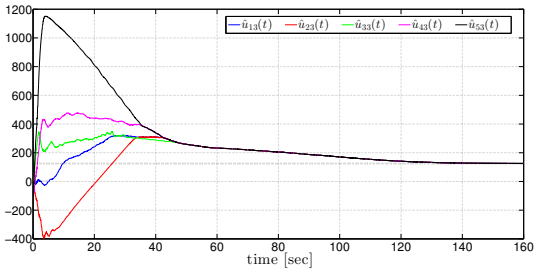

Figure 2.16: Evolution in time of $\hat{u}_3$ for each agent $i \in \mathcal{V}$.

value of u_i^* converges to a neighborhood of u_i^*. For this simulation the parameters used were $a = 0.2$, $\omega = [30, 25, 35, 40, 37.5]^\top$, $\omega_L = 1$, $\delta = 0.1$, $\gamma = 0.1$, and $k = 1.2$. The communication graph of the control system switches every 0.1 seconds between the three configurations shown in Figure 2.13.

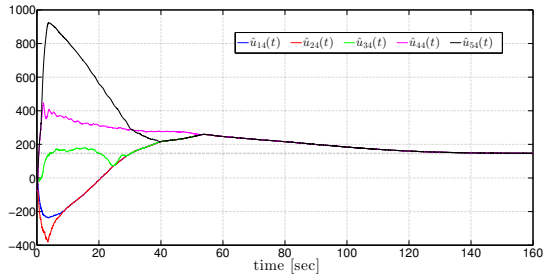

Figure 2.17: Evolution in time of $\hat{u}_4$ for each agent $i \in \mathcal{V}$.

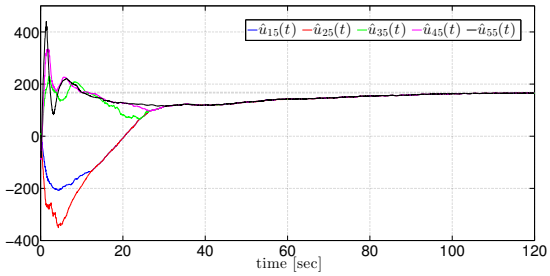

Figure 2.18: Evolution in time of $\hat{u}_5$ for each agent $i \in \mathcal{V}$.

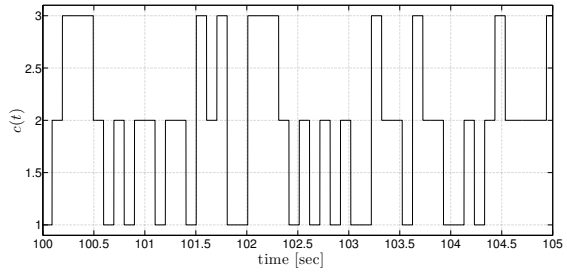

Figure 2.19: Evolution in time of the switching signal associated to the configuration of the communication graph.

2.2 Averaging-Based Hybrid Extremum Seeking for Hybrid Inclusions

Having established a ES framework for plants modeled as differential inclusions, we proceed to extend the results for the case when the plant is characterized by a hybrid system. In order to address this type of plants we rely on the results presented

in Appendix D, which allow us to consider singularly perturbed HDS with hybrid boundary layer dynamics.

2.2.1 Model of the Plant

We consider now a nonlinear hybrid plant with input $u \in \mathbb{R}^n$, output $y_\theta \in \mathbb{R}^m$, state $\theta \in \mathbb{R}^p$, dynamics of the form

$$\dot{\theta} \in F_\theta(\theta, u), \qquad \theta \in \Psi_{C,\theta}(u), \tag{2.49a}$$

$$\theta^+ \in G_\theta(\theta, u), \qquad \theta \in \Psi_{D,\theta}(u), \tag{2.49b}$$

and output function given by

$$y_\theta = h_\theta(\theta, u). \tag{2.50}$$

The set-valued mappings $F_\theta : \mathbb{R}^p \times \mathbb{R}^n \rightrightarrows \mathbb{R}^p$, $\Psi_{C,\theta} : \mathbb{R}^n \rightrightarrows \mathbb{R}^p$, $G_\theta : \mathbb{R}^p \times \mathbb{R}^n \rightrightarrows \mathbb{R}^p$, and $\Psi_{D,\theta} : \mathbb{R}^n \rightrightarrows \mathbb{R}^p$ are assumed to be nonempty, OSC and LB. The mapping F_θ is also assumed to be convex valued. The input u is assumed to be constrained to evolve in the set $U = \hat{U} + c\mathbb{B}$, where $c \in \mathbb{R}_{>0}$, and $\hat{U} \subset \mathbb{R}^n$ is a nonempty closed set. For the purpose of generality, the output mapping $h_\theta : \mathbb{R}^p \times \mathbb{R}^n \to \mathbb{R}^m$ is assumed to be vector-valued, and we define the mapping $\Psi_\theta(u) := \Psi_{C,\theta}(u) \cup \Psi_{D,\theta}(u)$. Systems that can be modeled by a HDS of the form (2.49) include traffic light control systems [201], switched systems with arbitrarily fast switching signals, as well as switching signals satisfying dwell-time constraints [202], and plants internally stabilized by control systems such as PWM control [203], quantized control systems [204] and reset linear control systems [78].

For a plant of the form (2.49)-(2.50), we are again interested in using measurements of the output y_θ in order to control the input u, without any knowledge of the mathematical form of the dynamics (2.49) and the output function (2.50), and aiming

to *optimize* the *steady-state input-to-output* mapping $J(u)$, i.e., the *response map*. For the purpose of generality, it is assumed that this *response map* can be vector-valued, such that Pareto optimization problems and game-theoretic learning problems can be captured by individual cost functions associated to the entries of the vector $J(u)$.

Under the assumption that the plant (2.49)-(2.50) generates a well-defined response map $J : \mathbb{R}^n \to \mathbb{R}^m$ (formally established in Assumption 10 below), the extremum seeking problem is again characterized by problem (2.7), and we consider that Assumption (4) holds again.

2.2.2 Hybrid Extremum Seeking Controllers with Hybrid Dither Generators and Hybrid Filters

In order to solve problem (2.7) with hybrid plants of the form 2.49, we now consider a class of set-valued hybrid extremum seeking controllers comprised of three main hybrid dynamical systems: 1) A hybrid dynamic Jacobian-based optimizer, with state $\hat{x}$; 2) a hybrid dynamic Jacobian generator, with state ξ; and 3) a hybrid dynamic dither generator, with state μ. We describe as follows each of these blocks.

Hybrid Jacobian-Based Optimizer

This block corresponds to a hybrid dynamical system with flow map taking as input a matrix $y_\xi \in \mathbb{R}^{m\times n}$ corresponding to an estimation of the Jacobian matrix $DJ(u)$ associated to the response map $J(u)$. This dynamical system is designed a priori for the particular *type* of optimization problem (2.7), e.g., standard convex and non-convex optimization [90], Pareto-Optimum seeking [205], Nash seeking in non-cooperative [105] or population games [101], distributed optimization, etc. The state of the hybrid optimizer is given by $\hat{x} := [\hat{x}_1^\top, \hat{x}_2^\top]^\top \in \mathbb{R}^\ell$, where $\hat{x}_1 \in \mathbb{R}^n$ and $\hat{x}_2 \in \mathbb{R}^{n_2}$

are auxiliary states, and $\ell = n + n_2$. The hybrid dynamics of the optimizer are given by the equations

$$\dot{\hat{x}} \in k \cdot F_{\hat{x}}(\hat{x}, y_\xi, \delta), \quad \hat{x} \in \hat{C} := \hat{C}_{x_1} \times \hat{C}_{x_2}, \tag{2.51a}$$

$$\hat{x}^+ \in G_{\hat{x}}(\hat{x}, \delta), \quad \hat{x} \in \hat{D} := \hat{D}_{x_1} \times \hat{D}_{x_2}, \tag{2.51b}$$

where $k = \omega_L \cdot \sigma$, $\omega_L := \epsilon \cdot \bar{\omega}$, $(\epsilon, \bar{\omega}, \sigma) \in \mathbb{R}^3_{>0}$ are tunable gains, $F_{\hat{x}} : \mathbb{R}^\ell \times \mathbb{R}^{n \times m} \times \mathbb{R}_{>0} \rightrightarrows \mathbb{R}^\ell$ and $G_{\hat{x}} : \mathbb{R}^\ell \times \mathbb{R}_{>0} \rightrightarrows \mathbb{R}^\ell$, $\delta \in \mathbb{R}_{>0}$ is a tunable parameter, $\hat{C} \subset \mathbb{R}^\ell$, $\hat{D} \subset \mathbb{R}^\ell$, and $\hat{C}_{x_1}, \hat{D}_{x_1} \subset \mathbb{R}^n$. The output of system (2.51) is given by

$$y_{\hat{x}} = h_{\hat{x}}(\hat{x}), \tag{2.52}$$

where $h_{\hat{x}} : \mathbb{R}^\ell \to \mathbb{R}^n$ is continuous.

As in the previous section, the hybrid Jacobian-based optimizer is designed under the assumption that the input signal y_ξ satisfies $y_\xi = DJ(\hat{x}_1) + e$, where e is a small approximation error. Thus, system (2.51) is designed based on the HDS

$$\dot{\hat{x}} \in \hat{F}_{\hat{x}}(\hat{x}, DJ(\hat{x}_1) + e, \delta), \quad \hat{x} \in \hat{C}, \tag{2.53a}$$

$$\hat{x}^+ \in G_{\hat{x}}(\hat{x}, \delta), \quad \hat{x} \in \hat{D}, \tag{2.53b}$$

where $e(t)$ is a uniformly bounded signal. In particular, it is assumed that system (2.53) satisfies Assumptions 5 and 6.

Several examples of hybrid learning dynamics of this form were presented in the previous section.

Finally, the hybrid optimizer (2.51) is designed such that the jumps generated by the dynamics (2.51b) do not change the values of the other states of the system. That

is, whenever $\hat{x}$ jumps according to (2.51b), the states ξ, μ, and θ are updated as $\xi^+ = \xi$, $\mu^+ = \mu$, $\theta^+ = \theta$.

A Hybrid Jacobian Generator

This block corresponds to a hybrid dynamical system having flows with input given by the matrix $f_\xi(y_\theta, y_\mu) \in \mathbb{R}^{n\times m}$, where $f_\xi : \mathbb{R}^n \times \mathbb{R}^n \to \mathbb{R}^{n\times m}$ maps the output of the plant y_θ, and the output of the dither generator block y_μ. The state of the hybrid Jacobian generator is given by $\xi \in \mathbb{R}^s$, where $s \in \mathbb{Z}_{\geq 1}$. The hybrid dynamics of ξ are given by

$$\dot{\xi} \in \omega_L \cdot F_\xi(\xi, f_\xi(y_\theta, y_\mu), a), \qquad \xi \in \Psi_{C,\xi}(\hat{x}), \tag{2.54a}$$

$$\xi^+ \in G_\xi(\xi, a), \qquad \xi \in \Psi_{D,\xi}(\hat{x}), \tag{2.54b}$$

where $a \in \mathbb{R}_{>0}$ is a small tunable parameter, and $F_\xi : \mathbb{R}^s \times \mathbb{R}^{n\times m} \times \mathbb{R}_{>0} \rightrightarrows \mathbb{R}^s$, $G_\xi : \mathbb{R}^s \times \mathbb{R}_{>0} \rightrightarrows \mathbb{R}^s$, $\Psi_{C,\xi} : \mathbb{R}^\ell \rightrightarrows \mathbb{R}^s$, $\Psi_{D,\xi} : \mathbb{R}^\ell \rightrightarrows \mathbb{R}^s$, and $\Psi_\xi(\hat{x}) = \Psi_{C,\xi}(\hat{x}) \cup \Psi_{D,\xi}(\hat{x})$. The output of (2.54) is given by

$$y_\xi = h_\xi(\xi), \tag{2.55}$$

which is the same input of the hybrid optimizer (2.51), and where $h_\xi : \mathbb{R}^s \to \mathbb{R}^{m\times n}$ is a continuous function. Although, in principle, the hybrid Jacobian generator is not needed by the extremum seeking control, it is commonly used to improve the transient performance of the closed-loop system by attenuating the oscillations induced by the dithering signals, and by allowing to increase the adaptation gain k in the optimization dynamics (2.51).

The hybrid Jacobian generator (2.54) is designed such that the jumps given by

the dynamics (2.54b) do not generate instantaneous changes in the other states of the system. In this way, the interconnection of the hybrid optimizer (2.51) and the hybrid Jacobian generator (2.54) generates two types of jumps, given by

$$\hat{x}^+ = \hat{x}, \qquad \hat{x} \in \hat{C}, \tag{2.56a}$$

$$\xi^+ \in G_\xi(\xi, a), \qquad \xi \in \Psi_{D,\xi}(\hat{x}), \tag{2.56b}$$

and

$$\hat{x}^+ \in G_{\hat{x}}(\hat{x}, \delta), \qquad \hat{x} \in \hat{D}, \tag{2.57a}$$

$$\xi^+ = \xi, \qquad \xi \in \Psi_{C,\xi}(\hat{x}) \cup \Psi_{D,\xi}(\hat{x}). \tag{2.57b}$$

The dynamics of the hybrid Jacobian generator (2.54) are designed under the assumption that $f_\xi = DJ(\hat{x}_1) + e$, where e is a uniformly bounded small error. Thus, under this assumption, the flows given by the interconnection of the hybrid optimizer (2.51) and the hybrid Jacobian generator (2.59) are given by

$$\dot{\hat{x}} \in k \cdot F_{\hat{x}}(\hat{x}, y_\xi, \delta), \qquad \hat{x} \in \hat{C}, \tag{2.58a}$$

$$\dot{\xi} \in \omega_L \cdot F_\xi(\xi, DJ(\hat{x}_1) + e, a), \quad \hat{\xi} \in \Psi_{C,\xi}(\hat{x}), \tag{2.58b}$$

Using the definition of k, and a new time scale $\tau = \sigma t$, for values of σ sufficiently small, it can be observed that the HDS given by the equations (2.56), (2.57), and (2.58) in the τ-time scale, is a SP-HDS of the form (D.1). This system has hybrid boundary

layer dynamics with flows given by

$$\dot{\hat{x}} = 0, \qquad \hat{x} \in \hat{C}, \tag{2.59a}$$

$$\dot{\xi} \in F_\xi(\xi, DJ(\hat{x}_1) + e, a), \quad \hat{\xi} \in \Psi_{C,\xi}(\hat{x}), \tag{2.59b}$$

and jumps given by

$$\hat{x}^+ = \hat{x}, \qquad \hat{x} \in \hat{C}, \tag{2.60a}$$

$$\xi^+ \in G_\xi(\xi, a), \qquad \xi \in \Psi_{D,\xi}(\hat{x}). \tag{2.60b}$$

Based on this, the hybrid dynamics (2.54) and the output function (2.55) are designed such that the following assumption holds.

Assumption 8 *Let δ^* be given by Assumption 5. Then for each $\delta \in (0, \delta^*)$ there exists an $a^* \in \mathbb{R}_{>0}$ such that for all $a \in (0, a^*)$ the SP-HDS* (2.56), (2.57), (2.58), *in the τ-time scale, with boundary layer dynamics* (2.59)-(2.60), *satisfies the following conditions:*

(a) The set-valued mappings $F_\xi(\cdot,\cdot,a)$, $G_\xi(\cdot,a)$, $\Psi_{C,\xi}(\cdot)$ and $\Psi_{D,\xi}(\cdot)$ are OSC and LB. Moreover, $F_\xi(\cdot,\cdot,a)$ is convex-valued for each $(\hat{x},\xi) \in \hat{C} \times \Psi_{C,\xi}(\hat{x})$.

(b) Definition 13 holds with $x_1 = \hat{x}$, $x_2 = \xi$, $F_1 = F_{\hat{x}}$, $F_2 := F_\xi$, $\tilde{C} = \{(\hat{x},\xi) : \hat{x} \in \hat{C}, \xi \in \Psi_{C,\xi}(\hat{x})\}$, $H_2 = G_\xi$, and set-valued mapping F^A given by

$$F^A(\hat{x}) := F_{\hat{x}}(\hat{x}, DJ(\hat{x}_1) + e, \delta), \tag{2.61}$$

where $e(\cdot)$ is a measurable function of order $O(a)$.

(c) The boundary layer dynamics (2.59)-(2.60) *do not generate purely discrete solu-*

tions, and system (2.56), (2.57), (2.58) *generates at least one complete solution from every initial condition.*

Note that the classic first order low pass filter commonly used in ESC, e.g., [96], [90], satisfies Assumption 8. However, Assumption 8 opens the door for more advanced hybrid filters that combine continuous and discrete-time dynamics, e.g., [78, Ex. 7.26].

A Hybrid Dither Generator

This block corresponds to a hybrid dynamical system generating the dithering signals $\mu \in \mathbb{R}^r$ used by the ESC in order to extract the gradient information of the response map J. The hybrid dynamics of the dither generator are given by

$$\dot{\mu} \in \epsilon \cdot F_\mu(\mu), \qquad \mu \in \Psi_{C,\mu}(\hat{x}, \xi), \tag{2.62a}$$

$$\mu^+ \in G_\mu(\mu), \qquad \mu \in \Psi_{D,\mu}(\hat{x}, \xi), \tag{2.62b}$$

where the mappings $F_\mu : \mathbb{R}^r \rightrightarrows \mathbb{R}^r$, $G_\mu : \mathbb{R}^r \rightrightarrows \mathbb{R}^r$, $\Psi_{C,\mu} : \mathbb{R}^\ell \times \mathbb{R}^s \rightrightarrows \mathbb{R}^r$, and $\Psi_{D,\mu} : \mathbb{R}^\ell \times \mathbb{R}^s \rightrightarrows \mathbb{R}^r$ are set-valued, and $\Psi_\mu(\hat{x}, \xi) = \Psi_{C,\mu}(\hat{x}, \xi) \cup \Psi_{D,\mu}(\hat{x}, \xi)$ and $\epsilon \in \mathbb{R}_{>0}$ is the same tunable parameter used in the definition of k in equation (2.51). The output of (2.62) is given by

$$y_\mu = h_\mu(\mu), \tag{2.63}$$

where $h_\mu : \mathbb{R}^r \to \mathbb{R}^{n \times m}$ is a continuous function.

Discrete-time updates of the dither generator, given by the equation (2.62b), do not generate instantaneous changes in the other states of the system. In this way, the interconnection of the hybrid dither generator (2.62), and the hybrid Jacobian generator and hybrid optimizer (2.56)-(2.58), generates a HDS with three types of

jumps given by

$$\hat{x}^+ = \hat{x}, \qquad \hat{x} \in \hat{C}, \tag{2.64a}$$

$$\xi^+ = \xi, \qquad \xi \in \Psi_{C,\xi}(\hat{x}), \tag{2.64b}$$

$$\mu^+ \in G_\mu(\mu), \qquad \mu \in \Psi_{D,\mu}(\hat{x}, \xi), \tag{2.64c}$$

$$\hat{x}^+ = \hat{x}, \qquad \hat{x} \in \hat{C}, \tag{2.65a}$$

$$\xi^+ \in G_\xi(\xi), \qquad \xi \in \Psi_{D,\xi}(\hat{x}), \tag{2.65b}$$

$$\mu^+ = \mu, \qquad \mu \in \Psi_{C,\mu}(\hat{x}, \xi) \cup \Psi_{D,\mu}(\hat{x}, \xi), \tag{2.65c}$$

$$x^+ \in G_{\hat{x}}(\hat{x}, \delta), \qquad \hat{x} \in \hat{D}, \tag{2.66a}$$

$$\xi^+ = \xi, \qquad \xi \in \Psi_{C,\xi}(\hat{x}) \cup \Psi_{D,\xi}(\hat{x}), \tag{2.66b}$$

$$\mu^+ = \mu, \qquad \mu \in \Psi_{C,\mu}(\hat{x}, \xi) \cup \Psi_{D,\mu}(\hat{x}, \xi), \tag{2.66c}$$

Note that the jumps (2.65) and (2.66) are related to the jumps (2.56) and (2.57). The hybrid dither generator is designed under the assumption that $y_\theta = J(u)$, with input u given by

$$u = h_u(y_{\hat{x}}, y_\mu), \tag{2.67}$$

where $h_u : \mathbb{R}^n \times \mathbb{R}^{n \times m} \to \mathbb{R}^n$ is a continuous mapping. Under this assumption, the flows given by the interconnection of the hybrid optimizer, the Jacobian generator, and

the dither generator are given by

$$\dot{\hat{x}} \in k \cdot F_{\hat{x}}(\hat{x}, \xi, \delta), \qquad \hat{x} \in \hat{C}, \tag{2.68a}$$

$$\dot{\xi} \in \omega_L \cdot F_{\xi}(\xi, f_{\xi}(J(u), y_{\mu}), a), \quad \xi \in \Psi_{C,\xi}(\hat{x}), \tag{2.68b}$$

$$\dot{\mu} \in \epsilon \cdot F_{\mu}(\mu), \qquad \mu \in \Psi_{C,\mu}(\hat{x}, \xi), \tag{2.68c}$$

where $u = h_u(y_{\hat{x}}, y_{\mu})$. Using a new time scale $\tau = \epsilon\bar{\omega}t$, and the definition of k, for ω_L sufficiently small, the HDS (2.64), (2.65), (2.66), (2.68), with flows in the τ-scale is a SP-HDS of the form (D.1) with $\bar{\omega}$ acting as a small parameter. The hybrid boundary layer dynamics of this system have flows

$$\dot{\hat{x}} = 0, \qquad \hat{x} \in \hat{C}, \tag{2.69a}$$

$$\dot{\xi} = 0, \qquad \xi \in \Psi_{C,\xi}(\hat{x}), \tag{2.69b}$$

$$\dot{\mu} \in F_{\mu}(\mu), \qquad \mu \in \Psi_{C,\mu}(\hat{x}, \xi), \tag{2.69c}$$

and jumps given by

$$\hat{x}^+ = \hat{x}, \qquad \hat{x} \in \hat{C}, \tag{2.70a}$$

$$\xi^+ = \xi, \qquad \xi \in \Psi_{C,\xi}(\hat{x}), \tag{2.70b}$$

$$\mu^+ \in G_{\mu}(\mu), \qquad \mu \in \Psi_{D,\mu}(\hat{x}, \xi). \tag{2.70c}$$

Based on this, the hybrid dither generator is designed such that the following assumption holds.

Assumption 9 *Let δ^* be generated by Assumption 5 and a^* be generated by Assumption 8. Then for each $\delta \in (0, \delta^*)$ and $a \in (0, a^*)$ the SP-HDS* (2.64),(2.65), (2.66), (2.68) *in the τ-time scale, with boundary layer dynamics* (2.69)-(2.70)*, satisfies the*

following conditions:

(a) The set-valued mappings F_μ, G_μ, $\Psi_{\mu,C}$, *and* $\Psi_{\mu,D}$ *are OSC and LB. The mapping* F_μ *is convex valued for each* $(\hat{x},\xi) \in \Psi_{C,\mu}(\hat{x},\xi)$.

(b) Definition 13 holds with $x_1 = [\hat{x}^\top, \xi^\top]^\top$, $x_2 = \mu$, $F_1 := F_{\hat{x}} \times F_\xi$, $F_2 := F_\mu$, $\tilde{C} = \{(x,z) : \hat{x} \in \hat{C}, \xi \in \Psi_{C,\xi}(\hat{x}), \mu \in \Psi_{C,\mu}(\xi)\}$, $H_2 = G_\mu$, *and*

$$F^A := F_{\hat{x}}(\hat{x}, y_\xi, \delta) \times F_\xi(\xi, DJ(\hat{x}_1) + e, a)$$

where $e(\cdot)$ *is a measurable function of order* $O(a)$.

(c) The boundary layer dynamics (2.69)-(2.70) *do not generate purely discrete or eventually discrete solutions, and system* (2.64),(2.65), (2.66), (2.68), *generates at least one complete solution from every possible initial condition.*

Assumption (9) is satisfied by the linear oscillator considered in [206], as well as by any nonlinear system rendering UGAS a compact set, and generating solutions that have the orthogonality property, e.g., [205, Def. 11]. System (2.62) also opens the door for nonsmooth and discontinuous dithering signals generated by switching mechanisms, e.g., [207], [208].

Closed-Loop System

The closed-loop system, shown in Figure 2.20, is given by the interconnection of the hybrid plant and the hybrid extremum seeking control. In the closed-loop system, the jumps of the plant state, given by (2.49b), do not generate instantaneous changes in the other states of the system. Thus, the closed-loop system has four types of jumps,

given by

$$\hat{x}^+ = \hat{x}, \qquad \hat{x} \in \hat{C}, \tag{2.71a}$$

$$\xi^+ = \xi, \qquad \xi \in \Psi_{C,\xi}(\hat{x}), \tag{2.71b}$$

$$\mu^+ = \mu, \qquad \mu \in \Psi_{C,\mu}(\hat{x}, \xi), \tag{2.71c}$$

$$\theta^+ \in G_\theta(\theta, u), \quad \theta \in \Psi_{D,\theta}(u), \tag{2.71d}$$

$$\hat{x}^+ = \hat{x}, \qquad \hat{x} \in \hat{C}, \tag{2.72a}$$

$$\xi^+ = \xi, \qquad \xi \in \Psi_{C,\xi}(\hat{x}), \tag{2.72b}$$

$$\mu^+ \in G_\mu(\mu), \quad \mu \in \Psi_{D,\mu}(\hat{x}, \xi), \tag{2.72c}$$

$$\theta^+ = \theta, \qquad \theta \in \Psi_{C,\theta}(u) \cup \Psi_{D,\theta}(u), \tag{2.72d}$$

$$\hat{x}^+ = \hat{x}, \qquad \hat{x} \in \hat{C}, \tag{2.73a}$$

$$\xi^+ \in G_\xi(\xi, a), \quad \xi \in \Psi_{D,\xi}(\hat{x}), \tag{2.73b}$$

$$\mu^+ = \mu, \qquad \mu \in \Psi_{C,\mu}(\hat{x}, \xi) \cup \Psi_{D,\mu}(\hat{x}, \xi), \tag{2.73c}$$

$$\theta^+ = \theta, \qquad \theta \in \Psi_{C,\theta}(u) \cup \Psi_{D,\theta}(u), \tag{2.73d}$$

$$x^+ \in G_{\hat{x}}(\hat{x}, \delta), \qquad \hat{x} \in \hat{D}, \tag{2.74a}$$

$$\xi^+ = \xi, \qquad \xi \in \Psi_{C,\xi}(\hat{x}) \cup \Psi_{D,\xi}(\hat{x}), \tag{2.74b}$$

$$\mu^+ = \mu, \qquad \mu \in \Psi_{C,\mu}(\hat{x}, \xi) \cup \Psi_{D,\mu}(\hat{x}, \xi), \tag{2.74c}$$

$$\theta^+ = \theta, \qquad \theta \in \Psi_{C,\theta}(u) \cup \Psi_{D,\theta}(u), \tag{2.74d}$$

and flows given by

$$\dot{\hat{x}} \in k \cdot F_{\hat{x}}(\hat{x}, \xi, \delta), \qquad \hat{x} \in \hat{C}, \tag{2.75a}$$

$$\dot{\xi} \in \omega_L \cdot F_{\xi}(\xi, f_{\xi}(y_\theta, y_\mu), a), \qquad \xi \in \Psi_{C,\xi}(\hat{x}), \tag{2.75b}$$

$$\dot{\mu} \in \epsilon \cdot F_{\mu}(\mu), \qquad \mu \in \Psi_{C,\mu}(\hat{x}, \xi), \tag{2.75c}$$

$$\dot{\theta} \in F_{\theta}(\theta, u), \qquad \theta \in \Psi_{C,\theta}(u). \tag{2.75d}$$

Finally, using the definitions of k and ω_L, we note that for values of ϵ sufficiently small, and in a new time scale defined as $\tau = \epsilon t$, the closed-loop HDS (2.71)-(2.75) is a SP-HDS of the form (D.1), with ϵ acting as small parameter, and with boundary layer dynamics having flows of the form

$$\dot{\hat{x}} = 0, \qquad \hat{x} \in \hat{C} \tag{2.76a}$$

$$\dot{\xi} = 0, \qquad \xi \in \Psi_{C,\xi}(\hat{x}) \tag{2.76b}$$

$$\dot{\mu} = 0, \qquad \mu \in \Psi_{C,\mu}(\hat{x}, \xi) \tag{2.76c}$$

$$\dot{\theta} \in F_{\theta}(\theta, u), \qquad \theta \in \Psi_{C,\theta}(u), \tag{2.76d}$$

and jumps given by

$$\hat{x}^+ = \hat{x}, \qquad \hat{x} \in \hat{C} \tag{2.77a}$$

$$\xi^+ = \xi, \qquad \xi \in \Psi_{C,\xi}(\hat{x}) \tag{2.77b}$$

$$\mu^+ = \mu, \qquad \mu \in \Psi_{C,\mu}(\hat{x}, \xi) \tag{2.77c}$$

$$\theta^+ \in G_\theta(\theta, u), \qquad \theta \in \Psi_{D,\theta}(u), \tag{2.77d}$$

These boundary layer dynamics characterize the class of response maps $J(u)$ that can be generated by the plant (2.49), such that the extremum seeking problem is well-defined.

Assumption 10 *Let δ^* be given by Assumption 5, and a^* be given by Assumption 8. Then, for each $\delta \in (0, \delta^*)$ and $a \in (0, a^*)$ the SP-HDS* (2.71)-(2.75) *in the τ-time scale, and with boundary layer dynamics* (2.76)-(2.77)*, satisfies the following conditions:*

1. *The set-valued mappings F_θ, G_θ, $\Psi_{C,\theta}$ and $\Psi_{D,\theta}$ are OSC and LB. The mapping F_θ is convex valued.*

2. *There exists a unique map $J : \mathbb{R}^n \to \mathbb{R}^m$ such that Definition 13 holds with $x_1 = [\hat{x}^\top, \xi^\top, \mu^\top]^\top$, $x_2 = \theta$, $F_1 := F_{\hat{x}} \times F_\xi \times F_\mu$, $F_2 := F_\theta$, $\tilde{C} = \{(x, z) : x \in \hat{C}, \xi \in \Psi_{C,\xi}(\hat{x}), \mu \in \Psi_{C,\mu}(\hat{x}, \xi), \theta \in \Psi_{C,\theta}(\hat{x}, \xi, \theta)\}$, $H_2 = G_\theta$, and*

$$F^A := F_{\hat{x}}(\hat{x}, y_\xi, \delta) \times F_\xi(\xi, f_\xi(J(u), y_\mu), a) \times F_\mu(\mu).$$

3. *The boundary layer dynamics* (2.76)-(2.77) *do not generate purely discrete or eventually discrete solutions.*

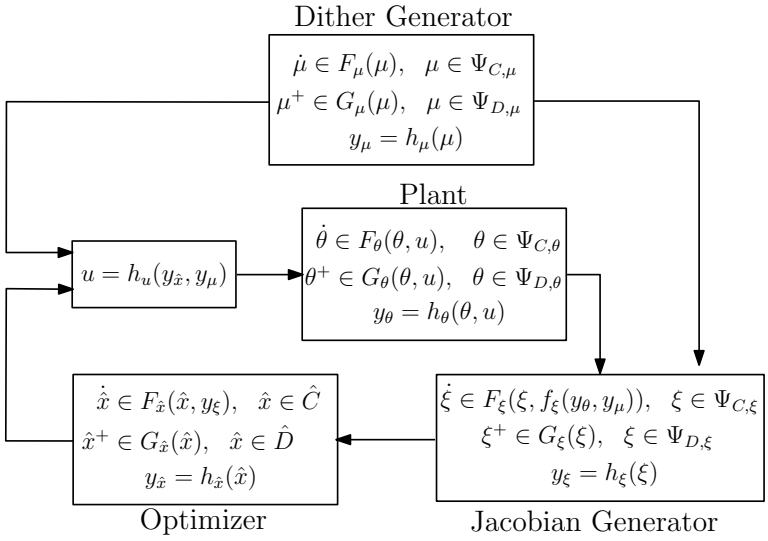

Figure 2.20: Closed-loop system with HESC.

Analysis of the Closed-Loop System

In order to establish the stability properties of the closed-loop system, we define the state $x := [\hat{x}^\top, \xi^\top, \mu^\top, \theta^\top]^\top \in \mathbb{R}^{\ell+s+r+p}$, and the compact sets

$$\mathcal{A}_\xi := \Psi_\xi(\mathcal{A}_{\hat{x}}), \quad \mathcal{A}_\mu := \Psi_\mu(\mathcal{A}_{\hat{x}}, \mathcal{A}_\xi), \tag{2.78a}$$

$$\mathcal{A}_\theta := \Psi_\theta\left(h_u(h_{\hat{x}}(\mathcal{A}_{\hat{x}}), h_\mu(\mathcal{A}_\mu))\right), \tag{2.78b}$$

$$\mathcal{A}_{\hat{x},\xi,\mu,\theta} := \mathcal{A}_{\hat{x}} \times \mathcal{A}_\xi \times \mathcal{A}_\mu \times \mathcal{A}_\theta. \tag{2.78c}$$

Using this construction, we obtain the following result for the closed-loop system (2.71)-(2.75).

Theorem 2 *Consider the HDS* (2.71)-(2.75)*, and the compact set* (5.10)*. Suppose that Assumptions 4, 8, 9, and 10 hold. Then, for each compact set* $K := K_{\hat{x}} \times K_\xi \times K_\mu \times K_\theta \subset \mathbb{R}^{\ell+s+r+p}$ *and each* $\nu > 0$ *such that* $\mathcal{A}_{\hat{x},\xi,\mu,\theta} + \nu\mathbb{B} \subset int(K)$*, there exists* δ^* *such that for each* $\delta \in (0, \delta^*]$ *there exists* a^* *such that for each* $a \in (0, a^*]$ *there exists* $\sigma^* \in \mathbb{R}_{>0}$ *such that for each* $\sigma \in (0, \sigma^*]$ *there exists* $\bar{\omega}^*$ *such that for each* $\bar{\omega} \in (0, \bar{\omega}^*]$ *there*

exists $\epsilon^* \in \mathbb{R}_{>0}$ *such that for each* $\epsilon \in (0, \epsilon^*]$ *there exists a ULAS compact set* $\mathcal{A}_{\epsilon,\bar{\omega},\sigma,a,\delta}$ *satisfying* $\mathcal{A}_{\epsilon,\bar{\omega},\sigma,a,\delta} \subset \mathcal{A}_{\hat{x},\xi,\mu,\theta} + \nu\mathbb{B}$*, with basin of attraction containing the set* K*.*

Theorem 2 is similar in spirit to Theorem 1. In particular, for each arbitrarily large compact set of initial conditions and each arbitrarily small neighborhood of the optimal solution of the ES problem, it is possible to tune the parameters of the control system such that convergence is achieved in finite time.

2.3 Neuro-Adaptive Hybrid Extremum Seeking for Differential Inclusions

We now proceed to study hybrid extremum seeking controllers based on neuro-adaptive architectures, which have been recently and successfully used to solve learning problems in dynamical systems [209]. In contrast to the averaging-based architectures, this type of HESCs implement a neural network in order to approximate the gradient of the response map of the plant. In particular, we focus on the hybrid extremum seeking controller shown in Figure 2.21. This scheme is comprised of four main blocks: (a) the neural network-based model-free gradient approximator; (b) the differential inclusion generating the dither signal μ; (c) the hybrid learning dynamics $\hat{\mathcal{H}}_\delta$; and d) a plant characterized by a differential inclusion, such as the one considered in Section 2.1.1. In contrast to the averaging-based HESC, which only requires an orthogonality property on the dithering signals, the neuro-adaptive hybrid extremum seeking control (NHESC) requires a classic persistency of excitation condition. We proceed now to the describe in detail the blocks (a), (b) and (c).

2.3.1 NN-based Model-Free Approximator

Under Assumption 4 the response map $J(\cdot)$ is smooth, which implies that there exists a complete independent basis set of functions $\{\phi_i(u)\}$ such that J and ∇J are uniformly approximated [210], i.e., there exist coefficients c_i such that

$$J(u) = \sum_{i=1}^{N} c_i \phi_i(u) + \sum_{i=N+1}^{\infty} c_i \phi_i(u) \tag{2.79}$$

$$\nabla J(u) = \sum_{i=1}^{N} c_i \frac{\partial \phi(u)}{\partial u} + \sum_{i=N+1}^{\infty} c_i \frac{\partial \phi(u)}{\partial u}, \tag{2.80}$$

where $\phi(u) = [\phi_1(u), \ldots, \phi_N(u)]^\top : \mathbb{R}^n \to \mathbb{R}^N$, and the last terms in (2.79)-(2.80) converge uniformly to 0 as $N \to \infty$. Therefore, given $N \in \mathbb{Z}_{\geq 1}$, (2.79) and (2.80) can be written as

$$J(u) = \phi(u)^\top w^* + \epsilon(u) \tag{2.81}$$

$$\nabla J(u) = \nabla \phi(u)^\top w^* + \nabla \epsilon(u), \tag{2.82}$$

where $w^* \in \mathbb{R}^N$. The mapping $\phi : \mathbb{R}^n \to \mathbb{R}^N$ is called the NN activation function vector, N the number of neurons in the hidden layer, and $\epsilon(\cdot)$ the NN approximation error. The following lemma, adapted from [211], [212], and [209, Lemma 1] establishes the approximation properties of the neurons in the hidden layer.

Lemma 2 *Let $\Omega \subset \mathbb{R}^n$ be a compact set. Then as $N \to \infty$ the approximation errors ϵ and $\nabla\epsilon$ satisfy $\epsilon \to 0$ and $\nabla\epsilon \to 0$, uniformly on compact sets. Moreover, for each fixed N and each compact set $K \subset \mathbb{R}^n$, there exist $(\bar{\epsilon}_1, \bar{\epsilon}_2, \bar{w}) \in \mathbb{R}^3_{>0}$ such that $\|\epsilon\| \leq \bar{\epsilon}_1$, $\|\nabla\epsilon\| \leq \bar{\epsilon}_2$, and $\|w^*\| \leq \bar{w}$.*

The main limitation for the direct implementation of equations (2.81) and (2.82) is that the ideal weights w^*, which provide the best approximation of order N for J and

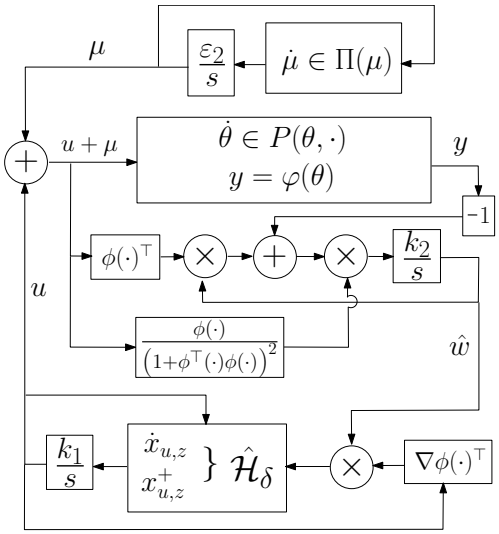

Figure 2.21: Modular scheme of NHESC

∇J, are unknown, and so, they have to be estimated online by using measurements of J. In order to do this, let u be fixed, and define the output of the NN as

$$\hat{J}(u) = \hat{w}^\top \phi(u), \tag{2.83}$$

where $\hat{w}$ is the estimated value of the NN weights w^*. Define the weight approximation error as

$$\tilde{w} = \hat{w} - w^*, \tag{2.84}$$

and the estimation error of J as

$$e = \hat{J} - J, \quad \text{or} \quad e = \tilde{w}^\top \phi(u) + \epsilon(u). \tag{2.85}$$

We aim to select $\hat{w}$ to minimize the squared residual error $E = \frac{1}{2} e^\top e$. To minimize E we propose the following learning dynamics based on the modified Levenberg-Marquardt

gradient descent algorithm

$$\dot{\hat{w}} = -\Gamma \frac{\phi}{(1+\phi^\top \phi)^2} e, \tag{2.86}$$

where $\Gamma \in \mathbb{R}_{\geq 0}$, which has a normalization term $(1+\phi^\top\phi)^2$ instead of the standard $(1+\phi^\top\phi)$, see also [213]. The learning dynamics (2.86) will be constrained to evolve in a compact set Ω_c that will be defined in the next section.

2.3.2 Signal Generator for Persistence of Excitation

Similar to standard adaptive architectures [1], in order to obtain convergence of the learning dynamics (2.86) to their correct values, a persistency of excitation condition is needed in ϕ. To achieve this, a dither signal $\mu : \mathbb{R}_{\geq 0} \to \mathbb{R}^n$ needs to be injected to u for all $t \geq 0$. This signal will be generated as the solution of the time-invariant differential inclusion

$$\dot{\mu} \in \Pi(\mu), \quad \mu \in \Psi, \tag{2.87}$$

where $\Pi : \mathbb{R}^n \rightrightarrows \mathbb{R}^n$, and $\Psi \subset \mathbb{R}^n$ is the flow set describing the points in the space where μ is allowed to evolve. System (2.87) needs to satisfy the following regularity assumption.

Assumption 11 *$\Pi(\cdot)$ is OSC, LB, and convex-valued relative to Ψ, and Ψ is compact.*

Note that Assumption 11 is not restrictive, and it is satisfied if, for instance, $P(\cdot)$ is single-valued and continuous. However, using set-valued mappings as signal generators allows us to consider a broader class of excitation signals compared to those generated by differential equations.

The following stability and completness assumption is also imposed on system (2.87).

Assumption 12 *For system* (2.87) *there exists a UGAS compact set* $\mathcal{A}_\mu \subset \Psi$*, and for each initial condition in* Ψ *there exists at least one complete solution* $\mu(\cdot)$*.*

Although the stability condition imposed by Assumption 12 is critical for our stability analysis of the closed-loop system, so is the persistently exciting (PE) property associated to the signal ϕ in the learning dynamics (2.86). We formalize the PE condition on ϕ with the following assumption:

Assumption 13 *Define* $\phi(t) := \phi(u+\mu(t))$*. Then, there exists constants* $(\beta_1, \beta_2, T) \in \mathbb{R}^3_{>0}$ *such that for each* $u \in \mathbb{R}^n$ *and each solution* $\mu(\cdot)$ *of* (2.87)*, the normalized time varying signal*

$$\bar{\phi}(t) := \frac{\phi(t)}{1 + \phi(t)^\top \phi(t)} \tag{2.88}$$

satisfies the PE property

$$\beta_1 I \leqslant \int_t^{t+T} \bar{\phi}(\tau)\bar{\phi}^\top(\tau)d\tau \leqslant \beta_2 I \tag{2.89}$$

for all $t \geq 0$*.*

Remark 9 *Note that under Assumption 12, and by the compactness of* Ψ*, for each fixed* u*, the signal* $\phi(t)$ *is uniformly bounded. Moreover, there will always exists a signal* ϕ *with unbounded time domain, such that the PE condition can actually be evaluated.*

Remark 10 *One can ensure that the signal* $\bar{\phi}(t)$ *is persistently exciting by adding exploration noise formed by sinusoids of different frequencies, see [1, Chapter 4].*

Using the PE property of $\bar{\phi}$, as well as the learning dynamics (2.86), and the change of variable (2.84), for each pair of positive numbers $(\rho, c) \in \mathbb{R}^2_{>0}$ we can study

the stability properties of the system

$$\left.\begin{aligned} \dot{u} &= 0 \\ \dot{\mu} &\in \Pi(\mu) \\ \dot{\tilde{w}} &= -\Gamma \frac{\phi(u+\mu)}{\left(1+\phi(u+\mu)^\top \phi(u+\mu)\right)^2} e \end{aligned}\right\}, \ (u,\, \mu, \tilde{w}) \in C_{\rho,c} \tag{2.90}$$

with flow set

$$C_{\rho,c} := (\rho\mathbb{B} \cap \mathbb{U}) \times \Psi \times \Omega_c, \tag{2.91}$$

where $\Omega_c := \{\tilde{w} \in \mathbb{R}^N : \frac{1}{2}\text{tr}\left\{\tilde{w}^\top \Gamma^{-1} \tilde{w}\right\} \leq c\}$, and e is defined as in (2.85). The following proposition establishes a stability result for this system with frozen input:

Proposition 6 *Consider system* (2.90) *with flow set* (2.91)*, and suppose that Assumptions 11-13 hold. Then, for each pair* $(\rho, c) \in \mathbb{R}^2_{>0}$*, and each* $\bar{\epsilon} \ll c$ *there exists a number* N^* *of NN such that for all* $N \geq N^*$ *there exists a compact set* $\mathcal{A}_c \subset \bar{\epsilon}\mathbb{B}$ *such that the set*

$$\mathcal{M}_\rho := \{(u, \mu, \tilde{w}) : u \in \rho\mathbb{B} \cap \mathbb{U}, (\mu, \tilde{w}) \in \mathcal{A}_\mu \times \mathcal{A}_c\} \tag{2.92}$$

is UGAS.

The stability result of Proposition 6, which assumes a frozen input u, will allows us to make use of singular perturbation arguments for time-invariant set-valued systems once the learning dynamics $\dot{u}$ are taken into consideration. This approach makes the design of the NHESC of *modular nature*, allowing us to design the learning dynamics of u independently of the dynamics of the NN.

Remark 11 *The proof of Proposition 6 hinges on invariance and well-posedness properties of the set-valued* time-invariant *systems. It also exploits the stability properties of* μ*, as well as the PE Assumption 13 on the* solutions *of the generator* (2.87)*, instead*

of using the weaker and more common (see [1, Ch. 4]) PE assumption in an arbitrary time-varying signal $\phi(\cdot)$. However, as noted before, several classes of dithers can be generated by system (2.87)*, including the classic sinusoids commonly used in adaptive schemes.*

2.3.3 Hybrid Learning Dynamics

Similar to the averaging-based HESCs considered in Sections 2.1 and 2.2, the optimization block $\hat{\mathcal{H}}$ in Figure 2.21, is modeled as a hybrid dynamical system of the form

$$\dot{x}_{u,z} \in \hat{F}_\delta\left(x_{u,z}, \nabla\phi(u)^\top \hat{w}\right), \quad x_{u,z} \in C_u \times C_z, \tag{2.93a}$$

$$x^+_{u,x} \in \hat{G}_\delta\Big(x_{u,z}\Big), \qquad\qquad x_{u,z} \in D_u \times D_z, \tag{2.93b}$$

where $x_{u,z} := (u^\top, z^\top)^\top \in \mathbb{R}^{n+r}$, z is an auxiliary state of dimension[3] $r \in \mathbb{Z}_{\geq 0}$, which can be used to model timers, automatas, logic modes, etc, $n+r = \ell$, the sets $C_u, D_u \subset \mathbb{R}^n$ and $C_z, D_z \subset \mathbb{R}^r$ define the flow and jump sets for u and z, respectively, and $\delta \in \mathbb{R}_{>0}$ is a tunable parameter that gives flexibility for the design of the set-valued mappings $\hat{F}_\delta : \mathbb{R}^\ell \times \mathbb{R}^n \rightrightarrows \mathbb{R}^\ell$ and $\hat{G}_\delta : \mathbb{R}^l \rightrightarrows \mathbb{R}^\ell$. As in the averaging-based case, the hybrid learning dynamics (2.93) are designed based on Assumption 5, and the following stability assumption:

Assumption 14 *The set $\mathbb{U}$ satisfies $C_u \cup D_u = \mathbb{U}$, and there exists a compact set $\Upsilon \subset C_z \times D_z$ such that the set $\mathcal{A}_{u,z} := \mathcal{O} \times \Upsilon$ is SGP-AS as $\delta \to 0^+$ for system* (2.93) *with $\nabla\phi(u)^\top \hat{w} = \nabla J(u)$.*

For the case that the mappings $\hat{F}_\delta$ and $\hat{G}_\delta$ are independent of any parameter δ, Assumption 14 is just a UGAS assumption on (2.93).

[3]The case $r = 0$ indicates that the auxiliary state z is omitted.

2.3.4 Main Result

The closed-loop system is obtained by combining the plant dynamics (2.1), the PE generator (2.87), the NN learning dynamics (2.86) with J replaced by the output of the plant $y = \varphi(\theta)$, and the hybrid seeking dynamics (2.93). The resulting system is a HDS $\mathcal{H} := \{C, F, D, G\}$ with state $x := (x_{u,z}^\top, \hat{w}^\top, \mu^\top, \theta^\top)^\top$ and equations

$$C := (C_u \times C_z) \times \Omega_c \times \Psi \times \Lambda_\theta \tag{2.94a}$$

$$\dot{x} \in F(x) := \begin{pmatrix} k_1 \cdot \hat{F}_\delta \left(x_{u,z}, \nabla\phi(u)^\top \hat{w}\right) \\ -k_2 \cdot \bar{\bar{\phi}}(u+\mu)\left(\hat{w}^\top \phi(u+\mu) - \varphi(\theta)\right) \\ -\varepsilon_2 \cdot \Pi(\mu) \\ P(\theta, u+\mu) \end{pmatrix} \tag{2.94b}$$

$$D := (D_u \times D_z) \times \Omega_c \times \Psi \times \Lambda_\theta \tag{2.94c}$$

$$x^+ \in G(x) := \hat{G}_\delta\big(x_{u,z}\big) \times \{\hat{w}\} \times \{\mu\} \times \{\theta\}, \tag{2.94d}$$

where $k_1 := \varepsilon_1 \cdot \varepsilon_2$, $k_2 := \varepsilon_2 \cdot \Gamma$, $(\varepsilon_1, \varepsilon_2) \in \mathbb{R}^2_{>0}$ are tunable parameters, and where

$$\bar{\bar{\phi}}(u+\mu) := \frac{\bar{\phi}(u+\mu)}{(1 + \phi(u+\mu)^\top \phi(u+\mu))}, \tag{2.95}$$

with $\bar{\phi}$ defined as in (2.88). The following theorem characterizes the stability properties of the neuro-adaptive HESC.

Theorem 3 *Suppose that all the assumptions of Section 2.3 hold. Then, for each compact set $\tilde{K} \subset \mathbb{R}^l$ satisfying $\mathcal{A}_{u,z} \subset int(\tilde{K})$, there exists a pair (c, λ_θ), such that for each $\varepsilon > 0$ there exists $N \in \mathbb{Z}_{>0}$, $w^* \in \mathbb{R}^N$, $\delta^* > 0$, such that for each $\delta \in (0, \delta^*)$ there exists $\epsilon_2^* > 0$ such that for each $\epsilon_2 \in (0, \epsilon_2^*)$ there exists $\epsilon_1 \in (0, \epsilon_1^*)$ and a UGAS set $\mathcal{A}_\varepsilon \subset (\mathcal{A}_{u,z} \times \{w^*\} \times \mathcal{A}_\mu \times \Lambda_\theta) + \varepsilon\mathbb{B}$ for the HDS (2.94) with restricted flow and jump*

sets

$$C_{\tilde{K}} := [(C_u \times C_z) \cap \tilde{K}] \times \Omega_c \times \Psi \times \Lambda_\theta \tag{2.96}$$

$$D_{\tilde{K}} := [(D_u \times D_z) \cap \tilde{K}] \times \Omega_c \times \Psi \times \Lambda_\theta. \tag{2.97}$$

Remark 12 *The proof of Theorem 6 is similar to the proof of [206, Thm. 1]. However, it has three main differences: First, using the NN model-free approximator allows us to eliminate one of the multiple time scales that emerge in the closed-loop system. Second, the averaging-based step of [206, Thm. 1] is replaced by a singular-perturbation argument that makes use of Proposition 6. Third, the amplitude of the dither signal μ does not necessarily have to be small in order to obtain a good approximation of the gradient of the response map J. Instead, the number of neurons in the hidden layer should be sufficiently large.*

2.3.5 Numerical Examples: Neuro-Adaptive HESC

We present two numerical examples of neuro-adaptive extremum seeking controllers.

SISO Static Plants

Suppose that the plant is a static map such that $y = J(u) := u^2$, which has a global minimum at $u^* = 0$. We want to achieve convergence to u^* in "finite-time", and with an approximately constant evolution rate. To achieve this objective we consider again the learning dynamics (2.35). The dither signal is generated by a linear periodic oscillator. The vector of basis functions is defined as $\phi = [u^2, u, 1]^\top$. Figure 2.22 shows the evolution of the vector of weights $\hat{w} = [\hat{w}_1, \hat{w}_2, \hat{w}_3]^\top$ converging to the actual values $w^* = [1, 5, 16]^\top$. The inset shows the evolution in time of the input u converging to the optimal value u^*. The parameters are $\Gamma = 500$, $k = 10$, $a = 2$, and $\omega = 40$.

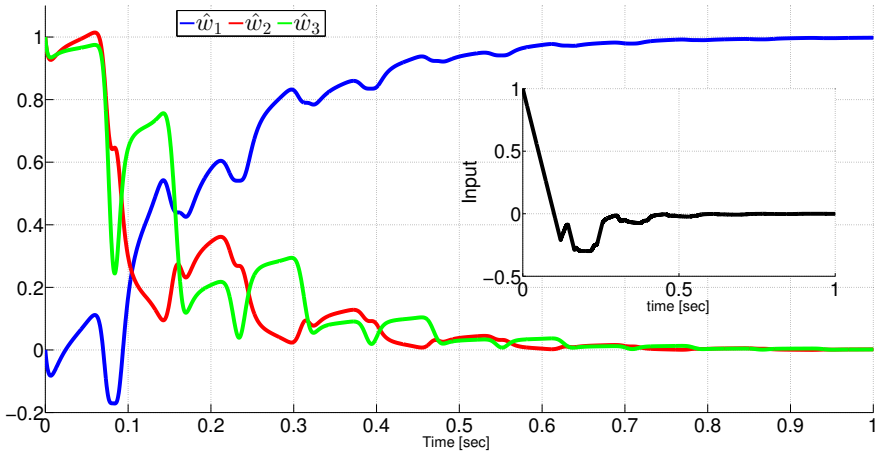

Figure 2.22: Evolution in time of $\hat{w}$ and u.

Multivariable Dynamic Plants

Consider a simple linear system with state $\theta \in \mathbb{R}^2$, dynamics given by $\delta \cdot \dot{\theta} = A\theta + Bu$, and output given by $y = (\theta_1 - 5)^2 + (\theta_2 - 4)^2$, where A and B are just the identity matrix I, $u \in \mathbb{R}^2$, and $\delta = 5 \times 10^{-4}$. Note that the output is a scalar nonlinear function of both states θ_1 and θ_2. The response map is obtained as $J = (u_1 - 5)^2 + (u_2 - 4)^2$, which attain its minimum at the point $u^* = [5, 4]^\top$. For this system, we use a vector of basis functions given by $\phi = [u_1^2, u_1, u_2^2, u_2, 1]^\top$. Note that although here for simplicity we consider quadratic functions, one could consider other types of polynomial or not polynomial basis functions [214] for non-quadratic response maps. We consider standard gradient descent as learning mechanism. Figure (2.23) shows the evolution in time of the weights w_i associated to each of the entries of the basis functions. Figure (2.24) shows the evolution of the control actions converging to the optimal point that minimizes the response map. Here $a = 2.5$, $k = 0.1$, $\Gamma = 200$, $\omega_1 = 40$, $\omega_2 = 45$.

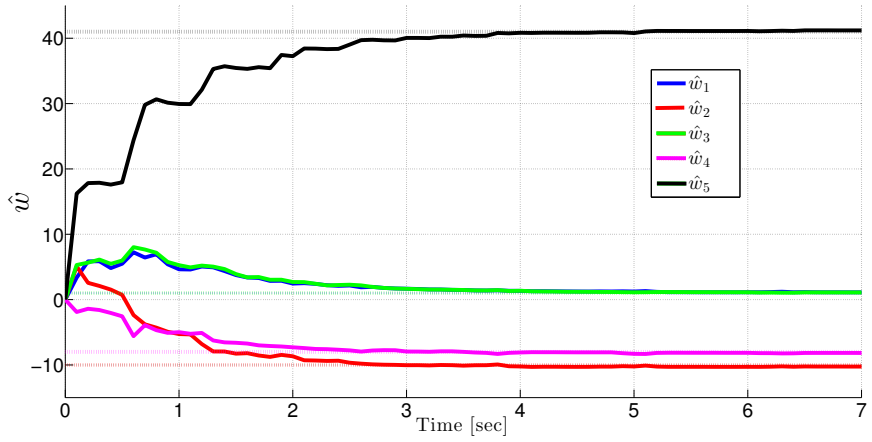

Figure 2.23: Evolution in time of $\hat{w}$.

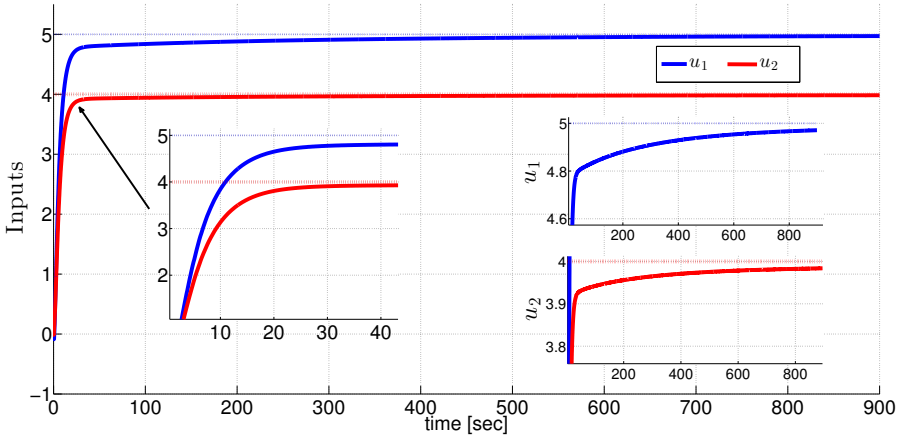

Figure 2.24: Evolution in time of u.

Chapter 3

Online Learning for Dynamic Pricing in Societal Systems

In this chapter, we study an application of the theoretical results of Section 2.3 in the context of societal systems [215]. In particular, we study the problem of designing model-free algorithms to control in real-time the incentives assigned to a population of users, aiming to maximize the welfare of the society. Our results rely on two main assumptions about the societal system under consideration. First, we assume that the entities of the society are faced with a decision making problem that can be modeled by a congestion game. Second, we assume that every entity of the society is rational and selfish, in the sense that each entity always implements an action that minimizes its own individual cost given the actions of the other users. Under these two assumptions, we show that a model-free cooperative controller can be designed such that the social welfare of the system is asymptotically maximized.

3.1 Societal Model and Problem Statement

We consider a population of users with a total mass m, where each user can choose between a finite set of available resources $\mathcal{V} := \{1, \dots, N\}$. Since the mass of users is constant, we can normalize the size of the population to 1, and for each $i \in \mathcal{V}$ we denote by x_i the share of users implementing the i^{th} resource. We call $x = [x_1, \dots, x_N]^\top$ the society state, and we note that x belongs to the simplex $\Delta = \{x \in \mathbb{R}^N_{\geq 0} : \mathbf{1}^\top x = 1\}$. Each strategy $i \in \mathcal{V}$ has a related cost given by $c_i(x_i)$, and we denote the vector of costs of the game as $c(x) = [c_1(x_1), \dots, c_N(x_N)]^\top$.

Example 3 *A simple example of a population game that fits our setting, is given by a routing problem, where a mass of drivers travels from point A to point B using a network of N different parallel paths. In this case each path can be seen as a resource, and the cost $c_i(\cdot)$ is a measure of the delay experienced by the users using the i^{th} path. When users make choices aiming to minimize their delay, we call the steady-state distribution that emerges in this game a Nash equilibria or Nash flow.*

3.1.1 Nash flows

When players aim to minimize their individual cost, the steady-state distribution $x_f \in \Delta$ that emerges in a congestion game is called a Nash flow or Wardrop equilibrium [216]. It turns out that congestion games are also potential games [121, Sect. 2.4], with potential function given by

$$P(x) = -\sum_{i}^{N} \int_0^{x_i} c_i(z)dz, \quad z \in \mathbb{R}. \tag{3.1}$$

Being a potential game simply means that the vector of costs $c(x)$ corresponds to the gradient of the potential function P. When the costs $c_i(\cdot)$ satisfy $\frac{\partial c_i(x_i)}{\partial x_i} > 0$ for all

x_i and $i \in \{1, \dots, N\}$, the potential function $P(\cdot)$ is strictly concave. In this case, Nash flows correspond to the maximizers of $P(x)$, i.e., the pair $(x_f, \mu) \in \mathbb{R}^N \times \mathbb{R}$ is the solution of the system of equations

$$\frac{\partial P(x_f)}{\partial x_i} + \lambda_i + \mu = 0, \quad \forall\, i \in \{1, \dots, N\} \tag{3.2a}$$

$$\mathbf{1}^\top x_f = 1, \tag{3.2b}$$

$$\lambda_i x_{f,i} = 0, \quad \lambda_i \geq 0, \quad \forall\, i \in \{1, \dots, N\} \tag{3.2c}$$

which correspond to the KKT first order conditions for maximizers of $P(x)$ in the simplex Δ. Since when $P(\cdot)$ is strictly concave the solution of (3.2) is unique, Nash flows are also unique. Moreover, since (3.1) is a separable function, condition (3.2a) can be rewritten as

$$-c_i(x_{f,i}) + \lambda_i + \mu = 0, \quad \forall\, i \in \{1, \dots, N\}. \tag{3.3}$$

3.1.2 Nash flows and Social Welfare

In a population game, the total welfare function $W(x_f)$ of the population is given by the negative sumation of the costs $c_i(x_f)$ multiplied by the share of users $x_{f,i}$ that implement the i^{th} strategy, i.e.,

$$W(x_f) = -\sum_{i=1}^{N} c_i(x_{f,i}) x_{f,i}. \tag{3.4}$$

When (3.4) is strictly concave, the *socially optimal* Nash flow x^* corresponds to the Nash flow that maximizes $W(\cdot)$ over Δ. Thus, x^* satisfies the KKT first order condi-

tions

$$\frac{\partial W(x^*)}{\partial x_i} + \lambda_i + \mu = 0, \quad \forall\, i \in \{1, \dots, N\} \tag{3.5a}$$

$$\mathbf{1}^\top x^* = m \tag{3.5b}$$

$$\lambda_i x_i^* = 0, \quad \lambda_i \geq 0, \qquad \forall\, i \in \{1, \dots, N\} \tag{3.5c}$$

and in this case equation (3.5) can be rewritten as

$$-\frac{\partial c_i(x^*)}{\partial x_i} x_i^* - c_i(x_i^*) + \lambda_i + \mu = 0, \quad \forall\, i \in \{1, \dots, N\}. \tag{3.6}$$

Since the solutions of (3.2) and (3.6) are in general not the same, Nash flows x_f are, in general, not socially socially optimal.

3.1.3 The role of the social planner

Since Nash flows are in general not socially optimal, a social planner who seeks to optimize the behavior of the overall society will be interested in designing incentive mechanisms for the population, such that the emerging collective behavior under this incentives leads to a socially optimal Nash flow, i.e., a distribution $x_f \in \Delta$ that is a solution of both (3.2) and (3.5). One of the most practical ways to incentive users corresponds to assign different tolls τ_i to each of the N resources of the game. In this way, under the assumption that users are sensitive to costs and tolls, a new congestion game with costs

$$\hat{c}_i(x_i) = c_i(x_i) + s \cdot \tau_i, \tag{3.7}$$

is induced by the social planner, where the sensitivity parameter s characterizes the impact of the toll on the users. The challenge for the social planer is then to design the

pricing mechanism for the tolls τ_i such that the Nash flow induced by the new game with costs $\hat{c}_i(\cdot)$ is now also a solution of (3.5). To achieve this goal two types of tolls have been mostly studied in the literature of pricing mechanisms: 1) flow varying tolls, and 2) fixed tolls.

3.1.4 Flow Varying Tolls

A flow varying toll is a static mapping $\tau : \Delta \to \mathbb{R}^N$ that maps flows to tolls. It is well known, e.g., [118], [121] that marginal pricing of the form

$$\tau_i(x_i) = \frac{\partial c_i(x_i)}{\partial x_i} x_i, \quad \forall \ \ i \in \{1, \dots, N\}, \tag{3.8}$$

incentives socially optimal Nash flows provided they induced potential game obtained with the cost $\hat{c}(x_i) = c_i(x) + \tau_i(x_i)$ is strictly concave. The dynamic implementation of the static pricing mechanism (3.8) then assumes that the user's behavior evolves according to some social dynamics depending on $\tau_i(x_i)$, whose equilibrium point will correspond to the socially optimal Nash flow x^*. Though this approach has been extensively studied in many settings, e.g., [118], [121], [123] some limitations prevent its application in practical environments. In particular, as noted in [114], users dislike fast-changing tolls, and they prefer prior information of the tolls before making a decision.

3.1.5 Fixed Tolls

The limitations of flow-varying tolls can be addressed by using fixed tolls [125], where the value of the toll is kept constant until the population of users converges to a steady state Nash flow. This convergence is usually application-dependent, and varies from seconds to days or weeks. Once the population achieves a steady state condition,

the values of the steady state Nash flow and the cost functions are measured, and the toll is recalculated following a particular update rule. This process is repeated until convergence to a toll that incentivizes a socially optimal Nash flow is achieved. In this chapter we will focus on designing adaptive model-free pricing mechanisms of this form.

3.1.6 Dynamic Pricing in Fully Utilized Affine Congestion Games

To keep our analysis tractable we consider in this work a particular class of congestion games characterized by the following assumption.

Assumption 15 *For the congestion game with $N \in \mathbb{Z}_{\geq 1}$ resources, and mass of users $m \in \mathbb{R}_{\geq 0}$, the following holds:*

- Affine Costs: *The vector of costs $c(x)$ is of the form $c(x) = Ax + b$, where $b \in \mathbb{R}^N$, and $A \in \mathbb{R}^{n \times n}$ is a positive definite diagonal matrix.*
- Full utilization: *The mass m of users is sufficiently large such that for any $\tau \in \mathbb{R}^N$ we have that the induced Nash flows always satisfy $x_{f,i} > 0$ for all resources $i \in \{1, \ldots, N\}$.* □

We term congestion games satisfying Assumption 15 with arbitrary matrix A as *fully utilized affine congestion games.*

Remark 13 *Note that although the conditions of Assumption 15 may seem too restrictive, affine congestion games emerge in many societal systems such as routing and traffic problems in parallel networks [113], power electrical systems and water distribution systems [117], and resource allocation models in biological and economic systems*

[217]. Additionally, the fully utilization assumption will actually be needed to hold only on compact sets selected a priori by the social planer or the pricing mechanism. In this way, it is natural to expect that when the set of tolls is bounded, and the mass of users is too large, or the number of resources is too small, there is always at least an $\epsilon > 0$ small share of users using every resource $i \in \mathcal{V}$. □

Clearly, for *fully utilized affine congestion games* with positive definite matrix A, the Welfare function (3.4) is a quadratic function that is strictly concave, and because of this there exists a unique socially optimal Nash flow $x^* \in \Delta$. However, the set of fixed optimal tolls that generate x^* is, in general, not unique, and not even bounded. We formally characterize this set by the following Lemma, which is proved in the Appendix.

Lemma 3 *Consider a congestion game satisfying Assumption 15. Then, the set of fixed tolls that generate socially optimal Nash flows is given by*

$$\mathcal{A} = \{\tau \in \mathbb{R}^N : \tau = \tau^* + \mu \mathbf{1},\ \mu \in \mathbb{R}\} \tag{3.9}$$

where $\tau^* = -\frac{b}{2}$. □

Based on the definition of $\mathcal{A}$, the dynamic adaptive pricing problem on fully utilized affine congestion games consists on designing "model-free" and decentralized algorithms that recursively adjust the tolls τ_i such that convergence to the unknown set $\mathcal{A}$ is achieved, thus indirectly steering the population towards the unique socially optimal Nash flow x^*. By "model-free" it is understood that such algorithms should not rely on the specific mathematical model and parameters of the congestion game, i.e., the parameters of the costs $c_i(\cdot)$ may be unknown. Instead, they must be data-driven and adaptable to changes in the game . Finally, since congestion games usually model large-

scale systems, it is desirable that the dynamic pricing mechanism associated to each resource $i \in \mathcal{V}$ shares information only with a subset of the other individual pricing mechanisms.

3.2 Adaptive Pricing Mechanisms in Static Societal Systems

In this section we design distributed dynamic pricing mechanisms for fully utilized affine congestion games for the case when the dynamics of the society are ignored. In this setting, it is assumed that there exists a static Oracle that delivers sampled values of all the relevant information of the game to the pricing mechanisms. We characterize this static *Oracle* by a *state* function $\mathcal{O}(\cdot)$ that maps incentives τ to Nash flows x_f, and by an *output* function $h_{\mathcal{O}}(\cdot)$ that delivers the values of x_f, $c(x_f)$, and $\nabla c(x_f)$ to the pricing mechanisms. We write this Oracle as the static system

$$x_f = \mathcal{O}(\tau), \qquad y = h_x(x_f), \tag{3.10}$$

where $\tau \mapsto \mathcal{O}(\tau) \subset F$, being $F \subset \Delta$ the set of solutions of (3.2) with induced cost (3.7), and

$$h_x(x_f) = \begin{pmatrix} h_{x,1}(x_f) \\ h_{x,2}(x_f) \\ h_{x,3}(x_f) \end{pmatrix} = \begin{pmatrix} x_f \\ c(x_f) \\ \mathrm{diag}(\nabla c(x_f)) \end{pmatrix}. \tag{3.11}$$

In order to learn the fixed optimal tolls τ in a distributed way, we assume that the Oracle delivers to the i^{th} resource only the tuple $\left\{x_{f,i}, c_i(x_{f,i}), \frac{\partial c_i(x_{f,i})}{\partial x_i}\right\}$ corresponding to sampled-values of the current Nash flow $x_{f,i}$, the current cost $c_i(x_{f,i})$, and the current marginal cost $\frac{\partial c_i(x_{f,i})}{\partial x_i}$.

3.2.1 Welfare-Gradient Dynamics are Full-Information Consensus Dynamics

To design distributed adaptive pricing mechanisms that only use local information, we start with the most basic pricing scheme which, although centralized, serves as the basic block for the adaptive distributed schemes presented in the next sections. In particular, consider a pricing mechanism based on welfare gradient dynamics of the form

$$\dot{\tau} = \nabla_\tau \tilde{W}(\tau), \tag{3.12}$$

where $\tilde{W} := W \circ \mathcal{O}(\tau)$. It turns out that, in affine congestion games with full utilization, the welfare gradient dynamics (3.12) describe a Laplacian flow with a Laplacian matrix having a particular structure.

Lemma 4 *Suppose that Assumption 15 holds and consider the static Oracle given by* (3.10)*. Then, the gradient dynamics* (3.12) *have the form*

$$\dot{\tau} = k\ \mathcal{L}_{\mathcal{G}_A}\Big(h_{x,2}(x_f) + h_{x,3}(x_f) \cdot h_{x,1}(x_f)\Big), \tag{3.13}$$

where $k = (\mathbf{1}^\top A^{-1}\mathbf{1})^{-1} \in \mathbb{R}$, and where $\mathcal{L}_{\mathcal{G}_A}$ is the out-degree Laplacian of an undirected graph $\mathcal{G}_A$ with adjacency matrix $A^{-1}\mathbf{1}\mathbf{1}^\top A^{-1}$. Moreover, system (3.13) *renders the set $\mathcal{A}$ in* (3.9) *globally asymptotically stable (GAS), and every solution converges to the fixed toll*

$$\tau^* + \frac{\mathbf{1}^\top(\tau(0) - \tau^*)}{N}\mathbf{1}. \tag{3.14}$$

Proposition (3.13) reveals that using welfare-gradient dynamics to learn the optimal tolls in fully utilized diagonal affine congestion games, is equivalent to implementing a Laplacian algorithm with the induced vector of cost functions $\hat{c}(x_f) =$

$c(x_f) + \text{diag}(\nabla c(x_f)) \cdot x_f$, where the Laplacian matrix $\mathcal{L}_{\mathcal{G}_A}$ characterizes a weighted undirected complete graph.

Although the welfare-gradient dynamics (3.13) render the set $\mathcal{A}$ GAS, their implementation requires the individual pricing mechanisms to share information with all the other mechanisms of the game. To alleviate this issue, we introduce in the next section a distributed version of (3.13) that allows the pricing mechanisms to update their tolls by only sharing information with their neighboring mechanisms.

3.2.2 A Class of Distributed Welfare-Gradient Dynamics

We consider pricing mechanisms sharing information via a graph $\mathcal{G}$ that satisfies the following assumption.

Assumption 16 (Graph Connectivity) *The individual pricing mechanisms share information via a communication graph $\mathcal{G}$ that is strongly connected and weighted-balanced.*

To achieve distributed learning of optimal tolls with the static Oracle (3.10), consider the now distributed pricing dynamics

$$\dot{\tau} = \mathcal{L}_{\mathcal{G}}\Big(h_{x,2}(x_f) + h_{x,3}(x_f) \cdot h_{x,1}(x_f)\Big), \tag{3.15}$$

where $\mathcal{L}_{\mathcal{G}}$ is the Laplacian matrix associated to the graph $\mathcal{G}$. The stability and convergence properties of (3.15) are characterized by the following proposition.

Proposition 7 *Suppose that Assumptions 15 and 16 hold. Then, the learning dynamics* (3.15) *render the set $\mathcal{A}$ GAS, and every solution converges to the fixed toll* (3.14).

Distributed pricing dynamics of the form (3.15) are indeed consistent with the characterization of socially optimal Nash flows presented in Section 3.1.2, since whenever the individual induced cost functions $\hat{c}_i(\cdot)$ with marginal utility tolls have all the same value μ, a socially optimal Nash flows emerges.

3.2.3 Learning Socially Optimal Tolls With A Performance Index

In some applications it may be of interest to converge to an optimal point $\tau^\star$ that not only generates socially optimal Nash flows, but that also minimizes a particular performance index $J(\cdot)$ defined over the set of optimal tolls $\mathcal{A}$. Examples of common performance indexes include

$$J(\tau) = \tau^\top x_f(\tau), \quad \text{and} \quad J(\tau) = \|\tau\|_p^p, \quad p \geq 1,$$

which correspond to the total revenue of the pricing mechanism, and the p-norm of the vector of tolls, respectively. For instance, when $p = 2$ the pricing mechanisms should converge to the toll $\tau^\star$ that solves the convex problem

$$\begin{aligned} &\min\ J(\tau) = \|\tau\|_2^2, \\ &\text{s.t.}\ \ \tau \in \mathcal{A}, \end{aligned} \tag{3.16}$$

where the set $\mathcal{A}$ is defined in (3.9). Using the definition of $\mathcal{A}$ in (3.9), this problem is equivalent to the unconstrained optimization problem

$$\min_{\mu \in \mathbb{R}} J(\mu) = \|\tau^* + \mu \mathbf{1}\|^2 = \sum_{i=1}^{N} J_i(\mu), \tag{3.17}$$

where $J_i(\mu) = (\mu + \tau_i^*)^2$, and τ^* was defined in Lemma 3. Note that here the scalar μ is the argument of the N different functions J_i. Using standard first order conditions for optimality it can be verified that the optimal solution $\mu^\star$ of (3.17) satisfies $-\mathbf{1}^\top b + 2\mu^\star N = 0$, such that

$$\mu^\star = \frac{\mathbf{1}^\top b}{2N} \text{ for (3.17)} \implies \tau^\star = -\frac{b}{2} + \frac{\mathbf{1}^\top b}{2N}\mathbf{1} \text{ for (3.16)}.$$

To generate distributed adaptive pricing mechanisms that converge to $\tau^\star$ using a static Oracle of the form (3.10), we can consider the learning dynamics

$$\begin{aligned} \dot{\tau} &= \mathcal{L}\left(h_{x,2}(x_f) + h_{x,3}(x_f)\cdot h_{x,1}(x_f) - 2z\right) - 2\cdot\nabla J(\tau) \\ \dot{z} &= \mathcal{L}\left(h_{x,2}(x_f) + h_{x,3}(x_f)\cdot h_{x,1}(x_f))\cdot x_f\right), \end{aligned} \tag{3.18}$$

where the cost J is defined as in (3.16). The following Proposition establishes the convergence properties of the dynamics (3.18).

Proposition 8 *Suppose that Assumption 15 holds, and consider a learning communication network having a Laplacian matrix $\mathcal{L}_\mathcal{G}$ satisfying Assumption 16. Then, each solution of* (3.18) *remains bounded, and τ converges to $\tau^\star$.*

Based on the proof of Proposition 8, the learning dynamics (3.18) can be seen as a type of saddle-point dynamics similar to those presented in [218], or [219]. Therefore the performance index $J(\cdot)$ in (3.16) can be generalized to other classes of strictly convex cost functions that may be of interest for the social planner. These cost functions can be used to generate barrier functions that bound τ [220], or to model additional performance index that incorporate political costs [221], or budget and environmental constraints [118], for example.

3.3 Adaptive Pricing Mechanisms in Dynamic Societal Systems

Since a Nash flow is a steady-state equilibrium concept, in practice an Oracle $\mathcal{O}(\cdot)$ will have to wait infinite time in order to report the steady state flow induced by a new toll acting on the social dynamics. To avoid this infinite waiting time, the results of the previous section assumed that the oracle $\mathcal{O}(\cdot)$ was actually characterized by the static functions (3.10). One can also interpret this assumption as an instantaneous convergence property on the social dynamics that describe the evolution of the social state. To dispense with this assumption we study in this section the problem of distributed learning of fixed-tolls with *dynamic* oracles. In particular, dynamic Oracles are simply social dynamics defined on the simplex that converge to a Nash flow for any fixed vector of incentives τ. In the classic literature of congestion and population games e.g., [183], [217], these social dynamics are usually modeled by Lipschitz continuous differential equations of the form

$$\dot{x} = F(x, c(x)), \quad x \in \Delta. \tag{3.19}$$

Stability properties of social dynamics of the form (3.19) have been recently studied in the literature using Lyapunov and passivity-based tools e.g., [222], [223], [121], [117]. To capture this, and more general set-valued social dynamics, we model dynamic Oracles as differential inclusions with inputs and outputs, of the form

$$\dot{x} \in F(x, u), \quad x \in \Delta, \quad u \in \mathbb{R}^N, \tag{3.20a}$$

$$y_x = h_x(x), \tag{3.20b}$$

where $F : \Delta \times \mathbb{R}^N \to T\Delta$ is a set-valued mapping assumed to be outer semicontinuous, locally bounded and convex valued, and which already encodes the vector of cost functions $c(\cdot)$ of the game. The input u is the effective vector of tolls perceived by the society, and the output mapping $h_x(\cdot)$ is defined as in (3.11) with the argument being now the state of the society x instead of the Nash flow x_f.

Dynamic Oracles modeled by equations of the form (3.20) must satisfy the following two assumptions.

Assumption 17 (Invariance of the simplex) *For all $u \in \mathbb{R}^N$ the differential inclusion* (3.20a) *renders the set Δ positively invariant.* □

Assumption 18 (Stability of Nash Flows) *Consider the social dynamics given by* (3.20) *and the Oracle mapping given by* (3.10) *that maps tolls to Nash flows. Then, under Assumption 15 for each fixed compact set $K \subset \mathbb{R}^N$, the K-constrained system*

$$\left.\begin{aligned} \dot{x} &\in F(x,u) \\ \dot{u} &= 0 \end{aligned}\right\}, \quad (x,u) \in \Delta \times K, \tag{3.21}$$

renders the set $M_K = \{(x_f, u) : x_f \in \mathcal{O}(u), u \in K\}$ GAS. □

Remark 14 *In words, Assumption 18 asks that for each fixed incentive τ, all solutions of* (3.20) *converge to the unique Nash flow x_f that solves* (3.2). □

With the new definition of the Oracle, the adaptive pricing dynamics are now of the form

$$\dot{\tau} = \alpha \, \mathcal{L}\Big(h_{x,2}(x) + h_{x,3}(x) \cdot h_{x,1}(x)\Big), \qquad \alpha \in \mathbb{R}_{>0}, \tag{3.22}$$

with output function

$$y_\tau = h_\tau(\tau) := \tau. \tag{3.23}$$

To characterize the convergence properties of the pricing dynamics (3.22) interconnected with the dynamic Oracle (3.20), let $(\rho, \varepsilon) \in \mathbb{R}^2_{>0}$, and define the compact set

$$K_\rho := \{\tau : \|\tau\|_{\mathcal{A}} \leq \rho \text{ and } \mathbf{1}^\top \tau \in \rho\mathbb{B}\}. \tag{3.24}$$

Based on this the following proposition is in order.

Proposition 9 *For each pair $(\rho, \varepsilon) \in \mathbb{R}^2_{>0}$ there exists $\alpha^* \in \mathbb{R}_{>0}$ such that for each $\alpha \in (0, \alpha^*]$ every complete solution (x, τ) of the interconnection of the learning dynamics* (3.22) *and the social dynamics* (3.20) *with $u = h_\tau(\tau)$,* constrained *to $K_\rho \times \Delta$, converges to an ε-neighborhood of the set $\{x^*\} \times \mathcal{A}$.*

Proposition 9 is obtained by means of singular-perturbation theory for set-valued dynamical systems with compact attractors, e.g., [224], thus the convergence of the solutions is indeed uniform. Since the set $\mathcal{A}$ in (3) is not compact, we are forced to constrain a priori the trajectories of τ in (3.22) to the compact set K_ρ, which can be selected arbitrarily large to encompass any complete solution of interest. We stress that constraining the trajectories of consensus dynamics to compact sets is indeed needed in most applications, since the stability properties of points in the set $\mathcal{A}$ are not robust to arbitrarily small perturbations. Thus, in order to avoid tolls that due to arbitrarily small perturbations "slide" along the set $\mathcal{A}$ and grow unbounded, one will need to constrain τ a priori to a compact set. Examples of dynamics for bounded consensus are presented in [220].

Remark 15 *If one is willing to impose additional regularity assumptions on the social dynamics* (3.20)*, e.g. a uniform Lipschitz condition with respect to τ, a convergence result can be obtained in Theorem 9 without a priori constraining the trajectories of τ. This follows by the result in [91] for non-bounded attractors. However, said results could still generate unbounded tolls.* □

We finish this section by discussing the case when the sensitivity s of the entire population has a known value that is not necessarily 1. In this case the set $\mathcal{A}$ will be given by (3.9) with $\tau^* = -\frac{b}{2s}$ Since the sensitivity multiplies the input u in the social dynamics (3.20), convergence to the optimal set $\mathcal{A}$ can be recovered by simply defining the output function $h_\tau(\tau)$ in (3.23) as $h_\tau(\tau) = \frac{\tau}{s}$.

3.4 Adaptive Pricing Mechanisms with Population Excitation

One of the standing assumptions in Sections 3.2 and 3.3, was the ability of the Oracle to generate sampled values of the marginal costs $\nabla c(x)$ as part of its output mapping. In practice, this implies that either the Oracle can directly sample the gradient of the costs $c_i(\cdot)$, or that the mathematical structure of $c_i(\cdot)$ is known for all $i \in \{1, \dots, N\}$. However, in most cyber-physical societal systems these assumptions are difficult to satisfy. In this section, we address this issue by making the observation that even though the results of the previous section can be seen as a robustness result for the distributed welfare dynamics under small perturbations induced by social dynamics that are not infinitely fast, they also open the door for the *exploitation* of the social dynamics (3.20) to learn information from the underlaying game based on the evolution of the social state x. This can be achieved by sharing ideas from adaptive control theory e.g., [1], [209].

In order to exploit the social dynamics to learn information from the game, for each pricing mechanism $i \in \mathcal{V}$, let $\breve{c}_i(x) := \breve{w}_i^\top \phi_i(x_i)$ be an approximation of the cost function $c_i(\cdot)$, where $\breve{w}_i \in \mathbb{R}^m$ is a vector of tunable weights, and $\phi_i : \mathbb{R} \to \mathbb{R}^m$ is a continuous vector valued basis function. A simple choice of basis functions for affine congestion

games is given by $\phi_i = [x_i, 1]^\top$, for all $i \in \{1, \dots, N\}$, since the true parameters are $w_i^* = [a_i, b_i]^\top$. In order to online learn this parameters consider the simple estimator

$$\dot{\breve{w}}_i = -\frac{\phi_i(x_i)}{\big(1 + \phi_i^\top(x_i)\phi_i(x_i)\big)^2}\Big(\breve{c}_i(x_i) - c_i(x_i)\Big), \tag{3.25}$$

which can be seen as a normalized gradient-based algorithm of the estimation error [1, Sec. 4.3.5]. System (3.25) only needs to mesaure the value of the social state x_i and cost function $c_i(x_i)$ associated to the i^{th} resource. Therefore, since now the only information that the individual pricing mechanism i requires is the pair $(x_i, c_i(x_i))$, the output (3.11) of the social dynamics is defined as

$$h_x(x) = \begin{pmatrix} h_{x,1}(x) \\ h_{x,2}(x) \end{pmatrix} = \begin{pmatrix} x \\ c(x) \end{pmatrix}. \tag{3.26}$$

To guarantee convergence of (3.25) to the true parameters w_i^*, the social state x_i must have enough excitation. To provide this excitation to the population, consider the time-invariant signal generator given by the differential inclusion

$$\dot{\mu}_i \in \Psi_i(\mu_i), \quad \mu_i \in \Lambda_i, \tag{3.27a}$$

$$y_i = h_{\mu,i}(\mu_i), \tag{3.27b}$$

where for each $i \in \{1, \dots, N\}$ the set $\Lambda_i \subset \mathbb{R}^\ell$ is compact, $\ell \in \mathbb{Z}_{\geq 1}$, the set-valued mapping $\Psi_i : \mathbb{R}^\ell \to \mathbb{R}^\ell$ is outer-semicontinuous, locally bounded, and convex-valued, and $h_{\mu,i} : \mathbb{R}^\ell \to \mathbb{R}$ is continuous. The signal generator is assumed to satisfy the following stability condition.

Assumption 19 *The dynamic signal generator* (3.27) *renders a nonempty compact set* $\mathcal{A}_{\mu,i} \subset \Lambda_i$ *GAS.* □

Assumption 19 is mainly needed to guarantee a uniform bound property on the signal μ. Standard signal generators of the form (3.27) include linear periodic oscillators defined on the circle $\Lambda_i = \mathbb{S}$, or nonlinear systems rendering asymptotically stable a limit cycle .

Using the excitation signal μ, and the output function (3.27b), the overall toll is now defined as

$$\tau_{\text{total}} = \tau + \text{diag}(a) \cdot h_\mu(\mu), \tag{3.28}$$

where $\mu := [\mu_1, \dots, \mu_N]^\top$, $\text{diag}(a)$ is a $N \times N$ diagonal matrix with diagonal entries given by the vector $a = [a_1, \dots, a_N]^\top$, with $a_i \in \mathbb{R}_{>0}$ for all $i \in \{1, \dots, N\}$, and $h_\mu := [h_{\mu,1}, \dots, h_{\mu,N}]^\top$. The nominal toll τ is generated by the distributed welfare-gradient dynamics

$$\dot{\tau} = \alpha \, \mathcal{L}\Big(h_{x,2} + \breve{w}^\top \nabla\phi(h_{x,1}) \cdot h_{x,1}\Big), \tag{3.29}$$

where $\alpha \in \mathbb{R}_{>0}$, and where

$$\breve{w}^\top \nabla\phi(h_{x,1}) = \text{diag}\left(\left[\breve{w}_1 \frac{\partial \phi_i(x_i)}{\partial x_i}, \dots, \breve{w}_N \frac{\partial \phi_N(x_N)}{\partial x_N}\right]\right).$$

Based on this, the main idea that we seek to convey in this section is that, if the signal generator (3.27) is designed such that for each fixed nominal toll τ in (3.28) the overall toll τ_{total} provides enough *excitation*, in the PE sense (see 2.89), to the population state, then the combination of the distributed welfare-gradient dynamics (3.22) and the parameter estimator (3.25) allows us to dispense with the assumption of the existence of a social Oracle that has perfect information of the game. To exploit this idea the signal μ generated by (3.27) must provide enough excitation to the social system.

Assumption 20 *Let $\rho \in \mathbb{R}_{\geq 0}$ and consider the system*

$$\left.\begin{aligned} \dot{\mu} &\in \Psi(\mu) \\ \dot{\tau} &= 0 \\ \dot{x} &\in F(x, \tau_{total}) \end{aligned}\right\}, \ (\mu, x, \tau) \in \Lambda \times \Delta \times K_\rho, \tag{3.30}$$

where $\Lambda := \Lambda_1 \times \ldots \times \Lambda_N$, $\Psi := \Psi_1 \times \ldots \times \Psi_N$, and K_ρ is defined as in (3.24)*. There exists $a^* \in \mathbb{R}_{>0}$ such that for all amplitude vectors $a \in \mathbb{R}^N_{>0}$ with entries satisfying $a_i \in (0, a^*]$ and all solutions of* (3.30)*, we have that the signals $\phi_i(x_i(t))$ satisfy* (2.89) *$i \in \{1, \ldots, N\}$.* □

Let $\mathcal{A}_\mu := \mathcal{A}_{\mu,1} \times \ldots \times \mathcal{A}_{\mu,N}$, where each $\mathcal{A}_{\mu,i}$ is given by Assumption 19. Let $\rho \in \mathbb{R}_{>0}$ and consider the compact set

$$\mathcal{A}_{\text{closed-loop}} = \mathcal{A}_\mu \times (\mathcal{A} \cap K_\rho) \times \{x^*\} \times \{w^*\}. \tag{3.31}$$

The following theorem generalizes the results of the previous sections.

Theorem 4 *Consider the closed-loop system obtained by the interconnection of: the signal generator* (3.27)*, the estimator* (3.25)*, the social dynamics* (3.20) *with input given by* (3.28) *and output given by* (3.26)*, and the learning mechanism* (3.22) *with input given by* (3.26) *and output given by* (3.23)*. Then, for each $(\rho, \varepsilon) \in \mathbb{R}^2_{>0}$ there exists $\alpha^* \in \mathbb{R}_{>0}$ such that for all $\alpha \in (0, \alpha^*]$ there exists $a^* \in \mathbb{R}_{>0}$ such that for all $a \in (0, a^*)$ every complete solution $(\mu, \tau, x, \breve{w})$ of the closed-loop system with τ constrained to K_ρ converges to $\mathcal{A}_{\text{closed-loop}} + \varepsilon\mathbb{B}$ in finite time.* □

In words Theorem 4 says for each compact set where the tolls are constrained, and for any arbitrarily small ε-neighborhood of the socially optimal state x^*, it is always possible to select the amplitude of the excitation signals and the gain of the

distributed welfare gradient dynamics, such that complete solutions of the adaptive pricing mechanism incentivize the society state x towards an ε-neighborhood of the socially optimal state x. This is achieved by using only measurements of x_i and the costs $c_i(x_i)$, i.e., the pricing mechanisms are agnostic with respect to the game.

3.5 Numerical Example

To illustrate the geometrical interpretation of the pricing mechanism, we present in this section a simple example of an affine congestion game with two resources, i.e., $\mathcal{V} = \{1, 2\}$, and matrices A and b with entries $a_1 = 3$, $a_2 = 2$, $b = 2.5$, $b = 2$. We consider first the case when the pricing mechanisms have access to a dynamic Oracle of the form (3.20), which delivers to each mechanism $i \in \mathcal{V}$ sampled values of $c_i(x_i)$ and $\frac{\partial c_i(x_i)}{\partial x_i}$. For the social dynamics we consider the Brown-von Neumann-Nash dynamics [], i.e.,

$$\dot{x}_i = \max\{0, \bar{c}_i(x, \tau)\} - x_i \sum_{j \in \mathcal{N}} \max\{0, \bar{c}_j(x, \tau)\} \tag{3.32}$$

where $\bar{c}_i(x, \tau) = \hat{c}_i(x_i, \tau_i) - \sum_{j \in \mathcal{V}} \hat{c}_j(x_j, \tau_j) x_j$, and

$$\hat{c}_i(x_i, \tau_i) = -(a_i x_i + b_i + \tau_i), \quad \forall\ i \in \mathcal{V}. \tag{3.33}$$

which satisfy Assumptions 17 and 18. We select the set $\mathcal{K}_\rho$ with $\rho = 10$ to make sure that every solution of interest was complete.

Figure 3.1 shows the convergence of the tolls to the unknown set $\mathcal{A}$ of optimal tolls that incentivize socially optimal states, from four different initial conditions. The red points denote the theoretical optimal toll (3.14). The evolution of the toll τ for the case when $\tau(0) = [-2, -2, 5]^\top$ is shown in Figure 3.2. The inset shows the evolution of the social state x towards the socially optimal Nash equilibrium. To address the

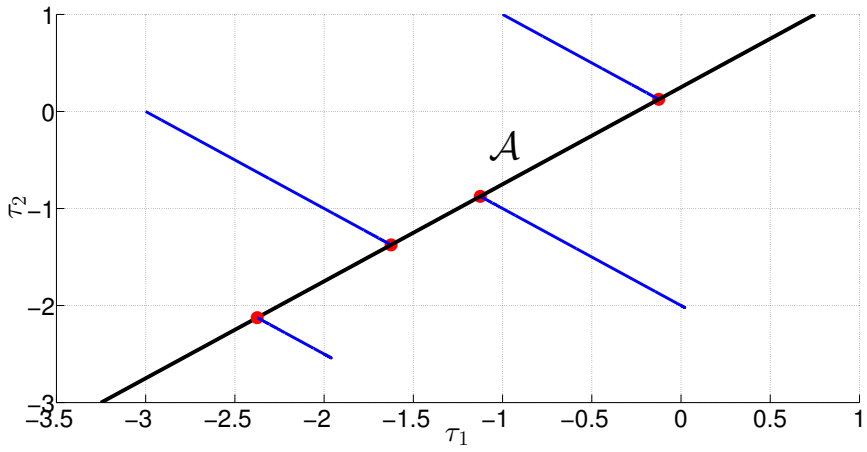

Figure 3.1: Convergence to the unknown set of optimal tolls $\mathcal{A}$, from 4 different initial conditions.

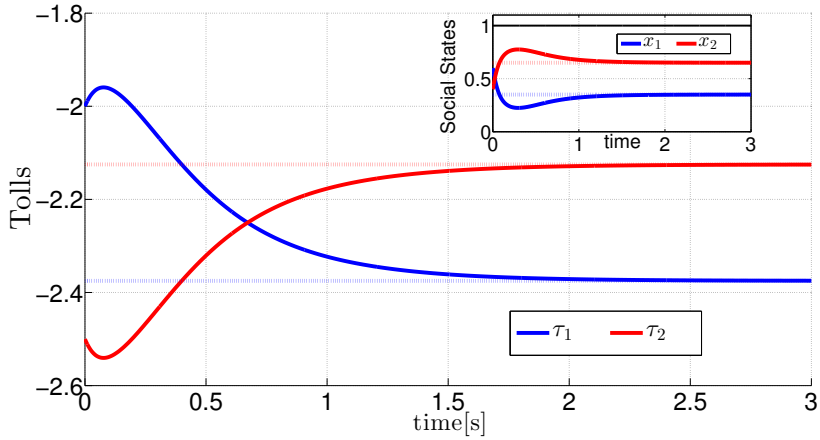

Figure 3.2: Evolution in time of the optimal toll

case when then parameters of the game are unknown for the pricing mechanisms, we also simulate the adaptive pricing mechanisms with population excitation presented in Section 3.4. In this case, for each pricing mechanism we use a signal generator (3.27) of the form

$$\begin{bmatrix} \dot{\mu}_{1,i} \\ \dot{\mu}_{2,i} \end{bmatrix} = \begin{bmatrix} 0 & -\omega_i \\ \omega_i & 0 \end{bmatrix} \begin{bmatrix} \mu_{1,i} \\ \mu_{2,i} \end{bmatrix}, \quad [\mu_{1,i}, \mu_{2,i}]^\top \in \mathbb{S},$$
$$\dot{\mu}_{3,i} = -\beta_i \cdot (\mu_{3,i} + \epsilon), \quad \beta_i, \epsilon \in \mathbb{R}^2_{>0},$$
$$y_i = h_{\mu,i}(\mu_i) = \mu_{3,i} \cdot \mu_{1,i}.$$

which generates an output that is an exponentially decaying sinusoid signal. Note that the dynamics of this system render the set $\mathbb{S} \times \{\epsilon\}$ UGAS, thus satisfying Assumption 19. The frequencies of the oscillator are selected as $\omega_1 = 40$ and $\omega_2 = 50$. Figure 3.3 shows the evolution in time of the pricing tolls τ_i converging to its optimal value on the set $\mathcal{A}$. Note that convergence to the optimal toll is achieved in approximately 6 seconds. Figure (3.4) shows the evolution in time of the social state, which slowly decays to a neighborhood of the optimal social state. Note that in practice the excitation signals $h_{\mu,i}$ are turned off after an initial learning phase, which in this case takes approximately 10 seconds. After turning off the excitation signal the social state x settles to a steady state value ε-close to the optimal social Nash flow x^*. This case is shown in Figure 3.5. Note that here the full utilization assumption is violated during the first second of the simulation. Nevertheless, convergence to the optimal set of tolls is still achieved.

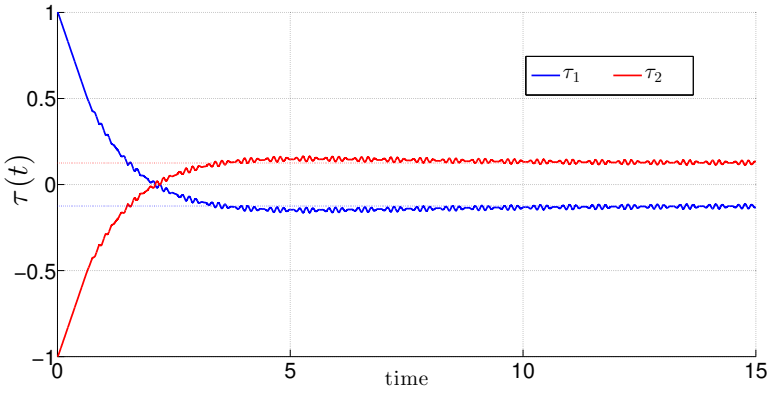

Figure 3.3: Evolution in time of the tolls.

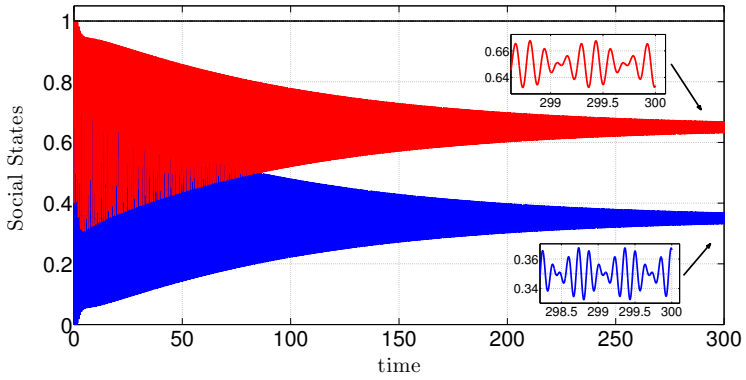

Figure 3.4: Evolution in time of the social state.

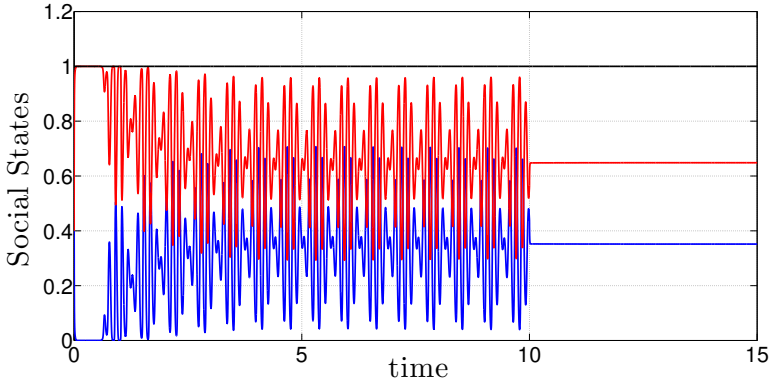

Figure 3.5: Evolution of the social state with excitation turned off after 10 seconds.

Chapter 4

Event-Triggered Sampled-Data Extremization

In the previous chapters we studied learning dynamics that require continuous measurements of the output of the plant in order to update the input. On the other hand, a different approach considered in the literature studies the problem of designing learning mechanisms where only periodic samples of the output of the plant can be obtained. This approach usually relies on stability and robustness results for standard periodic sampled-data systems. In this chapter, we show that, by considering a class of event-triggered controllers, it is possible to significantly improve the rate of convergence of the closed-loop sampled-data system. Moreover, we show that a variety of different set-valued discrete-time learning mechanisms can be implemented in a model-free way, provided some particular regularity conditions are satisfied.

4.1 Model and Problem Statement

Consider a plant with input $u \in \mathbb{R}^n$, state $\theta \in \mathbb{R}^p$, and output $y \in \mathbb{R}$, characterized in open-loop by the dynamics

$$(\theta, u) \in \mathbb{R}^p \times \mathbb{U} : \begin{cases} \dot{\theta} \in f(\theta, \alpha(\theta, u)) \\ \dot{u} = 0 \end{cases}, \quad y = \varphi(\theta), \tag{4.1}$$

where $\alpha : \mathbb{R}^p \times \mathbb{R}^n \to \mathbb{R}^n$ is a feedback law, $f : \mathbb{R}^p \times \mathbb{R}^n \rightrightarrows \mathbb{R}^p$ is a set-valued mapping, $\varphi : \mathbb{R}^p \to \mathbb{R}$ is an output function, and $\mathbb{U} := \hat{\mathbb{U}} + 1\mathbb{B} \subset \mathbb{R}^n$ is the set where the input u is constrained to evolve. The unitary inflation on $\hat{\mathbb{U}}$ is motivated by the fact that the controller will be designed such that the signal u will satisfy $u(t) \in \hat{\mathbb{U}} + a\mathbb{B} \subset \mathbb{U}$ for all $t \geq 0$, where $a \in (0, 1)$ is a tunable parameter. Note that since (4.1) is a purely continuous-time system we omit the discrete-time index j in this section.

Similarly to the previous chapters, we impose the following regularity conditions on the plant (4.1).

Assumption 21 *(Regularity) The set-valued mapping $P : \mathbb{R}^p \times \mathbb{R}^n \rightrightarrows \mathbb{R}^p$, defined as $P(\theta, u) := f(\theta, \alpha(\theta, u))$, is OSC, LB, and convex valued with respect to $\mathbb{R}^p \times \mathbb{U}$. The mapping $\varphi(\cdot)$ is continuously differentiable. The set $\hat{\mathbb{U}}$ is closed.*

Assumption 22 *(UGAS) There exists a feedback law $\alpha(\cdot, \cdot)$, and an OSC and LB set-valued mapping $H : \mathbb{R}^n \rightrightarrows \mathbb{R}^p$, such that for each $\rho > 0$ the set $M_\rho := \{(\theta, u) : \theta \in H(u), u \in \rho\mathbb{B} \cap \mathbb{U}\}$ is UGAS for system (4.1) with restricted flow set $\mathbb{R}^p \times (\rho\mathbb{B} \cap \mathbb{U})$. Moreover, for all $u \in \mathbb{U}$ and for each pair $\theta, \theta' \in H(u)$ we have that $\varphi(\theta) = \varphi(\theta')$.*

In this chapter we will also impose the following condition on the plant (4.1).

Assumption 23 *(Regularity at Equilibrium) Let P and H be defined as in Assumptions 21 and 22. Then, for each $u \in \mathbb{U}$ we have that $P(\theta, u) = \{0\}$ if and only if $\theta \in H(u)$.*

Using the definition of $H(\cdot)$ in Assumption 22, the *response map* associated to system (6.2) is again defined as

$$J(u) := \{\varphi(\theta) : \theta \in H(u)\}, \tag{4.2}$$

for all $u \in \mathbb{U}$. The following assumption characterizes the types of response maps J that we study.

Assumption 24 *(Regularity and Feasibility of J) The function $J(\cdot)$ is locally Lipschitz and regular [225, Def. 2.3.4], and there exists a nonempty compact set $\mathcal{A}_u \subset \hat{\mathbb{U}}$ corresponding to the solutions of the problem*

$$\textit{optimize} \quad f(J(u)), \quad \textit{s.t.} \quad u \in \hat{\mathbb{U}}. \tag{4.3}$$

Remark 16 *As in the previous section, the optimization problem* (4.3) *may correspond to a game theoretic problem or a distributed optimization problem defined on a multi-agent system.*

We assume that the mappings P, φ, H, and J are unknown or poorly known, precluding the implementation of model-based extremization algorithms. Based on this, the main goal in this chapter is to design efficient *learning dynamics* that regulate the input u of the plant (4.1) to a neighborhood of the optimal set $\mathcal{A}_u$ using only sequential *measurements* of the output y. To achieve this, we consider an event-triggered control (ETC) that will continuously monitor a triggering signal $z(t)$ related to the

plant (4.1) in order to evaluate the convergence of θ to a neighborhood of M_ρ. A high-level scheme of the closed-loop event-triggered system is shown in Figure 4.1 for the case when $z(t) = y(t)$. Since here we will focus our attention on output-based event-triggered control, the following "observability" assumption will be needed.

Assumption 25 *(Observability) Consider the set*

$$Z := \{(\theta, u) \in \mathbb{R}^{p+n} : \exists\ \zeta \in P(\theta, u)\ s.t.\ \nabla\varphi(\theta)^\top \zeta = 0\}.$$

Then, for each $K \subset \mathbb{R}^{p+n}$ and $\tilde{e} \in \mathbb{R}_{>0}$ there exists a $\delta \in \mathbb{R}_{>0}$ such that for all solutions (θ, u) of system (4.1) with initial condition in K, and all $T \geq 0$, we have that: $(\theta^\top, u^\top)^\top(t) \in Z + \delta\mathbb{B}$ for all $t \geq T \Rightarrow \theta(t) \in H(u(t)) + \tilde{e}\mathbb{B}$ for all $t \geq T$.

By exploiting the well-posedness and stability properties of system (4.1), as well as the "observability" property induced by Assumption 25, the following proposition can be established.

Proposition 10 *(ϵ-Observability) Suppose that Assumptions 21, 22, and 25 hold. Then, for each $K_0 := K_\theta \times (\mathbb{U} \cap \rho\mathbb{B}) \subset \mathbb{R}^{p+n}$ and $\tilde{e} \in \mathbb{R}_{>0}$ there exists $\epsilon \in \mathbb{R}_{>0}$ such that for all solutions (θ, u) of (4.1) with initial conditions in K_0, and all $T \geq 0$, we have that: $|\dot{y}(t)| \leq \epsilon$ for almost all $t \geq T \Rightarrow \theta(t) \in H(u(t)) + \tilde{e}\mathbb{B}$ for all $t \geq T$.*

Proposition 10 ensures that the condition $|\dot{y}(t)| \leq \epsilon$ for all $t \geq T$, with $T \geq 0$, is an indication of convergence of θ to $H(u)$. We stress that Assumption 25 is only needed for output-based event-triggered control. If, on the other hand, measurements of $\theta(t)$ are available, a state-based event-triggered approach may not require Assumption 25.

Remark 17 *In the classic sampled-data based learning approach, Proposition 10 is usually replaced by an assumption regarding the existence of a sufficiently large T such*

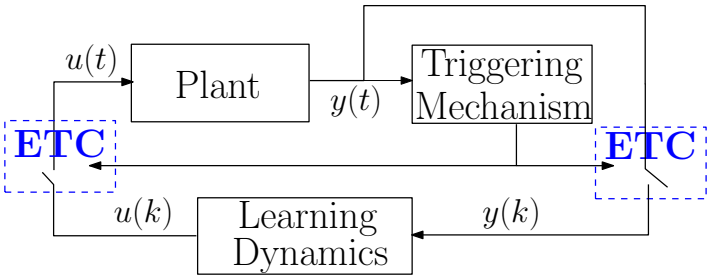

Figure 4.1: Closed-loop system with event-triggered control (ETC).

that, whenever a measurement of the output y is taken, the second containment in Proposition 10 holds, see [87, Assump. 1.4]. If, additionally, $\hat{\mathbb{U}}$ is also assumed to be bounded, the existence of such T can easily be established, see [135, Lemma 10].

4.2 Event-Based Triggering Mechanism

In this section, we first characterize a class of robust dynamic triggering mechanisms that receive uniformly sampled values of a triggering signal $z(t)$ related to system (4.1), guaranteeing that the control system is triggered only after a given event condition has been verified during a given time window. After this, we show how to use these mechanisms to achieve quasi-steady state triggering in plants satisfying Assumption 25.

4.2.1 Robust Triggering Mechanisms

Consider a class of dynamic triggering mechanisms that make use of three auxiliary states $(\tau, \gamma, \xi) \in [0,1] \times [0,1] \times \mathbb{R}^m$, a set $S \subset \mathbb{R}^m$, and a triggering signal

$$z = f_z(y, \theta), \tag{4.4}$$

where $f_z : \mathbb{R} \times \mathbb{R}^p \to \mathbb{R}$ maps information from the output and/or states of system

(4.1) to a real number. The state τ corresponds to a fast resetting clock, which is reset to 0 every ΔT seconds, where $\Delta T \in \mathbb{R}_{>0}$ is a small tuning parameter. Every time that τ is reset to 0 the triggering signal z is sampled, and its sampled value is used to update a memory state ξ as $\xi^+ \in G_\xi(\xi, z)$, where $G_\xi : \mathbb{R}^m \times \mathbb{R} \rightrightarrows \mathbb{R}^m$ is a set-valued mapping. Also, whenever τ is reset to 0 and $\xi \in \text{int}(S)$, a counter state γ is increased by a small quantity $\frac{r_e}{\gamma^*}$, where $(r_e, \gamma^*) \in (0,1) \times \mathbb{Z}_{>0}$. If $\xi \notin S$, the counter γ is reset to zero. Finally, since we aim to design *robust* triggering mechanisms that under small perturbations behave "similarly" to the nominal unperturbed mechanism, any of the two previously discussed updates for γ are allowed whenever $\xi \in \text{bd}(S)$, a condition that may emerge when $\xi \in \text{int}(S)$ and arbitrarily small perturbations act on ξ.

Assumption 26 (Regularity of Triggering Mechanism) *The set $S \subset \mathbb{R}^m$ satisfies int$(S) \neq \emptyset$. The set-valued mapping $G_\xi(\cdot,\cdot)$ satisfies (C3) with respect to $\mathbb{R}^m \times \mathbb{R}$, and $f_z(\cdot,\cdot)$ is continuous with respect to both arguments.*

Remark 18 *The design of the set S and the mappings f_z and G_ξ, are application-dependent. The mapping f_z must be selected based on the available measurements of system (4.1), e.g., $f_z = y$ for output-based event-triggered control, or $f_z = \theta$ for state-based event-triggered control. The set S characterizes a particular condition of interest that is periodically verified via measurements of z, e.g., tracking or regulation error, boundedness of the states, quasi-steady state conditions, etc. Finally, the mapping G_ξ can be use to simply assign sampled values of z to the entries of the memory state ξ, or it can be designed as a dynamic filter for smoothing z.*

Let the set valued mapping $\mathbb{I}_S : \mathbb{R}^m \rightrightarrows \mathbb{R}$ be defined as the outer semicontinuous

hull of the indicator function $\mathbb{1}_S(\cdot)$, i.e.,

$$\mathbb{I}_S(\xi) := \begin{cases} \{0,1\}, & \text{if } \xi \in \mathrm{Bd}(S) \\ 1, & \text{if } \xi \in \mathrm{int}(S) \\ 0, & \text{if } \xi \notin S. \end{cases} \tag{4.5}$$

Then, the previously discussed mechanism, interconnected with the plant (4.1), can be modeled as a HDS with overall state $x_{s,u} := (x_s^\top, u^\top)^\top \in \mathbb{R}^{N_s} \times \mathbb{R}^n$, where $x_s := (\tau, \gamma, \xi^\top, \theta^\top)^\top$, $N_s := 2 + m + p$, $m \in \mathbb{Z}_{>0}$, and data $\mathcal{H}_s$ given by

$$\mathcal{H}_s := \Big\{ C_s \times \mathbb{U}, F_s \times \{\mathbf{0}_n\}, D_s \times \mathbb{U}, G_s \times \{\mathrm{i}_d\} \Big\}, \tag{4.6}$$

where $\mathrm{i}_d : \mathbb{R}^n \to \mathbb{R}^n$ is the identity function, and where the mappings F_s, G_s, and sets C_s, D_s are defined as follows:

$$C_s := [0,1] \times [0,1] \times \mathbb{R}^m \times \mathbb{R}^p \,, \tag{4.7a}$$

$$\begin{pmatrix} \dot{\tau} \\ \dot{\gamma} \\ \dot{\xi} \\ \dot{\theta} \end{pmatrix} \in F_s(x_s, u) := \begin{pmatrix} \frac{1}{\Delta T} \\ 0 \\ \mathbf{0}_m \\ P(\theta, u) \end{pmatrix}, \tag{4.7b}$$

$$D_s := \{1\} \times [0,1] \times \mathbb{R}^m \times \mathbb{R}^p \,, \tag{4.7c}$$

$$\begin{pmatrix} \tau^+ \\ \gamma^+ \\ \xi^+ \\ \theta^+ \end{pmatrix} \in G_s(x_s, z) := \begin{pmatrix} 0 \\ \left\{ \min\left\{ \left(\gamma + \frac{r_e}{\gamma^*} \right) \cdot s, 1 \right\}, s \in \mathbb{I}_S(\xi) \right\} \\ G_\xi(\xi, z) \\ \theta \end{pmatrix}. \tag{4.7d}$$

Under Assumptions 21, 22, and 26, the HDS (4.6) is well-posed, and it corresponds

to a hybrid system that jumps every ΔT seconds, i.e., every time that $\tau = 1$. Note that the function $\min\{\cdot, 1\}$ in (4.7d) simply guarantees the positive invariance of the set $[0, 1]$ for the counter γ.

We characterize the behavior during jumps of the solutions of the HDS (4.6) in terms of *sub-event* and *event* sets. The *sub-event* sets are characterized mainly by the condition $\xi \in S$, while the *event-sets* require an additional lower bound on the counter state γ.

Definition 1 *A solution $x_{s,u}$ of (4.6) generates a* sub-event *(resp.* strict sub-event*) at the hybrid time $(t, j) \in dom(x_{s,u})$, if $x_{s,u}(t, j) \in D_{se} \times \mathbb{U}$ (resp. $x_{s,u}(t, j) \in \mathring{D}_{se} \times \mathbb{U}$), where*

$$D_{se} := \{1\} \times [0, 1] \times S \times \mathbb{R}^p, \tag{4.8a}$$

$$\mathring{D}_{se} := \{1\} \times [0, 1] \times int(S) \times \mathbb{R}^p. \tag{4.8b}$$

Definition 2 *A solution $x_{s,u}$ of (4.6) generates an* event *(resp.* strict event*) at the hybrid time $(t, j) \in dom(x_{s,u})$, if $x_{s,u}(t, j) \in D_e \times \mathbb{U}$ (resp. $x_{s,u}(t, j) \in \mathring{D}_e \times \mathbb{U}$), where*

$$D_e : = \{1\} \times [r_e, 1] \times S \times \mathbb{R}^p, \tag{4.9a}$$

$$\mathring{D}_e : = \{1\} \times (r_e, 1] \times int(S) \times \mathbb{R}^p. \tag{4.9b}$$

Using Definitions 1 and 2 we obtain the following lemma which relates the occurrence of events and sub-events:

Lemma 5 *Let $(\Delta T, \gamma^*) \in \mathbb{R}_{>0} \times \mathbb{Z}_{>0}$, and $r_e \in (0, 1)$. Let $K := \{0\} \times \{0\} \times K_\xi \times K_\theta \times K_u$, where $K_\xi \subset \mathbb{R}^m$, $K_\theta \subset \mathbb{R}^p$, and $K_u \subset \mathbb{R}^n$ are compact. Then, for all $x_{s,u} \in \mathcal{S}_{\mathcal{H}_s}(K)$*

generating an event at some time $(t^*, j^*) \in dom(x_{s,u})$ *we have that*

$$\sum_{k=0}^{\gamma^*} \mathbb{1}_{D_{se}} \left(x_s(t^* - k\Delta T, j^* - k) \right) = \gamma^* + 1, \tag{4.10}$$

and $t^* \geq (\gamma^* + 1)\Delta T$, $j^* \geq \gamma^*$.

It is easy to see that equality (4.10) is also a sufficient condition to guarantee that a solution $x_{s,u}$ is generating an event at the hybrid time (t^*, j^*). On the other hand, note that the simple verification of the condition $\xi \in S$ at the end times of the last $\gamma^* + 1$ consecutive intervals of ΔT seconds of flow is not a sufficient condition to guarantee that a given solution $x_{s,u}$ generates an event. This is because the occurrence of non-strict sub-events does not necessarily imply that γ must increase. This behavior is induced on purpose by using the outer semicontinuous hull $\mathbb{I}_S(\cdot)$ in (4.7d) instead of the standard indicator function, and it aims to give a robust characterization of the behavior of the solutions of system (4.6) under arbitrarily small disturbances that may be problematic when $\xi \in \mathrm{bd}(S)$.

The following lemma is instrumental in order to guarantee that *every* solution of system (4.6) will eventually generate a (strict) event during jumps.

Lemma 6 *Consider the HDS* (4.6). *Let* $(\Delta T, \gamma^*) \in \mathbb{R}_{>0} \times \mathbb{Z}_{>0}$ *and* $r_e \in (0, 1)$. *Suppose that Assumptions 21, 22, and 26 hold. Then, system* (4.6) *is forward complete and well-posed. Additionally, suppose that the following assumption holds:*

A1. *For each compact set* $K = K_s \times K_u \subset \mathbb{R}^{2+m+p+n}$ *there exists a* $T_{\varepsilon,K} \in \mathbb{R}_{>0}$ *such that for all* $x_{s,u} \in \mathcal{S}_{\mathcal{H}_s}(K)$ *and* $(t, j) \in dom(x_{s,u})$ *satisfying* $t + j > T_{\varepsilon,K}$ *we have that* $\xi(t, j) \in int(S)$.

Then, there exists a $T^* > T_{\varepsilon,K}$ *such that for all* $x_{s,u} \in \mathcal{S}_{\mathcal{H}_s}(K)$ *and* $(t, j) \in dom(x_{s,u})$ *satisfying* $t + j > T^*$ *we have that* $x_{s,u}(t, j) \in D_s \times K_u \Rightarrow x_{s,u}(t, j) \in \mathring{D}_e \times K_u$.

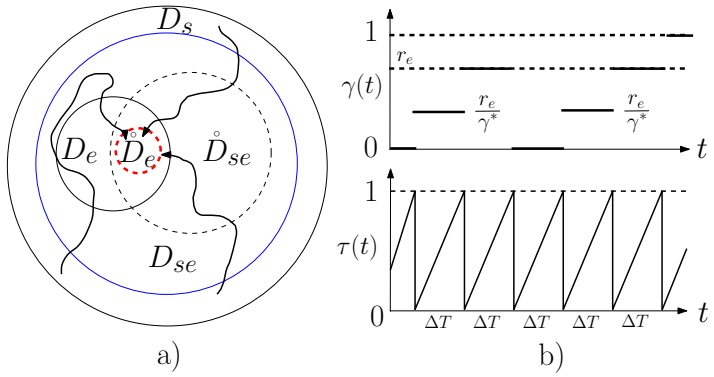

Figure 4.2: a) Three different solutions *during jumps*, eventually generating a strict-event. b) Evolution of γ and τ.

Lemma 6 says that if given a fixed input u the state ξ uniformly converges to int(S), then there exists a T^* such that for all $t + j \geq T^*$ every solution of (4.6) will generate a strict event (and an event) every time that a jump occurs. Figure 4.2-a) shows an abstract representation of the relation between the jump set and the sub-event and event-sets, as well as the different behaviors of the solutions of the HDS (4.6) during jumps. In particular, the simultaneous occurrence of an event and a non-strict sub-event may reset the timer γ to 0 forcing the state x_s out of the event set. However, under Assumptions 21, 22, 26, and **A1**, a strict-event will eventually occur. Figure 4.2-b) illustrates this for the case when $\gamma^* = 2$.

4.2.2 Event-triggered Closed-Loop System

The HDS (4.7) will be used to trigger a discrete-time control system with state $x_u \in \mathbb{R}^{N_u}$, given by the dynamics

$$x_u^+ \in G_u(x_u, y), \quad x_u \in D_u, \tag{4.11}$$

where y is the output of system (4.1), the input u is a state component of x_u, and $\mathbb{U} \subset D_u$. The control dynamics satisfy the following assumption.

Assumption 27 *(Regularity) The set-valued mapping $G_u : \mathbb{R}^{N_u} \times \mathbb{R} \to \mathbb{R}^{N_u}$ satisfies (C3) with respect to $D_u \times \mathbb{R}$. The set D_u satisfies (C1). For each $x_u \in D_u$ and $y \in \mathbb{R}$ there exists a $v \in G_u(x_u, y) \cap D_u$.*

Based on this, the event-triggered closed-loop HDS obtained by interconnecting (4.7) and (4.11) has a global state $x := (x_s^\top, x_u^\top)^\top \in \mathbb{R}^{N_s+N_u}$, and it is represented by the HDS $\tilde{\mathcal{H}} := \{\tilde{C}, \tilde{F}, \tilde{D}, \tilde{G}\}$ with data given by

$$\begin{aligned} \dot{x} \in \tilde{F}(x) &:= \begin{pmatrix} F_s(x_s, u) \\ \mathbf{0}_{N_u} \end{pmatrix}, \ \tilde{C} := C_s \times D_u, \\ x^+ \in \tilde{G}(x) &:= \tilde{G}_q(x_s, z, y), \qquad \tilde{D} := D_s \times D_u, \end{aligned} \tag{4.12}$$

where C_s, F_s, and D_s are given by (4.7a)-(4.7c), and the jump map $\tilde{G}_q$ is defined as

$$\tilde{G}_q := \begin{cases} \begin{pmatrix} G_s(x_s, z) \\ x_u \end{pmatrix}, & x_s \in D_s \backslash D_e \\ \begin{pmatrix} G_s(x_s, z) \\ x_u \end{pmatrix} \cup \begin{pmatrix} G_r(x_s) \\ G_u(x_u, y) \end{pmatrix}, & x_s \in D_e \backslash \mathring{D}_e \\ \begin{pmatrix} G_r(x_s) \\ G_u(x_u, y) \end{pmatrix}, & x_s \in \mathring{D}_e, \end{cases} \tag{4.13}$$

where G_s is given by (4.7d), z is defined as in (4.4), and the reset map G_r is given by

$$G_r(x_s) := (0, 0, \xi^\top, \theta^\top)^\top. \tag{4.14}$$

The following lemma characterizes the behavior of the HDS (4.12). The proof follows directly by Lemmas 5 and 6, and Assumption 27.

Lemma 7 *Consider the HDS* (4.12) *and suppose that Assumptions 21, 22, 26, and 27 hold. Then, system* (4.12) *is well-posed, and it generates at least one complete solution from every initial condition in* $\tilde{C} \cup \tilde{D}$. *Additionally, if Assumption* ***A1*** *holds, then every complete solution of system* (4.12) *triggers the control dynamics* (4.11) *infinitely often, and each pair of consecutive triggering times* $\{(t_1, j_1), (t_2, j_2)\}$ *satisfies* $t_2 + j_2 - t_1 - j_1 \geq T_L := (\gamma^* + 1)\Delta T + \gamma^*$.

Although Lemma 7 establishes a uniform *lower* bound for the amount of hybrid time that can pass between any two consecutive triggering times, as well as an infinitely often triggering property for the control dynamics, its does not entail a uniform *upper* bound for the amount of hybrid time that can pass between consecutive triggering times. However, under assumption **A1**, if a uniform bound can be established for x_u and θ, e.g., if $\mathbb{U}$ is also compact, said uniform upper bound between triggering times can be readily established. A detailed characterization of the stability properties of the control dynamics (4.11), and the closed-loop dynamics (4.12), will be addressed in Sections 4.3 and 4.4, respectively, for the case when $\mathbb{U}$ is only assumed to be closed.

Remark 19 *In system* (4.6) *the sub-event and event conditions are periodically verified every* ΔT *seconds. Since the control dynamics in* (4.13) *are triggered only when an event is detected, i.e.,* $x_s \in D_e$, *the control strategy in system* (4.12) *can be seen as a type of* periodic event-triggered control *(PETC) [128].*

4.2.3 An Application for Quasi-Steady State-based Triggering

According to Lemmas 5 and 7, systems of the form (4.12) verify online the satisfaction of the condition $\xi \in S$ during a window of time $(\gamma^* + 1)\Delta T$ before triggering the control system (4.11). For plants of the form (4.1), this type of mechanisms can be used to trigger a control system that requires a quasi-steady state condition of the

form $(\theta^\top, y)^\top(t) \in (H(u) \times \varphi(H(u))) + \tilde{\epsilon}\mathbb{B}$ for all $t \geq T^*$, for some $\tilde{\epsilon}$ sufficiently small, and some $T^* > 0$. For this purpose, consider a family of *steady-state identification mechanisms* that make use of a vector of $m \geq 2$ uniformly sampled measurements of the output y, given by

$$\bar{y}_{t_k} := \Big(y(t_k - (m-1)\Delta T), \ldots, y(t_k - \Delta T), y(t_k)\Big)^\top, \tag{4.15}$$

where $t_k \geq (m-1)\Delta T$. Each sequence $\bar{y}_{t_k}$ of the form (4.15) is mapped by a function $f_e(\cdot)$ that gives an approximation of $|\dot{y}(t_k)|$ on compact sets. This value is then compared with some tunable parameter $\epsilon \in \mathbb{R}_{>0}$ in order to obtain a conclusion pertaining to the validity of the bound $|\dot{y}(t_k)| \leq \epsilon$ at time t_k. By implementing this procedure for a sequence of vectors $\{\bar{y}_{t_k+\ell\Delta T}\}_{\ell=0}^{\ell^*}$ of the form (4.15), where $\ell^* \in \mathbb{Z}_{>1}$, a conclusion of whether or not the bound $|\dot{y}(t)| \leq \epsilon$ holds for almost all $t \in [t_k, t_k + \ell^*\Delta T]$, is obtained. This approach is aligned with several existing methods for online steady state identification in dynamical systems, where the function f_e can be used to model simple finite differences, or Runge-Kutta-based methods [191, Chapter 7], as well as more elaborated algorithms for triggering signals corrupted with noise [226]. Moreover, this methodology is easily adaptable for other numerical and statistical methods where the satisfaction of an ϵ-bound on a steady state index $f_e(\bar{y}_{t_k})$ is monitored, see [227], [228]. The following assumption aims to capture this idea.

Assumption 28 *(Data $(\Delta T, \gamma^*, f_e)$ of SSIM) Let $m \in \mathbb{Z}_{\geq 2}$, and suppose that Assumptions 21-23 hold. For each $\epsilon \in \mathbb{R}_{>0}$, each $\eta \in (0, \epsilon/2)$ and each compact set $K \subset \mathbb{R}^{p+n}$ there exists a continuous function $f_e : \mathbb{R}^m \to \mathbb{R}_{\geq 0}$, and a tuple $(\Delta T, \gamma^*) \in \mathbb{R}_{>0} \times \mathbb{Z}_{\geq 2m}$, such that for every solution of (4.1) with initial conditions in K the following holds:*

(a) For any $t_k \geq (m-1)\Delta T$ such that $\dot{y}(t_k)$ is defined, and any vector $\bar{y}_{t_k}$ having the

structure of (4.15), we have that $f_e(\bar{y}_{t_k}) \in \{|\dot{y}(t_k)|\} + \eta\mathbb{B}$.

(b) For any $t_k \geq \overline{T} := (\gamma^* - m)\Delta T$, *we have that if* $|\dot{y}(t)| \leq \epsilon,\ \forall\ t \in \{t_k - \overline{T}, t_k - \overline{T} + \Delta T, t_k - \overline{T} + 2\Delta T, \ldots, t_k\}$, *then* $|\dot{y}(t)| \leq \epsilon$, *for almost all* $t \geq t_k - \overline{T}$.

Remark 20 *Item (a) in Assumption 28 says that for each* $\eta > 0$ *it is possible to use a sequence of the form (4.15) with* ΔT *sufficiently small, such that an estimation of* $|\dot{y}(t_k)|$, *up to an* η*-bounded error, is obtained using an* m*-finite sequence of measurements of* y.

Remark 21 *Item (b) in Assumption 28 says that it is possible to select the sampling period* ΔT *sufficiently small, and* γ^* *sufficiently large, such that, if the bound* $|\dot{y}(t_k)| \leq \epsilon$ *is verified at a sequence of* $\gamma^* - m + 1$ *uniformly sampled points spanning the interval* $[t_k - \overline{T}, t_k]$, *then this* ϵ*-bound can be guaranteed for* almost all *time* $t \geq t_k - \overline{T}$. *Such* $\overline{T}$ *will always exist under Assumptions 21-23 (see Lemma 21 in Section H.2).*

There exists a vast amount of literature regarding numerical methods that satisfy Assumption 28. Simple examples include Euler based methods of different orders, Runge-Kutta methods [191, Chapter 7], as well as differentiators with smoothing for signals that are only locally absolutely continuous, or corrupted with noise [226], [229], [230].

Using data $(\Delta T,\ \gamma^*,\ f_e)$ satisfying Assumption 28, we can now make use of the triggering mechanism (4.6) to relate the occurrence of an event with the detection of a quasi-steady state condition in system (4.1). To achieve this, define the triggering signal (4.4) and the set S in (4.7d) as

$$f_z := y, \qquad S := \{\xi \in \mathbb{R}^m : f_e(\xi) \leq \varepsilon\}, \tag{4.16}$$

where $\varepsilon \in \mathbb{R}_{>0}$ is a tunable parameter. The mapping G_ξ can be defined as the linear system

$$\xi^+ = G_\xi(\xi, y) := A\xi + By, \tag{4.17}$$

with block matrices $A \in \mathbb{R}^{m\times m}$ and $B \in \mathbb{R}^{m\times 1}$ given by

$$A := \begin{bmatrix} \mathbf{0}_{m-1} & I \\ 0 & \mathbf{0}_{m-1}^\top \end{bmatrix}, \; B := \begin{bmatrix} \mathbf{0}_{m-1} \\ 1 \end{bmatrix}, \tag{4.18}$$

which simply assign a new measurement of $y(t)$ to the last entry of ξ, while the other entries satisfy the relation $\xi_i^+ = \xi_{i+1}$, for all $i = \{1, \dots, m-1\}$. This implies that, given any initial condition $\xi(0) \in \mathbb{R}^m$, after m jumps the state ξ in (4.17) will have the structure of (4.15), acting as a memory state.

The following proposition is the main result of this section, and it relates the occurrence of an event generated by a solution of system (4.6), with the convergence of θ and y to an ϵ-neighborhood of their steady state values.

Proposition 11 *Suppose that Assumptions 21-23, 25, and 28 hold, and consider the HDS* (4.6) *with f_z, S, and G_ξ defined as in* (4.16) *and* (4.17)*, respectively. Let $(\tilde{e}, \rho) \in \mathbb{R}^2_{>0}$, $r_e \in (0,1)$, and $K := K_s \times (\rho\mathbb{B} \cap \mathbb{U}) \subset \mathbb{R}^{2+m+p+n}$ be compact, where $K_s := K_\tau \times K_\gamma \times K_\xi \times K_\theta$, $[0,1] \subset K_\tau$, and $[0,1] \subset K_\gamma$. Then, there exist constants $(\underline{\varepsilon}, \overline{\varepsilon}, \Delta T, \gamma^*) \in \mathbb{R}^3 \times \mathbb{Z}_{\geq 2m}$ with $\overline{\varepsilon} > \underline{\varepsilon}$, and a nonnegative function $f_e : \mathbb{R}^m \to \mathbb{R}_{\geq 0}$, such that for each $\varepsilon \in (\underline{\varepsilon}, \overline{\varepsilon}]$:*

1. *Assumption **A1** holds with fixed set $K = K_s \times (\rho\mathbb{B} \cap \mathbb{U})$.*

2. *Let $K_0 := \{0\} \times \{0\} \times K_\xi \times K_\theta \times (\mathbb{U} \cap \rho\mathbb{B})$. If for each $x_{s,u} \in \mathcal{S}_{\mathcal{H}_s}(K_0)$ there exists $(t^*, j^*) \in dom(x_{s,u})$ such that $x_{s,u}(t^*, j^*) \in D_e \times (\mathbb{U} \cap \rho\mathbb{B})$, then for each $x_{s,u} \in \mathcal{S}_{\mathcal{H}_s}(K_0)$ and all $(t, j) \in dom(x_{s,u})$ satisfying $t > t^* - \overline{T}$ and $j > j^* - \frac{\overline{T}}{\Delta T}$*

we have that $x_s(t,j) \in \mathcal{A}_s^\rho + \tilde{e}\mathbb{B}$*, where*

$$\mathcal{A}_s^\rho := [0,1]^2 \times \varphi(H(\mathbb{U} \cap \rho\mathbb{B}))^m \times H(\mathbb{U} \cap \rho\mathbb{B}), \tag{4.19}$$

and where $H(\cdot)$ *is given by Assumption 22.*

4.3 Set-Valued Learning Dynamics

In this section, we characterize the family of control algorithms (4.11) that will be used to extremize the response map J of system (4.1) in the event-triggered closed-loop system (4.12). The design of these algorithms neglects the dynamics in (4.1), and assumes direct availability of measurements of J, i.e., $y = J(u)$. We consider algorithms that can be modeled as a time-invariant logic-based set-valued discrete-time system with state $x_u = (\hat{x}_u^\top, q)^\top \in \mathbb{R}^{N_u}$, given by

$$\begin{pmatrix} \hat{x}_u^+ \\ q^+ \end{pmatrix} \in G_u(x_u, y) := \begin{pmatrix} G_q(\hat{x}_u, y) \\ \ell(q) \end{pmatrix}, \tag{4.20a}$$

$$x_u \in D_u := D_{\hat{x}_u} \times Q, \tag{4.20b}$$

where the sets $D_{\hat{x}_u}$ and Q are defined as

$$D_{\hat{x}_u} := D_{\hat{u},\hat{z}} \times \mathbb{U} \times \mathbb{R}^\sigma, \quad Q := \{\underline{q}, \ldots, \bar{q}\} \subset \mathbb{Z}, \quad \underline{q} \leq \bar{q}, \tag{4.21}$$

and where $\sigma := |Q| - 1$, being $|Q|$ the cardinality of Q. The state $\hat{x}_u$ has three main components $\hat{x}_u := (\hat{x}_{u,z}^\top, u^\top, \hat{y}^\top)^\top \in \mathbb{R}^{2n+r+\sigma}$, where the *learning component state* $\hat{x}_{u,z}$ is defined as $\hat{x}_{u,z} := (\hat{u}^\top, \hat{z}^\top)^\top \in \mathbb{R}^{n+r}$. The set $D_{\hat{u},\hat{z}} := \hat{\mathbb{U}} \times D_{\hat{z}} \subset \mathbb{R}^{n+r}$ in (4.21) constrains the evolution of $\hat{x}_{u,z}$. The state $\hat{y} \in \mathbb{R}^\sigma$ is a memory state, and $q \in \mathbb{R}$ is a

logic-state constrained to evolve in Q. The function $\ell : Q \to Q$ is defined as

$$\ell(q) := \begin{cases} q+1, & \text{if } \ q \in \{\underline{q}, \ldots, \overline{q}-1\}, \\ \underline{q}, & \text{if } \ q = \overline{q}, \end{cases} \tag{4.22}$$

which orderly cycles through all the modes in Q. Let $\overline{y} := (\hat{y}^\top, y)^\top \in \mathbb{R}^{|Q|}$. Then, the set-valued mapping $G_q : \mathbb{R}^{2n+r+\sigma} \times \mathbb{R} \rightrightarrows \mathbb{R}^{2n+r+\sigma}$ in (4.20a) is defined as follows:
If $q = \underline{q}$ (*Learning - Dither Mode)*

$$G_q(\hat{x}_u, y) = \begin{pmatrix} (v_1^\top, v_2^\top)^\top \\ v_1 + a \cdot d_q(v_2) \\ \hat{y} \end{pmatrix}, \begin{pmatrix} v_1 \\ v_2 \end{pmatrix} \in G_\delta^L(\hat{x}_{u,z}, \overline{y}) \Bigg), \tag{4.23a}$$

If $q \in Q \backslash \{\underline{q}\}$ *(Dither-Measure modes)*,

$$G_q(\hat{x}_u, y) = \begin{pmatrix} \hat{x}_{u,z} \\ \hat{u} + a \cdot d_q(\hat{z}) \\ A\hat{y} + By \end{pmatrix}, \tag{4.23b}$$

where the matrices $A \in \mathbb{R}^{\sigma \times \sigma}$ and $B \in \mathbb{R}^\sigma$ in (4.23b) are given by (4.18) with m replaced by σ.

The key elements of the mapping G_q in (4.23a)-(4.23b) are the dither functions $d_q : \mathbb{R}^r \to \mathbb{R}^n$, which have a tunable gain $a \in (0, 1)$, and the learning set-valued mapping $G_\delta^L : \mathbb{R}^{n+r} \times \mathbb{R}^{|Q|} \rightrightarrows \mathbb{R}^{n+r}$, which is allowed to be parametrized by a tunable constant $\delta \in (0, 1)$. These mappings must satisfy the following regularity assumption.

Assumption 29 *(Regularity of G_δ^L and d_q)*

(a) For each $\delta \in [0,1]$: G_δ^L satisfies (C3) with respect to $D_{\hat{u},\hat{z}} \times \mathbb{R}^{|Q|}$. The set $D_{\hat{z}} \subset \mathbb{R}^r$ is closed. For each $\hat{x}_{u,z} \in D_{\hat{u},\hat{z}}$ and $\overline{y} \in \mathbb{R}^{|Q|}$ there exists a $v \in G_\delta^L(\hat{x}_{\hat{u},\hat{z}}, \overline{y}) \cap D_{\hat{u},\hat{z}}$.

(b) For each $q \in Q$ the mapping $d_q(\cdot)$ is continuous in $D_{\hat{z}}$, and $d_q(D_{\hat{z}}) \subset [-1,1]^n$.

Under Assumption 29 the control dynamics (4.20) satisfy Assumption 27. Note that the regularity conditions imposed by Assumption 29 are, indeed, mild. In fact, any δ-independent algorithm with a continuous right-hand side, of the form $\hat{x}_{u,z}^+ = g^L(\hat{x}_{u,z}, \overline{y})$, that renders the set $D_{\hat{u},\hat{z}}$ positively invariant, will satisfy item (a) in Assumption 29. If the algorithm is set-valued, Assumption 29 only asks for the existence of at least one complete solution from every initial condition. On the other hand, apart from the continuity of $d_q(\cdot)$ for each $q \in Q$, Assumption 29-(b) is simply a unitary bound on the amplitude of the dither signals.

Remark 22 *In contrast to [135, Lemma 28] we assume that G_δ^L is not only upper semicontinuous, but that it also OSC and LB. This allows us to guarantee the closedness of the graph of G_δ^L, a property that we will exploit in order to obtain a closed-loop HDS with good robustness properties.*

The choice of the mappings G_δ^L and d_q in (4.23) is application dependent, and it will be based on the concept of *target optimizing dynamical system* (TODS) and a property that we refer to as *finite differences approximability* (FDA).

4.3.1 Target Optimizing Dynamical Systems

A *target optimizing dynamical system* (TODS) is characterized by the following definition:

Definition 3 *Let the pair $(J, \hat{\mathbb{U}})$ satisfy Assumption 24. The time-invariant discrete-time dynamical system, with state $\hat{x}_{u,z} := (\hat{u}^\top, \hat{z}^\top)^\top \in \mathbb{R}^{n+r}$, jump set $D_{\hat{u},\hat{z}} = \hat{\mathbb{U}} \times D_z$,*

jump map $G_\delta^T : \mathbb{R}^{n+r} \rightrightarrows \mathbb{R}^{n+r}$*, and dynamics*

$$\hat{x}_{u,z}^+ \in G_\delta^T(\hat{x}_{u,z}), \quad \hat{x}_{u,z} \in D_{\hat{u},\hat{z}}, \tag{4.24}$$

is said to be a target optimizing dynamical system (TODS) with respect to $(J, \hat{\mathbb{U}})$*, if:*

(a) (Regularity) For each $\delta \in [0,1]$ *system* (4.24) *is well-posed.*

(b) (Stability) There exists a compact set $\Psi \subset D_{\hat{z}}$ *such that the set* $\mathcal{A}_{\hat{u},\hat{z}} := \mathcal{A}_u \times \Psi$ *is SGP-AS as* $\delta \to 0^+$*.*

In equation (4.24) the mapping G_δ^T is assumed to implicitly have all the necessary information of J required to render the set $\mathcal{A}_u \times \Psi$ SGP-AS. This information may correspond to direct measurements of J, the (sub) gradient ∂J, or the Hessian matrix $\mathbb{H}$ of J, for example. Depending on this information, the TODS (4.24) will describe a class of payoff-based learning dynamics, gradient-based learning dynamics, or Newton-based learning dynamics, respectively. The role of the auxiliary state $\hat{z}$ is to give additional flexibility for modeling logic states, timers, monitoring states, persistently exciting signals, etc. This allows us to consider a more general class of algorithms not studied so far in the context of sampled-data optimization. If the mapping G_δ^T is independent of $\hat{z}$, the sets $D_{\hat{z}}$ and Ψ can be neglected. TODS are well-posed by definition. Because of this, we do not consider constrained optimization or learning problems defined on sets that are not closed. Algorithms of the form $\hat{x}_{u,z}^+ = g_\delta^T(\hat{x}_{u,z})$ with a *discontinuous* right-hand side can also be considered provided their corresponding Krasovskii regularization, given by

$$\hat{x}_{u,z}^+ \in G_\delta^T(\hat{x}_{u,z}) := \bigcap_{\epsilon>0} \overline{g_\delta^L((\hat{x}_{u,z} + \epsilon\mathbb{B}) \cap D_{\hat{u},\hat{z}})}, \tag{4.25}$$

is also a TODS. Since item (b) in Definition 3 only asks for a SGP-AS property[1] in δ

[1]If system (4.24) does not depend on any parameter δ, item (b) in Definition 3 is equivalent to a

with respect to $\mathcal{A}_{\hat{u},\hat{z}}$, the dynamics (4.24) can be constructed via an Euler discretization of continuous-time or set-valued hybrid dynamical systems. This follows directly by [191, Example 7.5 & Theorem. 7.8]. Examples of *hybrid* learning dynamics that are suitable to obtain TODS via an Euler discretization are presented in [206]. Finally, note that TODS are defined only with respect to a feasible set $\hat{\mathbb{U}}$, and a payoff function J, which for a multi-agent systems scenario can be taken as a vector of the form $[J_1, \ldots, J_N]^\top$.

Example 4 (Smooth unconstrained optimization) *If J is C^2 and strictly concave, and $\hat{\mathbb{U}} := \mathbb{R}^n$, a discretized gradient system $\hat{u}^+ = G_\delta^T(\hat{u}) := \hat{u} + \delta \cdot \nabla J(\hat{u})$ is the simplest type of TODS satisfying the conditions of Definition 3. In this case, the regularization* (4.25) *of the discontinuous version $\hat{u}^+ = g_\delta^T(\hat{u}) := \hat{u} + \delta \cdot sgn(\nabla J(\hat{u}))$, is also a TODS.*

Example 5 (Optimal resource allocation) *If J is C^2 and strictly concave, and $\hat{\mathbb{U}} := \{\hat{u} \in \mathbb{R}^n_{\geq 0} : \mathbf{1}^\top \hat{u} = s\}$, where $s \in \mathbb{R}_{>0}$ is a limited resource, the set-valued dynamics $\hat{u}^+ \in G_\delta^T(\hat{u}) := \hat{u} - \delta \cdot \big(\hat{u} - s \cdot \arg\max_{w \in \hat{\mathbb{U}}} w^\top \nabla J(\hat{u})\big)$ describes a TODS, since this dynamics correspond to the discretized* best-response dynamics *[183, Section 6.1].*

Example 6 (Gradient systems with adversarial signals) *Let J be quadratic, strictly concave, and $\hat{\mathbb{U}} := \mathbb{R}^n$. The system $\hat{z}_1^+ = \frac{(1-\hat{z}_2)}{2}(\hat{z}_1 + 1 - \rho) + \frac{(1+\hat{z}_2)}{2} \max\{0, \hat{z}_1 - \rho\}$, $\hat{z}_2^+ \in \{-1, 1\}$, $\hat{u}^+ = \hat{u} + \delta \cdot \hat{z}_2 \nabla J(\hat{u})$, evolving on the set $D_{\hat{u},\hat{z}} := [0, M] \times \{-1, 1\} \times \mathbb{R}^n$, where $M \geq 1$ and $\rho \in (0, 1)$, models a gradient system subject to external jamming signals that aim to unstabilize the state $\hat{u}$ via the condition $\hat{z}_2 = -1$. Here $\hat{z}_1$ acts as a monitor state that guarantees that in any complete solution the state $\hat{z}_2$ is equal to 1 "sufficiently often", see [231, Lemma 3]. Thus, the parameters (δ, ρ) can be selected such that this system is a TODS.*

UGAS property.

4.3.2 Finite Differences Approximability

The direct implementation of a TODS to optimize J in $\hat{\mathbb{U}}$ will most likely require knowledge of the mathematical model of J, ∇J or $\mathbb{H}$, thus precluding its application in a black-box setting. Because of this, we consider TODS only as a "target" system, whose solutions we seek to approximate via an appropriate design of the learning mappings G_δ^L and the dither functions d_q in (4.23).

Assumption 30 *(*FDA*) Let the pair $(J, \hat{\mathbb{U}})$ satisfy Assumption 24, and let $(G_\delta^T, D_{u,z})$ be a TODS. Then, G_δ^L and d_q are such that for each compact set $K_{u,z} \subset D_{u,z}$, each $\rho \in (0,1)$, and each $\delta \in (0,1)$, there exists $a^* \in (0,1)$ such that for each $a \in (0, a^*)$ we have that if:*

$$\hat{y} = \begin{pmatrix} J(\hat{u} + a d_{\underline{q}}(\hat{z})) \\ J(\hat{u} + a d_{\underline{q}+1}(\hat{z})) \\ \vdots \\ J(\hat{u} + a d_{\bar{q}-1}(\hat{z})) \end{pmatrix}, \quad \begin{matrix} \tilde{y} = J(\hat{u} + a d_{\bar{q}}(\hat{z})) \\ \overline{y} = (\hat{y}^\top, \tilde{y})^\top \end{matrix}, \tag{4.26}$$

then $G_\delta^L(\hat{x}_{u,z}, \overline{y}) \subset G_\delta^T((\hat{x}_{u,z} + \rho\mathbb{B}) \cap D_{u,z}) + \rho\mathbb{B}$, for all $(\hat{u}, \hat{z}) \in K_{u,z}$.

In words, the FDA property implies that under an appropriate choice of the dither signals d_q, parameters (a, δ), and a sequence comprised of $|Q|$ measurements of J evaluated at points $\hat{u} + a d_q(\hat{z})$, for all $q \in Q$, the solutions of G_δ^L in (4.23a) will also be solutions of a ρ-perturbation of a TODS. The SGP-AS property in Definition 3 implies that Assumption 30 is similar in spirit to [87, Assumption 2] and [135, Assumption 16.(ii)-(iii)], although we do not make any extra assumption regarding the robustness of G_δ^L under additive perturbations in the vector $\overline{y}$. Indeed, these robustness properties will be obtained as a direct consequence of the structural properties of the learning mapping G_δ^L.

Example 7 *Let $(J, \hat{\mathbb{U}})$ satisfy Assumption 24, $J \in \mathcal{C}^2$, and consider the system*

$$\hat{x}^+_{u,z} \in G^T_\delta(\hat{x}_{u,z}) := \hat{G}_\delta(\hat{x}_{u,z}, k \cdot \nabla J(\hat{u})), \quad \hat{x}_{u,z} \in D_{\hat{u},\hat{z}}, \tag{4.27}$$

where $\hat{G}_\delta(\cdot,\cdot)$ satisfies (C3) with respect to $D_{\hat{u},\hat{z}} \times \mathbb{R}^n$, $D_{\hat{u},\hat{z}}$ is closed, and (4.27) *satisfies item (b) in Definition 3 for any $k > 0$. Then* (4.27) *is a TODS, and the learning mapping $G^L_\delta := \hat{G}_\delta(\hat{x}_{u,z}, E(\bar{y}))$, with $E(\bar{y}) = (\hat{y}_1 - \hat{y}_2, \ldots, \hat{y}_{2n-1} - y)^\top$, $Q = \{1, \ldots, 2n\}$, and dither functions $d_q = \boldsymbol{e}_{\frac{q+1}{2}}$ for q odd, and $d_q = -\boldsymbol{e}_{\frac{q}{2}}$ for q even, i.e., the Kiefer-Wolfowitz approach for the estimation of $(a \cdot \nabla J)$, satisfies Assumption 30. This observation follows by the upper-semicontinuity property of G^L_δ induced by (C3), which implies that in compact sets, any $O(a)$ estimation error of ∇J can be embedded in an additive ρ-inflation of* (4.27).

Many extremization algorithms satisfying the FDA property have the structure of (4.27). In particular, standard finite differences approximations can be used to approximate the gradient of J on compact sets whenever $J \in \mathcal{C}^2$. Moreover, any gradient-based time-invariant optimization algorithm with a continuous right-hand side can be combined with this approximation to satisfy Assumption 30. Other ways of generating the functions d_q can be found in [232, Section 5.5] for smooth response maps, or in [233] for nonsmooth response maps. A particular application of a TODS in nonsmooth networked systems is presented in the conference paper [161].

Remark 23 *Some TODS are able to guarantee convergence to the optimal set $\mathcal{A}_u$ by directly using unperturbed* measurements *of $J(u)$, i.e., without dithering, e.g., [183, ch. 7.2]. For this type of dynamics we can take $G^L_\delta := G^T_\delta$, $Q := \{0\}$, $d_0 := 0$, and the memory state $\hat{y}$ can be neglected.*

The following theorem, which is of semi-global practical nature, is the main result

of this section.

Theorem 5 *Consider the system (4.20) with $y \in J(u) + \tilde{e}\mathbb{B}$, $\tilde{e} \in \mathbb{R}_{>0}$, and suppose that Assumptions 24-30 hold. Let*

$$\mathcal{A}_{\hat{x}_u} := \mathcal{A}_{\hat{u},\hat{z}} \times \mathcal{A}_u \times J(\mathcal{A}_u)^\sigma, \tag{4.28}$$

where $\mathcal{A}_{u,z}$ is defined as in Definition 3-(b), and $\mathcal{A}_u$ is defined as in Assumption 24. Then, system (4.20) is well-posed, and for each $\nu \in \mathbb{R}_{>0}$ and each pair of compact sets $K_{\hat{x}_u} \subset \mathbb{R}^{2n+r+\sigma}$ and $K_q \subset \mathbb{R}$ satisfying $(\mathcal{A}_{\hat{x}_u} \times Q) + \nu\mathbb{B} \subset int(K_{\hat{x}_u} \times K_q)$, there exists $\delta^* \in (0,1)$ such that for all $\delta \in (0,\delta^*]$ there exists $a^* \in (0,1)$ such that for each $a \in (0,a^*]$ there exists $\tilde{e}^* \in (0,1)$ such that for each $\tilde{e} \in (0,\tilde{e}^*]$ there exists at least one complete solution from every point in $K_{\hat{x}_u} \times K_q$, as well as a ULAS compact set $\mathcal{A}_{\delta,a} \subset (\mathcal{A}_{\hat{x}_u} \times Q) + \nu\mathbb{B}$ with basin of attraction $\mathcal{B}_{\mathcal{A}_{\delta,a}}$ containing the set $K_{\hat{x}_u} \times K_q$.

4.4 Stability Analysis of the Closed-Loop System

We now proceed to analyze the complete closed-loop event-triggered system obtained by the hybrid dynamics (4.12) using the control dynamics (4.20) with y being the output of system (4.1). Since the control dynamics are parameterized by a logic state $q \in Q$ the closed-loop system can be seen as a logic-based automaton that allows flows of the plant (4.1) only when $x_s \in C_s$, i.e., when $\tau < 1$. Whenever $\tau = 1$ and an event occurs, the control state and the logic mode q are allowed to be updated. Figure 4.3 illustrates this automaton-like representation of system (4.12) for the case that $\underline{q} = 0$ and $\bar{q} = 1$.

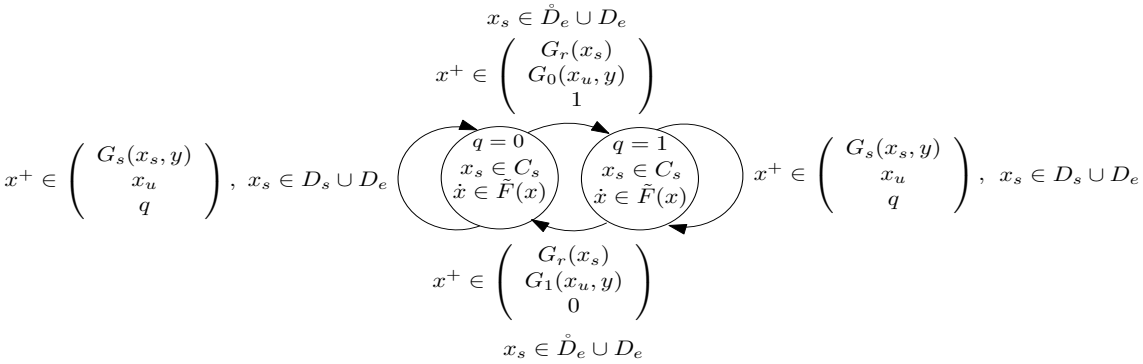

Figure 4.3: Automaton-like representation of the HDS (4.12) using the control dynamics (4.20) with only two modes, i.e., $Q = \{0, 1\}$.

Consider the compact set

$$\mathcal{A} := \mathcal{A}_s \times \mathcal{A}_{\hat{x}_u} \times Q, \tag{4.29}$$

where $\mathcal{A}_{\hat{x}_u}$ is defined as in (4.28), Q is defined as in (4.21), and $\mathcal{A}_s$ is defined as (4.19) with $\hat{\mathbb{U}} \cap \rho\mathbb{B}$ replaced by $\mathcal{A}_u$. The following semi-global practical asymptotic stability theorem corresponds to the main result of this chapter.

Theorem 6 *Consider the HDS (4.12) with control dynamics* (4.20)*, where y, S, and G_ξ are given by* (4.16) *and* (4.17)*, respectively. Suppose that Assumptions 37-25 and 28-30 hold. Then, the closed-loop HDS is well-posed, and for each $\nu \in \mathbb{R}_{>0}$ and each compact set $K \subset \mathbb{R}^{N_s+N_u}$ satisfying $\mathcal{A} + \nu\mathbb{B} \subset \mathit{int}(K)$, there exists $\delta^* \in \mathbb{R}_{>0}$ such that for each $\delta \in (0, \delta^*]$ there exists $a^* \in \mathbb{R}_{>0}$ such that for each $a \in (0, a^*]$ there exists data $(\Delta T, \gamma^*, f_e)$ and a pair $(\underline{\varepsilon}, \overline{\varepsilon})$, such that for each $\varepsilon \in (\overline{\varepsilon}, \underline{\varepsilon}]$: 1) There exists at least one complete solution from any initial condition in $K \cap (\tilde{C} \cup \tilde{D})$. 2) There exists a ULAS compact set $\mathcal{A}_\varepsilon \subset \mathcal{A} + \nu\mathbb{B}$ with basin of attraction $\mathcal{B}_{\mathcal{A}_\varepsilon} \supset K$.*

Theorem 6 characterizes the order in which the parameters of the closed-loop system must be tuned, being the constant δ the first parameter to be selected sufficiently small. Once this parameter has been selected one proceeds to tune the amplitude a, and finally

one proceeds to tune the parameters $(\Delta T, \gamma^*, \varepsilon)$ and the function f_e in order to detect the quasi-steady state condition with the sufficient accuracy. Since we only assume a "practical" derivative estimation characterized by item (a) in Assumption 28 (which is usually the best one can expect for noise corrupted signals), the sampling period ΔT needs to be selected sufficiently small, while the length of the vector (4.15) and the verification window $(\gamma^* - m)\Delta T$ need to be selected sufficiently large to avoid events that are not an indication of steady state.

Theorem 6 and [78, Lemma 7.20] allows us to directly obtain the following corollary, which exploits the well-posedness of the closed-loop system.

Corollary 2 *Consider the HDS (4.12) with data* $\tilde{\mathcal{H}} := \{\tilde{C}, \tilde{F}, \tilde{D}, \tilde{G}\}$ *and control dynamics* (4.20) *with output* y *of* (4.1). *Suppose that all assumptions from Theorem 6 hold, and let* $\mathcal{A}_\varepsilon$ *be the generated ULAS compact set. Then, for the* ρ*-perturbation of* $\tilde{\mathcal{H}}$*, given by the HDS with data*

$$\begin{aligned}
\tilde{C}^\rho &:= \{x : (x + \rho\mathbb{B}) \cap \tilde{C} \neq \emptyset\} \\
\tilde{F}^\rho &:= \overline{co}\ \tilde{F}((x + \rho\mathbb{B}) \cap \tilde{C}) + \rho\mathbb{B}, \\
\tilde{D}^\rho &:= \{x : (x + \rho\mathbb{B}) \cap \tilde{D} \neq \emptyset\} \\
\tilde{G}^\rho &:= \{v : v \in g + \rho\mathbb{B},\ g \in \tilde{G}((x + \rho\mathbb{B}) \cap \tilde{D})\},
\end{aligned} \tag{4.30}$$

the set $\mathcal{A}_\varepsilon$ *is SGP-AS (with respect to* $\mathcal{B}_{\mathcal{A}_\varepsilon}$*) as* $\rho \to 0^+$.

The margins of robustness given by Corollary 2 cover a variety of scenarios that are critical for the safe implementation of the output-based event-triggered control. These include: small additive perturbations with unknown directions acting on the measurements of the triggering signal z; mismatches and additive noises on τ, γ, and $(\xi, \hat{y})$; and small additive disturbances acting on the states $(\hat{x}_{u,z}, u, q)$ and on $d_q(\cdot)$.

4.4.1 Connections with the Periodic Sample-Data Approach

The standard approach for black-box optimization in sampled-data systems [133], [135], [87], periodically updates the control system by using a constant large sampling period T. Indeed, this approach can naturally be defined as a hybrid triggering mechanism with hybrid dynamics given by

$$\begin{aligned}
\begin{pmatrix} \dot{\tau} \\ \dot{\theta} \\ \dot{x}_u \end{pmatrix} &\in \begin{pmatrix} \frac{1}{\Delta T} \\ P(\theta, u) \\ \mathbf{0}_{N_u} \end{pmatrix}, \ C_s = [0,1] \times \mathbb{R}^p \times D_u \\
\begin{pmatrix} \tau^+ \\ \theta^+ \\ x_u^+ \end{pmatrix} &\in \begin{pmatrix} 0 \\ \theta \\ G_u(x_u, y) \end{pmatrix}, \ D_s = \{1\} \times \mathbb{R}^p \times D_u,
\end{aligned} \tag{4.31}$$

where the (strict) event set is now defined as $\mathring{D}_e := D_e := D_s$. In this case ΔT has now the role of T, and it is selected as the *worst case* settling time that guarantees a quasi-steady state condition for *all* solutions generated by the plant (4.1) from a given compact set of initial conditions. By using this definition for D_e and $\mathring{D}_e$, system (4.31) is consistent with the HDS (4.12), since now $D_s \backslash D_e = D_e \backslash \mathring{D}_e = \emptyset$, which implies that the jumps of the closed-loop system are completely characterized by the mapping $G_r \times G_u$ in (4.13). In this case the auxiliary states (γ, ξ) have no particular role, and the HDS (4.12) reduces to system (4.31). Since ΔT is now selected sufficiently large to guarantee an $\tilde{e}$-quasi-steady state condition at every jump, we have that the conclusions of Proposition 11.2 still hold (with appropriate set $\mathcal{A}_s^\rho$), thus, a stability result for system (4.31) can be seen as a corollary of Theorem 6, where the parameters $(\gamma^*, \varepsilon, r_e)$, and the function f_e, have no particular role. This approach was pursued in [161] in a networked systems scenario.

4.4.2 On the Convergence Rate of the Event-triggered Approach

In the standard periodic sampled-data optimization approach [133], [135], [87], which as mentioned before can also be modeled as (4.31), the updates of the control system occur in a periodic way, generating hybrid time domains of the form

$$[0,(1-\tau_0)\Delta T]\times\{0\}\cup\left(\bigcup_{k=0}^{\infty}[s_k,s_{k+1}]\times\{k+1\}\right), \tag{4.32}$$

where the sequence $\{s_k\}$ is generated by the recursion $s_{k+1}=s_k+\Delta T,\ \forall\, k\in\mathbb{Z}_{\geq 0},\ \ s_0=(1-\tau_0)\Delta T$, and where $\tau_0:=\tau(0,0)$. This type of hybrid time domains is independent of the initial conditions and dynamics of the plant (4.1), and illustrates the limitations imposed by using a large ΔT in (4.31). On the other hand, note that due to the equivalent $\mathcal{KL}$ characterization of the UGAS property of system (4.1), every time that u is updated to $u^+\neq u$ at some time t_i, the state of the plant will satisfy during flows a $\mathcal{KL}$ bound of the form[2]

$$|\theta(t)|_{H(u^+)}\leq\beta\left(|\theta\left(t_i\right)|_{H(u^+)},t-t_i\right), \tag{4.33}$$

for all t in the interval $[t_i,t_f]$, where t_f corresponds to the time where u^+ is updated again. Moreover, by Assumption 22, Proposition 11, and the construction of the jump map (4.13), at the time t_i the state of the plant will satisfy $|\theta(t_i)|_{H(u)}\leq\tilde{e}$. Due to the OSC and LB properties, the set-valued mapping $H(\cdot)$ is also upper semicontinuous [78, Lemma 5.15], which implies that for each u^+ and $\epsilon_1\in\mathbb{R}_{>0}$ there exists an $\epsilon_2\in\mathbb{R}_{>0}$ such that $H(u^+{+}\epsilon_2\mathbb{B})\subset H(u^+){+}\epsilon_1\mathbb{B}$. Thus, for any $\tilde{e}\in\mathbb{R}_{>0}$ and u^+ satisfying $\|u^+{-}u\|\leq\epsilon_2$ we have that $H(u)+\tilde{e}\mathbb{B}\subset H(u^+)+(\epsilon_1+\tilde{e})\mathbb{B}$. Without loss of generality we can take

[2]For simplicity we omit here the dependence of $\theta(t,j)$ on j.

$\epsilon_1 = \alpha_u(\epsilon_2)$, where $\alpha_u \in \mathcal{K}$. Thus, right after the controller is updated we have that $|\theta(t_i)|_{H(u^+)} \leq \alpha_u(\epsilon_2) + \tilde{e}$, and since $\alpha_u \in \mathcal{K}$ the upper bound on $|\theta(t_i)|_{H(u^+)}$ will decrease as ϵ_2 decreases. Moreover, $\alpha_u(\cdot)$ can be taken independent of u in a compact set sufficiently close to u^*. Therefore, for any learning dynamics of the form (4.20) that guarantees SGP-AS of a singleton $\mathcal{A}_u = \{u^*\}$, and for which the upper bound ϵ_2 will eventually decrease in a neighborhood of u^*, e.g., learning dynamics with a smooth right-hand side, the first argument of the $\mathcal{KL}$ function β in (4.33), i.e., the overshoot, will eventually decrease, thus leading to smaller settling times, and therefore smaller intervals of flow between updates of the discrete-time control dynamics, necessarily reducing the convergence time of the closed-loop system to a neighborhood of the optimal set. The reduction in the convergence time is achieved *without* deteriorating the basin of attraction and the residual set where solutions converge. Note, however, that it is easy to construct plants with a *discontinuous* right-hand side whose settling times do not depend on the norm of the input. Thus, to obtain a better estimate of the improvement on the convergence rate achieved by the event-triggered approach one would need additional information regarding the model of the plant. For instance, in [234], the authors show that for the smooth nonlinear system (and a more general class of systems) of the form $\dot{\theta}_1 = -\theta_1 + \theta_2^2 + u$, $\dot{\theta}_2 = -2\theta_2 + 2u$, $y = \theta_1 + \theta_2$, the $\tilde{e}$-settling time to the origin is approximately given by $-\log\left(\frac{\tilde{e}}{|u_s + 4u_s^2/3|}\right)$, where u_s is the normalized input. For this system, values of $\tilde{e} = 0.01$ and $|u_s| \leq 1$ lead to settling times decreasing from 5.5s to 0 as $|u_s| \to 0^+$, see [234]. In contrast to the event-triggered approach, this reduction in the settling time cannot be exploited by the periodic sampled-data system (4.31). We point out that this idea has been exploited in the process control and model-based optimization literature, e.g., [235, Ch. 9], although a rigorous stability analysis, as well as its study in the setting of set-valued *model-free* sampled-data learning and extremum seeking in nonlinear systems, was absent.

4.5 Numerical Example

Consider a switched system of the form

$$\epsilon\dot{\theta} = \begin{bmatrix} -1 & \frac{3}{2} - \frac{5}{4}p \\ -\frac{9}{4} + \frac{5}{4}p & -1 \end{bmatrix} \theta + \begin{bmatrix} 1 \\ \frac{9}{4} - \frac{5}{4}p \end{bmatrix} u \ , \tag{4.34a}$$

$$y = -(\theta_1 - 10)^2, \tag{4.34b}$$

where $\theta \in \mathbb{R}^2$, $u \in \mathbb{R}$, $\epsilon = 0.1$, and $p : [0, \infty) \to \{1, 2\}$ is a switching signal that is constant for at least $\delta_t > 0$ seconds. Since δ_t is arbitrarily small, to analyze all the solutions of system (4.34) one needs to consider the differential inclusion

$$\dot{\theta} \in P(\theta, u) := \overline{co} \ \cup_{p\in\{1,2\}} f_p(\theta, u), \tag{4.35}$$

where $f_p(\theta, u)$ corresponds to the right hand side of (4.34a). Indeed, every solution of (4.34) is also a solution of (4.35), and every solution of (4.35) can be generated by (4.34) under an appropriate selection of the switching signal p [78, Example 2.14]. Therefore the stability properties of system (4.34) are characterized by the stability properties of system (4.35). Since for each fixed u we have that $V = (\theta_1 - u)^2 + \theta_2^2$ is a common Lyapunov function for (4.34), it follows that (4.35) renders the singleton $H(u) := \{u\} \times \{0\}$ UGAS. Moreover, since the response map of (4.34) is given by $J(u) = -(u - 10)^2$, and system (4.35) is well-posed by construction, the plant satisfies Assumptions 37-24 with $\mathcal{A}_u = \{10\}$. Now, given any $\delta_t > 0$ arbitrarily small, the selection of the waiting time T for the classic periodic sampled-data optimization given by (4.31) must be based on the largest settling time among all the *worst case* settling time generated by *all solutions* of (4.35). For $\delta_t = 0.01$s the *worst case* T is given by the solution generated by the periodic switching signal p that jumps every δ_t seconds,

shown in Figure 4.4-b. These type of solutions generate a settling time approximately equal to 1.5 sec, which is more than double of the settling time generated by the solution associated to $\dot{p} = 0$ for all $t \geq 0$, which is approximately equal to 0.6s, for any $p \in \{1, 2\}$. For the dynamics (4.35) with output (4.34b) we have that $Z := \left\{(\theta, u) \in \mathbb{R}^2 \times \mathbb{R} : \theta_1 = 10, u = \theta_1 + \theta_2(1 - \frac{5}{4}\lambda), \lambda \in [0, 1]\right\}$, and no solution of (4.35) with $\dot{u} = 0$ can stay indefinitely in Z unless $\theta_1 = u$ and $\theta_2 = 0$. Thus, system (4.35) satisfies Assumption 25. Using the event-triggered approach, we simulate the solutions generated when $p(t)$ corresponds to the switching signals shown in Figure 4.4, and $\theta(0) = [0, 0]^\top$. The evolution of θ_1 for both of these solutions is shown in Figure 4.5, marked as "(a)" and "(b)", respectively. Additionally, we simulated the solution generated by the classic sampled-data system (4.31) for the switching signal in Figure 4.4-a. This solution is marked as "(c)" in Figure 4.5. For clarity we do not show the solution generated by system (4.31) with the switching signal of Figure 4.4-b since this solution is almost identical to the one generated using the switching signal (a), as both solutions are generated with the same *worst case* sampling period T=1.5s. Figures 4.5 and 4.6 illustrate the behavior discussed in Section 4.4.2: At the beginning of the simulation ($t \leq 20$ sec) the rate of convergence of the three solutions is almost the same. For $t >$ 20s the rate of convergence of solution (a) increases, since the event-triggered method exploits the fact that this solution requires settling times that are approximately half of the settling times of solutions (b). Note that although for $t \leq$ 120s the difference between the rates of convergence of solutions (b) and (c) is moderate, as $|u^+ - u| \to 0.2$, solution (b) accelerates, converging to the residual set $[9.9, 10.1]$ in approximately 300s, compared to solution (c), which converges in approximately 700s. Solution (a), which requires smaller settling times, converges in approximately 200s. The data of the SSIM was selected as: $\varepsilon = 0.06$, $\Delta T = 0.01$, $m = 2$, $\gamma^* = 10$, $r_e = 0.99$, and $f_e = |(\xi_1 - \xi_2)/\Delta T|$. The TODS employed corresponds

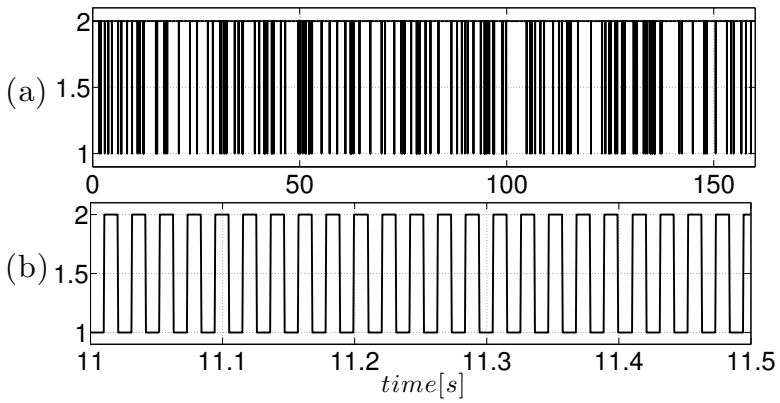

Figure 4.4: Switching signals $p(t)$ with: (a) low switching frequency, (b) high switching frequency.

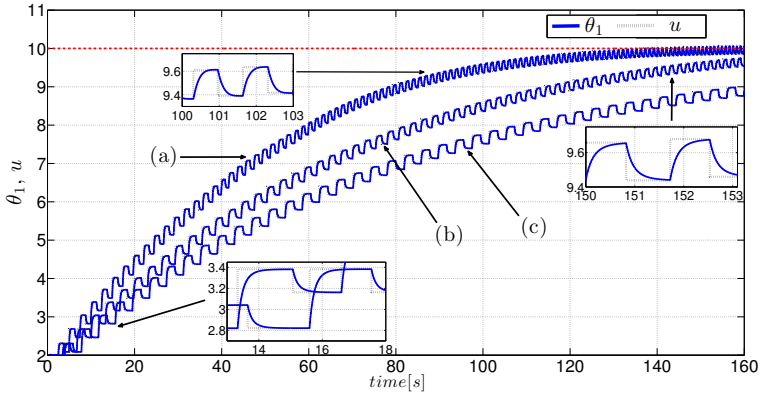

Figure 4.5: Trajectories of θ_1 (solid) and u (dashed), with (a)-(b), and without (c), event-triggered control.

to a standard continuous discretized gradient system as the one in Example 4. The parameters of the optimizer are selected as $a = 0.1$, $\delta = 0.1$, and we used $Q = \{0, 1\}$ and $d_0 = 1$, $d_1 = -1$. The signal $\dot{y}$, and its estimated value, are shown in Figure 4.7 for solutions (a) and (b). The evolution of γ is shown in Figure 4.8, illustrating how events in solution (a) are generated more frequently compared to solution (b).

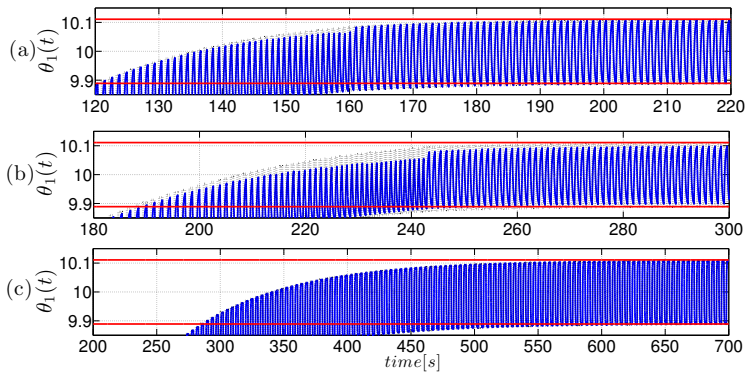

Figure 4.6: Solutions θ_1 of (4.34) converging to a neighborhood of u^*, with (a)-(b), and without (c), event-triggered control.

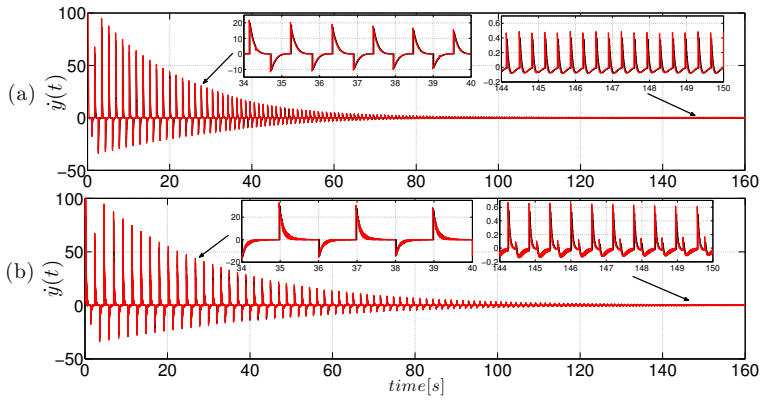

Figure 4.7: $\dot{y}(t)$ (red), and its estimated value (black).

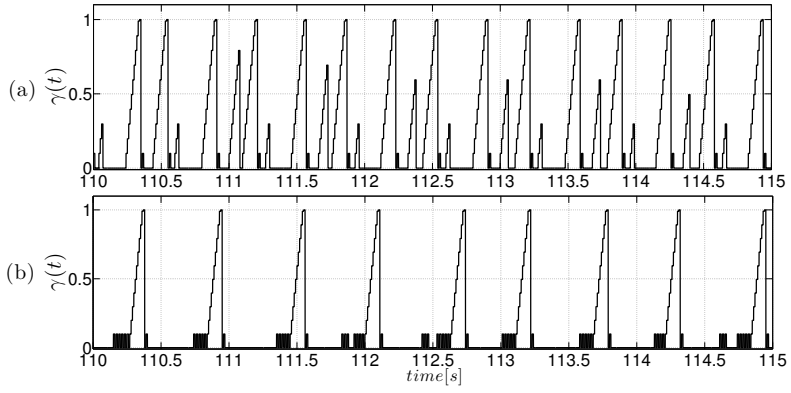

Figure 4.8: Evolution of γ for solutions (a) and (b).

Chapter 5

Robust Coordination of Networked Sampled-Data Systems

In networked multi-agent cyber-physical systems where agents have access to only local information, i.e., to the states and inputs/outputs of their neighboring agents, it is not possible to implement centralized architectures that require a synchronous and coordinated behavior of the agents. In order to overcome this limitation, in this chapter we study a methodology that allows to implement fully decentralized feedback mechanisms with good robustness properties, based on a centralized control system designed a priori. This methodology is based on a robust synchronization mechanism and a type of control system termed "pre-jump sampling control". We show that, by using these feedback mechanisms, the resulting closed-loop system exhibits desirable stability and robustness properties, which, in general, are difficult to obtain in networked cyber-physical systems.

5.1 Motivational Example

In networked multi-agent CPS with decentralized controllers, the interaction between multiple hybrid dynamical systems leads to complex behaviors due to the absence of a central node that coordinates the jumps. To illustrate this idea, and to prepare for the general discussion to follow, we present a simple motivational example using a MAS comprised of three sampled-data systems with linear dynamics and periodic discrete-time controllers.

5.1.1 Model of the System

Consider 3 sampled-data systems with scalar continuous-time dynamics given by

$$\delta\dot{\theta}_i = -\theta_i + u_i, \qquad y_i = \theta_i, \qquad \forall\ i \in \mathcal{V} := \{1,2,3\}, \tag{5.1}$$

where y_i is the output of the i^{th} plant. The parameter $\delta \in \mathbb{R}_{>0}$ is assumed to be small, inducing a fast transient modeling fast actuator dynamics, such as in [224]. The control dynamics of the sampled-data systems share information via a ring graph $\{1\} \to \{2\} \to \{3\} \to \{1\}$. We assume that agents also have access to the information of their own state. Each agent implements linear periodic discrete-time control dynamics of the form

$$u_i^+ = A_{i,z_i}u + B_i y, \qquad u_i \in \mathbb{R}, \tag{5.2a}$$

$$z_i^+ = z_i + 1 \ \text{ if } \ z_i \in \{0,1\}, \ \text{ or } \ z_i^+ = 0 \ \text{ if } \ z_i = 2, \tag{5.2b}$$

where $u = [u_1, u_2, u_3]^\top$, $y = [y_1, y_2, y_3]^\top$, and B_i is a row vector with the j^{th} entry different from zero only if j is a neighbor of agent i. For each agent $i \in \{1,2,3\}$ and each

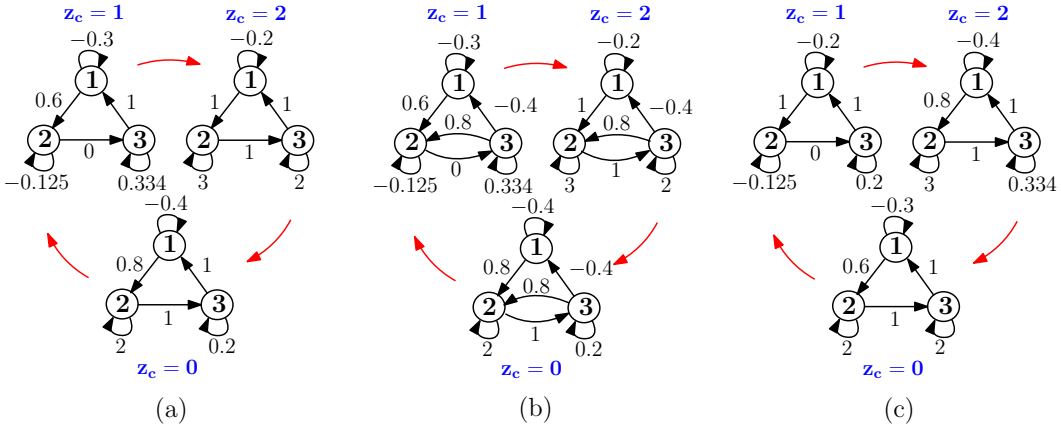

Figure 5.1: Three different collections of adjacency matrices $\{\tilde{A}_{z_c}\}$ associated with the networked periodic discrete-time system with dynamics (5.4). (a) Nominal stable system. (b) System obtained when agent 1 always updates its controller before the other agents. (c) System obtained when agents do not coordinate their logic mode z_{c_i} and $z(0) = [1, 0, 2]^\top$.

logic state $z_i \in \{0, 1, 2\}$ the matrices A_{i,z_i} are given as follows: $A_{1,0} = \left[-\frac{7}{5}, \frac{4}{5}, 0\right]$, $A_{1,1} = \left[-\frac{13}{10}, \frac{3}{5}, 0\right]$, $A_{1,2} = \left[-\frac{6}{5}, 1, 0\right]$; $A_{2,0} = [0, 1, 0]$, $A_{2,1} = \left[0, -\frac{9}{8}, -1\right]$, $A_{2,2} = [0, 2, 0]$; $A_{3,0} = \left[2, 0, -\frac{4}{5}\right]$, $A_{3,1} = \left[2, 0, -\frac{2}{3}\right]$, $A_{3,2} = [2, 0, 1]$. Since according to (5.2b) the logic state z_i models a periodic discrete-time parameter with period equal to 3, the control dynamics (5.2a) are also periodic.

As in [150], the plant dynamics (5.1) are interconnected in feedback with the periodic discrete-time dynamics (5.2) by means of an individual sampler/zero-order hold (S/ZOH) mechanism with periodic resetting clock $\tau_i \in \mathbb{R}_{\geq 0}$. This clock has a constant frequency ω, and it is reset to 0 every ω^{-1} seconds. Every time that τ_i is reset to zero, the S/ZOH samples the inputs and outputs of (5.1) and its neighbors, updates the states (u_i, z_i) via (5.2), and sends the new value of the input u_i^+ to the plant (5.1). Our goal is to design the row vectors B_i and any other necessary feedback mechanism, such that, for δ sufficiently small, the overall states (θ, u) of the networked multi-agent sampled-data system converge to a neighborhood of the origin.

5.1.2 Control Design

In order to design the matrices B_i, consider the case when $\delta = 0$ in (5.1), which corresponds to "instantaneous" actuator dynamics generating the steady state input-to-output condition $y_i = \theta_i = u_i$. The feedback interconnection with this static mapping in (5.2a) generates discrete-time scalar dynamics of the form

$$u_i^+ = \tilde{A}_{i,z_i} u, \text{ where } \tilde{A}_{i,z_i} = A_{i,z_i} + B_i. \tag{5.3}$$

Now, suppose that the three agents of the network are coordinated by a global logic state z_c with dynamics (5.2b), and by a global clock τ_c that simultaneously triggers the S/ZOH mechanisms and the control dynamics of *all* agents. Using (5.3) for all $i \in \mathcal{V}$, the *synchronous* discrete-time dynamics of the MAS can be written in vectorial form as

$$u^+ = \tilde{A}_{z_c} u, \quad \tilde{A}_{z_c} := \left[\begin{array}{c} \tilde{A}_{1,z_c}^\top, \ \tilde{A}_{2,z_c}^\top, \ \tilde{A}_{3,z_c}^\top \end{array} \right]^\top, \tag{5.4a}$$

$$z_c^+ = z_c + 1, \text{ if } z_c \in \{0, 1\}, \quad \text{or} \quad z_c^+ = 0 \text{ if } \ z_c = 2. \tag{5.4b}$$

Since the dynamics of agent i only depend on its own actions and the actions of its neighbors, the matrix $\tilde{A}_{z_c}$ in (5.4a) can be interpreted as a 3-periodic weighted *adjacency matrix* describing time-varying weights associated to the edges of the communication graph of the controllers. We assume that these weights only affect the dynamics (5.4), and not the communication between agents. This interpretation is shown in Figure 5.1 for three different collections $\{\tilde{A}_{z_c}\}_{z_c \in \{0,1,2\}}$.

The analysis of synchronous systems of the form (5.4) is significantly easier compared to the analysis of asynchronous MAS with dynamics (5.2). In fact, systems of the form (5.4) can be studied using standard algebraic or Lyapunov tools [236] . For

instance, since it is well known [236, pp. 15] that the origin is UGAS for the system (5.4a) if and only if the monodromy matrix $M := \tilde{A}_2\tilde{A}_1\tilde{A}_0$ is Schur stable, we can use $B_1 := [1, 0, 0]$, $B_2 := [0, 1, 1]$, and $B_3 := [-1, 0, 1]$ in (5.3) to obtain the weighted adjacency matrices $\{\tilde{A}_{z_c}\}_{z_c=0}^{2}$ shown in Figure 5.1-(a), which generate a Schur stable matrix M with eigenvalues $|\lambda(M)| = [0.0021, 0.8809, 0.8809]$. Since for $\delta > 0$ sufficiently small we have that every ω^{-1} seconds $y_i = u_i + O(\delta)$ in (5.2a), the synchronous and coordinated network of sampled-data systems with continuous-time dynamics (5.1), discrete-time dynamics (5.4), and global states (τ_c, z_c) will render the origin SGP-AS as $\delta \to 0$. Robustness to small perturbations of the form (G.14) follows by well-posedness of the synchronous system [78, Thm. 7.21].

5.1.3 Instability and Lack of Robustness due to Absence of Coordination

Once a robust feedback mechanism has been designed for the synchronous system given by equations (5.1) and (5.4) with global clock τ_c and global logic state z_c, a natural question to ask is whether or not the same matrices B_i can be used in the original asynchronous networked multi-agent sampled-data system with control dynamics (5.2) and individual states (τ_i, z_i). To explore this question, consider the initial conditions $\tau(0) = [0, 0, 0]$ and $z(0) = [1, 0, 2]$, and suppose that each agent individually updates its own state z_i according to the uncoupled dynamics (5.2b). When $\delta = 0$, we obtain again the synchronous control dynamics $u^+ = \tilde{A}_{z_c}u$, which will now periodically implement

the following matrices

$$\tilde{A}_0 = \begin{bmatrix} A_{1,1} \\ A_{2,0} \\ A_{3,2} \end{bmatrix}, \quad \tilde{A}_1 = \begin{bmatrix} A_{1,2} \\ A_{2,1} \\ A_{3,0} \end{bmatrix}, \quad \tilde{A}_2 = \begin{bmatrix} A_{1,0} \\ A_{2,2} \\ A_{3,1} \end{bmatrix}. \tag{5.5}$$

Clearly, these matrices are different from those defined in (5.4). Indeed, using the same matrices B_i defined in the previous section, we obtain this time a collection of weighted adjacency matrices $\{\tilde{A}\}_{z_c \in \{0,1,2\}}$ describing the three graphs shown in Figure 5.1-(c). In this case the monodromy matrix M has eigenvalues satisfying $|\lambda(M)| = [0.27,\ 0.036,\ 1.225]$, which implies that M is not Schur stable. Figure 5.2-(center) shows a numerical simulation illustrating the unstable behavior of the closed-loop system emerging from the given initial conditions. The inset shows the synchronous behavior of the clocks, as well as the uncoordinated behavior of the logic states z_i. The parameters of the system are selected $\delta = 0.1$ and $\omega = 0.5$.

On the other hand, suppose now that the initial values of the clocks $\tau_i(0)$ and the logic states $z_i(0)$ are common for all the agents, i.e., these states are initially synchronized. Consider any measurable perturbation $\epsilon : \mathbb{R}_{\geq 0} \to \mathbb{R}$ with $\sup_{t \geq 0} |\epsilon(t)| \leq \varepsilon$ and $\varepsilon \in \mathbb{R}_{>0}$ *arbitrarily small*, acting on the clock τ_1 of the S/ZOH mechanism of agent 1, such that the control dynamics (5.2) of agent 1 are triggered ε seconds before the control dynamics of agents 2 and 3. Since agent 1 updates its controller before agents 2 and 3, the closed-loop system will exhibit sequential updates of the control dynamics (5.2). In the simplest case, when $\delta = 0$, these sequential updates will generate control dynamics (5.3) for agents 2 and 3 given by

$$u_2^+ = \tilde{A}_{2,z_2}[u_1^+, u_2, u_3]^\top, \quad u_3^+ = \tilde{A}_{3,z_3}[u_1^+, u_2, u_3]^\top. \tag{5.6}$$

Replacing u_1^+ by its definition in (5.3), we obtain the control dynamics in vectorial form, given by

$$u^+ = \begin{bmatrix} \tilde{A}_{1,z_1} \\ \tilde{a}^1_{2,z_2}\tilde{a}^1_{1,z_1},\ \tilde{a}^1_{2,z_2}\tilde{a}^2_{1,z_1} + \tilde{a}^2_{2,z_2},\ \tilde{a}^1_{2,z_2}\tilde{a}^3_{1,z_1} + \tilde{a}^3_{2,z_2} \\ \tilde{a}^1_{3,z_3}\tilde{a}^1_{1,z_1},\ \tilde{a}^1_{3,z_3}\tilde{a}^2_{1,z_1} + \tilde{a}^2_{2,z_2},\ \tilde{a}^1_{3,z_3}\tilde{a}^3_{1,z_1} + \tilde{a}^3_{2,z_2} \end{bmatrix} u,$$

where $\tilde{a}^k_{i,z_i}$ is the k^{th} entry of the row vector $\tilde{A}_{i,z_i}$. Again, the emerging synchronous discrete-time system is different from the desired nominal system (5.4). In fact, if we implement the same matrices B_i designed in the previous section, the resulting 3-periodic weighted adjacency matrices $\{\tilde{A}_{z_c}\}_{z_c\in\{0,1,2\}}$ will correspond to the three graphs shown in Figure 5.1-(b). In this case, the monodromy matrix satisfies $|\lambda(M)| = [0.04,\ 0.02,\ 2.239]$, which is also not Schur stable. Figure 5.2-(left) shows a simulation illustrating the unstable behavior that emerges in this case. Note that here the states (τ_i, z_i) are essentially synchronized. Of course, the instability generated by the sequential jumps can also emerge if the clocks are not synchronized during the evolution of the system, or if any other ε-perturbation acting on the clocks triggers the S/ZOH mechanisms in sequential order. This implies that synchronization of the clocks and logic modes is, in general, not enough to guarantee *robust* asymptotic stability of the networked sampled-data system (5.2) under a feedback control designed for the synchronous system (5.4), even when the continuous-time dynamics (5.1) are neglected. Moreover, as we will show in the next section, the sequential jumps of the controllers in the networked MAS are unavoidable when a robust synchronization mechanism is implemented for the clocks.

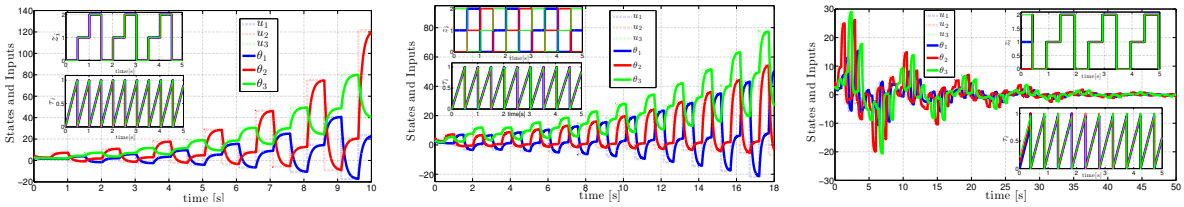

Figure 5.2: Agents with synchronized states τ_i and z_i, but without coordination mechanism $\mathcal{K}_{\rho_i}$ (left). Agents using $\mathcal{K}_{\rho_i}$, but without using $\mathcal{K}_{S_i}$ to synchronize z_i (center). Agents using both coordination mechanisms $\mathcal{K}_{S_i}$ and $\mathcal{K}_{\rho_i}$ (right).

5.1.4 A Universal Robust Coordination Mechanism

The lack of robustness discussed above is even more dramatic when the plant dynamics (5.1) are nonlinear, open-loop unstable, and set-valued, as well as when the control dynamics (5.2) are nonlinear and set-valued, such as those shown in Figure 5.3. However, as we will show in Section 5.3, it is indeed possible to design a feedback coordination mechanism that allows each agent i, with dynamics (5.1)-(5.2) and individual states $(\tau_i,\ z_i)$, to retain the stability properties, in a robust way, of the nominal synchronous system (5.4). In particular, as shown in Figure 5.5, the feedback coordination mechanism of each agent i is based on two main blocks: The block $\mathcal{K}_{S_i}$ will guarantee *global*, *robust*, and *decentralized*, synchronization of the states τ_i and z_i. The block $\mathcal{K}_{\rho_i}$ will guarantee that, under any sequential order of updates of the control dynamics (5.2a), the MAS with individual states $(\tau_i,\ z_i)$ will emulate the behavior of the synchronous system with global state (τ_c, z_c). Implementing this coordination mechanism, together with the matrices B_i designed for system (5.4), leads to the stable behavior shown in Figure 5.2-(right). The blocks $\mathcal{K}_{S_i}$ and $\mathcal{K}_{\rho_i}$ are "universal", in the sense that they can be used to coordinate a variety of networked multi-agent sampled-data systems with nonlinear and set-valued dynamics that implements a control system designed a priori to stabilize the networked system under the assumption of a global clock τ_c and a global logic state z_c. The design of $\mathcal{K}_{S_i}$ and $\mathcal{K}_{\rho_i}$ relies on robust stability

theory for set-valued hybrid dynamical systems, and these blocks can be implemented in a decentralized way.

5.2 Modeling Framework for a Class of CPS

We consider a multi-agent CPS with N agents, where each agent $i \in \mathcal{V} := \{1, 2, \ldots, N\}$ is an asynchronous sampled-data system comprised of three main parts:

(a) A continuous-time plant $\mathcal{P}_i$, modeled by a differential equation or inclusion, and an individual output y_i.

(b) A periodic discrete-time controller $\mathcal{C}_i$, modeled by a difference equation or inclusion, and parametrized by a periodic logic state z_i.

(c) A sampler/zero-order hold (S/ZOH) mechanism activated by an individual periodic resetting clock τ_i.

The *physical coupling* between the continuous-time dynamics $\mathcal{P}_i$ is characterized by a graph $\mathcal{G}_\mathcal{P} := \{\mathcal{V}, \mathcal{E}_\mathcal{P}\}$, whereas the *communication graph* between the individual controllers $\mathcal{C}_i$ is characterized by a graph $\mathcal{G}_\mathcal{C} = \{\mathcal{V}, \mathcal{E}_\mathcal{C}\}$. The graph $\mathcal{G}_\mathcal{C}$ also characterizes the access of each agent i to the clock information of its neighboring agents. In this section both graphs are assumed to be time-invariant. Next, we present the detailed model and assumptions behind each of the components (a), (b), (c) of each agent $i \in \mathcal{V}$.

5.2.1 Plant Dynamics

We consider nonlinear dynamical systems $\mathcal{P}_i$ with state $\theta_i \in \mathbb{R}^{p_i}$, input $u_i \in \mathbb{R}^{m_i}$, and output $y_i \in \mathbb{R}^{l_i}$. The governing dynamics are modeled by the set-valued system

$$\dot{\theta}_i \in P_i(\theta, u), \quad \theta_i \in \Theta_i, \quad u_i \in U_i, \tag{5.7a}$$

$$y_i = h_i(\theta, u), \tag{5.7b}$$

where $\theta := [\theta_1^\top, \ldots, \theta_N^\top]^\top \in \mathbb{R}^p$, $u = [u_1^\top, \ldots, u_N^\top]^\top \in \mathbb{R}^m$, $m = \sum_{i=1}^N m_i$, $p = \sum_{i=1}^N p_i$, $\Theta_i \subset \mathbb{R}^{p_i}$, $U_i \subset \mathbb{R}^{m_i}$, $P_i : \mathbb{R}^p \times \mathbb{R}^m \rightrightarrows \mathbb{R}^{p_i}$ is a set-valued mapping, and $h_i : \mathbb{R}^p \times \mathbb{R}^m \to \mathbb{R}^{l_i}$. Since the graph $\mathcal{G}_\mathcal{P}$ is time-invariant, we assume that it is embedded in the mappings P_i and h_i, i.e., even though we write these mappings as functions of the overall vectors θ and u, they only depend on the states θ_j and inputs u_j of the neighboring agents $j \in \mathcal{N}_{\mathcal{P}_i} := \{j : (i,j) \in \mathcal{E}_\mathcal{P}\}$. This graph, however, won't play any central role in our results. The model (5.7) is quite general and allows us to consider a variety of plants, including those with dynamics represented by non-Lipschitz or discontinuous differential equations, systems switching arbitrarily fast between a finite number of vector fields, and plants having unknown parameters that are known to lie on compact and convex sets [206], to just name a few. Aiming to exploit robustness properties for set-valued dynamical systems, we impose the following regularity assumption on system (5.7).

Assumption 31 *For each $i \in \mathcal{V}$ the following holds:* ***(a)*** *The set-valued mapping $P_i(\cdot,\cdot)$ is OSC, LB and convex valued relative to $\Theta \times U$.* ***(b)*** *The sets Θ_i and U_i are closed.* ***(c)*** *The function $h_i(\cdot,\cdot)$ is continuous.*

Item (a) in Assumption 31 is satisfied by any differential equation with a continuous right-hand side. It is also satisfied by the Krasovskii regularization of a discontinuous

vector field, provided it is LB [78, Lemma 5.16]. We also consider the following assumption, which simply asks that solutions generated by system (5.7a) are complete under fixed inputs.

Assumption 32 *Every solution of system* (5.7a) *with* $\dot{u} = 0$*, has an unbounded time domain.*

In situations where the plant (5.7a) does not satisfy Assumption 32 a priori, one may need to design a pre-stabilizing controller that ensures that solutions of the controlled system have no finite escape times.

5.2.2 Clock Dynamics

The S/ZOH mechanism of each agent has an individual clock $\tau_i \in \mathbb{R}_{\geq 0}$ with hybrid dynamics

$$\dot{\tau}_i = \omega, \qquad \tau_i \in [0, 1] \tag{5.8a}$$

$$\tau_i^+ = 0, \qquad \tau_i \in \{1\}, \tag{5.8b}$$

where the frequency $\omega \in \mathbb{R}_{>0}$ is assumed to be the same for all agents. In this hybrid system the clock flows with frequency ω until the condition $\tau_i = 1$ is satisfied, which resets τ_i^+ to zero. As in [141], we assume that each agent i has continuous access to the clock information τ_j of its neighboring agents $j \in \mathcal{N}_{\mathcal{C}_i}$.

5.2.3 Control Dynamics

In order to control the plant $\mathcal{P}_i$, each agent of the network implements a discrete-time controller $\mathcal{C}_i$ with states $[u_i^\top, z_i]^\top \in \mathbb{R}^{m_i+1}$. The state $u_i \in \mathbb{R}^{m_i}$ is the control signal, and z_i is a scalar periodic logic state defined on the finite set $Z := \{0, 1, 2, \ldots, \bar{z}\}$, where

$\bar{\mathrm{z}} \in \mathbb{Z}_{\geq 0}$ is a non-negative integer. The dynamics of the individual controllers are given by the periodic discrete-time set-valued dynamical system

$$u_i^+ \in G_{z_i}(u, y), \quad u_i \in U_i, \tag{5.9a}$$

$$z_i^+ = f_{\bar{\mathrm{z}}}(z_i) := \begin{cases} z_i + 1, & \text{if } z_i \in Z \backslash \{\overline{\mathrm{z}}\}, \\ 0, & \text{if } z_i \in \{\overline{\mathrm{z}}\}, \end{cases} \tag{5.9b}$$

where $y = [y_1^\top, y_2^\top, \ldots, y_N^\top]^\top \in \mathbb{R}^\ell$, with y_i defined as in (5.7b), and $\ell = \sum_{i=1}^N \ell_i$. In the update rule (5.9a) the mapping $G_{z_i} : \mathbb{R}^m \times \mathbb{R}^\ell \to \mathbb{R}^{m_i}$ is parametrized by the logic state z_i, which, according to (5.9b), is increased by one every time that the control dynamics (5.9a) are updated. This occurs until the condition $z_i = \bar{\mathrm{z}}$ is satisfied and the value of z_i^+ is reset back to zero. As in (5.7), the graph $\mathcal{G}_\mathcal{C}$ that characterizes the communication network between the controllers is embedded in the mapping G_{z_i}. This means that for each z_i, and each graph configuration $\mathcal{G}_\mathcal{C}$, the mapping G_{z_i} only depends on the individual signals (u_i, y_i) and the neighboring signals (u_j, y_j) for all $j \in \mathcal{N}_{\mathcal{C}_i} := \{j : (i, j) \in \mathcal{E}_\mathcal{C}\}$. As it is the case for the clock τ_i, we assume that each agent i has continuous access to the information of the logic states z_j associated with its neighbors $j \in \mathcal{N}_{\mathcal{C}_i}$.

Remark 24 *System* (5.9) *generalizes standard non-periodic discrete-time systems. In fact, by taking* $\overline{z} = 0$ *such that* $Z = \{0\}$*, we obtain that the mapping at the right hand side of* (5.9a) *is the same for all iterations.*

Using set-valued dynamical systems to model the control system allows us to consider controllers with continuous or discontinuous dynamics, as well as more elaborated set-valued algorithms that generate multiple potential updates at every iteration. Let $\Theta := \prod_{i \in \mathcal{V}} \Theta_i$ and $U := \prod_{i \in \mathcal{V}} U_i$. The following regularity assumption is considered on the mapping G_{z_i}.

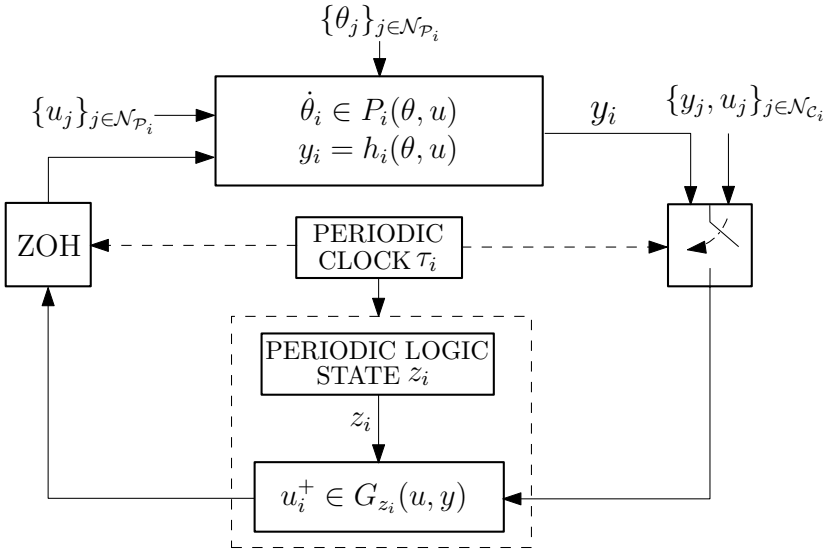

Figure 5.3: Structure of each sampled-data agent i of the networked system.

Assumption 33 *For each $i \in \mathcal{V}$ and each $z_i \in Z$ the mapping $G_{z_i}(\cdot,\cdot)$ is OSC and LB relative to $U \times h(\Theta, U)$*

Since we allow to constrain the state u_i to the set U_i, the following assumption is imposed on system (5.9) to guarantee that the interconnection of (5.7) and (5.9) generates at least one complete solution.

Assumption 34 *For each $(\theta, u, z_i) \in \Theta \times U \times Z$ we have that $G_{z_i}(u, h(\theta, u)) \cap U_i \neq \emptyset$.*

Equations (5.7), (5.8), and (5.9) comprise our baseline model for the asynchronous networked multi-agent sampled-data system. Figure 5.3 shows a conceptual representation of the structure of each agent. Each time that the clock τ_i is reset to zero according to (5.8), agent i proceeds to sample the inputs and outputs (u_i, y_i) and (u_j, y_j), for $j \in \mathcal{N}_{\mathcal{C}_i}$, generated by the dynamics (5.7b), and to update the control states (u_i, z_i) via the set-valued mapping (5.9).

5.2.4 Problem Statement

In this chapter, we are interested in designing robust distributed feedback mechanisms for networked multi-agent sampled-data systems with dynamics (5.7), (5.8), and (5.9). In particular, let $\mathcal{A}_\theta \subset \mathbb{R}^p$ and $\mathcal{A}_u \subset \mathbb{R}^m$ be nonempty compact sets defined a priori for a particular application. Let $\xi := [\theta^\top, u^\top]^\top$ and

$$\mathcal{A}_\xi := \mathcal{A}_\theta \times \mathcal{A}_u. \tag{5.10}$$

We wish to establish the existence of a $\mathcal{KL}$ function $\beta(\cdot,\cdot)$ such that for each $(\nu, \Delta) \in \mathbb{R}^2_{>0}$ it is possible to tune the parameters of the feedback mechanism such that for all $|\xi(0,0)|_{\mathcal{A}_\xi} \leq \Delta$ and all trajectories of ξ generated by the HDS that characterizes the networked sampled data system, the following bound holds:

$$|\xi(t,j)|_{\mathcal{A}_\xi} \leq \beta(|\xi(0,0)|_{\mathcal{A}_\xi}, t+j) + \nu. \tag{5.11}$$

Moreover, the feedback mechanisms must be robust with respect to small disturbances acting on the states and dynamics of the closed-loop system, i.e., we want to avoid that arbitrarily small perturbations on the inputs, outputs, states, and clocks, dramatically change the stability properties of the system. As shown in the motivational example of Section 5.1, this is a challenging task, since we don't preclude the existence of sequential jumps generated by ε perturbations acting on the clocks of each agent. In fact, as we will show in the next section, this sequential jumps are unavoidable when robust clock synchronization mechanisms are implemented.

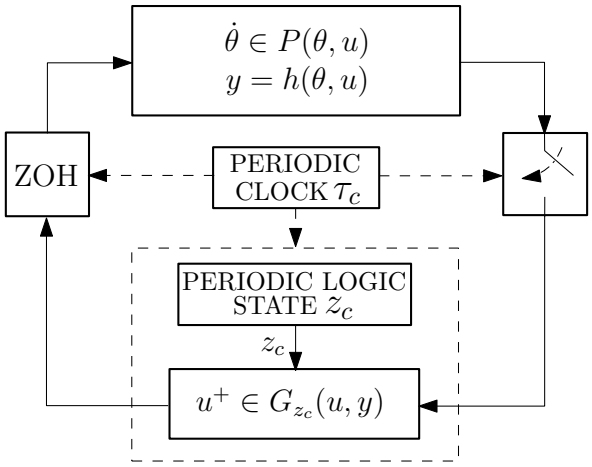

Figure 5.4: Networked multi-agent sampled-data system with centralized sampling and logic state.

5.3 Robust Hybrid Coordination Mechanisms

In order to design a decentralized feedback control that stabilizes the multi-agent sampled-data system with dynamics (5.7), (5.8), and (5.9), we propose an emulation-like approach, where the control system is designed to emulate the behavior of a feedback stabilization mechanism designed a priori for a synchronous networked system with a global clock τ_c, a global logic state z_c, and a unique S/ZOH mechanism for the MAS. This synchronized networked system with centralized sampling and periodic logic state z_c is shown in Figure 5.4, where $P(\theta, u) := P_1(\theta, u) \times \ldots \times P_N(\theta, u)$ and $G_{z_c}(u, y) = G_{z_1}(u, y) \times \ldots \times G_{z_N}(u, y)$, $z_i = z_c$ for all $i \in \mathcal{V}$. One can design control dynamics for this type of synchronous systems by using standard algebraic or Lyapunov-based tools that are not suitable for asynchronous systems, e.g., [236], [78]. Moreover, if the plants have trivial dynamics, i.e., $\dot{\theta} = 0$, and the set Z is a singleton, as in Remark 24, the closed-loop system corresponds to a synchronous non-periodic discrete-time system that can be analyzed using classic tools for discrete-time MAS, e.g., [237], [238], [239].

We model the synchronous networked system as a HDS with state $x_c := [\tau_c, z_c, \theta^\top, u^\top]^\top$

and data $\mathcal{H}_c := \{C_c, F_c, D_c, G_c\}$, given by

$$C_c := [0,1] \times Z \times \Theta \times U \tag{5.12a}$$

$$[\dot{\tau}_c, \dot{z}_c, \dot{\theta}^\top, \dot{u}^\top]^\top \in F_c := \{\omega\} \times \{0\} \times P(\theta, u) \times \{\mathbf{0}_m\} \tag{5.12b}$$

$$D_c := \{1\} \times Z \times \Theta \times U \tag{5.12c}$$

$$[\tau_c^+, z_c^+, \theta^{\top+}, u^{\top+}]^\top \in G_c = \{0\} \times \{f_{\bar{z}}(z_c)\} \times \ldots \\ \ldots \{\theta\} \times G_{z_c}(u, h(\theta, u)). \tag{5.12d}$$

where $f_{\bar{z}}$ is defined in (5.9b). For this centralized system, the control dynamics G_{z_c} are designed such that the following assumption holds.

Assumption 35 *For the HDS* (5.12) *the compact set* $\mathcal{A}_c := [0,1] \times Z \times \mathcal{A}_\xi$*, with* $\mathcal{A}_\xi$ *given by* (5.10)*, is UGAS.*

Under Assumptions 1-5, the HDS (5.12) is well-posed and robust to small perturbations. However, as shown in Section 5.1, the direct implementation of the control dynamics G_{z_c} in the original asynchronous networked system leads to closed-loop systems with zero margins of robustness, as well as asymptotic behaviors that are dependent on the initial conditions of the states. Therefore, to guarantee that the asynchronous MAS with controllers G_{z_i} retains the robust stability properties of the centralized system (5.12), we implement the control dynamics together with two decentralized robust synchronization and coordination mechanisms, $\mathcal{K}_{S_i}$ and $\mathcal{K}_{\rho_i}$, shown in Figure 5.5.

5.3.1 Robust Global Synchronization Using $\mathcal{K}_{S_i}$

For each agent $i \in \mathcal{V}$, we design a Lyapunov-based feedback mechanism $\mathcal{K}_{S_i}$ that guarantees global and robust synchronization in finite time of the states τ_i and z_i. Since a network of resetting clocks with equal frequency ω is equivalent to a network

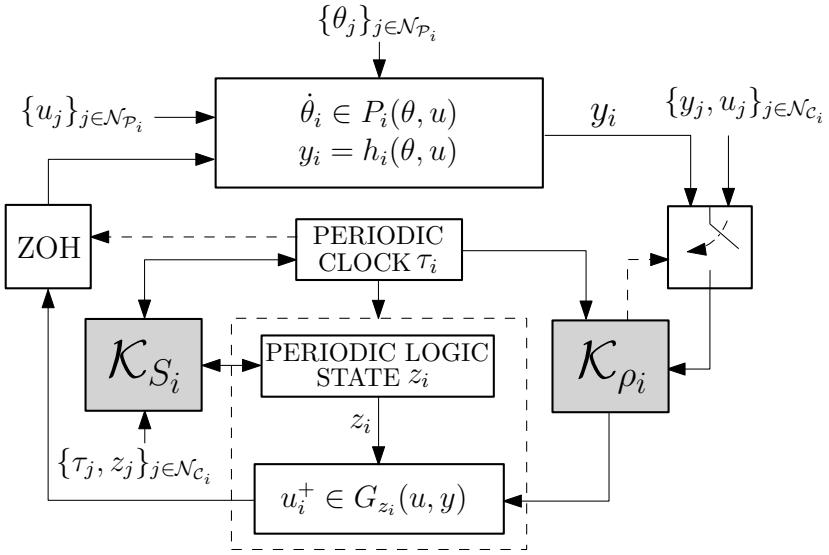

Figure 5.5: Networked system with robust synchronization and coordination mechanisms $\mathcal{K}_{S_i}$ and $\mathcal{K}_{\rho_i}$.

of oscillators flowing on the unit circle, global and robust synchronization of clocks is impossible using smooth feedback [157]. In fact, synchronization of periodic clocks and logic states is equivalent to synchronization of periodic oscillators flowing on a circle generated by the union of unitary arcs, each arc representing a different possible value of z_i, where the beginning of each arc corresponds to $\tau_i = 0$ and the end to $\tau_i = 1$, see Figures 5.7 and 5.8. In the language of robust hybrid dynamical systems, e.g., [78, Chapter 4], a robust synchronization mechanism must guarantee that for each $\tau_0 \in [0, 1]$, and each sequence of initial conditions $\{\tau_k(0, 0)\}_{k\in\mathbb{Z}_{\geq 0}}$ with components $\tau_{i,k}(0, 0)$ satisfying $0 \leq \tau_{1,k}(0, 0) \leq \ldots \leq \tau_{N,k}(0, 0) < \tau_0$ and $\lim_{k\to\infty} \tau_{1,k}(0, 0) = \ldots = \tau_{N,k}(0, 0) = \tau_0$, the sequence of solutions $\{\tau_k\}_{k\in\mathbb{Z}_{\geq 0}}$ must converge to a limiting solution as $k \to \infty$ that approximates the behavior that one obtains from the initial condition $\tau_1 = \ldots = \tau_N = \tau_0$. For the case when $\tau_0 = 1$, this condition implies that the clocks are sequentially reset with smaller and smaller times between resets, which implies that in the limiting case the resets must also be sequential, in this case with no time between resets. Since the initial conditions $\tau_i \in [0, 1]$ are arbitrary, a robust synchronization

mechanism must guarantee synchronization under *any* possible order of sequential resets of the clocks, i.e., any sequential order of the triggering mechanisms. Similarly, synchronization of the states z_i must be achieved from every possible initial condition in Z^N. Since the integer states z_i increment by one every time the controller i is updated, the synchronization goal for z_i is to guarantee the existence of a finite time T (uniform over all initial conditions) such that for all (t, j) satisfying $t + j > T$, the states z_i always agree on the same value during flows.

Based on this, for a HDS with state $[\tau^\top, z^\top]^\top$, with $\tau = [\tau_1, \ldots, \tau_N]^\top$, and $z = [z_1, \ldots, z_N]^\top$, we are interested in guaranteeing UGAS of the compact set

$$\mathcal{A}_{\tau,z} := \mathcal{A}_{\tau,z}^{\text{jump}_1} \cup \mathcal{A}_{\tau,z}^{\text{jump}_2} \cup \mathcal{A}_{\tau,z}^{\text{flow}} \subset [0,1]^N \times Z^N, \tag{5.13}$$

where the sets $\mathcal{A}_{\tau,z}^{\text{jump}_1}$, $\mathcal{A}_{\tau,z}^{\text{jump}_2}$, and $\mathcal{A}_{\tau,z}^{\text{flow}}$ are defined as

$$\begin{aligned}
\mathcal{A}_{\tau,z}^{\text{jump}_1} &:= \bigcup_{k \in Z \setminus \{0\}} \Big\{ (\tau, z) \in [0,1]^N \times Z^N : \tau_i + z_i = k,\ \forall\, i \in \mathcal{V} \Big\}, \\
\mathcal{A}_{\tau,z}^{\text{jump}_2} &:= \Big\{ (\tau, z) \in [0,1]^N \times Z^N : \tau_i + z_i \in \{0, \bar{\text{z}} + 1\},\ \forall\, i \in \mathcal{V} \Big\}, \\
\mathcal{A}_{\tau,z}^{\text{flow}} &:= \bigcup_{k \in Z} \Big([0,1] \times \{k\} \Big) \cdot \mathbf{1}_N.
\end{aligned}$$

Set $\mathcal{A}_{\tau,z}$ corresponds to the case where all agents have the same value of τ_i and z_i during flows, and where this values can differ only by one, in an ordered way, whenever z_i jumps to the next mode for some $i \in \mathcal{V}$. Figure 5.6 shows the set $\mathcal{A}_{\tau,z}$ for the case when $N = 2$ and $Z = \{0, 1, 2, 3\}$. In order to stabilize the set (5.13), we consider a hybrid mechanism $\mathcal{K}_{S_i}$ that works as follows:

(a) During flows, i.e., when $\tau_i \in [0, 1)$, the states (τ_i, z_i) of agent $i \in \mathcal{V}$ flow according

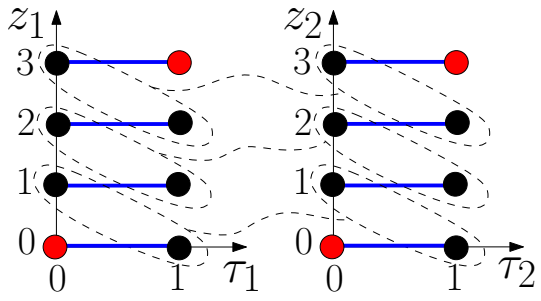

Figure 5.6: Set $\mathcal{A}_{\tau,z}$ for $\mathcal{V} = \{1, 2\}$ and $\mathcal{Z} = \{0, 1, 2, 3\}$. $\mathcal{A}_{\tau,z}^{\text{jump}_1}$ corresponds to the union of the encircled black dots with dash lines. $\mathcal{A}_{\tau,z}^{\text{jump}_2}$ corresponds to the set of red dots, and $\mathcal{A}_{\tau,z}^{\text{flow}}$ corresponds to the blue lines with same value of z_i.

to the dynamics

$$\dot{\tau}_i = \omega, \qquad \dot{z}_i = 0. \tag{5.15}$$

(b) Let $i \in \mathcal{V}$ be an agent of the network satisfying the condition $\tau_i = 1$. Then, agent i resets its clock according to (5.8b), and updates z_i as (5.9b). Simultaneously, all its neighboring agents j satisfying $i \in \mathcal{N}_{\mathcal{C}_j}$ update their states (τ_j, z_j) using the set-valued rule

$$[\tau_j^+, z_j^+] \in \mathcal{R}_j(z_i, \tau_j, z_j), \tag{5.16}$$

with mapping $\mathcal{R}_j$ defined as

$$\mathcal{R}_j := \Big\{ (\mathcal{L}_{\tau,j}(z_i, v, w), \mathcal{L}_{z,j}(z_i, z_j, w)) : v \in \mathcal{T}_j(\tau_j), \\ w \in \mathcal{Q}_j(\tau_j, z_j) \Big\},$$

where the functions $\mathcal{L}_{\tau,j}$ and $\mathcal{L}_{z,j}$ are defined as

$$\mathcal{L}_{\tau,j} := v \cdot \mathbb{I}_{\mathcal{O}}(z_i) \ + 1 \cdot w \cdot (1 - \mathbb{I}_{\mathcal{O}}(z_i)) \tag{5.17a}$$

$$\mathcal{L}_{z,j} := z_j \cdot \mathbb{I}_{\mathcal{O}}(z_i) + \bar{z} \cdot w \cdot (1 - \mathbb{I}_{\mathcal{O}}(z_i)), \tag{5.17b}$$

where $\mathcal{O} := Z \backslash \{\bar{z}\}$, and where the *coordination* set-valued mappings $\mathcal{T}_j : [0, 1] \rightrightarrows$

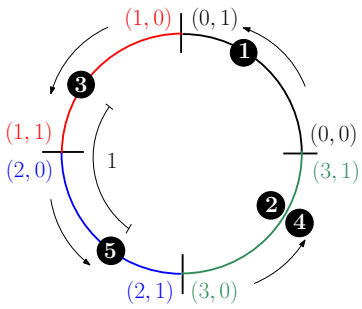

Figure 5.7: Agents with synchronized clocks τ_i, flowing with different values of z_i (colored).

$\{0,1\}$ and $\mathcal{Q}_j : [0,1] \times Z \rightrightarrows \{0,1\}$ are defined as

$$\mathcal{T}_j(\tau_j) := \begin{cases} \{1\} & \text{if } \tau_j \in (r_j, 1] \\ \{0,1\} & \text{if } \tau_j = r_j \\ \{0\} & \text{if } \tau_j \in [0, r_j), \end{cases} \tag{5.18a}$$

$$\mathcal{Q}_j(\tau_j, z_j) := \begin{cases} \{1\} & \text{if } z_j + \tau_j \in (r_j, \bar{\mathrm{z}} + 1] \\ \{0,1\} & \text{if } z_j + \tau_j = r_j \\ \{0\} & \text{if } z_j + \tau_j \in [0, r_j) \end{cases} \tag{5.18b}$$

where $r_j \in (0, N^{-1})$ for all $j \in \mathcal{V}$.

Finally, for those agents j such that $i \notin \mathcal{N}_{\mathcal{C}_j}$ the states (τ_j, z_j) are kept constant.

According to this update rule, each agent needs to know only the cardinality of $\mathcal{V}$ and the values (z_j, v_j) of its neighboring agents. Note that when $z_i < \bar{\mathrm{z}}$, the update of τ_j^+ for the neighboring agents j is entirely characterized by (5.18a), leaving the state z_j constant. On the other hand, when $z_i = \bar{\mathrm{z}}$ the updates of the states (τ_j, z_j) depend on the value w generated by the coordination mapping (5.18b), but it will only update τ_j either to 1 or 0. Figures 5.7 and 5.8 show a conceptual representation of the evolution of (z_i, τ_i) in a network with $\mathcal{V} = \{1,2,3,4,5\}$, and $Z = \{0,1,2,3\}$. The parentheses show the value (z_i, τ_i). The hybrid synchronization mechanism $\mathcal{K}_{S_i}$ described above

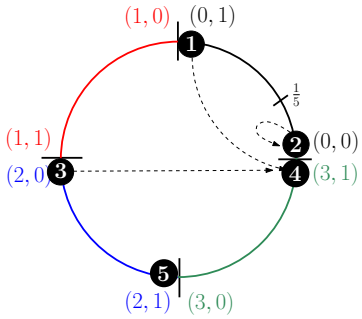

Figure 5.8: Jumps on z_i induced by agent 4, which shares information with agents {1,2,3}.

can formally be written as a HDS that generates every possible trajectory that emerges due to sequential jumps when more than one agent satisfies the condition $\tau_i = 1$. This HDS is given by the data

$$\begin{aligned} \left[\dot{\tau}^\top, \dot{z}^\top\right] &\in F_{\tau,z} := \{\omega \cdot \mathbf{1}_N\} \times \{\mathbf{0}_N\}, \;\; C_{\tau,z} := C_\tau \times Z^N \\ [\tau^\top, z^\top]^+ &\in G_{\tau,z}(\tau, z), \qquad D_{\tau,z} := D_\tau \times Z^N, \end{aligned} \tag{5.19}$$

where C_τ and D_τ are defined as

$$C_\tau = [0,1]^N, \quad D_\tau = \left\{\tau \in [0,1]^N : \max_{i \in \mathcal{V}} \tau_i = 1\right\}, \tag{5.20}$$

and where the jump map $G_{\tau,z}$ is defined as the outer semicontinuous hull of the mapping

$$G^0_{\tau,z}(\tau, z) := \Bigg\{ g \in \mathbb{R}^{2N} : g_i = [0, f_{\bar{z}}(z_i)]^\top,$$
$$g_j \in \begin{cases} \mathcal{R}_j(\tau, z), & \text{if } i \in \mathcal{N}_{\mathcal{C}_j} \\ \{\tau_j\} \times \{z_j\}, & \text{if } i \notin \mathcal{N}_{\mathcal{C}_j} \end{cases}, \; \forall \; j \; \neq \; i \Bigg\},$$

which is defined to be not empty only when $\tau_i = 1$ for some $i \in \mathcal{V}$ and $\tau_j \in [0, 1)$ for $j \neq i$. Based on this, $G_{\tau,z}$ satisfies $\text{graph}(G_{\tau,z}) = \text{cl}(\text{graph}(G^0_{\tau,z}))$.

The asymptotic and robustness properties of system (5.19) are characterized by the

following proposition.

Proposition 12 *Consider the hybrid synchronization mechanism $\mathcal{K}_{S_i}$ described by the HDS* (5.19)*. Suppose that the graph $\mathcal{G}_{\mathcal{C}}$ is strongly connected. Then the set $\mathcal{A}_{\tau,z}$ is UGAS. Moreover, the convergence to $\mathcal{A}_{\tau,z}$ is in finite time.*

Proof: The result follows as a special case of Theorem 8 in Section 5.4.

Remark 25 *For the case when $\bar{\boldsymbol{z}} = 0$, i.e., when the control dynamics are not periodic, the state z_i can be omitted and the set $\mathcal{O}$ is defined to be $\mathcal{O} = \{0\}$. In this case the set-valued mapping $\mathcal{R}_j$ reduces to $\mathcal{T}_j$ in* (5.18a)*, and the compact set* (5.13) *reduces to the set*

$$\mathcal{A}_{\tau,sync} := ([0,1] \cdot \mathbf{1}_N) \cup (\{0,1\}^N), \tag{5.21}$$

which was studied in [240].

5.3.2 Pre-Jump Sampling Control Using $\mathcal{K}_{\rho_i}$

As illustrated in Section 5.1, synchronization of the clocks and logic states is not enough to guarantee robust stability of the MAS. This is due to the sequential updates of the control dynamics (5.9) that can generate composite mappings such as those emerging in (5.6). Since the results of Section 5.3.1 show that sequential updates induced by the clocks are unavoidable when describing robust clock synchronization mechanisms, we now proceed to design a distributed coordination mechanism that, under the effect of sequential updates, allows agents to retain the stability properties of the centralized system (5.12). The key idea behind the coordination mechanism is that each agent $i \in \mathcal{V}$ will sample the value of the inputs and outputs of its neighboring agents just before resetting its clock. The sampled values will be stored in a memory state $s_i \in \mathbb{R}^{m+\ell}$, which will then be passed as argument to the mapping G_{z_i} in (5.9a)

to generate the new update u_i^+ whenever the clock τ_i is reset to zero. We call this strategy "pre-jump sampling control".

The main challenge in designing the hybrid mechanism that implements the pre-jump sampling control is to guarantee that the resulting system is well-posed, i.e., that small noise or ε-disturbances do not destroy the stability properties of the system. To achieve this, each agent $i \in \mathcal{V}$ is given a logic state α_i that takes values in the discrete set $\{0, 1\}$, where 0 corresponds to being ready to take a sample, and 1 corresponds to having already taken the sample. The sampling location in the interval $[0, 1]$ is denoted as $\rho_i \in (N^{-1}, 1)$, which is a tunable parameter. The i^{th} clock variable τ_i is allowed to flow continuously when $\alpha_i = 0$ and $\tau_i \in [0, \rho_i]$, as well as when $\alpha_i = 1$ and $\tau_i \in [\rho_i, 1]$. Jumps where a sample is taken should occur when $\tau_i = \rho_i$ and $\alpha_i = 0$, and they should toggle the state α_i to 1. Jumps that reset the clock to zero and toggle α_i to 0 should occur when $\tau_i = 1$ and $\alpha_i = 1$. Based on this idea, we define the sets

$$C_{i,0} := [0, \rho_i] \times \{0\}, \qquad C_{i,1} := [\rho_i, 1] \times \{1\} \tag{5.22a}$$

$$D_{i,0} := \{\rho_i\} \times \{0\}, \qquad D_{i,1} := \{1\} \times \{1\} \tag{5.22b}$$

$$C_i := C_{i,0} \cup C_{i,1}, \qquad D_i := D_{i,0} \cup D_{i,1}. \tag{5.22c}$$

The value of s_i is held constant during flows, and it is also not changed at jumps that correspond to resetting the clock τ_i to zero. However, whenever $(\tau_i, \alpha_i) \in D_{i,0}$ the value of s_i is updated to $[u^\top, h(\theta, u)^\top]^\top$. Note that although we set the dimension of s_i to $m+\ell$, the only components of s_i that need to be updated are the ones corresponding to the neighboring agents $j \in \mathcal{N}_{\mathcal{C}_i}$.

Remark 26 *For each agent $i \in \mathcal{V}$ the role of the state α_i is to guarantee a robust detection of the sampling instant ρ_i. This state is needed because the condition $\tau_i = \rho_i$*

can easily be "missed" under arbitrarily small measurement noise on τ_i. To avoid this phenomenon the memory state α_i is introduced, such that it keeps track of the side of the decision boundary in which the clock is located. See [157] and [241, pp. 35] for similar discussions in this direction.

5.3.3 Closed-loop System with Mechanisms $\mathcal{K}_{S_i}$ and $\mathcal{K}_{\rho_i}$

We now analyze the interconnection of the coordination mechanisms $\mathcal{K}_{S_i}$ and $\mathcal{K}_{\rho_i}$ with the control dynamics G_{z_i} designed for system (5.12).

Individual Agent Dynamics

The interconnection of the flow dynamics (5.7), control dynamics (5.9), resetting clocks (5.8), synchronization mechanism (5.19), and pre-sampling control with auxiliary states (α_i, s_i), leads to the following hybrid dynamics for each agent $i \in \mathcal{V}$

$$\begin{pmatrix} \dot{\tau}_i \\ \dot{\alpha}_i \\ \dot{z}_i \\ \dot{s}_i \\ \dot{\theta}_i \\ \dot{u}_i \end{pmatrix} \in \begin{pmatrix} \omega \\ 0 \\ 0 \\ 0 \\ P_i(\theta, h(\theta,u)) \\ 0 \end{pmatrix}, \quad \begin{array}{l} (\tau_i,\alpha_i) \in C_i \\ z_i \in Z,\ s_i \in U \times \mathbb{R}^\ell \\ \theta_i \in \Theta_i,\ u_i \in U_i \end{array} \tag{5.23a}$$

$$\begin{pmatrix} \tau_i^+ \\ \alpha_i^+ \\ z_i^+ \\ s_i^+ \\ \theta_i^+ \\ u_i^+ \end{pmatrix} \in \begin{pmatrix} \tau_i \\ 1 \\ z_i \\ \left[u^\top, h(\theta,u)^\top\right]^\top \\ \theta_i \\ u_i \end{pmatrix}, \quad \begin{array}{l} (\tau_i,\alpha_i) \in D_{i,0} \\ z_i \in Z,\ s_i \in U \times \mathbb{R}^\ell \\ \theta_i \in \Theta_i,\ u_i \in U_i \end{array} \tag{5.23b}$$

$$\begin{pmatrix} \tau_i^+ \\ \alpha_i^+ \\ z_i^+ \\ s_i^+ \\ \theta_i^+ \\ u_i^+ \end{pmatrix} \in \begin{pmatrix} 0 \\ 0 \\ f_{\bar{z}}(z_i) \\ s_i \\ \theta_i \\ G_{i,u,z}(s_i) \end{pmatrix}, \quad \begin{array}{l} (\tau_i,\alpha_i) \in D_{i,1} \\ z_i \in Z,\ s_i \in U \times \mathbb{R}^\ell \\ \theta_i \in \Theta_i,\ u_i \in U_i \end{array} \tag{5.23c}$$

$$\begin{pmatrix} \tau_i^+ \\ \alpha_i^+ \\ z_i^+ \\ s_i^+ \\ \theta_i^+ \\ u_i^+ \end{pmatrix} \in \begin{pmatrix} \left.\begin{array}{c} \mathcal{L}_{\tau,i}(z_i,v,w) \\ \mathcal{L}_{\tau,i}(z_i,v,w) \\ \mathcal{L}_{z,i}(z_i,z_j,w) \end{array}\right\}, \ v \in \mathcal{T}_i,\ w \in \mathcal{Q}_i \\ s_i \\ \theta_i \\ u_i \end{pmatrix}, \quad \begin{array}{l} (\tau_i,\alpha_i) \in C_i, \\ (\tau_j,\alpha_j) \in D_{j,1}, \\ j \in \mathcal{N}_{\mathcal{C}_i}, z_i \in Z, \\ s_i \in U \times \mathbb{R}^\ell, \\ \theta_i \in \Theta_i, u_i \in U_i. \end{array} \tag{5.23d}$$

During flows the states τ_i and θ_i evolve according to their continuous-time dynamics in (5.23a) and subject to the flow sets C_i, i.e., if $\tau_i \leq \rho_i$ flows are only allowed if $\alpha_i = 0$, while if $\tau_i \geq \rho_i$ flows are only allowed if $\alpha_i = 1$. Whenever the clock satisfies the condition $\tau_i = \rho_i$ with $\alpha_i = 0$, a jump is generated according to the mapping (5.23b), which toggles α_i to 1, and samples the states u_j and outputs y_j of the neighboring agents $j \in \mathcal{N}_{\mathcal{C}_i}$, storing said value in the state s_i. Toggling α_i to 1 will force the system to be in the set $C_{i,1}$, where the states of the agent will flow according to (5.23a) again, until the condition $\tau_i = 1$ is satisfied. This condition will force the states of the i^{th} agent to jump according to (5.23c). Finally, equation (5.23d) models the jumps induced by any neighbor j of agent i satisfying $\tau_j = 1$, i.e., the jumps that guarantee the synchronization during flows of the vectors τ and z.

Dynamics of the Closed-loop Networked MAS

To analyze the closed-loop MAS that emerges when each agent implements the dynamics (5.23), let $s = [s_1, \ldots, s_N]^\top \in \mathbb{R}^{mN+\ell N}$, $n = 3N + \ell N + mN + p + m$, and let the overall state be

$$x = \left[(\tau_1, \alpha_1, z_1)^\top, \ldots, (\tau_N, \alpha_N, z_N)^\top, s^\top, \theta^\top, u^\top\right]^\top.$$

Let $\tilde{f} := \omega \cdot f$, where $f \in \mathbb{R}^{3N}$ and $f_k = 1$ for all $k \in \{1, 4, 7, 10, \ldots, 3N-2\}$ and $f_k = 0$ otherwise. Using this construction the continuous-time dynamics of the MAS are given by

$$\dot{x} \in F(x) := \{\tilde{f}\} \times \{\mathbf{0}_N\} \times P(\theta, h(\theta, u)) \times \{\mathbf{0}_N\}. \tag{5.24}$$

Also, let $\tilde{C}_1 := (C_1 \times Z) \times \ldots \times (C_N \times Z)$ and $\tilde{C}_2 = (U \times \mathbb{R}^\ell) \times \ldots \times (U \times \mathbb{R}^\ell) \subset \mathbb{R}^{N\ell+Nm}$. The flow set for the MAS is then given by

$$C := \tilde{C}_1 \times \tilde{C}_2 \times \Theta \times U. \tag{5.25}$$

To cover all the jumps described by equation (5.23), the jump set is defined as

$$D := \left\{ x \in C : \max_{i \in \mathcal{V}} \left((1-\alpha_i)\frac{\tau_i}{\rho_i} + \alpha_i \tau_i \right) = 1 \right\}. \tag{5.26}$$

To construct the jump map that generates the jumps of equation (5.23), let $G^0 : \mathbb{R}^n \rightrightarrows \mathbb{R}^n$ be a set-valued mapping that is non-empty only at points $x \in D^0$, where

$$D^0 := \{x \in C : (1-\alpha_i)\frac{\tau_i}{\rho_i} + \alpha_i\tau_i = 1, \text{ for one and only one } i \in \mathcal{V}\}$$

Let $x \in D^0$, $(1-\alpha_i)\frac{\tau_i}{\rho_i} + \alpha_i\tau_i = 1$. Then $G^0(x)$ is defined as follows:

- If $\alpha_i = 0$, then

$$G^0(x) := x + e_{3i-1} + M_i \left([u^\top, h(\theta, u)^\top]^\top - s_i \right), \tag{5.27}$$

  where $e_{3i-1} \in \mathbb{R}^n$ is a vector of zeros except at the $3i-1$ entry, which is one, and $M_i \in \mathbb{R}^{n \times (m+\ell)}$ is a matrix of zeros, except in the $m+\ell$ rows from $3N + (i-1) \cdot (m+\ell) + 1$ to $3N + i \cdot (m+\ell)$, where it is set to the identity matrix. This models the jumps of (5.23b).

- If $\alpha_i = 1$, then $G^0(x)$ is defined as the set of vectors in $g \in \mathbb{R}^n$ such that the components that generate τ_i^+ and α_i^+ are zero, the component that generate z_i^+ is

$f_{\bar{z}}(z_i)$ given by (5.9b), the component that generates s_i^+ is s_i, and the component that generates u_i^+ belongs to $G_{z_i}(s_i)$. This models the jumps (5.23c). For $j \in \mathcal{N}_{\mathcal{C}_i}$ the components of g that generate $(\tau_j^+, \alpha_j^+, z_j^+, s_j^+, \theta_j^+, u_j^+)$ are updated as in (5.23d), and for $j \notin \mathcal{N}_{\mathcal{C}_i}$ the components of g that generate $(\tau_j^+, \alpha_j^+, z_j^+, s_j^+, \theta_j^+, u_j^+)$ are $(\tau_j, \alpha_j, z_j, s_j, \theta_j, u_j)$. This models the jumps (5.23d).

Using the previous construction, the jump map $G(x)$ for the overall system is defined as

$$x^+ \in G(x) := \overline{G^0(x)}. \tag{5.28}$$

where $\overline{G^0(x)}$ is the outer semicontinuous hull of $G^0(x)$.

Based on this, the resulting HDS has data $\mathcal{H} = \{C, F, D, G\}$ given by (5.25), (5.24), (5.26), and (5.28). For this system we are interested in studying the stability properties of the compact set

$$\mathcal{A} := \mathcal{A}_{\tau,\alpha,z} \times \mathcal{A}_s^N \times \mathcal{A}_\xi, \tag{5.29}$$

where $\mathcal{A}_{\tau,\alpha,z} \subset \mathbb{R}^{3N}$ and $\mathcal{A}_s \subset \mathbb{R}^{m+\ell}$ are defined as

$$\begin{aligned}\mathcal{A}_{\tau,\alpha,z} := \big\{&(\tau_1, \alpha_1, z_1) \times \ldots \times (\tau_N, \alpha_N, z_N) \in \tilde{C}_1 : \\ &(\tau^\top, z^\top)^\top \in \mathcal{A}_{\tau,z}\big\}, \\ \mathcal{A}_s := \mathcal{A}_u \times h(\mathcal{A}_\theta, \mathcal{A}_u),&\end{aligned}$$

and where $\mathcal{A}_{\tau,z}$ is given by (5.13), and $\mathcal{A}_\xi$ by (5.10). The following theorem is the first main result of this chapter.

Theorem 7 *Consider the HDS $\mathcal{H} = \{C, F, D, G\}$ with F given by (5.24), C given by (5.25), D given by (5.26), and G given by (5.28). Suppose that the graph $\mathcal{G}_\mathcal{C}$ is strongly connected. Let $\tilde{\rho}_i := 1 - \rho_i$, and $\tilde{\rho}^* = \max_{i\in\mathcal{V}}\{\tilde{\rho}_i\}$. Then system $\mathcal{H}$ is well-posed, and*

the set (5.29) *is SGP-AS as* $\tilde{\rho}^* \to 0^+$.

The SGP-AS result of Theorem 7 allow us to obtain a $\mathcal{KL}$ bound of the form (5.11) for the state x in the closed-loop HDS. Moreover, finite-time convergence of (τ, z), and compactness of the sets C_τ, D_τ, $\tilde{C}_1$ imply the existence of a similar $\mathcal{KL}$ bound for the state ξ, as in (5.11).

Remark 27 *According to Theorem 7, for values of* ρ_i *sufficiently close to* 1*, if each agent implements the coordination mechanisms* $\mathcal{K}_{S_i}$ *and* $\mathcal{K}_{\rho_i}$*, as well as a discrete-time controller* G_{z_i} *designed to stabilize the centralized system* (35)*, the resulting decentralized system with local clocks* τ_i *and logic states* z_i *will emulate the behavior of system* (35)*. Moreover, well-posedness of the resulting HDS confers desirable robustness properties to the MAS.*

5.4 Robust Synchronization in Time-Varying Graphs

In many applications, the topology of the graph that characterizes a communication network changes over time, and in some cases leads to disconnected graphs. In this section, we study the asymptotic properties of the synchronization mechanism $\mathcal{K}_{S_i}$ when $\mathcal{G}_\mathcal{C}$ is a time-varying graph that is strongly connected only "sufficiently often". To model this time-varying behavior, let $L \in \mathbb{Z}_{>0}$ be the number of possible configurations of directed unweighted graphs that are realizable with N ordered nodes and no self-loops. Let each of these configurations be represented by a logic state $q \in Q := \{1, 2, 3, \ldots, L\}$. Let $Q_s \subset Q$ be the set of indices associated only to strongly connected graphs, and let $Q'_s = Q \backslash Q_s$ be the set of indices associated to graphs that are not strongly connected. Figure 5.9 illustrates this idea in graphs with only two nodes. To characterize the time-varying behavior of the graph $\mathcal{G}_\mathcal{C}(t)$ we consider a switching

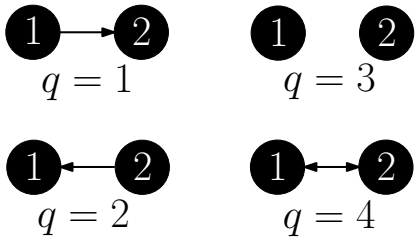

Figure 5.9: Graph configurations realizable with $N = 2$ nodes. In this case $L = 4$, $Q = \{1, 2, 3, 4\}$, $Q_s = \{4\}$, $Q'_s = \{1, 2, 3\}$.

signal $q : \mathbb{R}_{\geq 0} \to Q$ that indicates which of the configurations in Q is implementing the graph at time t. Using this signal we write the graph as $\mathcal{G}_{\mathcal{C},q}$ and the sets of neighbors as $\mathcal{N}_{\mathcal{C}_{i,q}}$.

Definition 4 *We say that a digraph $\mathcal{G}_{\mathcal{C},q}$ is (α, T)-persistently strongly connected (PSC) if there exists $(\alpha, T) \in \mathbb{R}^2_{>0}$ with $T > \alpha$ such that for each time interval I of length T there exists a subinterval $I_i := [t_i, t_{i+1}]$ satisfying $t_{i+1} - t_i = \alpha$, and an integer $q_\alpha \in Q_s$, such that $q(t) = q_\alpha$ for all $t \in I_i$.*

To analyze the stability and robustness properties of the synchronization mechanism $\mathcal{K}_{S_i}$ under switching graphs, we consider dynamic signal generators, such as those in [78, Sec. 2.4], with state $x_\mathcal{G} := [\sigma^\top, q]^\top \in \mathbb{R}^{\bar{\sigma}+1}$, and hybrid dynamics

$$\dot{x}_\mathcal{G} \in F_\mathcal{G}(x_\mathcal{G}), \quad x_\mathcal{G} \in C_\mathcal{G} \subset \mathbb{R}^{\bar{\sigma}} \times Q, \tag{5.30a}$$

$$x^+_\mathcal{G} \in G_\mathcal{G}(x_\mathcal{G}), \quad x_\mathcal{G} \in D_\mathcal{G} \subset \mathbb{R}^{\bar{\sigma}} \times Q. \tag{5.30b}$$

This signal generator uses an auxiliary state $\sigma \in \mathbb{R}^{\bar{\sigma}}$ to regulate the switching behavior of system (5.30). We make the following assumption on this system.

Assumption 36 *System* (5.30) *satisfies the following:*

*(a) The data $\mathcal{H}_\mathcal{G} = \{F_\mathcal{G}, C_\mathcal{G}, G_\mathcal{G}, D_\mathcal{G}\}$ satisfies **(C1)**, **(C2)**, and **(C3)**.*

(b) There exists $T > \alpha > 0$ such that the q-components of all trajectories $x_{\mathcal{G}}$ satisfy the conditions of Definition 4.

(c) There exist at least one complete solution.

(d) There exists a nonempty compact set $\mathcal{A}_{\mathcal{G}} \subset C_{\mathcal{G}} \cup D_{\mathcal{G}}$ that is UGAS for system (5.30).

The following example illustrates a HDS of the form (5.30) that satisfifes Assumption 36.

Example 8 *Consider the HDS with state $[\sigma_1, \sigma_2, q] \in \mathbb{R}^3$, and dynamics*

$$\begin{pmatrix} \dot{\sigma}_1 \\ \dot{\sigma}_2 \\ \dot{q} \end{pmatrix} \in \begin{pmatrix} [0, \alpha^{-1}] \\ [0, \gamma] - \mathbb{I}_{Q_s'}(q) \\ 0 \end{pmatrix}, \ (\sigma_1, \sigma_2, q) \in C_{\mathcal{G}} \tag{5.31a}$$

$$\begin{pmatrix} \sigma_1^+ \\ \sigma_2^+ \\ q^+ \end{pmatrix} \in \begin{pmatrix} \sigma_1 - 1 \\ \sigma_2 \\ Q \end{pmatrix}, \qquad (\sigma_1, \sigma_2, q) \in D_{\mathcal{G}}, \tag{5.31b}$$

where $\eta \in \mathbb{R}_{>0}$, $\gamma \in (0, 1)$, and

$$C_{\mathcal{G}} := [0, 1] \times [0, T_0] \times Q, \qquad D_{\mathcal{G}} := \{1\} \times [0, T_0] \times Q, \tag{5.32}$$

with $T_0 > 0$. By [78, Example 2.15], for any pair of hybrid times $(t_1, s_1) \leq (t_2, s_2)$, every complete individual solution of σ_1 generated by (5.31) satisfies the dwell-time condition $(s_2 - s_1) \leq 1 + \frac{1}{\alpha}(t_2 - t_1)$, where $(s_2 - s_1)$ is here the number of jumps in the time interval $t_2 - t_1$. Also, by [206, Lemma 7], every complete individual solution of σ_2 in (5.31) satisfies the time-ratio constraint $N_{t_2 - t_1} \leq T_0 + \gamma(t_2 - t_1)$, where $N_{t_2 - t_1}$ corresponds

to the total amount of time that $q \in Q_s'$ *during the interval* $t_2 - t_1$*. Therefore, any complete solution of the HDS* (5.31) *satisfies the dwell-time constraint and the time-ratio constraint. Moreover, by taking* $\gamma = 1 - \frac{\alpha+T_0}{T_0}$ *we have that whenever* $t_2 - t_1 = T$ *the time-ratio constraint simplifies to* $N_{t_2-t_1} \leq T - \alpha$*, that is* $T - N_t \geq \alpha$*. Since* $T - N_t$ *is the total amount of time in the interval* T *where* $q \in Q_s$ *holds, and the graph cannot switch faster than every* α *seconds, it must be the case that in any interval of length* $T + \alpha$ *there exists a subinterval of at least* α *seconds where* $q = q_\alpha$ *for some* $q_\alpha \in Q_s$*. Finally, note that the set* $C_\mathcal{G}$ *is UGAS for the HDS* (5.31)*. Thus, system* (5.31) *satisfies Assumption* (36)*.*

5.4.1 Main Result for Time-Varying Graphs

To analyze the hybrid synchronization mechanism $\mathcal{K}_{S_i}$ under switching graphs that are $(\alpha, T) - PSC$, we consider the interconnection of the HDS (5.30) with the HDS (5.19), where now the mapping $G_{\tau,z}$ is parameterized by the switching signal q, representing the graph $\mathcal{G}_\mathcal{C}(t)$. The complete system has state $x_{\tau,z} = [\tau^\top, z^\top, x_\mathcal{G}^\top]^\top$ and dynamics

$$x_{\tau,z} \in C_{x_{\tau,z}} := C_\tau \times Z^N \times C_\mathcal{G}, \tag{5.33a}$$

$$\dot{x}_{\tau,z} \in F_{x_{\tau,z}} := \{F_{\tau,z}\} \times F_\mathcal{G}, \tag{5.33b}$$

$$x_{\tau,z}^+ \in G_{x_{\tau,z}} := \begin{cases} G_1(x_{\tau,z}) & \text{if } x_{\tau,z} \in D_1 \backslash D_2 \\ G_1(x_{\tau,z}) \cup G_2(x_{\tau,z}) & \text{if } x_{\tau,z} \in D_1 \cap D_2 \\ G_2(x_{\tau,z}) & \text{if } x_{\tau,z} \in D_2 \backslash D_1, \end{cases} \tag{5.33c}$$

$$x_{\tau,z} \in D_{x_{\tau,z}} = D_1 \cup D_2, \tag{5.33d}$$

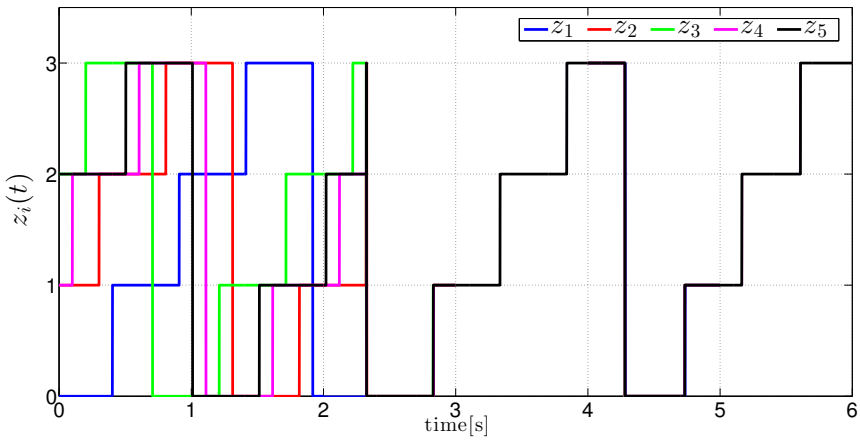

Figure 5.10: Evolution of z along time.

where the set-valued mappings G_1 and G_2 are defined as

$$G_1(x_{\tau,z}) := \{\tau\} \times \{z\} \times G_{\mathcal{G}}, \quad G_2(x_{\tau,z}) := G_{\tau,z,q} \times \{\mathcal{G}_c\}, \tag{5.34}$$

and the sets D_1 and D_2 are now defined as

$$D_1 := [0,1]^N \times Z^N \times D_{\mathcal{G}}, \; D_2 := D_\tau \times Z^N \times C_{\mathcal{G}}. \tag{5.35}$$

For system (5.33) we obtain the following theorem.

Theorem 8 *Let $\mathcal{G}_{\mathcal{C}}(t)$ be a (α, T)-PSC graph. If card$(Z) \cdot \omega^{-1} < \alpha$, the HDS with data $\mathcal{H}_{x_{\tau,z}} := \{F_{x_{\tau,z}}, C_{x_{\tau,z}}, G_{x_{\tau,z}}, D_{x_{\tau,z}}\}$, renders the set $\mathcal{A}_{\tau,z} \times \mathcal{A}_{\mathcal{G}}$ UGAS Moreover, the convergence of (τ, z) to $\mathcal{A}_{\tau,z}$ is in finite time.*

5.4.2 Numerical Example: Noisy Synchronization

Consider a network of 5 agents, i.e., $\mathcal{V} = \{1, 2, 3, 4, 5\}$, with clocks τ_i and logic modes z_i with dynamics (5.8) and (5.9b), respectively, and $\bar{z} = 3$. We implement the synchronization mechanism described by the HDS $\mathcal{H}_{x_{\tau,z}}$ in a time-varying graph (5.31)

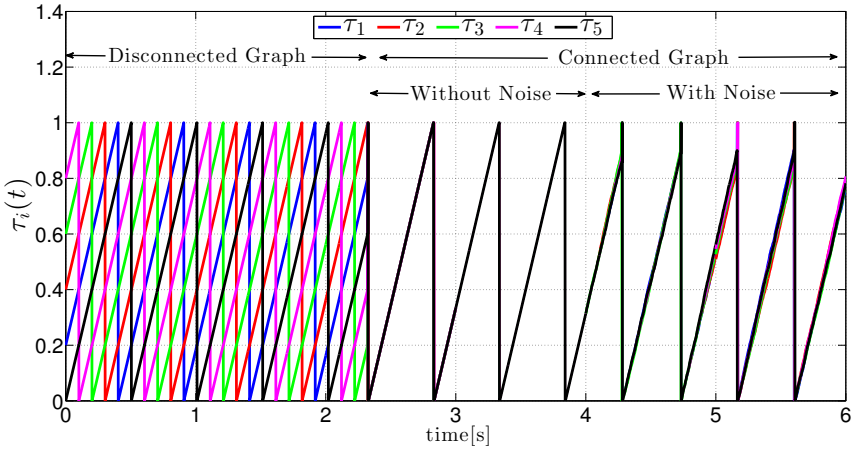

Figure 5.11: Evolution of τ along time.

switching every 2.3 seconds. The parameters of the clock synchronization algorithm (5.18a) are selected as $r_i = 0.1$ for all $i \in \mathcal{V}$, and the frequency of the clocks is selected as $\omega = 0.5$. The graph $\mathcal{G}_c$ is initially disconnected until it switches at time $t = 2.3$ into a ring configuration for the next two periods. To test the robustness properties of the synchronization mechanism, for each agent $i \in \mathcal{V}$ we add small noise ε_i to the clock measurements τ_i after the first four seconds of simulation. This corrupted clock measurements are used by the mapping $\mathcal{T}_i(\tau_i + \varepsilon_i)$ in the synchronization mechanism (5.18a). The noise ε_i is generated as a scalar with random direction and amplitude equal to 0.1, which is 10% of the maximum amplitude of the clocks. Also, after the first 4 seconds of simulation, a random bounded drift d_i is added to the dynamics $\dot{\tau}_i = \omega + d_i$ of each agent's clock. Figures 5.10 and 5.11 show the evolution in time of the logic modes and clocks. After the graph switches into a connected configuration, synchronization of the clocks and logic modes is achieved in finite time. Once the noise is added to the clocks (at $t = 4$ sec), the synchronization is maintained in a "practical" way.

Chapter 6

Intermittent Stochastic Nash Seeking in Sampled-Data Systems

Many decision making problems in multi-agent systems can be analyzed using game theoretic models. In this chapter, we study one of these models, namely a non-cooperative game, where each player is a dynamical system mathematically modeled as a periodic sampled-data system. Our goal is to design a decentralized feedback mechanism to control the actions of each player, such that the overall vector of actions converges to the Nash equilibrium of the game. Due to privacy and robustness concerns, we are interested in using stochastic learning dynamics instead of classic deterministic approaches. Because of this, we pay particular attention to the role of causality in the stability properties of the closed-loop system. Since the closed-loop system is modeled by a stochastic hybrid dynamical system, the results of this chapter rely on the mathematical background presented in Appendices J and K.

6.1 Problem Statement

Consider a network of $n \in \mathbb{Z}_{\geq 0}$ sampled-data systems, also called agents, where each agent $i \in \{1, \ldots, n\}$ consists of three elements: 1) A continuous-time plant $\mathcal{P}_i$; 2) a discrete-time controller $\mathcal{C}_i$; 3) a resetting clock that characterizes the times at which the sampler/hold mechanism samples the output of the plant and updates the control signal. We proceed to characterize in detail each of these components.

6.1.1 Plant Dynamics and Game Structure

The continuous-time plant $\mathcal{P}_i$ associated to the i^{th} agent is characterized by a differential inclusion with individual state $\theta_i \in \mathbb{R}^{p_i}$, input $u_i \in \mathbb{R}$, and given by

$$\dot{\theta}_i \in f_i\big(\theta, \alpha_i(\theta, u)\big), \qquad y_i = \varphi_i(\theta, u), \tag{6.1}$$

where $\alpha_i : \mathbb{R}^p \times \mathbb{R}^n \to \mathbb{R}^n$ is a feedback law, pre-designed to stabilize the plant, $f_i : \mathbb{R}^p \times \mathbb{R}^n \rightrightarrows \mathbb{R}^p$ is a set-valued mapping, $\varphi_i : \mathbb{R}^p \times \mathbb{R}^n \to \mathbb{R}$ is the output function, $\theta = (\theta_1^\top, \ldots, \theta_n^\top)^\top$, $u = (u_1, \ldots, u_n)^\top$, and $p := \sum_{i=1}^n p_i$. For each plant $i \in \{1, \ldots, n\}$ the dynamics (6.1) are assumed to depend only on the states θ_j and inputs u_j of its neighboring interacting plants j, which are characterized by a time-invariant strongly connected directed graph $\mathcal{G}_\mathcal{P} = (\mathcal{V}, \mathcal{E}_\mathcal{P})$, where $\mathcal{V} := \{1, \ldots, n\}$ is the set of nodes, and $\mathcal{E}_\mathcal{P}$ is the set of directed edges. The interaction graph $\mathcal{G}_\mathcal{P}$ can be understood as the graph that describes the interconnection between the *physical* dynamics of the plants of the network.

In general, the mappings $(f_i, \alpha_i, \varphi_i)$, as well as the structure of $\mathcal{G}_P$, are assumed to be *unknown*. However, as in the previous chapters, we impose the following regularity assumption on system (6.1).

Assumption 37 *(Regularity) Let $F_i : \mathbb{R}^p \times \mathbb{R}^n \rightrightarrows \mathbb{R}^p$ be defined as $F_i(\theta, u) := f_i(\theta, \alpha_i(\theta, u))$. For each $i \in \mathcal{V}$, the set-valued mapping $F_i(\cdot, \cdot)$ is OSC, LB, and convex valued with respect to $\mathbb{R}^p \times \mathbb{R}^n$, and $\varphi_i(\cdot)$ is continuous.* □

Let us define $F(\theta, u) := F_1(\theta, u) \times \ldots \times F_n(\theta, u)$, where each set-valued mapping $F_i(\cdot, \cdot)$ is defined as in Assumption 37. Then, the overall network of plants with a fixed input $u \in \mathbb{R}^n$ can be represented as a single set-valued system with dynamics

$$\dot{\theta} \in F(\theta, u), \quad \dot{u} = 0, \quad (\theta, u) \in \mathbb{R}^p \times \mathbb{R}^n. \tag{6.2}$$

For system (6.2) we impose the following regularity and stability assumptions, also considered in the previous chapters.

Assumption 38 *(Regularity and Stability) There exists a nonempty OSC and LB set-valued mapping $H : \mathbb{R}^n \rightrightarrows \mathbb{R}^p$, such that for each $\rho \in \mathbb{R}_{>0}$, the compact set $\mathbb{M}_\rho := \{(\theta, u) : \theta \in H(u), u \in \mathbb{R}^n \cap \rho\mathbb{B}\}$ is globally asymptotically stable for system (6.2) with restricted flow set $\mathbb{R}^p \times (\mathbb{R}^n \cap \rho\mathbb{B})$.* □

Assumption 39 *(Regularity of Output) Let $H(\cdot)$ be given by Assumption 38. For each $i \in \mathcal{V}$, each $u \in \mathbb{R}^n$, and each pair $\theta, \theta' \in H(u)$, we have that $\varphi_i(\theta, u) = \varphi_i(\theta', u)$.* □

The response map associated to each agent i is defined as $J_i(u) := \{\varphi_i(\theta, u) : \theta \in H(u)\}$, for all $i \in \mathcal{V}$, where $H(\cdot)$ is defined as in Assumption 38. Note that under Assumption 39 the response map is well-defined. We assume that the response maps have a quadratic structure of the form

$$J_i(u) = u^T Q_i u + u^T L_i + C_i, \quad \forall\, i \in \{1, \ldots, n\}, \tag{6.3}$$

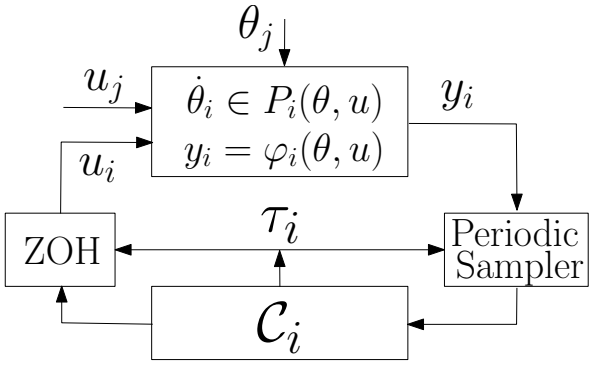

Figure 6.1: Sampled-data associated to each player of the game.

where without loss of generality we assume that $Q_i = Q_i^T \in \mathbb{R}^{n\times n}$, $L_i \in \mathbb{R}^n$, and $C_i \in \mathbb{R}$.

Assumption 40 *Let A denote the $n \times n$ matrix whose i^{th} row is the i^{th} row of Q_i. There exists $w \in \mathbb{R}^n_{>0}$ such that $I(w)A$ is symmetric and negative definite.* □

Under Assumption 40 the matrix A is Hurwitz, and therefore invertible. Moreover, the non-cooperative game characterized by the response maps J_i will be a potential game with unique Nash equilibrium given by

$$u^* = (u_1^*, \ldots, u_n^*)^\top = -0.5A^{-1}B, \tag{6.4}$$

where B denotes the $n \times 1$ column vector whose i^{th} entry is the i^{th} entry of L_i. This fact follows from the following Lemma whose proof was presented in [231].

Lemma 8 *Under Assumption 40, the quadratic game* (6.3) *is a weighted potential game as verified by the potential function*

$$W(u) := u^T I(w)Au + u^T I(w)B - 0.5(u^*)^T I(w)B \tag{6.5}$$

which is negative definite with respect to $u = u^*$. □

Note that the payoff functions, and therefore the game, are defined based on the graph $\mathcal{G}_{\mathcal{P}}$.

Remark 28 *In the deterministic setting it is straightforward to consider the case when J_i is not quadratic, see for instance [105] or [242]. This is usually achieved either via a linearization-based stability analysis, or via a "semi-global" analysis based on Taylor-series expansions. However, for the stochastic case, semi-global, and in fact, local results, are more difficult to characterize than the type of stability results that we pursue here (see [243, Section 7.1]). Hence, for ease of presentation, we confine our analysis to quadratic payoff functions*

6.1.2 Resetting Clock and Control Communication Structure

For each agent $i \in \mathcal{V}$ the resetting clock that coordinates the periodic sampler and the zero-order hold is modeled by a state $\tau_i \in \mathbb{R}_{\geq 0}$, which in open-loop evolves according to the following uncoupled hybrid dynamics

$$\dot{\tau}_i = \frac{1}{T}, \quad \tau_i \in [0, 1] \tag{6.6a}$$

$$\tau_i^+ = 0, \qquad \tau_i \in \{1\}, \tag{6.6b}$$

where $T \in \mathbb{R}_{>0}$ is a tunable sampling period assumed to be the same for all agents. The control system $\mathcal{C}_i$ associated to each agent i, has access to measurements of the output y_i of its own plant $\mathcal{P}_i$, gathered every time that the clock τ_i reaches the end of its period, i.e., when $\tau_i = 1$, as well as to the values of the control and clock states of its neighboring agents, which are characterized by a directed graph $\mathcal{G}_{\mathcal{C}} := \{\mathcal{V}, \mathcal{E}_{\mathcal{C}}\}$, i.e., the sampler/hold and control system j shares information with system i if and only if $(j, i) \in \mathcal{E}_{\mathcal{C}}$. The control communication digraph $\mathcal{G}_{\mathcal{C}}$ satisfies the following assumption.

Assumption 41 *The communication digraph $\mathcal{G}_{\mathcal{C}}$ is time-invariant and strongly connected.*

Figure 6.1 shows the sampled-data structure of each individual player $i \in \mathcal{V}$.

6.2 Stochastic Learning in Static Games

In order to design the control dynamics for each sampled-data system, we start by considering the case where each agent is characterized by a static mapping J_i, i.e., agents have no dynamics. After this, in the next section, we extend the results to the setting of dynamic agents.

6.2.1 Static Game under Persistent Attacks

In order to learn the Nash equilibrium of the game generated by the payoff functions $J_i(\hat{u})$, we consider a class of stochastic learning dynamics where each agent has an individual state $\hat{x}_i := (\alpha_i, \ell_i, \hat{u}_i) \in \mathbb{R}^3$, and dynamics of the form

$$\hat{x}_i^+ \in \hat{G}_{\delta,i}\left(\hat{x}_i, v_i\right), \ \hat{x}_i \in \hat{D}_i := \{0,1\} \times [0, M] \times \mathbb{R}, \tag{6.7}$$

where $M \geq 1$, and where the set-valued mapping $\hat{G}_{\delta,i}$ is defined as

$$\hat{G}_{\delta,i} := \left\{ \begin{array}{c} \{0,1\} \\ (1-\alpha_i)(\ell_i + 1 - \rho) + \alpha_i \max\{0, \ell_i - \rho\} \\ \hat{u}_i + \delta_{s,i}\alpha_i v_i \cdot \Big[J_i(u_a) - J_i(u_b)\Big] \end{array} \right\}, \tag{6.8}$$

where v_i is a random input, $\rho \in (0,1)$, $\delta_{s,i} = k_{s,i}\sqrt{\delta}$, and

$$u_a := \hat{u} + I(\delta_p)I(\alpha)v, \quad u_b := \hat{u} - I(\delta_m)I(\alpha)v, \tag{6.9}$$

with $\delta_p = [\delta_{p,1}, \ldots, \delta_{p,n}]^\top$, $\delta_m = [\delta_{m,1}, \ldots, \delta_{m,n}]^\top$, where $\delta_{p,i} = k_{p,i}\sqrt{\delta}$, $\delta_{m,i} = k_{m,i}\sqrt{\delta}$, $(k_{p,i}, k_{m,i}, k_{s,i}) \in (0,1]^3$, $\delta \in (0,1)$, and $I(\cdot) = diag(\cdot)$.

Modeling the "on" and "off" attacks

In the dynamics (6.7) the state $\alpha_i \in \{0,1\}$ models external attacks that can persistently turn off the controller of the i^{th} agent. In particular, the condition $\alpha_i = 0$ represents the i^{th} agent being attacked, which induces the control updated $\hat{u}_i^+ = \hat{u}_i$, i.e., agent i^{th} cannot update the value of this controller. On the other hand, the condition $\alpha_i = 1$ represents the i^{th} agent not being attacked, and it induces the nominal learning dynamics

$$\hat{u}_i^+ = \hat{u}_i + \delta_{s,i} v_i \cdot \Big[J_i(u_a) - J_i(u_b) \Big]. \tag{6.10}$$

This modeling framework has been shown to be useful in different engineering applications in communication networks and power systems [244], [245]. On the other hand, modeling the attacking signal $\alpha : \mathbb{Z}_{\geq 0} \to \{0,1\}$ as a function generated by the difference inclusion

$$\alpha_i^+ \in \{0,1\}, \tag{6.11}$$

allows us to consider an entire variety of different attacking signals.

A Time-ratio Constraint on the Attacking Signals

The individual auxiliary state ℓ_i in (6.8) is used to monitor the amount of time that each agent is under attack. The dynamics of this state can be used to induce constraints on the amount of time that α_i can be equal to 1 in a particular window of time, i.e., to bound how "persistent" are the attacks. In particular, the interconnection of the dynamics of the attacks and the dynamics of the auxiliary state ℓ_i are given by

a constrained difference inclusion with states (α_i, ℓ_i) and dynamics

$$\begin{cases} \alpha_i^+ \in \{0,1\} \\ \ell_i^+ = (1-\alpha_i)(\ell_i + 1 - \rho) + \alpha_i \cdot \max\{0, \ell_i - \rho\}, \end{cases} \quad (\alpha_i, \ell_i) \in \{0,1\} \times [0, M], \quad (6.12)$$

where $\rho \in (0,1)$. For this system it is not difficult to see that the condition $\alpha_i = 0$ will force ℓ_i to increase beyond M in a finite number of steps, at which point such a solution would be forced to stop. Therefore, complete solutions generated by system 6.12 must guarantee that $\alpha_i = 1$ "sufficiently often". The following lemma formalizes this observation.

Lemma 9 *For each complete solution $k \to (\alpha_i(k), \ell_i(k))$ of (6.12) and integers $j_1 \leq j_2$, we have*

$$\sum_{k=j_1}^{j_2-1} \Big(1 - \alpha_i(k)\Big) \leq M + \rho(j_2 - j_1). \quad (6.13)$$

Moreover, any function $\alpha_i : \mathbb{Z}_{\geq 0} \to \{0,1\}$ satisfying (6.13) can be generated by the system (6.12). □

Remark 29 *The condition (6.13) can also be interpreted as a discrete-time persistency of excitation (PE) condition on the participation variable q_i; indeed, it is equivalent to the condition*

$$\sum_{k=j_1}^{j_2-1} \alpha_i(k) \geq -M + (1-\rho)(j_2 - j_1). \quad (6.14)$$

Thus, whenever $j_2 - j_1 \geq (M+1)/(1-\rho)$ there must be some $k \in \{j_1, \ldots, j_2 - 1\}$ such that $\alpha_i(k) = 1$.

Stochastic Learning Dynamics

The stochastic learning dynamics that update $\hat{u}$ in (6.7), make use of a random dither signal v_i to probe the individual payoff functions J_i. These random variables are selected to satisfy $v_i \in \{-1, 1\}$ for all $i \in \mathcal{V}$, as well as the following assumption:

Assumption 42 *The sequence of random variables $\{\mathbf{v}_j\}_{j=1}^{\infty}$ defined on a probability space $(\Omega, \mathcal{F}, \mathbb{P})$ is i.i.d. with zero mean and identity correlation matrix; that is, $\mathbb{E}[\mathbf{v}_j] = 0$ and $\mathbb{E}\left[\mathbf{v}_j \mathbf{v}_j^T\right] = I$ for each $j \in \mathbb{Z}_{\geq 0}$.* □

Under Assumptions 40 and 42, the stability properties of the stochastic learning dynamics are characterized by the following theorem.

Theorem 9 *Consider the individual stochastic learning dynamics under attacks, modeled by the stochastic difference inclusion* (6.7)*, and define the stochastic difference inclusion*

$$\hat{x}^+ \in \hat{G}_\delta(\hat{x}, v) := \hat{G}_{\delta,1}(\hat{x}, v) \times \ldots \times \hat{G}_{\delta,n}(\hat{x}, v) \tag{6.15a}$$

$$\hat{x} \in \hat{D} := \hat{D}_1 \times \ldots \times \hat{D}_n, \tag{6.15b}$$

as well as the compact set

$$\mathcal{A}_{\hat{x}} := \{0, 1\}^n \times \{0, M\}^n \times \{u^*\}, \tag{6.16}$$

where u^* is the Nash equilibrium given by (6.4) for the quadratic game defined by the payoff function (6.3)*. Then, under Assumptions 40 and 42, and the discrete-time PE condition* (6.14)*, for each $\rho \in (0, 1)$ and $M \geq 1$, the compact set $\mathcal{A}$ is mean-square practically exponentially stable*[1] *in δ.* □

[1]The notion of mean-square practical exponential stability is presented in Definition 16 in the Appendix.

A trivial consequence of Theorem 9 is that an open neighborhood of the Nash equilibrium is also practically positive recurrent[2].

Corollary 3 *For the quadratic game defined by the payoff function* (6.3) *under Assumptions 40, 42, and the PE condition* (6.14) *with* $\rho \in (0,1)$ *and* $M \geq 1$*, the compact set* $\mathcal{A}$*, defined in* (6.16)*, is uniformly globally practically positive recurrent (UGPPR).* □

Remark 30 *The result of Theorem 9 implies that maximal solutions* $\mathbf{x} \in \mathcal{S}_r(x)$ *of system* (6.7)*, with* $x \in D$*, can be guaranteed to be ultimately bounded (in a mean square sense) inside a small residual set containing* $\mathcal{A}$*, which in turn can be made arbitrarily small by decreasing the parameter* δ*. On the other hand, the result of Corollary 3 says that, on average, solutions of the stochastic system will hit an open neighborhood of the set* $\mathcal{A}$ *in finite time.*

To illustrate the previous results consider a non-cooperative game with 3 players, characterized by quadratic cost functions with the following matrices:

[2]The notion of practical positive recurrence is presented in Definition 14 in the Appendix.

$$Q_1 := \begin{bmatrix} -6 & 3 & -1 \\ 3 & 2 & 1 \\ -1 & 1 & 2 \end{bmatrix}, \quad L_1 := \begin{bmatrix} 10 \\ 5 \\ 15 \end{bmatrix}, \tag{6.17a}$$

$$Q_2 := \begin{bmatrix} 3 & 6 & 1 \\ 6 & -9 & 4 \\ 1 & 4 & 3 \end{bmatrix}, \quad L_2 := \begin{bmatrix} 15 \\ 20 \\ 25 \end{bmatrix}, \tag{6.17b}$$

$$Q_3 := \begin{bmatrix} 2 & -3 & -0.5 \\ -3 & -1 & 1 \\ -0.5 & 1 & -3 \end{bmatrix}, \quad L_3 := \begin{bmatrix} 20 \\ 10 \\ 30 \end{bmatrix}, \tag{6.17c}$$

If we select $w = [1, 0.5, 2]^\top$, then $I(w)A$ is symmetric and negative definite with $k_A = [-12.44, -3.384, -2.175]$. Also, there exists a unique Nash equilibrium given by $u^* = [2.62, 5.73, 6.47]^\top$. We define $M = 5$, $\rho = 0.5$, $\delta_s = [0.005, 0.005, 0.01]^\top$, and $\delta_{m,i} = 0.01$, $\delta_{p,i} = 0.02$, for all $i \in \{1, 2, 3\}$. The initial conditions of the actions are set up as $u(0) = [5, 1, 2]^\top$. We generate a sample path associated with a complete solution of the closed-loop system, where at each iteration each player has %50 of probability of being attacked, except when $\alpha_i = 1$ must hold such that PE condition is satisfied. Figure 6.2 shows the complete solution associated with this sample path converging to a neighborhood of the Nash equilibrium. We also show in Figure 6.3 and Figure 6.4 the solutions of $\ell(k)$ and $q(k)$, respectively, during the first 500 iterations of the simulation.

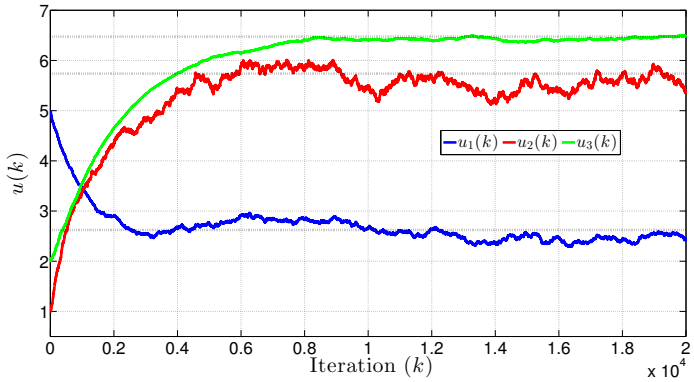

Figure 6.2: Evolution in time of the control state $\hat{u}$, under causal attacks satisfying condition 6.14.

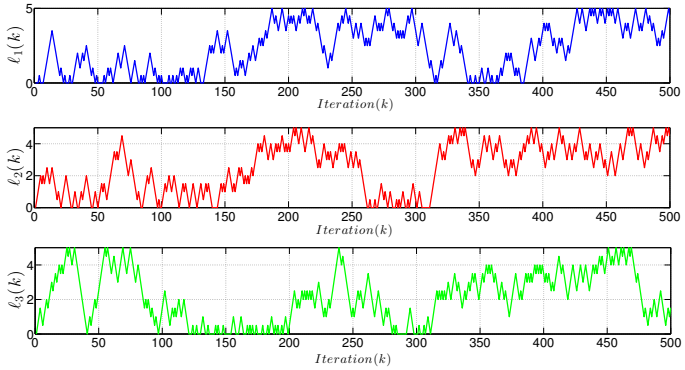

Figure 6.3: Evolution in time of the auxiliary states $\ell(k)$ used to induce condition 6.14 on the attacking signals α_i.

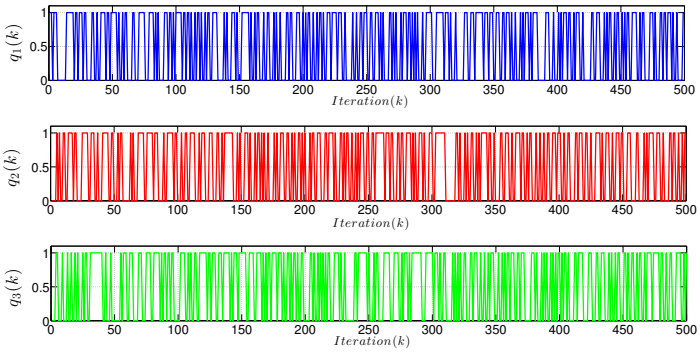

Figure 6.4: Evolution in time of the attacks α_i.

6.2.2 Static Game with Permanent Attacks

In some adversarial scenarios, the attacks influencing the behavior of the agents may not satisfy the PE condition (6.14). Instead, the attacks may be able to permanently damage the control systems of some of the agents. We model this scenario by considering the existence of $r < n$ "stubborn" agents in the game, whose control systems have been compromised, generating fixed inputs with dynamics of the form

$$\hat{u}_{p,i}^{+} = u_i^* + d_{p,i} \tag{6.18a}$$

$$\hat{u}_{m,i}^{+} = u_i^* + d_{m,i}, \tag{6.18b}$$

and probing signals $u_{p,i}$ and $u_{m,i}$, for each $i = \{s+1, \ldots, n\}$, where $s = n - r$ is now the number of agents that are still running a Nash seeking algorithm, which, without loss of generality, we assume to be the first s agents. For non-cooperative games with stubborn agents, the stability properties of the stochastic learning dynamics are now characterized by the following theorem.

Theorem 10 *Consider the stochastic learning dynamics under attacks, modeled by the stochastic difference inclusion* (6.15)*, and the stubborn agents with dynamics* (6.18)*. Then, under Assumptions 40 and 42, and the PE condition* (6.14)*, for each* $\rho \in (0,1)$ *and* $M \geq 1$*, the compact set* $\mathcal{A}$ *is mean-square d-input-to-state practically stable*[3] *in* δ*, where* $d = [d_p^\top, d_m^\top]^\top$*.* □

Figure 6.5 shows the evolution in time of the trajectories of the control state $\hat{u}$ for the numerical example associated with the matrices (6.17), where now player 3 is stubborn, and where $d_p = 0.4$ and $d_m = 0.2$.

[3]The notion of mean-square input-to-state practical stability is presented in Definition 17 in the Appendix.

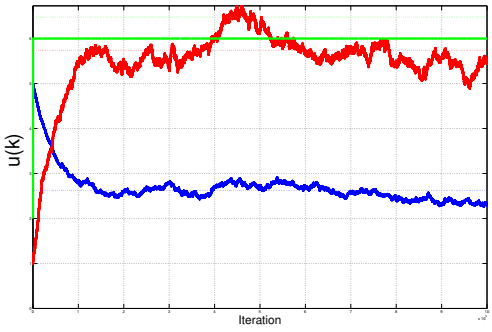

Figure 6.5: Evolution in time of the states $\hat{u}$ for the case when player 3 is stubborn.

6.3 Stochastic Learning in Dynamic Games Under Causal Attacks

The stochastic learning dynamics presented in the previous section rely on two main assumptions: 1) for each agent $i \in \mathcal{V}$ direct measurements of the payoff function J_i evaluated at the points u_a and u_b are available for all time; 2) the construction of the update rule for $\hat{u}$ in (6.8) assumes that the measurements $J_i(u_a)$ and $J_i(u_b)$ are evaluated at the same nominal point $\hat{u}$, and same state α. These two conditions preclude the direct application of the dynamics (6.15) in a network of sampled-data systems, as the one presented in Section 6.1, since the presence of continuous-time dynamics induce a lag of at least T seconds between measurements of the output of the plant. Nevertheless, both issues can be addressed by an appropriate design of a distributed hybrid mechanism that guarantees the necessary level of synchronization and coordination among the agents, such as the one considered in Chapter 5. In order to analyze the stability properties of the stochastic closed-loop system that emerges when this synchronization and coordination mechanism is used, we proceed to formulate the stochastic dynamics (6.8) as a centralized logic-based control system that can be implemented in a sampled-data system. Subsequently, we use the results of Chapter

5 to obtain a fully decentralized control system that retains the stability properties of the centralized system

6.3.1 Learning with Central Coordinator

The interconnection of the plant (6.2) and the dynamics (6.7) is modeled by a logic-based SHDS with 4 logic modes, characterized by a logic state $z_c \in Z := \{1, 2, 3, 4\}$, a centralized timer $\tau_c \in \mathbb{R}_{>0}$, and distributed controllers $\mathcal{C}_i$ with states $x_{u,i} := (s_i, u_i, \hat{x}_i^\top, \hat{y}_i^\top) \in \mathbb{R}^7$, where $s_i \in \mathbb{R}$ is here an auxiliary state that keeps track of the value of the random variable v_i during each *learning iteration*, $u_i \in \mathbb{R}$ is the input of the i^{th} plant, $\hat{x}_i \in \mathbb{R}^3$ is the same state used in (6.8), and $\hat{y}_i \in \mathbb{R}^2$ is an auxiliary state used to keep track of the two measurements of the output of the plant i, needed to implement the dynamics (6.8). Defining $x_u := (x_{u,1}^\top, \ldots, x_{u,n}^\top)^\top$, $D_{u,i} := \{-1, 1\} \times \mathbb{R} \times \hat{D}_i \times \mathbb{R}^2$, and $D_u := D_{u,1} \times \ldots \times D_{u,n}$, the closed-loop system can be modeled by a SHDS represented by $\mathcal{H}_c := (C_c, F_c, D_c, G_c)$, with overall state $x_c := (\tau_c, z_c, x_u^\top, \theta^\top)^\top \in \mathbb{R}^m$,

$m = 2 + 7n + p$, and data

$$C_c := [0,1] \times \{2,3\} \times D_u \times \mathbb{R}^p, \tag{6.19a}$$

$$\dot{x}_c \in F_c(x_c) := \begin{pmatrix} \frac{1}{T} \\ 0 \\ \mathbf{0}_{7n} \\ F(\theta, u) \end{pmatrix}, \tag{6.19b}$$

$$D_c := \Big((\{1\} \times Z) \cup ([0,1] \times \{1,4\}) \Big) \times D_u \times \mathbb{R}^p, \tag{6.19c}$$

$$x_c^+ \in G_c(x_c, v) := \begin{pmatrix} f_\tau(\tau_c, z_c) \\ f_z(z_c) \\ G_\delta^q(x_u, v, \tilde{y}) \\ \mathbf{0}_p \end{pmatrix}, \tag{6.19d}$$

where $\tilde{y} = (\tilde{y}_1, \ldots, \tilde{y}_n)^\top$ in (6.19d) corresponds to a vector of measurements of the outputs of the plants (6.1), i.e., $\tilde{y}_i = \varphi_i(\theta, u)$. The mappings f_τ and f_z in (6.19d) are given by

$$f_\tau(\tau_c, z_c) := \begin{cases} 0 & \text{if } \ z_c \in \{2,3\} \\ \tau_c & \text{if } \ z_c \in \{1,4\}, \end{cases} \tag{6.20a}$$

$$f_z(z_c) := \begin{cases} z_c + 1 & \text{if } \ z_c \in \{1,2,3\} \\ 1 & \text{if } \ z_c = \{4\}. \end{cases} \tag{6.20b}$$

Note that these dynamics are slightly different from those of the centralized system of Chapter 5, since, due to the definition of the jump set, system (6.19) is not allowed to flow when $z_c \in \{1,4\}$.

The logic-based stochastic set-valued mapping that characterizes the jumps of the

network is defined as $G_\delta^{z_c}$ in (6.19d) is defined as $G_\delta^{z_c}(\hat{x}, v) := G_{\delta,1}^{z_c}(\hat{x}, v) \times \ldots \times G_{\delta,n}^{z_c}(\hat{x}, v)$, where for each $i \in \mathcal{V}$ and each $z_c \in Z$ the map $G_{\delta,i}^{z_c}$ is defined as

$$G_{\delta,i}^1 = \left(s_i, \varepsilon_i \cdot \text{sat}((\hat{u}_i + \delta_{p,i}\alpha_i s_i)/\varepsilon_i), \hat{x}_i^\top, \hat{y}_i^\top\right)^\top, \tag{6.21a}$$

$$G_{\delta,i}^2 = \left(s_i, \varepsilon_i \cdot \text{sat}((\hat{u}_i - \delta_{p,i}\alpha_i s_i)/\varepsilon_i), \hat{x}_i^\top, (\tilde{y}_i, \hat{y}_{i,2})^\top\right)^\top \tag{6.21b}$$

$$G_{\delta,i}^3 = \left(s_i, u_i, \hat{x}_i^\top, (\hat{y}_{i,1}, \tilde{y}_i)^\top\right)^\top \tag{6.21c}$$

$$G_{\delta,i}^4 = \left(v_i, u_i, \hat{G}_{\delta,i}(\hat{x}_i, s_i, \hat{y}_i),\ \hat{y}_i^\top\right)^\top, \tag{6.21d}$$

with $\text{sat}(\cdot)$ in (6.21a)-(6.21b) being the saturation function, $\varepsilon_i \in \mathbb{R}_{>0}$ satisfies $|u_i^*| \leq \varepsilon_i$, and $\hat{G}_{\delta,i}(\hat{x}_i, s_i, \hat{y}_i)$ in (6.21d) is given by (6.8) with $J_i(u_a)$ replaced by $\hat{y}_{i,1}$, $J(u_b)$ replaced by $\hat{y}_{i,2}$, and v_i replaced by s_i. We point out that the introduction of the saturation function in (6.21a)-(6.21b) is motivated merely for purposes of analysis. In general, the positive constants ε_i can be selected arbitrarily large to characterize any solution of practical interest.

Note that the behavior generated by the SHDS (6.19) can be seen as a logic-based automaton where flows given by (6.19b) are allowed only during the modes 2 and 3. This implies that whenever $z_c \in \{1, 4\}$ a jump is induced, and the state x_c is updated according to the dynamics (6.19d). Note also that, according to the definition of the jump set in (6.19c), agents can jump out of the modes 2 and 3 only if $\tau_c = 1$. Moreover, by the definition of the mappings f_τ and f_{z_c} in (6.20), each time that the agents jump from the modes 2 and 3 the timer is reset to 0. Finally, note that every time that there is a jump the logic state z_c is incremented by 1, except when $z_c = 4$, a case that forces z_c to be reset to 1. Since the maximum amount of time that the entire system can spend in the modes 2 or 3 is ΔT seconds, we have that every agent of the network visits in order every mode in the set Z infinitely often. In this way, every time that a solution of the SHDS (6.19) hits for the first time the mode 1 after passing by all the

modes Z, we say that the solution has completed a *learning iteration.*

The following proposition will be fundamental for our results. It follows directly by the regularity and stability properties of system (6.2).

Proposition 13 (Slow sampling) *Consider the dynamical system (6.2) with restricted flow set $\mathbb{R}^p \times K_u$. Let $K_\theta \subset \mathbb{R}^p$, and suppose that Assumptions 37 and 38 hold. Let $\mathbb{M}_{\tilde{\rho}}$ be defined as in Assumption 38, with $\tilde{\rho} > 0$. Then, for each pair $(\rho, \tilde{\rho}) \in \mathbb{R}^2_{>0}$ and each compact set K_θ there exists a sufficiently large sampling period $\Delta T > 0$ such that*

$$[\theta(t)^\top, u(t)^\top]^\top \in \mathbb{M}_{\tilde{\rho}} + \rho\mathbb{B}, \tag{6.22}$$

for all $t \geq \Delta T$, $(\theta(0)^\top, u(0)^\top)^\top \in K_\theta \times K_u$. □

Let us denote $\tilde{x} := (u^\top, s^\top, \hat{y}^\top, \theta^\top)^\top$, where $\hat{y} = (\hat{y}_1^\top, \dots, \hat{y}_n^\top)^\top$. The stability properties of the SHDS (6.19) are characterized with respect to the compact set $\mathcal{A}_{\hat{x}}$ given by (6.16), and the compact sets

$$\mathcal{A}_{\tau,z} := \Big(([0,1] \times \{2,3\}) \cup (\{0\} \times \{1,4\}) \Big), \tag{6.23}$$

$$\begin{aligned} \tilde{\mathbb{M}} : = \Big\{ \tilde{x} \in \mathbb{R}^{4n+p} : u = u^*,\ s \in \{-1,1\}^n, \\ \hat{y}_i = J_i(u) \cdot [1,1]^\top \ \forall\ i \in \mathcal{V}, \theta \in H(u), \Big\}. \end{aligned} \tag{6.24}$$

The following theorem establishes the stability and convergence properties of the centralized stochastic system.

Theorem 11 (Stability with Central Coordinator) *For the SHDS (6.19) there exist $\beta_{\tau,q}$, $\beta_{\tilde{x}} \in \mathcal{KL}$, $(\sigma, \gamma, \alpha) \in \mathbb{R}^3$, $\delta^* \in (0,1)$, and $\lambda < 1/\delta^*$, such that for each $\delta \in (0, \delta^*)$ and each compact set $K_\theta \subset \mathbb{R}^p$ there exists $\Delta T^* \in \mathbb{R}_{\geq 0}$, such that for all $\Delta T \geq \Delta T^*$ and $x_c(0,0) \in [0,1] \times Z \times D_u \times K_\theta$ there exists a $\rho_{\delta,\hat{x}(0,0)} \in \mathbb{R}_{>0}$ and $j^* \in \mathbb{Z}_{\geq 0}$*

such that for all $(t,j) \in dom(\mathbf{x}_c)$,

$$|\tau_c(t,j), z_c(t,j)|_{\mathcal{A}_{\tau,q}} \leq \beta_{\tau,q}(|\tau_c(0,0), q_c(0,0)|_{\mathcal{A}_{\tau,q}}, t+j) \tag{6.25}$$

$$\mathbb{P}\big(|\tilde{\mathbf{x}}(t,j)|_{\tilde{\mathbb{M}}} \leq \beta_{\tilde{x}}(|\tilde{x}(0,0)|_{\tilde{\mathbb{M}}}, t+j) + \delta, \quad \forall\ (t,j) \in dom(\mathbf{x}_c)\big) = 1 \tag{6.26}$$

$$\mathbb{E}\left[\|\hat{\mathbf{x}}(t, \underline{\mathbf{j}}(t))\|^2_{\mathcal{A}_{\hat{x}}}\right] \leq \sigma(1-\delta\lambda)^{h(t)}\rho_{\delta,\hat{x}(0,0)} + \gamma\delta^{\alpha},\ \forall\ t \geq 0, \tag{6.27}$$

where $\underline{\mathbf{j}}(t)$ *is the smallest integer* j *such that* (t,j) *is in the domain of the solution, and* $h(t) := \max\{0, \frac{t-\Delta T}{\Delta T+1}\}$. □

6.3.2 Distributed Learning without Central Coordinator

In the absence of a global clock τ_c and a global logic mode z_c, a distributed mechanism able to globally synchronize and coordinate the states τ_i and q_i is needed. To achieve this, we consider a hybrid algorithm similar to the one considered in Chapter 5. This algorithm makes use of an OSC reset map $R_i : \mathbb{R} \rightrightarrows \mathbb{R}$ defined as

$$R_i(\tau_i) := \begin{cases} 0 & \tau_i \in [0, r_i) \\ \{0,1\} & \tau_i = r_i \\ 1 & \tau_i \in (r_i, 1], \end{cases} \quad , \quad r_i \in \left(0, \frac{1}{n}\right), \tag{6.28}$$

where r_i is an individual parameter selected by each agent $i \in \mathcal{V}$. The algorithm is modeled by a *deterministic* HDS represented as $\mathcal{H}_{\tau,z} := \{C_{\tau,z}, F_{\tau,z}, D_{\tau,z}, G_{\tau,z}\}$, with states $(\tau, z) \in \mathbb{R}^n \times Z^n$, and data given by

$$C_{\tau,z} := [0,1]^n \times \{2,3\}^n, \tag{6.29a}$$

$$\begin{pmatrix} \dot{\tau} \\ \dot{z} \end{pmatrix} = F_{\tau,z}(\tau,z) := \begin{pmatrix} \omega \cdot \mathbf{1}_n \\ \mathbf{0}_n \end{pmatrix}, \tag{6.29b}$$

$$D_{\tau,z} := \Big\{ (\tau,z) \in [0,1]^n \times Z^n : \max_{i\in\mathcal{V}} \tau_i = 1, \text{ or } \max_{i\in\mathcal{V}} z_i = 4, \text{ or } \min_{i\in\mathcal{V}} z_i = 1 \Big\}, \tag{6.29c}$$

$$\begin{pmatrix} \tau^+ \\ z^+ \end{pmatrix} \in \overline{G}_{\tau,z}(\tau,z), \tag{6.29d}$$

where $\overline{G}_{\tau,z}$ is the outer semicontinuous hull of a mapping $G_{\tau,z}$ generating the entries of the vectors τ and z as follows:

(a) Let $i \in \mathcal{V}$ be an agent satisfying $\tau_i = 1$ or $z_i \in \{1,4\}$, then its states are updated as

$$\tau_i^+ = f_\tau(\tau_i, z_i), \quad z_i^+ = f_z(z_i), \tag{6.30}$$

where f_τ and f_z are given by (6.20).

(b) Let $j \in \mathcal{V}$ be an agent satisfying $(i,j) \in \mathcal{E}$, and $z_j \in \{2,3\}$, then its states are updated as follows:

If $(z_i, z_j) \in \{2,3\}^2$, then

$$\tau_j^+ \in R_j(\tau_j), \qquad z_j^+ = z_j. \tag{6.31}$$

If $(z_i, z_j) \in \{1\} \times \{2\}$, then

$$\tau_j^+ = \tau_j, \qquad z_j^+ \in z_j + R_j(\tau_j). \tag{6.32}$$

If $(z_i, z_j) \in \{1\} \times \{3\}$, then

$$\tau_j^+ = \tau_j, \qquad z_j^+ \in z_j + (1 - R_j(\tau_j)). \tag{6.33}$$

(c) Let $j \in \mathcal{V}$ be an agent satisfying either $(i,j) \notin \mathcal{E}$ or $(z_i, z_j) \notin \{1,2,3\} \times \{2,3\}$, then $\tau_j^+ = \tau_j$, $z_j^+ = z_j$.

According to the HDS (6.29), each time that the states of at least one agent are in the jump set (6.29c), this agent signals the value of its states (τ_i, z_i) to all the neighboring agents satisfying $(i,j) \in \mathcal{E}$, and updates its states according to (6.30), while the neighboring agents j update their states according to (6.31), (6.32), or (6.33), depending on the values of z_i and their individual state z_j. If multiple agents have states in the jump set (6.29c), they will jump sequentially, the order being not important since the outer semicontinuous hull of $G_{\tau,z}$ captures all possible orders of jumps. Note that according to (6.29), the agents can flow only whenever all states (τ, z) belong to the flow set (6.29a). This *does not* mean that agents need full information of the network in order to flow, but rather it exploits the fact that jumps occur instantaneously, such that whenever an agent decides to flow, every agent that was in the jump set has already jumped.

We proceed to establish the stability properties of the HDS (6.29) with respect to the "synchronized" compact set

$$\mathcal{A}_{sync} := \bigcup_{z \in \{2,3\}} \Big([0,1] \cdot \mathbf{1}_n \times \{z\}^n \Big) \cup \mathcal{A}_2 \cup \mathcal{A}_3, \tag{6.34}$$

where the compact sets $\mathcal{A}_2$ and $\mathcal{A}_3$ are given by

$$\mathcal{A}_2 := \Big((\{0\} \times \{3\}) \cup (\{1\} \times \{2\}) \Big)^n$$
$$\mathcal{A}_3 := \Big((\{0\} \times Z \backslash \{3\}) \cup (\{1\} \times \{3\}) \Big)^n.$$

The following proposition characterizes the stability and convergence properties of the synchronization dynamics.

Proposition 14 *Consider the network of sampled-data systems described in Section 6.1, where each controller $\mathcal{C}_i$ has an individual clock τ_i, and logic state $z_i \in Z$, and implements the dynamics (6.29). Then, the compact set $\mathcal{A}_{sync}$, given by (6.34), is uniformly globally asymptotically stable (UGAS).* □

Using the synchronization mechanism, the distributed Nash seeking dynamics for the network of asynchronous sampled-data systems are given by a SHDS $\mathcal{H} := (C, F, D, G)$, with state $x := (\tau^\top, z^\top, x_u^\top, \theta^\top)^\top \in \mathbb{R}^m$, $m = 9 \cdot n + p$, and data given by

$$\dot{x} \in F(x) := \begin{pmatrix} F_{\tau,z}(\tau, z) \\ \mathbf{0}_{7 \cdot n} \\ F(\theta, u) \end{pmatrix}, \; C := C_{\tau,z} \times D_u \times \mathbb{R}^p, \tag{6.35a}$$

$$x^+ \in \overline{G}(x, v), \qquad D := D_{\tau,z} \times D_u \times \mathbb{R}^p, \tag{6.35b}$$

where the sets $C_{\tau,z}$ and $D_{\tau,z}$ are given by (6.29a) and (6.29c), respectively, the mapping $F_{\tau,z}$ is given by (6.29b), and the stochastic jump map $\overline{G}(x, v)$ is the outer semicontinuous hull of a set-valued mapping $G(x, v)$ defined as follows: Let $x \in D$ and $\tau_i = 1$ or $z_i \in \{1, 4\}$. Then, $G(x, v)$ is the set of vectors $g \in \mathbb{R}^m$ such that the components that generate τ_i^+ and q_i^+ are given by (6.30), the component that generate $x_{u,i}$ is given by (6.21), and the component that generate θ_i^+ is given by θ_i. For the rest of the agents

$j \neq i$, the components that generate $x_{u,j}^+$ and θ_j^+ are given by $x_{u,j}$ and θ_j. Similarly, for the agents $j \neq i$, if $(i,j) \in \mathcal{E}$ and $(z_i, z_j) \in \{2,3\}^2$, then the components that generate τ_j^+ and z_j^+ are given by (6.31). If $(i,j) \in \mathcal{E}$ and $(z_i, z_j) \in \{1\} \times \{2\}$ then τ_j^+ and z_j^+ are updated as (6.32), and for those agents j satisfying $(i,j) \in \mathcal{E}$ and $(z_i, z_j) \in \{1\} \times \{3\}$ the components τ_j^+ and z_j^+ are updated as (6.33). The rest of the agents keep (τ_j, z_j) constant.

The following theorem characterizes the convergence properties of the closed-loop decentralized stochastic hybrid dynamical system.

Theorem 12 *For the SHDS (6.35) there exists $\beta_{\tau,z}$, $\beta_{\tilde{x}} \in \mathcal{KL}$, $(\sigma, \gamma, \alpha) \in \mathbb{R}^3$, $\delta^* \in (0,1)$, and $\lambda < 1/\delta^*$, such that for each $\delta \in (0, \delta^*)$ and each compact set $K_\theta \subset \mathbb{R}^p$ there exists $\Delta T^* \in \mathbb{R}_{\geq 0}$, such that for all $\Delta T \geq \Delta T^*$ and $x_c(0,0) \in [0,1] \times Z \times D_u \times K_\theta$ there exists a $\rho_{\delta,\hat{x}(0,0)} \in \mathbb{R}_{>0}$ and $j^* \in \mathbb{Z}_{\geq 0}$ such that $|\tau(t,j), z(t,j)|_{\mathcal{A}_{sync}} \leq \beta_{\tau,z}(|\tau(0,0), z(0,0)|_{\mathcal{A}_{sync}}, t+j)$ and $\hat{\mathbf{x}}$, $\tilde{\mathbf{x}}$ satisfies equations (6.27)-(6.26).* □

We illustrate this convergence result by means of a numerical example in a networked sampled-data system with 5 agents. The communication network is characterized by a ring graph $\mathcal{G}_\mathcal{P}$, and the continuous-time dynamics of the sampled-data systems are

given by

$$
\begin{aligned}
\begin{pmatrix} \dot{\theta}_{1,1} \\ \dot{\theta}_{1,2} \end{pmatrix} &\in \begin{pmatrix} -\theta_{1,1}^5 - (1+\theta_{5,1})\theta_{1,1}^3 \\ -\mathrm{sgn}(\theta_{1,2} - u_1) \end{pmatrix}, \\
\begin{pmatrix} \dot{\theta}_{2,1} \\ \dot{\theta}_{2,2} \\ \dot{\theta}_{2,3} \end{pmatrix} &= \begin{pmatrix} -\theta_{2,1}^3 + \theta_{5,1} \\ \theta_{2,3} - u_2 \\ -(1+\theta_{2,2}^2)\theta_{2,2} - (\theta_{2,3} - u_2) + \theta_{2,1} \end{pmatrix}, \\
\begin{pmatrix} \dot{\theta}_{3,1} \\ \dot{\theta}_{3,2} \end{pmatrix} &= \begin{pmatrix} -\theta_{3,1} + \theta_{1,2} - u_1 \\ -\theta_{3,2} + \theta_{3,1} + u_3 \end{pmatrix}, \\
\begin{pmatrix} \dot{\theta}_{4,1} \\ \dot{\theta}_{4,2} \end{pmatrix} &\in \begin{pmatrix} -\theta_{4,1} + \theta_{2,2} \\ -\theta_{4,2} + \theta_{4,1} + u_4 \end{pmatrix}, \\
\begin{pmatrix} \dot{\theta}_{5,1} \\ \dot{\theta}_{5,2} \end{pmatrix} &\in \begin{pmatrix} -\theta_{5,1} - 2\theta_{5,1}^3 + (1+\theta_{5,1}^2)\theta_{3,1} \\ -\mathrm{sgn}(\theta_{5,2} - u_5) + \theta_{5,1} \end{pmatrix},
\end{aligned}
$$

where $\mathrm{sgn}(s) := [-1, 1]$ if $s = 0$. The output functions are defined as $y_1 = -2 \cdot \theta_{1,2}^2 + \theta_{4,3}^2 + 20 \cdot \theta_{1,2} + \theta_{43} + 5$, $y_2 = -5 \cdot \theta_{2,2}^2 + \theta_{5,2}^2 + 150 \cdot \theta_{2,2} + \theta_{5,2} + 10$, $y_3 = -4 \cdot \theta_{3,2}^2 + \theta_{1,2}^2 + \theta_{1,2} - 20 \cdot \theta_{3,2} + 10$, $y_4 = -\theta_{4,3}^2 + \theta_{2,2}^2 + 50 \cdot \theta_{4,3} + \theta_{2,2} - 15$, $y_5 = -3 \cdot \theta_{5,2}^2 + \theta_{3,2}^2 + 70 \cdot \theta_{5,2} + \theta_{3,2} - 50$. This network satisfies Assumptions 38-39 with a single-valued mapping $H(u) = (0, u_1)^\top \times (0, 0, u_2)^\top \times (0, u_3)^\top \times (0, u_4)^\top \times (0, u_5)^\top$. Thus, the response maps J_i are well-defined quadratic functions with unique NE given by $u^* = [5, 15, 2.5, 25, 11.66]^\top$, satisfying Assumption 40 with $w = [1, 1, 1/2, 1/3, 2]$. Figure 6.6 shows a simulation of the HDS (6.35) generating a sample-path where at each learning iteration (i.e., mode 4) each sampled-data system is attacked with a probability of 50%, except at the times when the PE-like condition forces the attacking signal to satisfy $\alpha_i = 1$. The initial conditions of the clocks and logic modes are

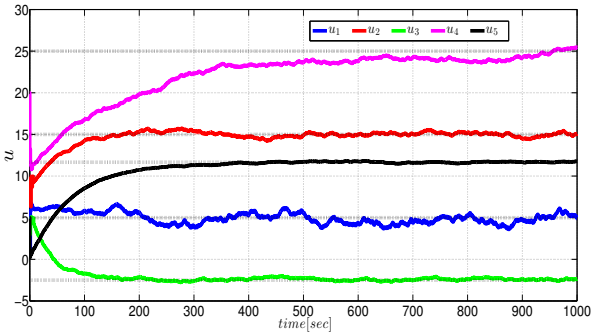

Figure 6.6: Trajectories of u converging to u^*.

selected as $\tau(0,0) = [0.2, 0.4, 0.6, 0.8, 1]$ and $q(0,0) = [2, 3, 2, 3, 4]$. The parameters of the simulation are selected as $M = 5$, $\rho = 0.5$, $\delta_{s,i} = 0.02$, $\delta_{p,i} = \delta_{m,i} = 0.1$, $r_i = 0.1$ for all $i \in \mathcal{V}$, and $\Delta T = 0.5$.

Appendix A

Hybrid Dynamical Systems

In this dissertation we consider set-valued HDS aligned with the framework presented in [78], which allows us to exploit a sequential compactness property that is useful to establish robustness properties in HDS with regular data. A HDS with state $x \in \mathbb{R}^n$ is modeled by the equation

$$\begin{aligned} \dot{x} \ &\in F(x) \qquad x \in C \\ x^+ &\in G(x) \qquad x \in D, \end{aligned} \tag{A.1}$$

where $\dot{x}$ stands for the derivative of x with respect to time, and x^+ represents the value of x after an instantaneous jump. The set-valued mappings $F : \mathbb{R}^n \rightrightarrows \mathbb{R}^n$ and $G : \mathbb{R}^n \rightrightarrows \mathbb{R}^n$ are called the flow map and the jump map, respectively, and they describe the evolution of the system when x belongs to the flow set C, or/and the jump set D, respectively. System (A.1) is represented by the notation $\mathcal{H} := \{C, F, D, G\}$, where C, F, D and G comprise the *data* of $\mathcal{H}$. Note that HDS of the form (A.1) generalize purely continuous-time systems and purely discrete-time systems. Namely, continuous-time dynamical systems can be seen as a HDS of the form (A.1) with $D = \emptyset$, while discrete-time dynamical systems can be seen as a HDS of the form (A.1) with $C = \emptyset$.

This fact allows us to make use of a unified framework to analyze the different types of systems considered in this thesis, irrespective of the nature of the sets C and D.

We proceed to review some relevant definitions for HDS of the form (A.1). Further details and illustrative examples are presented in [78].

A.1 Solutions and Stability Concepts for HDS

Solutions of (A.1) are defined on *hybrid time domains*. A set $E \subset \mathbb{R}_{\geq 0} \times \mathbb{Z}_{\geq 0}$ is called a *compact* hybrid time domain if $E = \cup_{j=0}^{J-1}([t_j, t_{j+1}], j)$ for some finite sequence of times $0 = t_0 \leq t_1 \ldots \leq t_J$. The set E is a hybrid time domain if for all $(T, J) \in E$, $E \cap ([0, T] \times \{0, \ldots, J\})$ is a compact hybrid time domain.

Definition 5 *A function $x : dom(x) \mapsto \mathbb{R}^n$ is a hybrid arc if $dom(x)$ is a hybrid time domain and $t \mapsto x(t, j)$ is locally absolutely continuous for each j such that the interval $I_j := \{t : (t, j) \in dom(x)\}$ has nonempty interior. A hybrid arc x is a* solution *to (A.1) if $x(0, 0) \in \overline{C} \cup D$, and the following two conditions hold:*

1. *For each $j \in \mathbb{Z}_{\geq 0}$ such that I_j has nonempty interior: $x(t, j) \in C$ for all $t \in int(I_j)$, and $\dot{x}(t, j) \in F(x(t, j))$ for almost all $t \in I_j$.*

2. *For each $(t, j) \in dom(x)$ such that $(t, j + 1) \in dom(x)$: $x(t, j) \in D$, and $x(t, j + 1) \in G(x(t, j))$.*

Since F and G are set-valued, and $C \cap D$ may not be empty, the solutions generated by the HDS (A.1) from an initial condition $x(0, 0) \in \mathbb{R}^n$ may not necessarily be unique.

Definition 6 *A hybrid solution x is said to be forward pre-complete if its domain is compact or unbounded, i.e., if the flows do not generate finite escape times. A hybrid solution is said to be forward complete if its domain is unbounded. A hybrid solution is*

maximal if there does not exist another solution ψ to $\mathcal{H}$ such that dom(x) is a proper subset of dom(ψ), and $x(t,j) = \psi(t,j)$ for all $(t,j) \in$ dom(x). System $\mathcal{H}$ is said to be forward (pre) complete from a compact set $K_0 \subset \mathbb{R}^n$ if all maximal solutions x with $x(0,0) \in K_0$, describing the set $\mathcal{S}_{\mathcal{H}}(K_0)$, are forward (pre) complete.

Definition 7 *Let $\mathcal{H}$ be a hybrid system of the form (A.1), and $\mathcal{A} \subset \mathbb{R}^n$ be a compact set. The set $\mathcal{A}$ is said to be* uniformly globally asymptotically stable *(UGAS) for $\mathcal{H}$ if there exists a $\mathcal{KL}$ function β such that any maximal solution x to $\mathcal{H}$ satisfies $|x(t,j)|_{\mathcal{A}} \leq \beta(|x(0,0)|_{\mathcal{A}}, t+j)$, for all $(t,j) \in$ dom(x).*

Note that Definition 7 does not insist that each maximal solution must have an unbounded time domain, neither in the t direction nor in the j direction. However, if the time domain of a particular solution is unbounded, then that particular solution must converge to $\mathcal{A}$.

The following is the local version of Definition 7.

Definition 8 *Let $\mathcal{H}$ be a hybrid system of the form (A.1), $\mathcal{A} \subset \mathbb{R}^n$ be a compact set, and $\mathcal{B}_{\mathcal{A}}$ be an open set satisfying $\mathcal{A} \subset \mathcal{B}_{\mathcal{A}}$. The set $\mathcal{A}$ is said to be* uniformly locally asymptotically stable *(ULAS) for $\mathcal{H}$ with basin of attraction $\mathcal{B}_{\mathcal{A}}$, if there exists a $\mathcal{KL}$ function β and a proper indicator $\omega(\cdot)$[1] of $\mathcal{A}$ on $\mathcal{B}_{\mathcal{A}}$ such that all solutions x to $\mathcal{H}$ with $x(0,0) \in \mathcal{B}_{\mathcal{A}}$ satisfy $\omega(x(t,j)) \leq \beta(\omega(x(0,0)), t+j)$, for all $(t,j) \in$ dom(x).*

Since we are interested in designing feedback mechanisms with good robustness properties, we will always consider systems of the form (A.1) that satisfy the following conditions:

(C1) The sets C and D are closed.

[1] A function $\omega : \mathcal{B}_{\mathcal{A}} \to \mathbb{R}_{\geq 0}$ is a proper indicator of $\mathcal{A}$ on $\mathcal{B}_{\mathcal{A}}$ if it is continuous, $\omega(x_i) \to \infty$ when $i \to \infty$ if either $|x_i| \to \infty$ or the sequence $\{x_i\}_{i=1}^{\infty}$ approaches the boundary of $\mathcal{B}_{\mathcal{A}}$, and $\omega(x) = 0$ if and only if $x \in \mathcal{A}$.

(C2) F is OSC and LB relative to C, $C \subset \text{dom}(F)$, and $F(x)$ is convex for every $x \in C$.

(C3) G is OSC and LB relative to D, and $D \subset \text{dom}(G)$.

A.2 Some Robustness and Invariance Results for HDS

We now review some useful theoretical results for HDS satisfying conditions (C1)-(C3). The following definition will be useful to analyze the stability and convergence properties of parametrized HDS.

Definition 9 *For a HDS parametrized by a small positive parameter ε, given by $\mathcal{H}_\varepsilon := \{C_\varepsilon, F_\varepsilon, D_\varepsilon, G_\varepsilon\}$, a compact set $\mathcal{A} \subset \mathbb{R}^n$ is said to be semi-globally practically asymptotically stable (SGP-AS) as $\varepsilon \to 0^+$ if there exists a function $\beta \in \mathcal{KL}$ such that the following holds: For each $\Delta > 0$ and $\nu > 0$ there exists $\varepsilon^* > 0$ such that for each $\varepsilon \in (0, \varepsilon^*)$ each solution x of $\mathcal{H}_\varepsilon$ that satisfies $|x(0,0)|_\mathcal{A} \leq \Delta$ also satisfies*

$$|x(t,j)|_\mathcal{A} \leq \beta(|x(0,0)|_\mathcal{A}, t+j) + \nu, \quad \textit{for all} \quad (t,j) \in \textit{dom}(x). \tag{A.2}$$

Remark 31 *If the sets C_ε and D_ε are compact, SGP-AS is equivalent to* global practical asymptotic stability *(GP-AS), since Δ can be selected sufficiently large to encompass every initial condition where the solutions of $\mathcal{H}_\varepsilon$ are defined.*

The following lemma, adapted from [78, Lemma 7.20], establishes SGP-AS of a compact set $\mathcal{A}$ for a well-posed HDS with persistent disturbances.

Lemma 10 *Let $\mathcal{H}$ be a well-posed HDS of the form (A.1) rendering a nonempty compact set $\mathcal{A} \subset \mathbb{R}^n$ UGAS. Then, for the perturbed HDS $\mathcal{H}_\rho$ with data given by*

$$F_\rho(x) := \overline{co}\ F((x + \rho\mathbb{B}) \cap C) + \rho\mathbb{B} \tag{A.3a}$$

$$G_\rho(x) := \{v \in \mathbb{R}^n : v \in g + \rho\mathbb{B}, g \in G((x + \rho\mathbb{B}) \cap D)\} \tag{A.3b}$$

$$C_\rho := \{x \in \mathbb{R}^n : (x + \rho\mathbb{B}) \cap C \neq \emptyset\} \tag{A.3c}$$

$$D_\rho := \{x \in \mathbb{R}^n : (x + \rho\mathbb{B}) \cap D \neq \emptyset\}, \tag{A.3d}$$

the set $\mathcal{A}$ is SGP-AS as $\rho \mapsto 0^+$.

The following definition is taken from [246, Sec. 3].

Definition 10 *Consider the HDS $\mathcal{H}$ given by (A.1), and let $K \subset \mathbb{R}^n$ be a compact set. The Ω-limit set from K of (A.1) is defined as $\Omega_\mathcal{H}(K) := \{x \in \mathbb{R}^n : x = \lim_{i\to\infty} x_i(t_i, j_i), x_i \in \mathcal{S}_\mathcal{H}(K), (t_i, j_i) \in dom(x_i), t_i + j_i \to \infty\}$.*

The following lemma, adapted from [78, Corollary 7.7], provides sufficient conditions to establish UGAS of Ω-limit sets for a well-posed HDS of the form (A.1).

Lemma 11 *Suppose that $\mathcal{H}$ is a well-posed HDS of the form (A.1). Let $K \subset \mathbb{R}^n$ be compact, and suppose that $\Omega_\mathcal{H}(K)$ is nonempty and satisfies $\Omega_\mathcal{H}(K) \subset int(K)$, and that the reachable set from K is bounded. Then, the set $\Omega_\mathcal{H}(K)$ is UGAS for system (A.1) with restricted flow set $C \cap K$, and restricted jump set $D \cap K$.*

Non-emptiness of $\Omega_\mathcal{H}(K)$ can be guaranteed, for example, by establishing the existence of at least one bounded complete solution with an initial condition in K [246, Remark 2]. Lemma 11, together with Definition 9, allow us to establish the following lemma for well-posed HDS.

Lemma 12 *Let $\mathcal{H}_\varepsilon := \{C, F_\varepsilon, D, G_\varepsilon\}$ be a well-posed HDS of the form (A.1) rendering a nonempty compact set $\mathcal{A}$ SGP-AS as $\varepsilon \to 0^+$. Let $\Delta > v > 0$, and define $K_\Delta := \mathcal{A} + \Delta\mathbb{B}$. Suppose that for all $\varepsilon > 0$ sufficiently small there exists at least one complete solution $x \in \mathcal{S}_{\mathcal{H}_\varepsilon}(K_\Delta)$. Then there exists a ε^* such that for all $\varepsilon \in (0, \varepsilon^*)$ there exists a UGAS compact set $\Omega^\varepsilon_{\mathcal{H}'}(K_\Delta) \subset \mathcal{A} + v\mathbb{B}$ for the restricted hybrid system $\mathcal{H}' := \{C \cap K_\Delta, F_\varepsilon, D \cap K_\Delta, G_\varepsilon\}$.*

If the data of the HDS is not restricted to the compact set K_Δ we obtain the following local result.

Lemma 13 *Suppose that a HDS $\mathcal{H}_\varepsilon := \{C_\varepsilon, F_\varepsilon, D_\varepsilon, G_\varepsilon\}$ satisfying **(C1) – (C3)** renders a compact set $\mathcal{A} \subset \mathbb{R}^n$ SGP-AS as $\varepsilon \to 0^+$. Then, for each compact set $K_\Delta \subset \mathbb{R}^n$ and each $\delta \in \mathbb{R}_{>0}$ such that $\mathcal{A} + \delta\mathbb{B} \subset \mathit{int}(K_\Delta)$ there exists an $\varepsilon^* \in \mathbb{R}_{>0}$ such that for each $\varepsilon \in (0, \varepsilon^*)$ there exists a ULAS compact set $\Omega_\varepsilon(K_\Delta) \subset \mathcal{A} + \delta\mathbb{B}$ with basin of attraction $\mathcal{B}(\Omega_\varepsilon(K_\Delta))$ satisfying $K_\Delta \subset \mathcal{B}(\Omega_\varepsilon(K_\Delta))$.* □

The following result exploits the OSC and LB properties of well-posed set-valued mappings.

Lemma 14 *Let $F : \mathbb{R}^n \times \mathbb{R}^n \rightrightarrows \mathbb{R}^n$ satisfy* (**C2**)*, and let $f : \mathbb{R}^n \to \mathbb{R}^n$ be continuous. Then, for each compact set $K \in \mathbb{R}^n$ and each $\rho \in \mathbb{R}_{>0}$ there exists a $\delta \in \mathbb{R}_{>0}$ such that*

$$F(x, f(x) + \delta\mathbb{B}) \subset F(x + \rho\mathbb{B}, f(x + \rho\mathbb{B})) + \rho\mathbb{B}, \tag{A.4}$$

for all $x \in K$.

Proof: Suppose the statement is false. Then, there exists a compact set $K \subset \mathbb{R}^n$ and an $\rho \in \mathbb{R}_{>0}$ such that for each $i \in \mathbb{Z}_{\geq 1}$ there exists an $x_i \in K$ such that

$$F\left(x_i, f(x_i) + \frac{1}{i}\mathbb{B}\right) \not\subset F\left(x_i + \rho\mathbb{B}, f(x_i + \rho\mathbb{B})\right) + \rho\mathbb{B}. \tag{A.5}$$

Since $\{x_i\}_{i=1}^{\infty}$ is a bounded sequence it has a convergent subsequence that we will not relabel. Let $x_i \to x'$, and define $M_1 := x' + \frac{\rho}{2}\mathbb{B}$. Then, $M_1 \times f(M_1)$ is compact, and there exists an $i^* \in \mathbb{Z}_{\geq 1}$ such that for all $i \geq i^*$ we have that $|x_i - x'| \leq \rho/2$. Using continuity of f we obtain that for all $i \geq i^*$

$$F\left(x_i, f(x_i) + \frac{1}{i}\mathbb{B}\right) \subset F\left(M_1, f(M_1) + \frac{1}{i}\mathbb{B}\right). \tag{A.6}$$

Since F satisfies **(C2)** it is also upper semicontinuous [78, Lemma 5.15], and then by [247, Claim 3], there exists an $i^{**} \in \mathbb{Z}_{\geq 1}$ such that for all $i \geq i^{**}$

$$F\left(M_1, f(M_1) + \frac{1}{i}\mathbb{B}\right) \subset F\big(M_1, f(M_1)\big) + \rho\mathbb{B}. \tag{A.7}$$

Also, for all $i > i^*$ we have that $y \in M_1 \Rightarrow y \in x_i + \rho\mathbb{B}$, and then

$$F(M_1, f(M_1)) + \rho\mathbb{B} \subset F(x_i + \rho\mathbb{B}, f(x_i + \rho\mathbb{B})) + \rho\mathbb{B}. \tag{A.8}$$

Using $i > \max\{i^*, i^{**}\}$ and (A.6), (A.7), (A.8), we get the desired contradiction. ■

Appendix B

Singularly Perturbed Hybrid Systems with Non-Hybrid Boundary Layer Dynamics

In this section, we use $\dot{x}_t$ to describe the derivative of x with respect to the time scale t. The following definition, together with Lemma 15, subsumes the main results presented in [224] for *singularly perturbed HDS (SP-HDS) with a well-defined boundary layer and reduced system.*

Definition 11 (SP-HDS with Reduced Dynamics) *Let $x = [x_1^\top, x_2^\top]^\top \in \mathbb{R}^n$, where $x_1 \in \mathbb{R}^{n_1}$ and $x_2 \in \mathbb{R}^{n_2}$. Let $\varepsilon > 0$ and $\tilde{K} \subset \mathbb{R}^{n_2}$ be compact. We say that the hybrid system $\mathcal{H}_\varepsilon := \{C \times \tilde{K}, F, D \times \tilde{K}, G\}$ given by*

$$\begin{bmatrix} I_{n_1} & \mathbf{0} \\ \mathbf{0} & \varepsilon I_{n_2} \end{bmatrix} \dot{x}_t \in F(x) \qquad x \in C \times \tilde{K}, \tag{B.1a}$$

$$x^+ \in G(x) \qquad x \in D \times \tilde{K}, \tag{B.1b}$$

is a SP-HDS with a well-defined boundary layer and reduced system *if it satisfies the following conditions:*

1. *The data* $\{C \times \tilde{K}, F, D \times \tilde{K}, G\}$ *satisfies conditions* (**C1**)-(**C3**).

2. *Let* $\tau = t/\varepsilon$ *and* $\rho \in \mathbb{R}_{>0}$. *For the boundary layer system of (B.1), defined as*

$$\dot{x}^{bl}_{\tau} \in \begin{bmatrix} \boldsymbol{0} & \boldsymbol{0} \\ \boldsymbol{0} & I_{n_2} \end{bmatrix} F(x^{bl}), \qquad x^{bl} \in (C \cap \rho\mathbb{B}) \times \tilde{K}, \tag{B.2}$$

there exists an OSC, LB set-valued mapping $H : \mathbb{R}^{n_1} \rightrightarrows \mathbb{R}^{n_2}$, *with* $H(x^{bl}_1)$ *being a nonempty subset of* $\tilde{K}$ *for each* $x^{bl}_1 \in C$, *such that for each* $\rho > 0$ *the compact set*

$$M_\rho := \{(x^{bl}_1, x^{bl}_2) : x^{bl}_1 \in C \cap \rho\mathbb{B}, x^{bl}_2 \in H(x^{bl}_1)\} \tag{B.3}$$

is UGAS.

3. *For the reduced system of (B.1), defined as*

$$\dot{x}_1 \in F^r(x_1), \qquad x_1 \in C \tag{B.4a}$$

$$x^+_1 \in G^r(x_1), \qquad x_1 \in D, \tag{B.4b}$$

where

$$\begin{aligned} F^r(x_1) : = \overline{co}\ \{v_1 \in \mathbb{R}^{n_1} : (v_1, v_2) \in F(x_1, x_2), \\ x_2 \in H(x_1), v_2 \in \mathbb{R}^{n_2}\}, \end{aligned} \tag{B.5a}$$

$$G^r(x_1) := \{v_1 \in \mathbb{R}^{n_1} : (v_1, v_2) \in G(x_1, x_2),$$
$$(x_2, v_2) \in \tilde{K} \times \tilde{K}\}, \tag{B.5b}$$

there exists a UGAS compact set $\mathcal{A} \subset \mathbb{R}^{n_1}$.

The following Lemma, which is a direct consequence of [224, Theorem 1] characterizes the stability properties of the set $\mathcal{A} \times \tilde{K}$ for a *well-posed SP-HDS with a well-defined boundary layer and reduced system.*

Lemma 15 *For a* SP-HDS with a well-defined boundary layer and reduced system*, the set* $\mathcal{A} \times \tilde{K}$ *is SGP-AS as* $\varepsilon \to 0^+$.

Proof: The result follows directly by noting that conditions (1), (2), and (3), in Definition 11, fulfill the required assumptions for the application of [224, Theorem 1]. ■

In the same way, *SP-HDS with a well-defined boundary layer and average system* are characterized by Definition 12 and Lemma 16, the later being a simple extension of [248, Theorem 2].

Definition 12 (SP-HDS with Average Dynamics) *Let* $x = [x_1^\top, x_2^\top, x_3^\top]^\top \in \mathbb{R}^n$, *where* $x_1 \in \mathbb{R}^{n_1}$, $x_2 \in \mathbb{R}^{n_2}$, *and* $x_3 \in \mathbb{R}^{n_3}$. *Let* $\varepsilon > 0$ *and* $\tilde{K} \subset \mathbb{R}^{n_3}$ *be a compact set. We say that the hybrid system* $\mathcal{H}_\varepsilon := \{C \times \tilde{K}, F, D \times \tilde{K}, G\}$ *given by*

$$\begin{bmatrix} I_{n_1} & \mathbf{0} & \mathbf{0} \\ \mathbf{0} & I_{n_2} & \mathbf{0} \\ \mathbf{0} & \mathbf{0} & \varepsilon I_{n_3} \end{bmatrix} \dot{x}_t \in F(x), ((x_1, x_2), x_3) \in C \times \tilde{K}, \tag{B.6a}$$

$$x^+ \in G(x), ((x_1, x_2), x_3) \in \ D \times \tilde{K}, \tag{B.6b}$$

where $F := F_1 \times F_2 \times F_3$, $F_1 : \mathbb{R}^{n_1+n_2} \rightrightarrows \mathbb{R}^{n_1}$ $F_2 : \mathbb{R}^n \to \mathbb{R}^{n_2}$, $F_3 : \mathbb{R}^{n_2+n_3} \to \mathbb{R}^{n_3}$, *is*

a SP-HDS with a well-defined boundary layer and average system, *if it satisfies the following conditions:*

1. *The data* $(C \times \tilde{K}, F, D \times \tilde{K}, G)$ *satisfies* (**C1**)-(**C3**).

2. *Let* $\tau = t/\varepsilon$ *and* $\rho \in \mathbb{R}_{>0}$. *For the boundary layer system of (B.6), defined as*

$$\begin{aligned} \dot{x}^{bl}_{1_\tau} &= \boldsymbol{0} \\ \dot{x}^{bl}_{2_\tau} &= \boldsymbol{0} \qquad , \big((x^{bl}_1, x^{bl}_2), x^{bl}_3\big) \in (C \cap \rho\mathbb{B}) \times \tilde{K}, \\ \dot{x}^{bl}_{3_\tau} &= F_3(x^{bl}) \end{aligned} \tag{B.7}$$

   there exists a compact set $M^A_\rho \subset (C \cap \rho\mathbb{B}) \times \tilde{K}$, *a class-*$\mathcal{L}$ *function* $\sigma_L(M^A_\rho)(\cdot)$, *and a continuous function* $F^A_2 : C \to \mathbb{R}^{n_2}$, *such that, for each* $L > 0$, *and function* $x^{bl}_{3_\tau} : [0, L] \to \tilde{K}$ *that is a solution of (B.7), the following holds: i)* $\left|\frac{1}{L}\int_0^L (F_2(x_1, x_2, x^{bl}_3) - F^A_2(x_1, x_2))ds\right| \leq \sigma_L(M^A_\rho)(L)$, *(ii) the set* M^A_ρ *is UGAS for system (B.7).*

3. *For the average system of (B.6), defined as*

$$\begin{pmatrix} \dot{x}^A_1 \\ \dot{x}^A_2 \end{pmatrix} \in F^A(x^A_1, x^A_2), \qquad (x^A_1, x^A_2) \in C, \tag{B.8a}$$

$$\begin{pmatrix} x^{A+}_1 \\ x^{A+}_2 \end{pmatrix} \in G^A(x^A_1, x^A_2), \qquad (x^A_1, x^A_2) \in D, \tag{B.8b}$$

   where $F^A = F_1 \times F^A_2$, F^A_2 *is defined as in item (2), and* G^A *is given by*

$$\begin{aligned} G^A := \big\{ &(v_1, v_2) \in \mathbb{R}^{n_1+n_2} : (v_1, v_2, v_3) \in G(x^A_1, x^A_2, x_3), \\ &(x_3, v_3) \in \tilde{K} \times \mathbb{R}^{n_3} \big\}, \end{aligned} \tag{B.9}$$

there exists a UGAS compact set $\mathcal{A} \subset \mathbb{R}^{n_1+n_2}$.

Lemma 16 *For a* well-posed SP-HDS with a well-defined boundary layer and average system*, the set* $\mathcal{A} \times \tilde{K}$ *is SGP-AS as* $\varepsilon \to 0^+$.

Proof: The proof of Lemma 16 follows a similar path as the proof of [248, Theorem 2], with the addition that we exploit the fact that F_1 is independent of the fast state x_3, as well as the non-dependence of F_3 on x_1. We extend the SP-HDS (B.6) by introducing an auxiliary state $\eta \in \mathbb{R}^{n_2}$, a small constant $\mu \geq 0$, and by intercepting the flow and jump sets C and D by a compact set K (that is constructed as Eq. (31) in [248]). Specifically we consider the extended hybrid system H_K given by

$$\left.\begin{aligned} \dot{x}_1 &\in F_1(x_1, x_2) \\ \dot{x}_2 &= F_2(x_1, x_2, x_3) \\ \dot{x}_3 &= \tfrac{1}{\varepsilon} F_3(x_2, x_3) \\ \dot{\eta} &= \tfrac{1}{\varepsilon}\left[F_2(x_1, x_2, x_3) - F_2^A(x_1, x_2) - \mu\eta\right] \end{aligned}\right\}, \qquad \text{(B.10a)}$$

$$((x_1, x_2), x_3, \eta) \in C \cap K \times \tilde{K} \times \mathbb{R}^{n_2},$$

$$\left.\begin{aligned} x^+ &\in G(x) \\ \eta^+ &= 0 \end{aligned}\right., \ ((x_1, x_2), x_3, \eta) \in D \cap K \times \tilde{K} \times \mathbb{R}^{n_2}. \qquad \text{(B.10b)}$$

Consider the change of variables $\bar{x}_1 = x_1$ and $\bar{x}_2 = x_2 - \varepsilon\eta$. Using (B.10) and the definition of $G^A(x)$ in (B.9) we obtain the auxiliary system given by

$$\left.\begin{aligned} \dot{\bar{x}}_1 &\in F_1(\bar{x}_1, \bar{x}_2 + \varepsilon\eta) \\ \dot{\bar{x}}_2 &= F_2^A(\bar{x}_1, \bar{x}_2 + \varepsilon\eta) + \mu\eta \end{aligned}\right., \quad \bar{x} + \varepsilon\eta \in C, \qquad \text{(B.11a)}$$

$$\bar{x}^+ \in G^A(\bar{x}_1, \bar{x}_2 + \varepsilon\eta), \qquad \bar{x} + \varepsilon\eta \in D. \qquad \text{(B.11b)}$$

Since the data of the system (B.10) satisfies item (1) in Definition 12, F_1 is independent of x_3, and F_2 is continuous, by [248, Lemma 4] we have that for any $\delta > 0$ and compact set $K \subset \mathbb{R}^{n_1+n_2}$ there exists $(\mu, \varepsilon^*) \in \mathbb{R}^2_{>0}$ such that, for all $\varepsilon \in (0, \varepsilon^*]$, each solution (x, η) of system (B.10) with $\eta(0,0) = 0$ satisfies $\mu|\eta(t,j)| \leq \delta$, for all $(t,j) \in \mathrm{dom}(x)$, impliying that solutions $\bar{x}(t,j)$ of system (B.11) will also be solutions of an inflated system $\mathcal{H}^A_\delta$ given by

$$\dot{\bar{x}} \in F^A(\bar{x} + \delta\mathbb{B}), \quad \bar{x} \in C_\delta, \tag{B.12a}$$

$$\bar{x}^+ \in G^A(\bar{x} + \delta\mathbb{B}), \quad \bar{x} \in D_\delta. \tag{B.12b}$$

where C_δ and D_δ are defined as in equations (A.3c) and (A.3d). From this point the proof follows the same steps as in the proof of Theorems 1 and 2 in [248] using closeness of solutions of systems $\mathcal{H}^A_\delta$ and $\mathcal{H}^A$, the uniform stability of $\mathcal{A}$ for the system $\mathcal{H}^A$, and Lemma 10. ■

Appendix C

Proof of Theorem 1

The proof of Theorem 1 is based on singular perturbation and averaging theory for HDS with non-hybrid boundary layers [224], [248]. To prove Theorem 1 we start by obtaining the average-reduced HDS in the slowest time-scale, which will correspond to a perturbed version of the learning dynamics (2.11). Making use of Lemmas 12 and 10 we will establish the existence of a UGAS Ω-limit set for this average-reduced system with restricted flow and jump sets. After this, we will repeatedly use Lemmas 12, 15, and 16, to establish a global practical stability results for the optimal compact set for the average system in the quasi-steady state, for the non-average quasi-steady state system, and finally for the original system (2.12). We divide the proof in 5 main steps:

Step 1: We start by considering the case when the dynamics of θ are negligible, such that direct measurements of the response map are available, i.e., $y = J(u)$. In this case we consider a hybrid dynamical system in the λ-time scale (which only affect the flows), where $\lambda = \epsilon\overline{\omega}t$, given by $\mathcal{H}_s := \{(C_u \times C_z) \times \Lambda_\xi \times \mathbb{S}^n, F_s, (D_u \times D_z) \times \Lambda_\xi \times \mathbb{S}^n, G_s\}$, with state $x_s := \left[x_{u,z}^\top, \xi^\top, \mu^\top\right]^\top \in \mathbb{R}^{\ell+3n}$, and $\overline{\omega}$ acting as a small perturbation param-

eter. The data of this system is given by

$$F_s := \begin{pmatrix} \sigma \hat{F}_\delta(x_{u,z}, \xi) \\ -(\xi - \frac{2}{a} J(u) \cdot \mathbb{D}\ \mu) \\ \overline{\omega}^{-1} \Phi(\kappa)\ \mu \end{pmatrix},\ (C_u \times C_z) \times \Lambda_\xi \times \mathbb{S}^n, \tag{C.1a}$$

$$G_s := \begin{pmatrix} \hat{G}_\delta(x_{u,z}) \\ \xi \\ \mu \end{pmatrix}, \quad (D_u \times D_z) \times \Lambda_\xi \times \mathbb{S}^n. \tag{C.1b}$$

System (C.1) is a SP-HDS of the form (B.6), with $\overline{\omega}$ acting as small parameter. For this system the boundary layer dynamics, in the $\tau_{\overline{\omega}} := \lambda/\bar{\omega}$-time scale, simply correspond to the oscillator $\dot{\mu} = \Phi(\kappa)\ \mu$, which generates a vector of periodic solutions with even components given by $\mu_{2i}(\tau_{\bar{\omega}}) = -\sin(\kappa_i \tau_{\bar{\omega}})\mu_{2i-1}(0) + \cos(\kappa_i \tau_{\bar{\omega}})\mu_{2i}(0)$, and odd components given by $\mu_{2i-1}(\tau_{\bar{\omega}}) = \cos(\kappa_i \tau_{\bar{\omega}})\mu_{2i-1}(0) + \sin(\kappa_i \tau_{\bar{\omega}})\mu_{2i}(0)$, for each $i \in \{1, \ldots, n\}$, rendering the compact set $\mathbb{S}^n$ UGAS. Moreover, by the selection of the constants κ_i, the matrix $\mathbb{D}$, and the fact that J is analytic, a Taylor series expansion of $J(\hat{u} + a\mathbb{D}\mu)$ with respect to $\hat{u}$ can be performed, obtaining that $J(\hat{u} + a\mathbb{D}\mu) = J(\hat{u}) + a(\mathbb{D}\mu)^\top \nabla J(\hat{u}) + O(a^2)$. By defining $T = 2\pi \cdot \mathrm{LCM}(1/\kappa_1, \ldots, 1/\kappa_n)$, and using the facts that $\int_0^T \mu_{2i-1}(s)ds = 0$, $\int_0^T \mu_{2i-1}(s)\mu_{2j-1}(s)ds = 0$ for all $i \neq j$, and $\frac{1}{T}\int_0^T \mu_{2i-1}(s)^2 ds = \frac{1}{2}$, for all $i \in \{1, \ldots, n\}$, we obtain that $\psi_a(\hat{u}^A) := \frac{1}{T}\int_0^T \frac{2}{a} J(\hat{u} + a\mathbb{D}\mu(s))\,(\mathbb{D}\mu(s))\,ds = \nabla J(\hat{u}^A) + O(a)$. Therefore, system (C.1) has a well defined boundary layer system of the form (B.7), and average system of the form (B.8), with state $x_s^A := \left[x_{u,z}^{A^\top}, \xi^{A^\top}\right]^\top \in \mathbb{R}^{\ell+n}$, given by $\mathcal{H}_s^A := \left\{C_u \times C_z \times \Lambda_\xi, F_s^A, D_u \times D_z \times \Lambda_\xi, G_s^A\right\}$, which in the λ-time scale has

the following data

$$F_s^A := \begin{pmatrix} \sigma \hat{F}_\delta(x_{u,z}^A, \xi^A) \\ -\xi^A + \psi_a(\hat{u}^A) \end{pmatrix}, \ (C_u \times C_z) \times \Lambda_\xi, \tag{C.2a}$$

$$G_s^A := \begin{pmatrix} \hat{G}_\delta(x_{u,z}^A) \\ \xi^A \end{pmatrix}, \qquad (D_u \times D_z) \times \Lambda_\xi. \tag{C.2b}$$

In the γ-time scale, with $\gamma = \sigma\lambda$, and σ acting as a small perturbation parameter, the data (C.2) is given by

$$F_s^A := \begin{pmatrix} \hat{F}_\delta(x_{u,z}^A, \xi^A) \\ -\frac{1}{\sigma}\left(\xi^A - \psi_a(\hat{u}^A)\right) \end{pmatrix}, \quad (C_u \times C_z) \times \Lambda_\xi, \tag{C.3a}$$

$$G_s^A := \begin{pmatrix} \hat{G}_\delta(x_{u,z}^A) \\ \xi^A \end{pmatrix}, \qquad (D_u \times D_z) \times \Lambda_\xi. \tag{C.3b}$$

For σ small, system (C.3) is a SP-HDS of the form (B.1), where the flow dynamics of ξ^A evolve on a faster time scale compared to the flow dynamics of $x_{u,z}^A$. The boundary layer dynamics (B.2) associated to system (C.3), with state $x^{A,bl} := [x_{u,z}^{A,bl\top}, \xi^{A,bl\top}]^\top \in \mathbb{R}^{\ell+n}$, are characterized in the $\tau = \gamma/\sigma$-time scale by the mapping

$$F_s^{A,bl}(x^{A,bl}) := \begin{pmatrix} 0 \\ -\xi^{A,bl} + \psi_a(\hat{u}^{A,bl}) \end{pmatrix}, \tag{C.4}$$

with flow set $[(C_u \times C_z) \cap \rho\mathbb{B}] \times \Lambda_\xi$, for each $\rho > 0$. These linear boundary layer dynamics render the set $M_\rho := \{(x_{u,z}^{A,bl}, \xi^{A,bl}) : x_{u,z}^{A,bl} \in (C_u \times C_z) \cap \rho\mathbb{B}, \xi^{A,bl} \in H_a(\hat{u}^{A,bl})\}$

UGAS, where

$$H_a(\hat{u}^{A,bl}) := \begin{cases} \psi_a(\hat{u}^{A,bl}), & \tilde{u} \in C_u \cup D_u, \\ \emptyset, & \tilde{u} \notin C_u \cup D_u. \end{cases} \tag{C.5}$$

In the same way, the reduced dynamics (B.4) associated to system (C.3) are given by the HDS $\mathcal{H}_s^{A,r} := \{C_u \times C_z, F_s^{A,r}, D_u \times D_z, G_s^{A,r}\}$, with state $x_{u,z}^{A,r} \in \mathbb{R}^\ell$, which in the γ-time scale has the following data:

$$\dot{x}_{\gamma_{u,z}}^{A,r} \in F_s^{A,r} := \hat{F}_\delta \left(x_{u,z}^{A,r}, \psi_a(\hat{u}^{A,r}) \right), \quad (C_u \times C_z), \tag{C.6a}$$

$$x_{u,z}^{+A,r} \in G_s^{A,r} := \hat{G}_\delta \left(x_{u,z}^{A,r} \right), \qquad (D_u \times D_z). \tag{C.6b}$$

System (C.6) thus approximates the behavior of the HESC (2.12) in the slowest time scale.

Step 2: Let $\Delta > \nu > 0$ be given and define $\tilde{K} := \mathcal{A} + \Delta\mathbb{B}$. We make the observation that due to the definition of ψ_a system (C.6) is an $O(a)$-perturbed version of the hybrid learning dynamics (2.11). Let Lemma 12 generate δ^* with the pair $(\Delta, \frac{\nu}{5})$, and let $\delta \in (0, \delta^*)$. Using Assumption 6, and by Lemma 12, there exists a compact set $\Omega_{\hat{\mathcal{H}}}^\delta(\tilde{K}) \subset \mathcal{A} + \frac{\nu}{5}\mathbb{B} \subset \text{int}(\tilde{K})$ that is UGAS for the learning dynamics (2.11) with restricted flow and jump set $(C_u \times C_z) \cap \tilde{K}$ and $(D_u \times D_z) \cap \tilde{K}$. Since this restricted system is well-posed and its restriction is compact, we have that by Lemma 10 and Remark 31, its inflated version (A.3) will render the set $\Omega_{\hat{\mathcal{H}}}^\delta(\tilde{K})$ GP-AS with respect to the inflation size. Moreover, by the definition of $O(a)$, there exists a $k_\Delta > 0$ such that $\hat{F}_\delta \left(x_{u,z}^{A,r}, \psi_a(\hat{u}^{A,r}) \right) \subset \overline{co}\ \hat{F}_\delta \left(x_{u,z}^{A,r}, \nabla J(\hat{u}^{A,r}) + a k_\Delta \mathbb{B} \right)$, for all $x_{u,z}^{A,r} \in \tilde{K}$. Using Lemma

14 we have that for each $\rho \in \mathbb{R}_{>0}$ there exists an $a^* \in (0,1)$ such that for all $a \in (0, a^*)$

$$\overline{co}\hat{F}_\delta\left(x_{u,z}^{A,r}, \nabla J(\hat{u}^{A,r}) + ak\mathbb{B}\right) \subset \overline{co}\hat{F}_\delta\left(x_{u,z}^{Ar} + \rho\mathbb{B}, \nabla J(\hat{u}^{A,r} + \rho\mathbb{B})\right) + \rho\mathbb{B},$$

for all $\hat{u}^{A,r} \in \tilde{K}$, which implies that for any ρ we can select a sufficiently small such that solutions of system (C.6) with restricted flow and jump set are also solutions of the inflated HDS (A.3) associated to the learning dynamics (2.11), with restricted flow and jump set. Therefore, the set $\Omega^{\delta}_{\hat{\mathcal{H}}}(\tilde{K})$ is also GP-AS for system (C.6) with restricted flow and jump set $(C_u \times C_z) \cap \tilde{K}$ and $(D_u \times D_z) \cap \tilde{K}$, as $a \to 0^+$, where without loss of generality we assumed the existence of a function $\alpha(\cdot) \in \mathcal{K}$ such that $\rho = \alpha(a)$. Now, by Assumption 5, item (d), the $O(a)$ perturbation on the gradient ∇J does not preclude the existence of at least one complete solution of system (C.6) from every possible initial condition. Let Lemma 12 generate $a^{**} \in (0, a^*)$ for the HDS (C.6) using again $(\Delta, \nu/5)$. Let $a \in (0, a^{**})$. Then, there exists a compact set $\Omega^{\delta,a}_{\mathcal{H}_s^{A,r}}(\tilde{K}) \subset \mathcal{A} + \frac{2\nu}{5}\mathbb{B}$, that is UGAS for system (C.6) with restricted flow and jump set $(C_u \times C_z) \cap \tilde{K}$ and $(D_u \times D_z) \cap \tilde{K}$.

Step 3: The restricted reduced system (C.6) has compact flow and jump sets, and $\psi_a(\cdot)$ in (C.5) is continuous, therefore there exists a $\lambda_\xi \in \mathbb{R}_{>0}$ such that for each $x_{u,z} \in (C_u \times C_z) \cap \tilde{K}$ we have that $H_a(\hat{u}) \subset \lambda_\xi \mathbb{B} =: \Lambda_\xi$, thus satisfying the condition (2) in Definition 11. By the UGAS stability of the set $\Omega^{\delta,a}_{\mathcal{H}_s^{A,r}}(\tilde{K})$ for system (C.6) with flow set $(C_u \times C_z) \cap \tilde{K}$ and jump set $(D_u \times D_z) \cap \tilde{K}$, and the UGAS stability of the compact set M_ρ for the boundary layer system (C.4), we obtain via Lemma, 15 GP-AS as $\sigma \to 0^+$ of the set $\Omega^{\delta,a}_{\mathcal{H}_s^{A,r}}(\tilde{K}) \times \Lambda_\xi$ for the average system (C.3), with restricted flow set $\left[(C_u \times C_z) \cap \tilde{K}\right] \times \Lambda_\xi$, and jump set $\left[(D_u \times D_z) \cap \tilde{K}\right] \times \Lambda_\xi$. Since this system is well-posed, and complete solutions are always guaranteed by selecting λ_ξ sufficiently

large, we can now use again Lemma 12 to generate σ^* using $(\Delta, \nu/5)$ and the compact set $K'' := \tilde{K} \times K''_\xi$, where $\Lambda_\xi \subset \text{int}(K''_\xi)$. Then, for each $\sigma \in (0, \sigma^*)$ there exists a UGAS compact set $\Omega^{\delta,a,\sigma}_{\mathcal{H}^A_s}(K'') \subset \left(\mathcal{A} + \frac{3v}{5}\mathbb{B}\right) \times \Lambda_\xi$, for the average system (C.3) with flow set given by $\Big[(C_u \times C_z) \cap \tilde{K} \times \Lambda_\xi\Big] \cap K'' = \Big[(C_u \times C_z) \cap \tilde{K}\Big] \times \Lambda_\xi$, and jump set given by $\Big[(D_u \times D_z) \cap \tilde{K} \times \Lambda_\xi\Big] \cap K'' = \Big[(D_u \times D_z) \cap \tilde{K}\Big] \times \Lambda_\xi$. Since the result holds for system (C.3) in the γ-time scale it also holds for system (C.2) in the λ-time scale.

Step 4: By definition, all solutions of the boundary layer dynamics of (C.1) are complete and defined on $\mathbb{S}^n$. Thus, system (C.1) satisfies condition (2) in Definition 12. Combining the UGAS property of the set $\Omega^{\delta,a,\sigma}_{\mathcal{H}^A_s}(K'')$ for the average system (C.2) with restricted data, and the UGAS of the set $\mathbb{S}^n$ for the boundary layer dynamics of system (C.1), we get, by Lemma 16, SGP-AS of the set $\Omega^{\delta,a,\sigma}_{\mathcal{H}^A_s}(K'') \times \mathbb{S}^n$ as $\overline{\omega} \to 0^+$ for system (C.1). Applying again Lemma 11 with $(\Delta, \nu/5)$ and $K''' := \tilde{K} \times K'''_\xi \times K'''_\mu$, where $\Lambda_\xi \subset \text{int}(K'''_\xi)$, and $\mathbb{S}^n \subset \text{int}(K'''_\mu)$, we generate $\overline{\omega}^*$, and select $\omega \in (0, \omega^*)$, obtaining the existence of a UGAS compact set $\Omega^{\delta,a,\sigma,\bar{\omega}}_{\mathcal{H}_s}(K''') \subset \left(\mathcal{A} + \frac{4\nu}{5}\mathbb{B}\right) \times \Lambda_\xi \times \mathbb{S}^n$ for the quasi-steady state system (C.1), with restricted flow set $\Big[(C_u \times C_z) \cap \tilde{K} \times \Lambda_\xi \times \mathbb{S}^n\Big] \cap K''' = \Big[(C_u \times C_z) \cap \tilde{K}\Big] \times \Lambda_\xi \times \mathbb{S}^n$, and restricted jump set given by $\Big[(D_u \times D_z) \cap \tilde{K} \times \Lambda_\xi \times \mathbb{S}^n\Big] \cap K''' = \Big[(D_u \times D_z) \cap \tilde{K}\Big] \times \Lambda_\xi \times \mathbb{S}^n$.

Step 5: Finally, consider the complete system interconnected with the plant (2.1), given in the closed-loop form by Eq. (2.12). Rewriting the flow and jump maps of (2.12) in the ς-time scale, where $\varsigma = \epsilon t$ we obtain

$$F_\epsilon := \begin{pmatrix} \overline{\omega}\sigma \hat{F}_\delta(x_{u,z}, \xi) \\ -\overline{\omega}\left(\xi - \frac{2}{a}\varphi(\theta, u) \cdot \mathbb{D} \cdot \mu\right) \\ \Phi(\kappa_i) \cdot \mu \\ \epsilon^{-1} g(\theta, \hat{u} + a\mathbb{D} \cdot \mu) \end{pmatrix}, \; G := \begin{pmatrix} \hat{G}_\delta(x_{u,z}) \\ \xi \\ \mu \\ \theta \end{pmatrix}, \tag{C.7}$$

with flow and jump set defined as in Theorem 1. System (C.7) is of the form (B.1), with ϵ acting as small parameter. The boundary layer dynamics (B.2) in this case correspond to the dynamics of the plant, given by (2.1), with frozen input u. By Assumptions 1 and 2 this boundary layer dynamics are well-posed and render the set $\mathbb{M}_\rho$ UGAS. Moreover, using LB of the quasy-steady-state manifold $H(\cdot)$, there exists a $\lambda_\theta \in \mathbb{R}_{>0}$ such that for any $u \in (C_u \cap \tilde{K}) + a\mathbb{B} \subset \mathbb{U}$ the containment $H(u) \subset \lambda_\theta \mathbb{B}$ holds, thus satisfying condition (2) in Definition 11. Also, by Assumption 3, the function $J(u)$ is well-defined, and the reduced system associated to (C.7) in the $\alpha = \overline{\omega}\varsigma$-time scale corresponds to the same system (C.1) with restricted flow and jump set, and whose stability properties were already established in Step 4. Therefore, we can use again Lemma 15 to obtain that system (C.7) with flow set $\left[(C_u \times C_z) \cap \tilde{K}\right] \times \Lambda_\xi \times \mathbb{S}^n \times \Lambda_\theta$ and jump set $\left[(D_u \times D_z) \cap \tilde{K}\right] \times \Lambda_\xi \times \mathbb{S}^n \times \Lambda_\theta$ renders the set $\Omega^{\delta,a,\sigma,\bar{\omega}}_{\mathcal{H}_s}(K''') \times \Lambda_\theta$ SGP-AS as $\epsilon \to 0^+$. Since complete solutions for this system can always be guaranteed by selecting λ_θ sufficiently large, we can apply again Lemma 12 with $(\Delta, \nu/5)$ and compact set $K'''' := \tilde{K} \times K''''_\xi \times K''''_\mu \times K''''_\theta$, where $\Lambda_\xi \subset \text{int}(K''''_\xi)$, $\mathbb{S}^n \subset \text{int}(K''''_\mu)$, and $\Lambda_\theta \subset \text{int}(K''''_\theta)$, obtaining the existence of an ϵ^* such that for each $\epsilon \in (0, \epsilon^*)$ there exists a compact set $\Omega^{\delta,a,\sigma,\bar{\omega},\epsilon}_{\mathcal{H}}(K'''') \subset (\mathcal{A} + v\mathbb{B}) \times \Lambda_\xi \times \mathbb{S}^n \times \Lambda_\theta$ that is UGAS for the closed-loop system (C.7) with restricted jump and flow set given by $\left[(C_u \times C_z) \cap \tilde{K}\right] \times \Lambda_\xi \times \mathbb{S}^n \times \Lambda_\theta$ and jump set $\left[(D_u \times D_z) \cap \tilde{K}\right] \times \Lambda_\xi \times \mathbb{S}^n \times \Lambda_\theta$. Theorem 1 follows by noting that for any pair $\Delta > \nu$, uniform convergence to an arbitrarily small ν-neighborhood of $\mathcal{A}$, from initial conditions of x_{uz} in arbitrarily large compact sets $\tilde{K}$, can be achieved by decreasing in order the parameters $(\delta, a, \sigma, \bar{\omega}, \epsilon)$ (note that, unlike Definition 9, the resulting $\mathcal{KL}$ function will depend on these parameters). Finally, note that if $C_u \times C_z$ and $D_u \times D_z$ are bounded, Δ can always be selected sufficiently large to satisfy $(C_u \times C_z) \cap \tilde{K} = C_u \times C_z$ and $(D_u \times D_z) \cap \tilde{K} = D_u \times D_z$, obtaining the global practical result for the original system (C.7) as in Corollary 1. ■

C.1 Proof of Lemma 1.

The first part of the Lemma follows by noting that

$$\begin{aligned} 0 \leq \tau_2(t,j) &\leq \tau_2(s,i) + \rho(t-s) - \int_s^t \mathbb{I}_{Q_u}(q(r,j(r)))dr \\ &\leq T_0 + \rho(t-s) - \int_s^t \mathbb{I}_{Q_u}(q(r,j(r)))dr, \end{aligned}$$

For the second part, choose

$$\tau_2(0,0) = T_0, \tag{C.8a}$$

$$\dot{\tau}_2 = \begin{cases} \eta_2 - \mathbb{I}_{Q_u}(q) & \tau_2 < T_0, \\ -\mathbb{I}_{Q_u}(q) & \tau_2 = T_0. \end{cases} \tag{C.8b}$$

The solution can track the hybrid time domain E as long as it does not reach the condition

$$\tau_2(s,i) = 0 \tag{C.9a}$$

$$q(s,i) \in Q_u \tag{C.9b}$$

$$(t,i) \in E \text{ for some } t > s. \tag{C.9c}$$

Let (p,k) be the largest time preceding (s,i) such that $\tau(p,k) = T_0$. There exists such a time due to (C.8a). The conditions in (C.8b) together with (C.9a) imply

$$0 = T_0 + \eta_2(s-p) - \int_p^s \mathbb{I}_{Q_u}(q(r,j(r)))dr. \tag{C.10}$$

Then, since $\eta_2 \in [0, 1)$, the condition (C.9b)-(C.9c) and the fact that q is constant along flows imply

$$\begin{aligned}\int_p^t \mathbb{I}_{Q_u}(q(r, j(r)))dr &= \int_p^s \mathbb{I}_{Q_u}(q(r, j(r)))dr + (t - s) \\ &= T_0 + \eta_2(s - p) + (t - s) \\ &> T_0 + \eta_2(s - p) + \eta_2(t - s) = T_0 + \eta_2(t - p),\end{aligned}$$

which violates the time-ratio constraint (2.18). ■

Appendix D

Singularly Perturbed Hybrid Systems with Hybrid Boundary Layer

We consider now singularly perturbed hybrid dynamical systems (SP-HDS) with state $x = [x_1^\top, x_2^\top]^\top$, $x_1 \in \mathbb{R}^{n_1}$, $x_2 \in \mathbb{R}^{n_2}$, and dynamics in the $\tau = \varepsilon t$-time scale, given by

$$\left.\begin{array}{l} \frac{dx_1}{d\tau} \in F_1(x_1, x_2) \\ \varepsilon \frac{dx_2}{d\tau} \in F_2(x_1, x_2) \end{array}\right., \quad (x_1, x_2) \in C_s \times \Psi_C(x_1), \tag{D.1a}$$

$$\left.\begin{array}{l} x_1^+ = x_1 \\ x_2^+ \in H_2(x_1, x_2) \end{array}\right., \quad (x_1, x_2) \in C_s \times \Psi_D(x_1), \tag{D.1b}$$

$$\left.\begin{array}{l} x_1^+ \in G_1(x_1) \\ x_2^+ \in G_2(x_1, x_2) \end{array}\right., \quad (x_1, x_2) \in D_s \times \Psi(x_1), \tag{D.1c}$$

where $\Psi_C, \Psi_D : \mathbb{R}^{n_1} \rightrightarrows \mathbb{R}^{n_2}$, $F_1 : \mathbb{R}^{n_1+n_2} \rightrightarrows \mathbb{R}^{n_1}$, $F_2 : \mathbb{R}^{n_1+n_2} \rightrightarrows \mathbb{R}^{n_2}$, $G_2, H_2 : \mathbb{R}^{n_1+n_2} \rightrightarrows \mathbb{R}^{n_2}$, $\Psi(x_1) = \Psi_C(x_1) \cup \Psi_D(x_1)$, and $\varepsilon \in \mathbb{R}_{>0}$ is a small constant. The set-valued

mappings $\Psi_C,\ \Psi_D,\ F_1,\ F_2,\ G_1,\ G_2,\ H_2$, are assumed to be locally bounded and outer-semicontinuous. The set-valued mappings F_1, F_2 are additionally assumed to be convex-valued. The sets C_s and D_s are assumed to be closed and nonempty. For system (D.1) we will use the notation $F = F_1 \times F_2$, and $\tilde{C} := \{(x_1, x_2) : x \in C_s, x_2 \in \Psi_C(x_1)\}$.

Systems of the form (D.1) are studied in [249] and [203]. In the HDS (D.1) the state x_2 evolves faster than the state x_1 during flows. Also, during jumps induced by the condition $x_1 \in C_s$ and $x_2 \in \Psi_D(x_1)$, the state x_2 is updated according to H_2, and the state x_1 remains constant. To analyze system (D.1) we introduce the boundary layer dynamics in the standard time scale t, given by

$$\begin{aligned} \dot{x}_1^{bl} &= 0 \\ \dot{x}_2^{bl} &\in F_2(x_1^{bl}, x_2^{bl}) \end{aligned} \quad , \quad (x_1^{bl}, x_2^{bl}) \in C_s \times \Psi_C(x_1), \tag{D.2a}$$

$$\begin{aligned} x_1^{bl\,+} &= x_1^{bl} \\ x_2^{bl\,+} &\in H_2(x_1^{bl}, x_2^{bl}) \end{aligned} \quad , \quad (x_1^{bl}, x_2^{bl}) \in C_s \times \Psi_D(x_1). \tag{D.2b}$$

Based on these boundary layer dynamics, the *average system* associated to the HDS (D.1) is defined as follows.

Definition 13 *Consider the hybrid dynamical system*

$$\frac{dx_1}{d\tau} \in F^A(x_1), \quad x_1 \in C_s, \tag{D.3a}$$

$$x_1^+ \in G_1(x_1), \quad x_1 \in D_s. \tag{D.3b}$$

We say that system (D.3) *is a* well-defined average system *for the HDS* (D.1) *if the mapping $F^A : \mathbb{R}^{n_1} \rightrightarrows \mathbb{R}^{n_1}$ is OSC, LB, convex-valued, and non-empty for each $x_1 \in C_s$, and if for each compact set $K \subset \mathbb{R}^{n_1}$ there exists a continuous function $\sigma_K : \mathbb{R}_{>0} \to \mathbb{R}_{\geq 0}$ that decreases to zero as it argument increases, such that for each $L > 0$, each*

$x \in C_s \cap K$, *each solution* x_2^{bl} *to the boundary layer system* (D.2) *with* $dom(x_2^{bl}) \cap ([L,\infty] \times \mathbb{Z}_{\geq 0}) \neq \emptyset$ *and each measurable function* $f_1 : [0,L] \to \mathbb{R}^n$ *that satisfies* $f_1(s) \in F_1(x_1, x_2^{bl}(s,j))$ *for each* $j \in \mathbb{Z}_{\geq 0}$ *and almost all* $t \in [0,L] \cap \{t : (t,j) \in dom(x_2^{bl})\}$, *there exists a measurable function* $f^A : [0,L] \to \mathbb{R}^{n_1}$ *with* $f^A(s) \in F^A(x_1)$ *such that* $\frac{1}{L}\left\| \int_0^L \left(f_1(s) - f^A(s)\right) ds \right\| \leq \sigma_K(L)$. □

In order to characterize the stability properties of system (D.1) based on the stability properties of the average system (D.3), we need to take into account that the time domain of the solutions of the average system do not take into account the jumps associated to the boundary layer dynamics (D.2). In order to account for this difference, a mapping $\tilde{x}_1$ is defined as follows:

$$\text{graph}(\tilde{x}_1) = \cup_{(t,j)\in \text{dom}(x)} \{s(t,j), k(t,j), x_1(t,j)\}, \tag{D.4}$$

where $s(t,j)$ is a timer that counts the flow time of system (D.1), and $k(t,j)$ is a timer that counts the jumps given by (D.1c). Note that the values of $\tilde{x}_1$ match those of x_1. Thus convergence of $\tilde{x}_1$ as $s + k \to \infty$ will necessarily imply convergence for the original state x_1. Based on this, and using Definition 13, the next Theorem follows by the results in [249, Thm. 2] relaxed to local stability.

Theorem 13 *Consider the SP-HDS* (D.1)*, and suppose that the hybrid boundary layer dynamics* (D.2) *do not generate purely discrete solutions. Also, suppose that the SP-HDS has a well-defined average system* (D.3) *in the sense of Definition 13, and that this average system renders ULAS a compact set* $\mathcal{A} \subset C_s \cup D_s$ *with some* $\mathcal{KL}$ *function* β *and basin of attraction* $\mathcal{B}_\mathcal{A}$*. Then, there exists a proper indicator* ω *for* $\mathcal{A}$ *on* $\mathcal{B}_\mathcal{A}$ *such that for each compact set* $K \subset \mathcal{B}_\mathcal{A}$ *and each* $\nu \in \mathbb{R}_{>0}$ *there exists an* $\varepsilon^* \in \mathbb{R}_{>0}$ *such that for each* $\varepsilon \in (0, \varepsilon^*)$ *every solution of the singularly perturbed HDS* (D.1) *with* $x_1(0,0) \in K$, $\tilde{x}_1$ *constructed as in* (D.4)*, and* $s(0,0) = k(0,0) = 0$ *generates the bound*

$$\omega(\tilde{x}_1(s,k)) \leq \beta(\omega(\tilde{x}_1(0,0)), s+k) + \nu, \tag{D.5}$$

for all $(s(t,j), k(t,j))$ *such that* $(t,j) \in dom(x)$. □

Note that the bound (D.5) does not decrease when the HDS (D.1) jumps according to (D.1b). Thus, in order to obtain convergence of x_1 towards $\mathcal{A} + \nu\mathbb{B}$ it is required that system (D.1) generates complete solutions that flow or jump according to (D.1a) or (D.1c). Finally, note that if x_1 converges to $\mathcal{A}+\nu\mathbb{B}$, by definition of the flow and jump set of x_2 in (D.1), we have that x_2 will converge to the set $\Psi(\mathcal{A}+\nu\mathbb{B})$. Using the fact that OSC and LB of Ψ imply upper-semicontinuity of Ψ [78, Lemma 5.15], we have that for any $\tilde{\nu} \in \mathbb{R}_{>0}$ there exists a sufficiently small $\nu < \tilde{\nu}$ such that $\Psi(\mathcal{A}+\nu\mathbb{B}) \subset \Psi(\mathcal{A}) + \tilde{\nu}\mathbb{B}$, which in turn implies that one can select ν sufficiently small in Theorem 13 to establish convergence of the states (x_1, x_2) in finite time (from compact sets in $\mathcal{B}_{\mathcal{A}}$) towards the set $(\mathcal{A} \times \Psi(\mathcal{A})) + \tilde{\nu}\mathbb{B}$.

Appendix E

Proof of Theorem 2

Proof: Fix K and ν, such that $\mathcal{A}_{\hat{x},\xi,\mu,\theta} + \nu\mathbb{B} \subset \text{int}(K)$. Using OSC and LB of the mappings Ψ_ξ, Ψ_μ, and Ψ_θ, and continuity of h_u and h_μ, there exists ν_a such that $\Psi_\theta\left(h_u(h_{\hat{x}}(\mathcal{A}_{\hat{x}} + \nu_a\mathbb{B}), h_\mu(\mathcal{A}_\mu + \nu_a\mathbb{B}))\right) + \nu_a\mathbb{B} \subset \Psi_\theta\left(h_u(h_{\hat{x}}(\mathcal{A}_{\hat{x}}), h_\mu(\mathcal{A}_\mu))\right) + \nu\mathbb{B}$. Using this ν_a, there exists a $\nu_b > 0$ such that $\Psi_\mu(\mathcal{A}_{\hat{x}} + \nu_b\mathbb{B}, \mathcal{A}_\xi + \nu_b\mathbb{B}) + \nu_b\mathbb{B} \subset \Psi_\xi(\mathcal{A}_{\hat{x}}, \mathcal{A}_\xi) + \frac{\nu_a}{2}\mathbb{B}$. Using this ν_b, there exists $\nu_c > 0$ such that $\Psi_\xi(\mathcal{A}_{\hat{x}} + \nu_c\mathbb{B}) + \nu_c\mathbb{B} \subset \Psi_\xi(\mathcal{A}_{\hat{x}}) + \frac{\nu_b}{2}\mathbb{B}$. Based on this, we divide the proof in 4 main steps:

Step 1: By Lemma 13, there exists a ULAS compact set $\Omega_\delta(K_{\hat{x}}) \subset \mathcal{A}_{\hat{x}} + \frac{\nu_c}{3}\mathbb{B}$ for system (2.53) with $e = 0$, with basin of attraction $\mathcal{B}_{\Omega_\delta(K_{\hat{x}})}$ satisfying $K_{\hat{x}} \subset \mathcal{B}_{\Omega_\delta(K_{\hat{x}})}$. Since the system satisfies **(C1)-(C3)**, and $e(t)$ is of order $O(a)$, by Lemmas 11 and 12, the set $\Omega_\delta(K_{\hat{x}})$ is SGP-AS as $a \to 0^+$. Using again Lemma 13 with $\frac{\nu_c}{3}$ we obtain the existence of a ULAS compact set $\Omega_{\delta,a}(K_{\hat{x}}) \subset \mathcal{A}_{\hat{x}} + \frac{2\nu_c}{3}\mathbb{B}$ for system (2.53), with basin of attraction $\mathcal{B}_{\Omega_{\delta,a}(K_{\hat{x}})}$ satisfying $K_{\hat{x}} \subset \mathcal{B}_{\Omega_{\delta,a}(K_{\hat{x}})}$.

Step 2: The previous step established ULAS of the set $\Omega_{\delta,a}(K_{\hat{x}})$ for system (2.53). Since system (2.53) is the average system associated to the SP-HDS given by the equations (2.56), (2.57), and (2.58), by Assumption 8 and Theorem 13 we obtain the existence of an σ^* such that for each $\sigma \in (0, \sigma^*)$ the trajectories of the slow state $\hat{x}$ of

the SP-HDS (2.56), (2.57), and (2.58) satisfying $\hat{x}(0,0) \in K_{\hat{x}}$, also generate a bound of the form (D.5) with residual term $\frac{\nu_c}{3}$, constructed as in (D.4). Since by assumption the SP-HDS generates complete solutions, and the boundary layer dynamics do not generate purely-discrete solutions, the bound (D.5) and the construction (D.4) imply the convergence in finite time of the state $\hat{x}$ to a $\frac{\nu_c}{3}$-neighborhood of the compact set $\Omega_{\delta,a}(K_{\hat{x}})$. In turn, this implies the convergence of $\hat{x}$ to $\mathcal{A}_{\hat{x}} + \nu_c\mathbb{B}$ in finite time. Using the properties of ν_c, we obtain that the states $(\hat{x}, \xi)$ converge in finite time to the set $\mathcal{A}_{\hat{x},\xi} + \frac{\nu_b}{2}\mathbb{B}$, where $\mathcal{A}_{\hat{x},\xi} := \mathcal{A}_{\hat{x}} \times \mathcal{A}_{\xi}$. Using again Lemma 13, there exists a ULAS compact set $\Omega_{\delta,a,\sigma}(K_{\hat{x}} \times K_{\xi}) \subset \mathcal{A}_{\hat{x},\xi} + \frac{\nu_b}{2}\mathbb{B}$, with basin of attraction satisfying $K_{\hat{x}} \times K_{\xi} \subset \mathcal{B}_{\Omega_{\delta,a,\sigma}(K_{\hat{x}} \times K_{\xi})}$.

Step 3: The previous step established ULAS of the set $\Omega_{\delta,a,\sigma}(K_{\hat{x}} \times K_{\xi})$ for the HDS (2.56), (2.57), and (2.58). Since the HDS (2.56), (2.57), and (2.58) is the average system associated to the SP-HDS given by the equations (2.64), (2.65), (2.66), (2.68), by Assumption 9 and Theorem 13, we obtain the existence of an $\bar{\omega}^*$ such that for each $\bar{\omega} \in (0, \bar{\omega}^*)$ the trajectories of the slow states $(\hat{x}, \xi)$ of the SP-HDS (2.64), (2.65), (2.66), (2.68) satisfying $[\hat{x}^\top(0,0), \xi^\top(0,0)]^\top \in K_{\hat{x}} \times K_{\xi}$, also generate a bound of the form (D.5) with $\frac{\nu_b}{2}$, constructed as in (D.4). Therefore, using the properties ν_b, the states $(\hat{x}, \xi, \mu)$ will converge in finite time to the set $\mathcal{A}_{\hat{x},\xi,\mu} + \frac{\nu_a}{2}\mathbb{B}$, where $\mathcal{A}_{\hat{x},\xi,\mu} := \mathcal{A}_{\hat{x}} \times \mathcal{A}_{\xi} \times \mathcal{A}_{\mu}$. By Lemma 13 there exists a ULAS compact set $\Omega_{\delta,a,\sigma,\bar{\omega}}(K_{\hat{x}} \times K_{\xi} \times K_{\mu}) \subset \mathcal{A}_{\hat{x},\xi,\mu} + \frac{\nu_a}{2}\mathbb{B}$, with basin of attraction satisfying $K_{\hat{x}} \times K_{\xi} \times K_{\mu} \subset \mathcal{B}_{\Omega_{\delta,a,\sigma,\bar{\omega}}(K_{\hat{x}} \times K_{\xi} \times K_{\mu})}$.

Step 4: The previous step established ULAS of the set $\Omega_{\delta,a,\sigma,\bar{\omega}}(K_{\hat{x}} \times K_{\xi} \times K_{\mu})$ for the HDS (2.64), (2.65), (2.66), (2.68). Since this HDS is the average system associated to the complete SP-HDS given by the equations (2.71)-(2.75), by Assumptions 10 and Theorem 13, we obtain the existence of an ϵ^* such that for each $\epsilon \in (0, \epsilon^*)$ the trajectories of the slow states $(\hat{x}, \xi, \mu)$ of the SP-HDS (2.71)-(2.75), satisfying $[\hat{x}^\top(0,0), \xi^\top(0,0), \mu^\top(0,0)]^\top \in K_{\hat{x}} \times K_{\xi} \times K_{\mu}$, also generate a bound of the form (D.5)

with residual term $\frac{\nu_a}{2}$, constructed as in (D.4). Using the properties of ν_a we obtain finite time convergence of the states $(\hat{x}, \xi, \mu, \theta)$ to the set $\mathcal{A}_{\hat{x},\xi,\mu,\theta} + \nu\mathbb{B}$, which, by Lemma 13 implies the existence of a ULAS compact set $\Omega_{\delta,a,\sigma,\bar{\omega},\epsilon}(K_{\hat{x}} \times K_\xi \times K_\mu \times K_\theta) \subset \mathcal{A}_{\hat{x},\xi,\mu,\theta} + \nu\mathbb{B}$, with basin of attraction satisfying $K_{\hat{x}} \times K_\xi \times K_\mu \times K_\theta \subset \mathcal{B}_{\Omega_{\delta,a,\sigma,\bar{\omega},\epsilon}(K_{\hat{x}} \times K_\xi \times K_\mu \times K_\theta)}$.

Appendix F

Proof of Theorem 3

F.1 Proof of Proposition 6

Since u is constant and μ is generated by the uncoupled PE signal generator (2.87) which renders the set $\mathcal{A}_\mu$ UGAS, it suffices to study the behavior of the dynamics of $\hat{w}$. Moreover, since u is constrained to lie in the compact set $\rho\mathbb{B} \cap \mathbb{U}$, and μ is uniformly bounded, we can take $\phi(t)$ in (2.90) as an independent absolutely continuous function of time. Now, consider the radially unbounded Lyapunov function

$$V_{\tilde{w}} = \frac{1}{2}\text{trace}\left\{\tilde{w}^T\Gamma^{-1}\tilde{w}\right\}, \tag{F.1}$$

and note that $\dot{\tilde{w}} = \dot{\hat{w}}$. Taking the derivative of (F.1) one gets

$$\begin{aligned}
\dot{V}_{\tilde{w}} &= \text{trace}\left\{\dot{\tilde{w}}^T \Gamma^{-1} \tilde{w}\right\} \\
&= \text{trace}\left\{\left(-\Gamma \frac{\phi}{(1+\phi^\top\phi)^2}(\tilde{w}^\top\phi + \epsilon)\right)^\top \Gamma^{-1}\tilde{w}\right\} \\
&= \text{trace}\left\{\left(-\Gamma \frac{\bar{\phi}}{(1+\phi^\top\phi)}(\tilde{w}^\top\phi + \epsilon)\right)^\top \Gamma^{-1}\tilde{w}\right\} \\
&= \text{trace}\left\{\left(-\Gamma\bar{\phi}\left(\tilde{w}^\top\bar{\phi} + \frac{\epsilon}{1+\phi^\top\phi}\right)\right)^\top \Gamma^{-1}\tilde{w}\right\} \\
&= -\text{trace}\left\{\tilde{w}^T\bar{\phi}\bar{\phi}^T\tilde{w}\right\} + \text{trace}\left\{\epsilon\cdot\bar{\phi}^T\frac{1}{(1+\phi^T\phi)}\tilde{w}\right\}.
\end{aligned}$$

When $\epsilon = 0$ we have that $\dot{V}_w$ reduces to

$$\dot{V}_{\tilde{w}} = -\text{trace}\left\{\tilde{w}^T\bar{\phi}\bar{\phi}^T\tilde{w}\right\}, \tag{F.2}$$

which can be rewritten as

$$\dot{V}_{\tilde{w}} = -\text{trace}\left\{\frac{e^2}{(1+\phi^\top\phi)^2}\right\} \leq 0. \tag{F.3}$$

This implies that $\sup_{t\geq 0}|V_{\tilde{w}}(t)| < \infty$ and $\sup_{t\geq 0}\|\tilde{w}(t)\| < \infty$. Moreover, (F.3) and (F.1) imply that for each $c \in \mathbb{R}_{>0}$ the compact set

$$\Omega_c := \{\tilde{w} \in \mathbb{R}^N : V_{\tilde{w}}(\tilde{w}) \leq c\}, \tag{F.4}$$

is positively invariant under the dynamics (2.86), which guarantees the existence of complete solutions for system (2.90). Using the PE condition on $\bar{\phi}$, and equation (F.2), it follows by [1, Theorem 4.3.2] or [209, Thm. 1] that $\tilde{w}$ converges to zero exponentially fast. Now, if $\epsilon \neq 0$, using the PE condition, one has that $\dot{V}_{\tilde{w}}$ is negative

if [209, Thm. 1],

$$\|\tilde{\omega}^\top \bar{\phi}\| \geq \frac{\|\epsilon\|}{\|1+\phi^T\phi\|}. \tag{F.5}$$

Note that $\|1+\phi^T\phi\| \geq 1$. Moreover, given the fact that u is constrained to the compact set $\rho\mathbb{B} \cap \mathbb{U}$, by Lemma 2 the condition $\|\epsilon\| \leq \bar{\epsilon}_1$ can be guaranteed for any $\bar{\epsilon}_1 < \bar{\epsilon} \ll c$ by taking N sufficiently large. Therefore, for any $\bar{\epsilon}_1$ there exists a N^* such that for any $N \geq N^*$ (F.5) is satisfied if

$$\|\tilde{w}^\top \bar{\phi}\| \geq \bar{\epsilon}_1. \tag{F.6}$$

Then, since $\|\bar{\phi}(t)\| < 1$ for all $t \geq 0$, using the Cauchy-Schwarz inequality we have that $\dot{V}_{\tilde{\omega}}$ will be negative outside the set

$$\Omega_{\bar{\epsilon}} := \{\tilde{w} \in \mathbb{R}^N : \|\tilde{w}\| \leq \bar{\epsilon}_1\}. \tag{F.7}$$

Finally, define $B_{\bar{\epsilon}} := \bar{\epsilon}\mathbb{B} \subset \mathbb{R}^N$ and note that for sufficiently small $\bar{\epsilon}_1$ one has that $\Omega_{\bar{\epsilon}_1} \subset B_{\bar{\epsilon}} \subset \text{int}(\Omega_c)$. Then, $\tilde{w}(t)$ is guaranteed to converge exponentially fast and in finite time to $B_{\bar{\epsilon}}$. Since the flow set in (2.90) is compact, the previous arguments, and Assumption 12, imply by [78, Corollary 7.7] and [206, Lemma 1] that there exists a compact set $\mathcal{A}_c \subset w^* + \bar{\epsilon}\mathbb{B}$ such that the set $(\rho\mathbb{B} \cap \mathbb{U}) \times \mathcal{A}_\mu \times \mathcal{A}_c$ is UGAS for system (2.90).

F.1.1 Proof of Theorem 3

The proof is divided in 4 steps:

Step 1: Suppose the dynamics of θ are negligible, such that $y = J(u)$, i.e., the plant is just a static mapping $J(\cdot)$. Then, the resulting HDS in the λ-time scale (which only affects the flows) with $\lambda := \varepsilon_1 \cdot \varepsilon_2 \cdot t$, has data $\mathcal{H}_s := \{C_s, F_s, D_s, G_s\}$, state

$x_s := \left[x_{u,z}^\top, \hat{w}, \mu^\top\right]^\top$, and is characterized by the equations

$$C_s := (C_u \times C_z) \times \Omega_c \times \Psi, \tag{F.8a}$$

$$F_s := \begin{pmatrix} \hat{F}_\delta(x_{u,z}, \nabla\phi(u)^\top \hat{w}) \\ \frac{1}{\varepsilon_1} \cdot \Gamma \bar{\bar{\phi}}(u+\mu)\left(\hat{w}^\top \phi(u+\mu) - J(u+\mu)\right) \\ \frac{1}{\varepsilon_1} \cdot \Pi(\mu) \end{pmatrix}, \tag{F.8b}$$

$$G_s := \begin{pmatrix} \hat{G}_\delta(x_{u,z}) \\ \hat{w} \\ \mu \end{pmatrix}, \quad D_s := (D_u \times D_z) \times \Omega_c \times \Psi. \tag{F.8c}$$

System (F.8) is a singularly perturbed HDS [224], with ε_1 acting as small positive parameter. For this system the *boundary layer* dynamics, in the $\tau_{\varepsilon_1} := \lambda/\varepsilon_1$-time scale, correspond to the same dynamics (2.90), where the "slow" variable u is assumed to be frozen. By Proposition 6, for each pair $(\rho, c) \in \mathbb{R}^2_{>0}$, and each $\bar{\epsilon} \ll c$ there exists a number N^* of NN such that for all $N \geq N^*$ the compact set $\mathcal{A}_{bdl} \subset \mathcal{A}_\rho + \bar{\epsilon}\mathbb{B}$ is UGAS for this *boundary layer* dynamics. Also, the *reduced system* associated to the singularly perturbed HDS (F.8) corresponds to the learning dynamics with an additive $\bar{\epsilon}$-bounded perturbation on the estimated gradient $\nabla\phi^\top\hat{w}$, i.e.,

$$\dot{x}_{u,z} \in \hat{F}_\delta\left(x_{u,z}, \nabla\phi(u)^\top\hat{w} + \bar{\epsilon}\mathbb{B}\right), \; x_{u,z} \in C_u \times C_z, \tag{F.9a}$$

$$x^+_{u,x} \in \hat{G}_\delta\Big(x_{u,z}\Big), \qquad x_{u,z} \in D_u \times D_z. \tag{F.9b}$$

Step 2: Let $\Delta > \nu > 0$ be given and define $\tilde{K} := \mathcal{A}_{u,z} + \Delta\mathbb{B}$. Let Lemma 12 in the Appendix generate δ^* with the pair $(\Delta, \frac{\nu}{4})$, and let $\delta \in (0, \delta^*)$. Then, by Assumption 14, and Lemma 11 in the Appendix, there exists a compact set $\Omega^\delta(K_\Delta) \subset \mathcal{A}_{u,z} + \frac{\nu}{4}\mathbb{B} \subset \text{int}(K_\Delta)$ that is UGAS for the learning dynamics with restricted flow and jump set

$(C_u \times C_z) \cap K_\Delta$ and $(D_u \times D_z) \cap K_\Delta$. Then, by Lemmas 14 and 10 in the Appendix, the perturbed system (F.9) with restricted flow and jump set $(C_u \times C_z) \cap K_\Delta$ and $(D_u \times D_z) \cap K_\Delta$ renders the set $\Omega^\delta(K_\Delta)$ GP-AS as $\bar{\epsilon} \to 0^+$. Moreover, by Lemma 2, without loss of generality we can assume that there exists a function $\alpha(\cdot) \in \mathcal{K}$ such that $\varepsilon = \alpha\left(\frac{1}{N}\right)$, such that $\Omega^\delta(K_\Delta)$ is GP-AS as $N \to \infty$. Using again $(\Delta, \nu/4)$ let Lemma 12 generate N^*. Let $N \geq N^*$ such that $\bar{\epsilon}$ can be chosen sufficiently small. Then, there exists a compact set $\Omega^{\delta,N}(K_\Delta) \subset \mathcal{A} + \frac{2\nu}{4}\mathbb{B}$ that is UGAS for system (F.9) with restricted flow and jump set $(C_u \times C_z) \cap K_\Delta$ and $(D_u \times D_z) \cap K_\Delta$.

Step 3: Since the restriction of system (F.9) has compact flow and jump set, we can chose $c \gg \bar{\epsilon}$ such that $\{w^*\} + \bar{\epsilon}\mathbb{B} \subset \Omega_c$, thus [224, Assumption 2] is satisfied by the compact set (2.92). By the UGAS stability of the set $\Omega^{\delta,N}(K_\Delta)$ for the *reduced* system (F.9) with flow set $(C_u \times C_z) \cap K_\Delta$ and jump set $(D_u \times D_z) \cap K_\Delta$, and the UGAS stability of the compact set $\mathcal{M}_\rho$ for the *boundary layer* system (2.90), we obtain via [224, Thm. 1] GP-AS as $\varepsilon_1 \to 0^+$ of the set $\Omega^{\delta,N}(K_\Delta) \times \Psi \times \Omega_c$ for system (F.8) with restricted flow set $((C_u \times C_z) \cap K_\Delta) \times \Psi \times \Omega_c$, and jump set $((D_u \times D_z) \cap K_\Delta) \times \Psi \times \Omega_c$. Since this system is well-posed, and complete solutions are always guaranteed under the given assumptions, we can now use again Lemma 12 to generate ε_1^* using $(\Delta, \nu/5)$ and the compact set $K'' := K_\Delta \times K''_{\mu,c}$, where $\Psi \times \Omega_c \subset \text{int}(K''_{\mu,c})$. Then, for each $\varepsilon \in (0, \varepsilon^*)$ there exists a UGAS compact set $\Omega^{\delta,N,\varepsilon_1}(K'') \subset \left(\mathcal{A} + \frac{3\nu}{4}\mathbb{B}\right) \times \Psi \times \Omega_c$, for system (F.8) with flow set given by $((C_u \times C_z) \cap K_\Delta \times \Psi \times \Omega_c) \cap K'' = ((C_u \times C_z) \cap K_\Delta) \times \Psi \times \Omega_c$, and jump set given by $((D_u \times D_z) \cap K_\Delta \times \Psi \times \Omega_c) \cap K'' = ((D_u \times D_z) \cap K_\Delta) \times \Psi \times \Omega_c$. Since the result holds for system (F.8) in the λ-time scale it also holds for system (F.8) in the t-time scale.

Step 4: Finally, consider the complete system (2.94) taking into account the dynamics of the plant (2.49). Rewriting the flow and jump maps of (2.94) in the ς-time

scale, where $\varsigma = \epsilon_2 t$ we obtain

$$F_{\epsilon_1} := \begin{pmatrix} \varepsilon_1 \cdot \hat{F}_\delta \left(x_{u,z}, \nabla\phi(u)^\top \hat{w} \right) \\ -\Gamma \bar{\bar{\phi}}(u+\mu) \left(\hat{w}^\top \phi(u+\mu) - \varphi(\theta) \right) \\ \Pi(\mu) \\ \frac{1}{\varepsilon_2} P(\theta, u+\mu) \end{pmatrix}, \tag{F.10a}$$

$$G := \begin{pmatrix} \hat{G}_\delta(x_{u,z}) \\ \mu \\ \hat{u} \\ \theta \end{pmatrix}, \tag{F.10b}$$

with flow and jump set defined as in (2.94a) and (2.94c). System (F.10) is also a singularly perturbed HDS [224], with ε_1 acting as small parameter. The *boundary layer* dynamics now correspond to the dynamics of the plant (2.49), with frozen input $\tilde{u} = u + \mu$, which under Assumptions 37 and 38 is well-posed and renders the set $\mathbb{M}_\rho$ UGAS. Moreover, using local boundedness of the quasy-steady-state manifold $H(\cdot)$ and compactness of Ψ, there exists a $\lambda_\theta \in \mathbb{R}_{>0}$ and $\lambda_\mu \in \mathbb{R}_{>0}$, such that $\Psi \subset \lambda_\mu \mathbb{B}$, and for any $\tilde{u} \in (C_u \cap K_\Delta) + \lambda\mathbb{B}$ the containment $H(\tilde{u}) \subset \lambda_\theta \mathbb{B}$ holds, thus satisfying [224, Assumption 2]. Also, by Assumption 39, the response map function $J(\tilde{u})$ is well-defined, and the *reduced system* associated to (F.10) in the $\lambda = \varepsilon_1 \cdot \varsigma$ time scale corresponds to the same system (F.8) with restricted flow and jump set, and whose stability properties were already established in Step 3. Therefore, using again [224, Thm 1.] we obtain that the HDS (F.10) with flow set $((C_u \times C_z) \cap K_\Delta) \times \Psi \times \Omega_c \times \Lambda_\theta$ and jump set $((D_u \times D_z) \cap K_\Delta) \times \Psi \times \Omega_c \times \Lambda_\theta$ renders the set $\Omega^{\delta,N,\varepsilon_1}(K'') \times \Lambda_\theta$ SGP-AS as $\varepsilon_2 \to 0^+$. For this system complete solutions can always be guaranteed by selecting λ_θ sufficiently large. Therefore, using again Lemma 12 with $(\Delta, \nu/4)$ and compact set

$K'''' := K_\Delta \times K''''_{\mu,c} \times K''''_\theta$, where $\Psi \times \Omega_c \subset \text{int}(K''''_{\mu,c})$, and $\Lambda_\theta \subset \text{int}(K''''_\theta)$, we obtain the existence of $\varepsilon_2^* > 0$ such that for each $\varepsilon_2 \in (0, \varepsilon_2^*)$ there exists a compact set $\Omega^{\delta,N,\varepsilon_1,\varepsilon_2}(K'''') \subset (\mathcal{A} + v\mathbb{B}) \times \Psi \times \Omega_c \times \Lambda_\theta$ that is UGAS for the closed-loop system (F.10) with restricted jump and flow set given by $((C_u \times C_z) \cap K_\Delta) \times \Psi \times \Omega_c \times \Lambda_\theta$ and jump set $((D_u \times D_z) \cap K_\Delta) \times \Psi \times \Omega_c \times \Lambda_\theta$. The result of the theorem follows by noting that for any pair $\Delta > \nu$, uniform convergence to an arbitrarily small ν-neighborhood of $\mathcal{A}$, from initial conditions of x_{uz} in arbitrarily large compact sets K_Δ can be achieved by decreasing, in order, the constants $\left(\delta, \frac{1}{N}, \varepsilon_1, \varepsilon_2\right)$. ■

Appendix G

Proofs of Chapter 3

The following Lemma gives some instrumental facts for the proofs of Lemma 18 and Proposition 7.

Lemma 17 *Let $A \in \mathbb{R}^{N\times N}$ be a positive definite diagonal matrix, and consider the matrix $Q \in \mathbb{R}^{N\times N}$ defined as*

$$Q := \left(I - \frac{A^{-1}}{\mathbf{1}^\top A^{-1}\mathbf{1}}\mathbf{1}\mathbf{1}^\top\right)A^{-1}. \tag{G.1}$$

Then, the following holds:

1. *$Q = k\mathcal{L}_{\mathcal{G}_A}$ where $\mathcal{L}_{\mathcal{G}_A}$ is the out-degree Laplacian of a weighted graph with symmetric adjacency matrix $Adj := A^{-1}\mathbf{1}\mathbf{1}^\top A^{-1}$, and k is a scalar defined as $k = (\mathbf{1}^\top A^{-1}\mathbf{1})^{-1}$.*

2. *Q is symmetric and for any $x \in \mathbb{R}^N$*

$$x^\top Q x = \frac{k}{2}\sum_{i,j=1}^{N}\bar{a}_{i,j}(x_i - x_j)^2, \quad \forall\ x \in \mathbb{R}^N. \tag{G.2}$$

where $\bar{a}_{i,j}$ is the entry (i,j) of $A^{-1}\mathbf{1}\mathbf{1}^\top A^{-1}$.

3. $Q\mathbf{1} = \mathbf{0}$ *and* $\mathbf{1}^\top Q = \mathbf{0}^\top$.

4. Q *is positive semidefinite.*

5. *The largest eigenvalue of* Q *satisfies* $\lambda_{max} \leq 2k\|D_{out}\mathbf{1}\|_\infty$, *where* D_{out} *is the out-degree matrix of Adj.*

6. $rank(Q) = n - 1$ *and* $\lambda_2 > 0$, *where* λ_2 *is the second smallest eigenvalue of* Q.

7. $\tilde{\mathcal{L}}AQ = \tilde{\mathcal{L}}$, *for any Laplacian matrix* $\tilde{\mathcal{L}}$

Proof:

1. Note that Adj has out-degree matrix

$$\begin{aligned} D_{\text{out}} &:= \text{diag}(\text{Adj } \mathbf{1}) = \text{diag}((A^{-1}\mathbf{1}\mathbf{1}^\top A^{-1})\mathbf{1}) \\ &= k^{-1}\text{diag}(A^{-1}\mathbf{1}) \\ &= k^{-1}A^{-1}. \end{aligned}$$

   Since the out-degree Laplacian of a graph with adjacency matrix Adj is defined as $\mathcal{L} := D_{out} - \text{Adj}$, [Bullo, Sec. 6.1], we get

$$\begin{aligned} \mathcal{L}_{\mathcal{G}_A} &= k^{-1}A^{-1} - A^{-1}\mathbf{1}\mathbf{1}^\top A^{-1} \\ &= k^{-1}(I - kA^{-1}\mathbf{1}\mathbf{1}^\top)A^{-1} \\ &= k^{-1}Q. \end{aligned}$$

2. Since $\text{Adj} = A^{-1}\mathbf{1}\mathbf{1}^\top A^{-1}$ is symmetric, then $\mathcal{L}_{\mathcal{G}_A}$, and therefore Q, are also symmetric. Equation (G.2) is obtained expanding $x^\top Qx$.

3. The first part follows directly by the fact that $\mathcal{L}\mathbf{1} = \mathbf{0}$ for any Laplacian matrix $\mathcal{L}$. The second part follows by the symmetry of Q.

4. The eigenvalues of Q different from 0 have strictly-positive real part. This follows by the fact that this property holds for any Laplacian matrix $\mathcal{L}_{\mathcal{G}_A}$.

5. Follows by the fact that the largest eigenvalue of $\mathcal{L}_{\mathcal{G}_A}$ is upper bounded by $\lambda_{max} \leq 2\|D_{out}\mathbf{1}\|_\infty$.

6. Follows by the fact that the graph of $\mathcal{L}_{\mathcal{G}_A}$ is connected and undirected, such that $\text{rank}(\mathcal{L}) = n - 1$. Since the rank of a matrix is invariant under scalar multiplication, we obtain the result for Q.

7. Expanding

$$\tilde{\mathcal{L}}AQ = k\tilde{\mathcal{L}}A(k^{-1}A^{-1} - A^{-1}\mathbf{1}\mathbf{1}^\top A^{-1}) \tag{G.5a}$$

$$= \tilde{\mathcal{L}} - k\tilde{\mathcal{L}}\mathbf{1}\mathbf{1}^\top A^{-1} \tag{G.5b}$$

where the last term is zero due to the fact that $\tilde{\mathcal{L}}\mathbf{1} = \mathbf{0}$. ■

Before presenting the proof of Lemma 3, we characterize the Oracle mapping $\mathcal{O}(\cdot)$ that maps tolls to Nash flows in fully utilized affine congestion games with a positive definite diagonal matrix A.

Lemma 18 *Under Assumption 15 the Oracle $\mathcal{O}(\cdot)$ satisfies*

$$x_f = \mathcal{O}(\tau) = -Q(b + \tau) + \frac{A^{-1}}{\mathbf{1}^\top A^{-1}\mathbf{1}}\mathbf{1}, \tag{G.6}$$

where Q is given by (G.1)*. Moreover, Q is positive semidefinite and $\mathcal{N}(Q) = span\{\mathbf{1}\}$.*

□

Proof: The fact that $\mathcal{N}(Q) = \mathbf{span}\{\mathbf{1}\}$ follows by items 3) and 6) in Lemma 17.

Now to obtain Q, note that any Nash flow $x_f \in \text{int}(\Delta)$ corresponds to the solution of the linear program (3.2) with equation (3.2a) replaced by equation (3.3), i.e.,

$$\left[\begin{array}{c|c} A & \mathbf{1} \\ \hline \mathbf{1}^\top & 0 \end{array}\right] \left[\begin{array}{c} x \\ \hline -\mu \end{array}\right] = - \left[\begin{array}{c} b+\tau \\ \hline -1 \end{array}\right]. \tag{G.7}$$

This system has a square matrix of the form $\left[\begin{array}{c|c} A & B^\top \\ \hline B & 0 \end{array}\right]$ which, provided A and $BA^{-1}B$ are invertible, has inverse of the form

$$\left[\begin{array}{c|c} A^{-1} - A^{-1}B^\top (BA^{-1}B)^{-1}BA^{-1} & A^{-1}B^\top (BA^{-1}B^\top)^{-1} \\ \hline (BA^{-1}B^\top)^{-1}BA^{-1} & -(BA^{-1}B^\top)^{-1} \end{array}\right]$$

Thus, solving for x we get

$$x_f(\tau) = -\left(I - \frac{A^{-1}\mathbf{1}\mathbf{1}^\top}{\mathbf{1}^\top A^{-1}\mathbf{1}}\right) A^{-1}(b+\tau) + \frac{A^{-1}}{\mathbf{1}^\top A^{-1}\mathbf{1}}\mathbf{1}. \tag{G.8}$$

which gives a closed expression for the Oracle mapping $x_f(\tau) = \mathcal{O}(\tau)$.

G.1 Proof of Lemma 3

For affine congestion games satisfying Assumption 15 the total welfare (3.4) in terms of the Nash flows x_f can be written as

$$W(x_f) = -(x_f^\top A x_f + b^\top x_f), \tag{G.9}$$

which for the case when x is a Nash flow x_f, can be written in terms of τ by means of the Oracle $\mathcal{O}(\cdot)$. In particular, using the chain rule we get

$$\nabla W(\tau)^\top = (2Ax_f(\tau) + b)^\top Q \tag{G.10}$$

and using the mapping $\tau \mapsto x_f(\tau)$ defined in (G.8), we obtain

$$\nabla W(\tau)^\top = \left(2A(-\left(I - \frac{A^{-1}\mathbf{1}\mathbf{1}^\top}{\mathbf{1}^\top A^{-1}\mathbf{1}}\right)A^{-1}(b+\tau)\right. \tag{G.11}$$

$$\left. + \frac{A^{-1}}{\mathbf{1}^\top A^{-1}\mathbf{1}}\mathbf{1}) + b\right)^\top Q. \tag{G.12}$$

Expanding terms we get

$$\nabla W(\tau)^\top = -2(b+\tau)^\top QAQ + 2\frac{\mathbf{1}A^{-1}AQ}{\mathbf{1}^\top A^{-1}\mathbf{1}} + b^\top Q - 2\tau^\top QAQ,$$

and using items 3) and 7) of Lemma 17, we get

$$\nabla W(\tau)^\top = (-b - 2\tau)^\top Q. \tag{G.13}$$

Thus the set of minimizers of $W(\tau)$ correspond to the points $\tau' \in \mathbb{R}^N$ satisfying $\nabla W(\tau) = 0$, i.e.,

$$\tau' \in \tau^* + \mathcal{N}(Q), \quad \text{where } \tau^* = -\frac{b}{2}. \tag{G.14}$$

Since by Lemma 18 we have that $\mathcal{N}(Q) = \text{span}\{\mathbf{1}\}$, we get that the set of optimal fixed tolls is

$$\mathcal{A} = \{\tau \in \mathbb{R}^N : \tau^* + \mu, \quad \mu \in \mathbb{R}\}. \tag{G.15}$$

This establishes the result. ■

The following Lemma recalls some stability properties of Laplacian flows.

Lemma 19 *Consider the Laplacian flow*

$$\dot{y} = -\mathcal{L}_{\mathcal{G}} y, \tag{G.16}$$

and suppose that $\mathcal{G}$ is strongly connected and weighted balanced. Then, we have that the set span$\{\mathbf{1}\}$ is GAS. ■

G.2 Proof of Lemma 4

From the proof of Lemma 3 and equation (G.10) we have that the gradient dynamics can be written as

$$\dot{\tau} = \nabla W(\tau) = -Q(Ax_f(\tau) + b + Ax_f(\tau)) \tag{G.17}$$

which by item 1) in Lemma 17, is of the form (3.13). Moreover, using equation (G.13) and item 1) in Lemma 17 we get the dynamics

$$\dot{\tau} = -k\mathcal{L}_A(b + 2\tau). \tag{G.18}$$

Equilibrium points of (G.18) are given by the set of points $\tau = -\frac{b}{2} + \mathcal{N}(\mathcal{L}_A)$. Since by item 1) in Lemma 17 the matrix $\mathcal{L}_A$ corresponds to the Laplacian matrix of a connected, undirected graph, we have that $\mathcal{N}(\mathcal{L}_A) = \text{span}\{1\}$, thus the set of equilibrium points of (G.18) corresponds to the set $\mathcal{A}$. Finally, consider the change of variable $\tilde{\tau} = \tau - \tau^*$,

where τ^* is defined in Lemma 3. The resulting system has dynamics

$$\dot{\tilde{\tau}} = -2k\mathcal{L}_A\tilde{\tau}. \tag{G.19}$$

The result of the lemma follows by Lemma 19.

G.3 Proof of Proposition 7:

Using the Oracle mapping $\mathcal{O}(\cdot)$ given by (G.8) we get the vector field of the learning dynamics in terms of $\tilde{\tau} = \tau - \tau^*$, i.e.,

$$\begin{aligned} x_f &= -\left(I - \frac{A^{-1}\mathbf{1}\mathbf{1}^\top}{\mathbf{1}^\top A^{-1}\mathbf{1}}-\right)A^{-1}(b+\tilde{\tau}+\tau^*) + \frac{A^{-1}}{\mathbf{1}^\top A^{-1}\mathbf{1}}\mathbf{1}. \\ &= -Q\tilde{\tau} - Qb - Q\tau^* + \frac{A^{-1}}{\mathbf{1}^\top A^{-1}\mathbf{1}}\mathbf{1} \end{aligned} \tag{G.20a}$$

Using the Oracle mapping (G.8) we get the learning dynamics in terms of $\tilde{\tau}$.

$$\begin{aligned} \dot{\tau} &= \mathcal{L}\left(2Ax_f + b\right) \\ &= \mathcal{L}\left(2A\left(-Q\tilde{\tau} - Qb - Q\tau^* + \frac{A^{-1}}{\mathbf{1}^\top A^{-1}\mathbf{1}}\mathbf{1}\right) + b\right) \\ &= -2\mathcal{L}AQ\tilde{\tau} - 2\mathcal{L}AQb - 2\mathcal{L}AQ\tau^* + 2\mathcal{L}A\frac{A^{-1}}{\mathbf{1}^\top A^{-1}\mathbf{1}}\mathbf{1} + \mathcal{L}b \\ &= -2\mathcal{L}\tilde{\tau} - 2\mathcal{L}b - 2\mathcal{L}\tau^* + \mathcal{L}b \\ &= -2\mathcal{L}\tilde{\tau} - \mathcal{L}b - 2\mathcal{L}\tau^* \end{aligned}$$

where in the last step we used facts 7) and 3) of Lemma 17. Since $\dot{\tau} = \dot{\tilde{\tau}}$, and using the definition of τ^* in 3, we get that

$$\dot{\tilde{\tau}} = -2\mathcal{L}\tilde{\tau} \tag{G.21a}$$

By Lemma 3 the set of optimal tolls is

$$\mathcal{A} = \{\tau \in \mathbb{R}^N : \tau = \tau^* + \mu \mathbf{1},\ \mu \in \mathbb{R}\}, \tag{G.21b}$$

which in the $\tilde{\tau}$-error space can be written as

$$\begin{aligned}\mathcal{A} &= \{\tilde{\tau} \in \mathbb{R}^N : \tilde{\tau} = \mu \mathbf{1},\ \mu \in \mathbb{R}\} \\ &= \{\tilde{\tau} \in \mathbb{R}^N : \tilde{\tau}_i = \tilde{\tau}_j,\ \forall\ (i,j) \in \{1,\dots,N\}\} \\ &= \text{span}\{\mathbf{1}\}. \end{aligned} \tag{G.21ca}$$

Based on this, the result of the proposition follows now by Lemma 19.

G.4 Proof of Proposition 8

The learning dynamics can be written as

$$\dot{\tau} = \mathcal{L}\left(c(x) + \nabla c(x) x\right) - 2\mathcal{L}z - 2\nabla J(\tau) \tag{G.4}$$

$$\dot{z} = \mathcal{L}\left(c(x) + \nabla c(x) x\right). \tag{G.5}$$

Using the transformation (G.20a) as in the proof of Theorem 7, we get the dynamics in terms of $\tilde{\tau}$

$$\dot{\tilde{\tau}} = -2\mathcal{L}\tilde{\tau} - 2\mathcal{L}z - 2\nabla J(\tilde{\tau} + \tau^*) \tag{G.6a}$$

$$\dot{z} = -2\mathcal{L}\tilde{\tau} \tag{G.6b}$$

and note that subject to $\mathcal{A}$ in (G.21b), $\tilde{\tau} = \mu \mathbf{1}$. Thus, using (3.17), converging to the optimal $\tilde{\tau}$ that maximizes J in the $\tilde{\tau}$-space is equivalent to converging to $\mu^\star$. Since

system (G.6) is just a time-scaled version of the saddle-point dynamics considered in [218]. Therefore, under Assumptions 16 and 15, by [218, Thm. 4.1]solutions of system G.6 remain bounded, with bound depending on the initial condition, and $\tilde{\tau}$ converges to the point that maximizes J, i.e., $\mu^\star$. In turn, using the fact that $\tilde{\tau} = \tau - \tau^*$ we obtain that $\tau \to \tau^\star$. ■

G.5 Proof of Proposition 9

We verify that all the Assumptions from [224, Thm. 1] are satisfied. In fact, by the linearity of the dynamics (3.22), and the regularity assumptions on the set-valued mapping F in (3.20a), Assumption 1 in [224] is satisfied. Also, since $\tau \mapsto \mathcal{O}(\tau)$ is single-valued and continuous, and $\mathcal{O}(\tau) \subset \Delta$ for all $\tau \in \mathbb{R}^N$, we have that the quasi-steady-state manifold is well posed and satisfies Assumption 2 of [224]. Next, since the "boundary layer dynamics" correspond in this case to the social dynamics (3.20), Assumption 18 implies that Assumption 3 in [224] is satisfied. Finally, note that the "reduced dynamics" associated to the interconnection of the learning dynamics and (3.20) corresponds to equation (3.22) with x replaced by the its equilibrium value, which according to Assumption 18 is generated by the mapping $\mathcal{O}(\cdot)$. Therefore, the reduced system is precisely the distributed welfare dynamics (3.15). By Proposition 7, this dynamics render the set $\mathcal{A}$ GAS. Moreover, for each $\gamma \in \mathbb{R}$ they also render the set $\mathbf{1}^\top \tau(0) = \gamma$ positively invariant. Therefore, constrained to the set K_ρ, they render the compact set $\mathcal{A} \cap K_\rho$ UGAS. Thus the reduced system satisfies Assumption 4 of [224]. Since all the assumptions required to apply [224, Thm. 1] are satisfied, we obtain convergence of complete solutions to the set $\{(\mathcal{A} \cap K_\rho) \times \Delta\} + \varepsilon\mathbb{B}$. Finally, by noting that the closed-loop system has no discrete-dynamics we can further use Assumption 18 to replace the set Δ by $\mathcal{O}(\mathcal{A})$. Since $\mathcal{A}$ is the set of optimal tolls, and the socially

optimal Nash flow x^* is unique, by definition of mapping $\mathcal{O}(\cdot)$ we get that $\mathcal{O}(\mathcal{A}) = x^*$.

G.6 Proof of Theorem 4

The proof of Theorem 4 is based on standard adaptive control arguments for model-free estimators, singular perturbation arguments for set-valued dynamical systems, and regularity properties of set-valued dynamical systems. Based on this we divide the proof on three steps:

Step 1: Let $\rho \in \mathbb{R}_{>0}$ and consider the dynamical system (3.30). Since by Assumption 17 the population state x satisfies $x(t) \in \Delta$ for all $t \geq 0$ and all $\tau_{\text{total}} \in \mathbb{R}^N$, we have that $x \in \mathcal{L}_\infty$, which by continuity of $\phi(\cdot)$ implies that $\phi \in \mathcal{L}_\infty$. Now consider the individual estimator given by (G.7), which in the error coordinates $\tilde{w}_i = \breve{w}_i - w_i^*$ is given by

$$\dot{\tilde{w}}_i = -\frac{\phi_i(x_i)}{\left(1 + \phi_i^\top(x_i)\phi_i(x_i)\right)^2}\phi_i(x)^\top \tilde{w}_i, \tag{G.7}$$

and the Lyapunov-like function $V_{\tilde{w}} = \frac{1}{2}\tilde{w}_i^\top \tilde{w}_i$. Taking the derivative of V along the trajectories of (G.7) we get

$$\dot{V}_{\tilde{w}} = -\tilde{w}_i^\top \left(\frac{\phi_i(x_i)}{\left(1 + \phi_i^\top(x_i)\phi_i(x_i)\right)^2}\phi_i(x)^\top \tilde{w}_i \right) \tag{G.8}$$

Defining $\bar{\phi}_i := \frac{\phi_i(x)}{(1+\phi_i^\top(x)\phi_i(x))}$ we get that

$$\dot{V}_{\tilde{w}} = -\tilde{w}_i^\top \left(\bar{\phi}_i(x_i)\bar{\phi}_i(x)^\top \right) \tilde{w}_i \tag{G.9}$$

And since $x \in \mathcal{L}_\infty$, under the PE assumption 20 we get by [1, Theorem 4.3.2], exponential convergence of $\tilde{w}_i$ to zero, i.e, $\breve{w}_i \to w_i^*$ for all $i \in \{1, \ldots, N\}$.

Step 2: The "boundary layer" dynamics obtained when $\alpha = 0$ are now given by

$$\begin{aligned}
&\dot{\mu} \in \Psi(\mu) \\
&\dot{\tau} = 0 \\
&\dot{x} \in F(x, \tau_{\text{total}}) \\
&\dot{\breve{w}}_i = -\frac{\phi_i(x_i)}{\left(1 + \phi_i^\top(x_i)\phi_i(x_i)\right)^2}\phi_i(x)^\top \tilde{w}_i, \ \forall\ i \in \{1, \dots, N\}
\end{aligned}$$

with states evolving on the sets

$$(\mu, x, \tau, \breve{w}) \in \Lambda \times \Delta \times K_\rho \times \mathbb{R}^{Nm}. \tag{G.11}$$

and by Step 1 and Assumption 18, system (G.10) renders the set $\mathcal{A}_{\mu,i} \times K_\rho \times M_{K'} \times \{w^*\}$ UGAS, where $K' := \{z : z = \tau + \text{diag}(a) \cdot h_\mu(\mu), \tau \in K_\rho, \mu \in \Lambda\}$.

Step 3: The "reduced system" constrained to K_ρ is given by the toll dynamics evaluated at the steady-state of x and $\breve{w}$, are given by:

$$\dot{\tau} = \alpha \cdot \mathcal{L} \cdot \Big(c(x_s) + (w^*)^\top \phi(x_s) x_s, \breve{w})\Big), \tag{G.12}$$

with $x_s \in \{\tau + \text{diag}(a) \cdot \mu : \mu \in \Lambda\}$. Since $h_1^x(\cdot)$, $h_2^x(\cdot)$, $h_3^x(\cdot)$, and $h_\mu(\cdot)$ are continuous, and μ is uniformly bounded, for each $\delta > 0$ there exists an $a^{**} > 0$ such that for all $a \in (0, a^{**}]$

$$\begin{aligned}
&\mathcal{L}\Big(h_{2,s}^x(x_s) + h_{3,s}^x(x_s) h_{1,s}^x(x_s)\Big) \\
&\qquad \subset \mathcal{L}\Big(h_2^x(x_f) + h_3^x(x_f) h_1^x(x_f)\Big) + \delta\mathbb{B} \\
&\qquad = \mathcal{L}\Big(c(x_f(\tau)) + \nabla c(x_f(\tau)) x_f(\tau)\Big) + \delta\mathbb{B}
\end{aligned} \tag{G.13}$$

Thus, constrained to K_ρ, and with $a \in (0, \min\{a^*, a^{**}\})$, where a^* comes from the PE assumption, solutions of the reduced system (G.12) are also solutions of the differential inclusion

$$\dot{\tau} \in \mathcal{L}\Big(c(x_f(\tau)) + \nabla c(x_f(\tau))x_f(\tau)\Big) + \delta\mathbb{B} \tag{G.14}$$

Equation (G.13) corresponds to a δ-perturbed version of the distributed welfare gradient dynamics, which by the result of Proposition 7 render the set $\mathcal{A} \cap K_\rho$ UGAS when the trajectories of τ are constrained to K_ρ. Since equation G.14 with $\delta = 0$ is just a linear ODE, by standard robustness results with respect to compact attractors for systems with a continuous right hand side, e.g., [250], we obtain that for each $\varepsilon \in \mathbb{R}_{>0}$ there exists a $\delta^* \in \mathbb{R}_{>0}$ and a compact set $\mathcal{A}_\varepsilon \subset \mathbb{R}^N$ that is ε-close to $\mathcal{A}$, such that for all $\delta \in (0, \delta^*]$ it is UGAS under the dynamics (G.14), with solutions constrained to K_ρ. Since every solution of (G.12) is also a solution of (G.14), we get that the set $\mathcal{A}_\varepsilon$ is also UGAS for the reduced dynamics (G.12) with trajectories constrained to K_ρ.

The proof finishes by noting that all assumptions from [224, Theorem 1] are satisfied, and since there are no discrete-time dynamics in the closed-loop system, all complete solutions $(\mu, \tau, x, \breve{w})$ converge uniformly to a ε-neighborhood of the set

$$\mathcal{A}_{\text{closed-loop}} = \mathcal{A}_\mu \times (\mathcal{A} \cap K_\rho) \times \mathcal{O}(\mathcal{A} \cap K_\rho) \times \{w^*\} \tag{G.15}$$

$$= \mathcal{A}_\mu \times (\mathcal{A} \cap K_\rho) \times \{x^*\} \times \{w^*\}. \tag{G.16}$$

■

Appendix H

Proofs of Chapter 4

In this section, we present the proof of Chapter 4.

Proof of Lemma 5: By the construction of (4.7) we have that if $\tau(0,0) = \gamma(0,0) = 0$, then a solution $x_{s,u}$ of (4.6) can generate an event at a time $(t,j) \in \text{dom}(x_{s,u})$ only if: 1) $x_{s,u}$ generated sub-events in each of its previous γ^* jumps, a condition that is necessary in order to have at least $\gamma = r_e$, and 2) $x_{s,u}$ is also generating a sub-event at the time (t,j). Since this implies that the condition $\xi \in S$ was verified at the end times of the last $(\gamma^* + 1)$ consecutive intervals of flow, each flow having a duration of ΔT seconds, and using the definition of the sets D_e and D_{se} we obtain equality (4.10), which in turn implies that $t^* \geq (\gamma^* + 1)\Delta T$ and $j^* \geq \gamma^*$. ■

Proof of Lemma 6: Completness follows by the absence of finite escape times in (4.1), and the construction of the jump map (4.7d). The second part of the lemma follows by the fact that if $\xi(t,j) \in \text{int}(S)$ for all $(t,j) \in \text{dom}(x_{s,u})$ such that $t+j > T_{\epsilon,K}$, then for all $t + j > T_{\epsilon,K} + (\gamma^* + 2)\Delta T + \gamma^* + 1 =: T^*$, γ will satisfy $\gamma \in (r_e, 1]$ every time that $x_{s,u} \in D_s \times K_u$. ■

H.1 Proof of Proposition 10

To prove Proposition 10 we first generate the following lemma.

Lemma 20 *Suppose that Assumption 21 holds. For each compact set $K \subset \mathbb{R}^{n+p}$ and each $\delta > 0$, there exists an $\epsilon \in \mathbb{R}_{>0}$ such that $|\nabla\varphi(\theta)^\top \zeta| \leq \epsilon \Rightarrow \ (\theta, u) \in Z + \delta\mathbb{B}$, for all $(\theta, u) \in K$ and all $\zeta \in P(\theta, u)$.* ■

Proof: We prove the Lemma for the case that $Z \cap K \neq \emptyset$ since otherwise the result is trivial. Suppose the statement of Lemma 20 is false. Then there exists a compact set $K \subset \mathbb{R}^{n+p}$ satisfying $K \cap Z \neq \emptyset$, and a $\delta > 0$ such that for each $i \in \mathbb{Z}_{\geq 0}$ there exists $(\theta_i, u_i) \in K$ and $\xi_i \in P(\theta_i, u_i)$ such that:

$$|\nabla\varphi(\theta_i)^\top \zeta_i| \leq \frac{1}{i+1} \quad \text{and} \quad (\theta_i, u_i) \notin Z + \delta\mathbb{B}. \tag{H.1}$$

Since $(\theta_i, u_i) \in K$ for all $i \in \mathbb{Z}_{\geq 0}$, there exists a convergent subsequence (not relabeled) satisfying $(\theta_i, u_i) \to (\theta^*, u^*) \in K$. Thus, $\exists\ M > 0$ such that $|\theta_i| \leq M$ and $|u_i| \leq M$ for all $i \in \mathbb{Z}_{>0}$. By LB of $P(\cdot, \cdot)$ we have that the sequence $\xi_i \in P(\theta_i, u_i)$ satisfies $|\xi_i| < M'$ for all $i \in \mathbb{Z}_{>0}$ and for some $M' > 0$, which implies the existence of a convergent subsequence (not relabeled) $\xi_i \to \xi^*$. Using OSC of $P(\cdot, \cdot)$ we have that $\xi^* \in P(\theta^*, u^*)$. Since (H.1) implies that $0 \leq |\nabla\varphi(\theta_i)^\top \zeta_i| \leq \frac{1}{i+1}$, we get $\lim_{i\to\infty} |\nabla\varphi(\theta_i)^\top \zeta_i| = 0$. By continuity of the absolute value and inner product we get $\lim_{i\to\infty} |\nabla\varphi(\theta_i)^\top \zeta_i| = |\nabla\varphi(\theta^*)^\top \zeta^*|$. Therefore $(\theta^*, u^*) \in Z$, and since $(\theta_i, u_i) \to (\theta^*, u^*)$ as $i \to \infty$, there exists $i^* \in \mathbb{Z}_{\geq 0}$ such that $(\theta_i, u_i) \in Z + \delta\mathbb{B}$ for all $i \geq i^*$, which contradicts (H.1). ■

Proof of Proposition 10: By Assumption 22 and [78, Lemma 7.8] the reachable set from K_0 in infinite time, denoted $\mathcal{R}(K_0)$, is compact. Using $\mathcal{R}(K_0)$ and δ let Lemma 20 generate ϵ. Then, since $(\theta^\top, u^\top)^\top(t) \in \mathcal{R}(K_0)$ for all $t \geq 0$, and $\dot{\theta}(t) \in F(\theta(t), u(t))$

for almost all $t \geq 0$, we have that for any $T \geq 0$ and almost all $t \geq T$

$$|\nabla\varphi(\theta(t))^\top \dot{\theta}(t)| \leq \epsilon \;\Rightarrow\; (\theta^\top, u^\top)^\top(t) \in Z + \delta\mathbb{B}, \tag{H.2}$$

but since $\theta(\cdot)$ and $u(\cdot)$ are continuous functions, and $Z + \delta\mathbb{B}$ is a closed set, we have that the right hand side of (H.2) must hold for all $t \geq T$. Indeed, for any $T > 0$ suppose that there exists a $t^* \geq T$ in a set of measure zero such that $(\theta^\top, u^\top)(t^*) \in \mathbb{R}^{n+p}\backslash(Z + \delta\mathbb{B})$. But since $\mathbb{R}^{n+p}\backslash(Z + \delta\mathbb{B})$ is an open set, there exists a $\nu > 0$ such that $(\theta^\top, u^\top)(t) \in \mathbb{R}^{n+p}\backslash(Z + \delta\mathbb{B})$ for all $t \in t^* + \nu\mathbb{B}^\circ$, which contradicts the assumption that the set where t^* belongs is of measure zero. ■

H.2 Proof of Proposition 11

We first show that for systems of the form (4.1), under Assumptions 21-23, the limit $|\dot{y}(t)| \xrightarrow[t\to\infty]{} 0^+$ is well-defined.

Lemma 21 *Consider system* (4.1) *with restricted flow set* $\mathbb{R}^p \times (\mathbb{U} \cap \rho\mathbb{B})$. *Suppose that Assumptions 21-23 hold. Then, for each pair* $(\epsilon, \rho) \in \mathbb{R}^2_{>0}$ *and each compact set* $K_\theta \subset \mathbb{R}^p$ *there exists a* $t^* \in \mathbb{R}_{>0}$ *such that if* $(\theta^\top, u^\top)^\top(0) \in K_\theta \times (\mathbb{U} \cap \rho\mathbb{B})$ *then* $\dot{y}(t) \in \epsilon\mathbb{B}$ *for almost all* $t \geq t^*$. ■

Proof: By the chain rule we have that $|\dot{y}(t)| = |\nabla\varphi(\theta(t))^\top \dot{\theta}(t)|$, where $\dot{\theta}(t) \in P(\theta(t), u(t))$ for almost all $t \geq 0$. Using Holder's inequality we obtain that $|\dot{y}|$ satisfies $|\dot{y}(t)| \leq \|\nabla\varphi(\theta(t))\|\|\dot{\theta}(t)\|$ for all $\dot{\theta}(t) \in P(\theta(t), u(t))$ and almost all $t \geq 0$. By the UGAS property of M_ρ there exists $M > 0$ such that $\theta(t) \in M\mathbb{B}$ for all $t \geq 0$, which by continuity of $\nabla\varphi(\cdot)$ implies that $\|\nabla\varphi(\theta(t))\| \leq M'$ for all $t \geq 0$ and for some $M' > 0$. Moreover, since P is OSC and LB it is also upper semicontinuous [78, Lemma 5.15], which implies the existence of an $\epsilon_2 \in \mathbb{R}_{>0}$ such that $P(H(\rho\mathbb{B} \cap \mathbb{U}) + \epsilon_2\mathbb{B}, \rho\mathbb{B} \cap \mathbb{U}) \subset$

$P(H(\rho\mathbb{B}\cap\mathbb{U}),\rho\mathbb{B}\cap\mathbb{U})+\frac{\epsilon}{M'}\mathbb{B}=\frac{\epsilon}{M'}\mathbb{B}$. Using again UGAS of M_ρ we obtain the existence of a time $t^*>0$ such that $\theta(t)\in H(\rho\mathbb{B}\cap\mathbb{U})+\epsilon_2\mathbb{B}$ for all $t\geq t^*$, which implies that $|\dot{y}(t)|\leq\epsilon$ for almost all $t\geq t^*$. ■

Proof of Proposition 11 Let $(\tilde{e},\rho)\in\mathbb{R}^2_{>0}$, K_0, and K and $r_e\in(0,1)$ be given. We start by proving the second part of the proposition. Let Proposition 10 generate ϵ, and let $\eta\in(0,\epsilon/2)$. Let Assumption 28 generate the triple $(\Delta T,\gamma^*,f_e)$. Define $\bar{\varepsilon}:=\epsilon-\eta$, and let $\varepsilon\in(0,\bar{\varepsilon}]$. By the structure of the set K_0, the HDS (4.6), and the discussion in Section 4.2.1, the condition $x_{s,u}(\ell,\jmath)\in D_e\times\mathbb{U}$ necessarily implies that the condition $\xi\in S$, i.e., $f_e(\xi)\leq\varepsilon$, was verified γ^*+1 times up to the continuous time ℓ, each verification separated by a flow of ΔT seconds, since otherwise γ would have been reset to 0. During the last γ^*-m+1 verifications the state ξ will have the structure (4.15), and by Item (a) in Assumption 28 we conclude that $\left|\dot{y}(\bar{t},j)|-f_e(\xi(\bar{t},j))\right|\leq\eta$ for all $\bar{t}\in\mathrm{dom}_t(x_{s,u})$ such that $\bar{t}=\sup I^j$ for each $I^j:=\{t:(t,j)\in\mathrm{dom}(x_{s,u})\}$ with $j\in\{\jmath,\jmath-1\ldots,\jmath-(\gamma^*-m)\}$, which correspond to the last γ^*-m+1 nonempty intervals of flow of the solution. Using the reverse triangle inequality we have that $|\dot{y}(t,j)|-|f_e(\xi(t))|\leq|\dot{y}(t,j)-f_e(\xi(t))|$, which implies $|\dot{y}(t,j)|\leq\eta+\varepsilon\leq\epsilon$ for a sequence of uniformly sampled (γ^*-m+1) points in time, with sampling period of ΔT. By Item (b) in Assumption 28 this implies that $|\dot{y}(t,j)|\leq\epsilon$, for almost all $t\geq\ell-(\gamma^*-m)\Delta T$. Then, item 2) of the proposition follows directly by the positive invariance of the set $[0,1]$ for the dynamics of τ and γ, by Proposition 10, and by noting that during the last γ^*-m jumps each entry of the state ξ was updated with a measurement of y, and since $\gamma^*-m\geq m$ we have that every entry ξ_i of ξ corresponded to a measurements of $y(t,j)$ after the time $\ell-(\gamma^*-m)\Delta T$.

To prove the first part of the proposition define $\underline{\varepsilon}:=\eta$, and let $\varepsilon\in(\underline{\varepsilon},\bar{\varepsilon}]$. Note that by Assumption 22 the state θ converges uniformly to the set $H(\mathbb{U}\cap\rho\mathbb{B})$. Let $\epsilon_2\in(0,\varepsilon-\eta)$. Then, by Lemma 21 there exists a $T_2>0$ such that for all $x_{su}\in\mathcal{S}_{\mathcal{H}_s}(K)$

and almost all $(t,j) \in \mathrm{dom}(x_{su})$ satisfying $t+j \geq T_2$ the inequality $|\dot{y}(t,j)| \leq \epsilon_2$ holds. Then, after at must m jumps separated by $(\Delta T - 1)$ intervals of flow, the state ξ will have the structure of (4.15), and by Item (a) in Assumption 28, we have that for almost all $t+j \geq T_2 + m + \Delta T(m-1)$ the bound $\left| f_e(\xi(t,j)) - |\dot{y}(t,j)| \right| \leq \eta$ holds. Using again the reverse triangle inequality we obtain that $f_e(\xi(t,j)) \leq \eta + \epsilon_2 < \varepsilon$. ■

H.3 Preliminaries of Proofs of Theorems 1 and 2

Throughout this and the next section, given two sets A and B we use $A \oplus B := \{a+b : a \in A, b \in B\}$ to represent their Minkowski sum, and given two nonnegative scalars $s_2 \geq s_1$ we define $A + [s_1, s_2]B := \bigcup_{s \in [s_1, s_2]} (A \oplus sB)$.

The following Lemma, corresponding to [78, Corollary 7.7 and Lemma 7.12], gives sufficient conditions for ULAS of $\Omega_{\mathcal{H}}$-limit sets.

Lemma 22 *Suppose that a HDS satisfies (C1)-(C3). Let $K \subset \mathbb{R}^n$ be compact, and suppose that there exists a $\rho \in \mathbb{R}_{>0}$, such that every solution $x \in \mathcal{S}_{\mathcal{H}}(K)$ satisfies $x(t,j) \in \rho\mathbb{B}$ for all $(t,j) \in dom(x)$. Suppose also that $\Omega_{\mathcal{H}}(K)$ is nonempty and satisfies $\Omega_{\mathcal{H}}(K) \subset int(K)$. Then, $\Omega_{\mathcal{H}}(K)$ is ULAS with basin of attraction containing K.* ■

The next proposition follows by [78, Lemma 7.20].

Proposition 15 *Let $(G_\delta^T, D_{\hat{u},\hat{z}})$ be a TODS with respect to $(J, \hat{\mathbb{U}})$. Then, for each $\epsilon \in \mathbb{R}_{>0}$ and each compact $K \subset \mathbb{R}^{n+r}$ satisfying $\mathcal{A}_{\hat{u},\hat{z}} + \epsilon\mathbb{B} \subset int(K)$, there exists $\delta^* \in (0,1)$ such that for each $\delta \in (0, \delta^*]$ there exists $\rho^* \in (0,1)$ such that for all $\rho \in (0, \rho^*]$ there exists $(M, j^*) \in \mathbb{R}^2_{>0}$ such that every complete solution of the ρ-perturbation (4.30) of $(G_\delta^T, D_{\hat{u},\hat{z}})$, with initial condition in K, satisfies $\hat{x}_{u,z}(j) \in M\mathbb{B}$ for all $j \geq 0$, and $\hat{x}_{u,z}(j) \in \mathcal{A}_{\hat{u},\hat{z}} + \epsilon\mathbb{B}$, for all $j \geq j^*$.* ■

H.4 Proof of Theorem 5

The following claim is a direct consequence of the continuity of $J(\cdot)$ and $d_q(\cdot)$, and the LB property of G^L_δ.

Claim 1 *Let $K_{\hat{u},\hat{z}} := K_{\hat{u}} \times K_{\hat{z}} \subset \mathbb{R}^{n+r}$, and $K_{\hat{y}} \subset \mathbb{R}$ be compact. Define $K_J := \bigcup_{q\in Q} J\left(K_{\hat{u}} + [0,1]d_q(K_{\hat{z}})\right) + [0,1]\mathbb{B}$. Then, there exists a positive $M_0 \in \mathbb{R}_{>0}$ such that $\bigcup_{\delta\in[0,1]} G^L_\delta(K_{\hat{u},\hat{z}}, (K_{\hat{y}} \cup K_J)^\sigma \times K_J) \cup K_{\hat{u},\hat{z}} \subset M_0\mathbb{B}$.* ■

The proof of Theorem 5 follows three steps:

1) *Uniform convergence of $\hat{x}_{u,z}$ when $\tilde{e} = 0$:* Set $\tilde{e} = 0$, and let $\epsilon \in \mathbb{R}_{>0}$, $K_{\hat{x}_u} := K_{\hat{u},\hat{z}} \times K_u \times K_{\hat{y}} \subset \mathbb{R}^{2n+r+\sigma}$ and $K_q \subset \mathbb{R}$ be such that $(\mathcal{A}_{\hat{x}_u} \times Q) + \nu\mathbb{B} \subset \text{int}(K_{\hat{x}_u} \times K_q)$. Let Assumptions 29 and 30 generate the TODS $(G^T_\delta, D_{u,z})$ and the functions $d_q(\cdot)$. Let Claim 1 generate M_0. Using M_0 and ϵ let Proposition 15 generate $\delta' \in (0,1)$, and $\rho' \in (0,1)$ for each $\delta \in (0,\delta')$. Let $\rho \in (0,\rho')$. Using this δ and ρ let Assumption 30 generate $a' \in (0,1)$, and choose $a \in (0,a')$. Then, by the structure of the jump map, for each complete solution x_u of (4.20) with initial conditions in $K_{\hat{x}_u} \times K_q$ there exists a $j_{q_0} \in \mathbb{R}_{>0}$ satisfying $j_{q_0} \leq 2\bar{q} + 1$, such that: $q(j_{q_0}) = \underline{q}$, the state $\hat{y}$ and the output y are given by (4.26), and the state $\hat{x}_{u,z}$ has been updated at most once according to the mapping G^L_δ. By the construction of the sets in Claim 1 we have that $\hat{x}_{u,z}(j_{q_0}) \in M_0\mathbb{B}$. Finally, note that for all $j \geq j_{q_0}$, whenever $q(j) = \underline{q}$ the state $\hat{y}$ and the output y will always have the structure of (4.26), which by Assumption 30 implies that the solutions generated by the learning dynamics G^L_δ will also be solutions of the ρ-inflation $G^T_\delta(\hat{x}_{u,z} + \rho\mathbb{B}) + \rho\mathbb{B}$. Since $\hat{x}_{u,z}(j_{q_0}) \in M_0\mathbb{B}$ and $\hat{x}_{u,z}$ is kept constant whenever $q \neq \underline{q}$, we have that by the selection of the constants (δ, a), and for $\rho \in \mathbb{R}_{>0}$ sufficiently small, the state $\hat{x}_{u,z}$ retains the boundedness and convergence properties of the ρ-perturbed TODS, which by Proposition 15 implies the existence of a $j^* \in \mathbb{R}_{>0}$ such that $\hat{x}_{u,z}(j) \in \mathcal{A}_{\hat{u},\hat{z}} + \epsilon\mathbb{B}$ for all $j \geq j^*$.

2) *Omega-limit set for the learning dynamics:* Let $\nu \in \mathbb{R}_{>0}$ and the compact sets $K_{\hat{x}_u} := K_{\hat{u},\hat{z}} \times K_u \times K_{\hat{y}} \subset \mathbb{R}^{2n+r+\sigma}$, and $K_q \subset \mathbb{R}$ be such that $(\mathcal{A}_{\hat{x}_u} \times Q) + \nu\mathbb{B} \subset \text{int}(K_{\hat{x}_u} \times K_q)$. Let $\tilde{\nu} \in (0, \nu/2)$. By continuity of $J(\cdot)^\sigma$ and compactness of $\mathcal{A}_u$ there exists a $\delta_3 > 0$ such that $J(\mathcal{A}_u + \delta_3\mathbb{B})^\sigma \subset J(\mathcal{A}_u)^\sigma + \tilde{\nu}\mathbb{B} \subset \text{int}(K_{\hat{y}})$. Let $\delta_1, \delta_2 \in (0, \tilde{\nu})$. By the assumption on $K_{\hat{x}_u}$ it follows that $\mathcal{A}_{\hat{u},\hat{z}} + \delta_1\mathbb{B} \subset \text{int}(K_{\hat{u},\hat{z}})$, and $\mathcal{A}_u + \delta_2\mathbb{B} \subset \text{int}(K_u)$. By the previous discussion in numeral 2), for each $\epsilon < \tilde{\nu}$ there exists a $\underline{\delta}^*$, such that for each $\delta \in (0, \underline{\delta}^*)$ there exists a $\underline{\rho}^*$ such that for each $\underline{\rho} \in (0, \underline{\rho})^*$ there exists an $\underline{a}^*$ such that for each $\underline{a} \in (0, \underline{a}^*)$ the component $\hat{x}_{u,z}$ of every complete solution of (4.20) with initial conditions in $K_{\hat{x}_u} \times K_q$ will satisfy $\hat{x}_{u,z}(j) \in \mathcal{A}_{\hat{u},\hat{z}} + \epsilon\mathbb{B} \subset \mathcal{A}_{\hat{u},\hat{z}} + \tilde{\nu}\mathbb{B} \subset \text{int}(K_{\hat{u},\hat{z}})$ for all $j \geq j^*$, for some $j \in \mathbb{Z}_{\geq 2\kappa+2}$. Choose ϵ and its generated $\underline{a}^*$ sufficiently small, such that $\epsilon < \delta_1$ and $\epsilon + \underline{a}^* < \min\{\delta_3, \delta_2\}$. Since by construction of the dynamics of u we have that $u(j) \in \hat{u}(j) + a\mathbb{B}$ for all $j \geq 2$, and $a < \underline{a}^*$, the previous item also implies that $u(j) \in \mathcal{A}_u + (\epsilon + \underline{a}^*)\mathbb{B}$ for all $j \geq j^*$. Since $\epsilon + \underline{a}^* < \delta_2$ we have that $u(j) \in \mathcal{A}_u + \tilde{\nu}\mathbb{B} \subset \text{int}(K_u)$ for all $j \geq j^*$. Since the state $\hat{y}(j)$ corresponds to a vector of measurements of $J(\cdot)$ evaluated at $u(j)$, the previous item implies that $\hat{y}_i(j) \in J(\mathcal{A}_u + (\epsilon + \underline{a}^*)\mathbb{B})$, for all $i \in \{\underline{q}, \ldots, \bar{q} - 1\}$, and for all $j \geq j^*$. Since $\epsilon + \underline{a}^* < \delta_3$ we have that $\hat{y}(j) \in J(\mathcal{A}_u + (\underline{a}^* + \epsilon)\mathbb{B})^\sigma \subset J(\mathcal{A}_u)^\sigma + \tilde{\nu}\mathbb{B} \subset \text{int}(K_{\hat{y}})$ for all $j \geq j^*$. From the previous arguments, and the fact that $Q \subset \text{int}(K_q)$, we have that every solution of (4.20) with initial conditions in $K_{\hat{x}_u} \times K_q$ will satisfy $x_u(j) \in (\mathcal{A}_{\hat{u},\hat{z}} + \tilde{\nu}\mathbb{B}) \times (\mathcal{A}_u + \tilde{\nu}\mathbb{B}) \times (J(\mathcal{A}_u)^\sigma + \tilde{\nu}\mathbb{B}) \times Q \subset (\mathcal{A}_{\hat{x}_u} \times Q) + \frac{\nu}{2}\mathbb{B}$. This fact, together with Definition of Omega limit sets in the Appendix, implies that $\Omega_{u,q}(K_{\hat{x}_u} \times K_q) \subset (\mathcal{A}_{\hat{x}_u} \times Q) + \frac{\nu}{2}\mathbb{B}$, which by Lemma 22 implies ULAS of $\Omega_{u,q}(K_{\hat{x}_u} \times K_q)$, with basin of attraction $\mathcal{B}_{\Omega_{u,q}}$ containing the set $K_{\hat{x}_u} \times K_q$.

3) *Robustness with respect to $\tilde{e}$:* Finally, note that under the given assumptions, system (5) is well-posed. Therefore, since $\Omega_{u,q}(K_{\hat{x}_u} \times K_q)$ is ULAS when $y = J(u)$, it is SGP-AS (w.r.t. $\mathcal{B}_{\Omega_{u,q}}$) as $\tilde{e} \to 0^+$ when $y \in J(u) + \tilde{e}\mathbb{B}$. This implies that

for any $\nu \in (0, \frac{\nu}{2})$ and for the same compact set of initial conditions and constants (δ, a), there exists an $\tilde{e}^* \in (0,1)$ such that for all $\tilde{e} \in (0, \tilde{e}^*)$ convergence of $\hat{x}_{u,q}$ to $\Omega_{u,q}(K_{\hat{x}_u} \times K_q) + \frac{\nu}{2} \subset (\mathcal{A}_{\hat{x}_u} \times Q) + \nu\mathbb{B}$ is achieved in finite time. Using Lemma 22 we obtain the stability result. ■

H.5 Preliminary results for the proof of Theorem 6

To prove Theorem 6 we first generate the following lemma, which follows by Assumption 29, and Lemma 7.

Lemma 23 *Let $\nu \in \mathbb{R}_{>0}$, and $K \subset \mathbb{R}^{N_s+N_u}$ be a compact set satisfying $\mathcal{A} + \nu\mathbb{B} \subset int(K)$. Suppose that Assumptions 21, 22, and 29 hold. Then, for any $(\varepsilon, \Delta T, \gamma^*) \in \mathbb{R}_{>0} \times \mathbb{R}_{>0} \times \mathbb{Z}_{\geq 2m}$, any $(a, \delta, r_e) \in (0,1)^3$, any nonnegative continuous function $f_e : \mathbb{R}^m \to \mathbb{R}_{\geq 0}$, and any initial condition $x(0,0) \in K$, there exists at least one complete solution for the HDS (4.12) using z, S, and G_ξ as in (4.16) and (4.17), respectively.* ■

The following lemma is just a re-statement of the stability property induced by Assumption 22, the continuity of $\varphi(\cdot)$, and the upper semicontinuity of $H(\cdot)$.

Lemma 24 *Let $\nu \in \mathbb{R}_{>0}$ and consider system (4.1) under Assumption 22. Then, for each $\delta_2 \in (0, \nu)$ there exists $\delta_1 \in (0, \delta_2)$ such that if $(\theta, u)(0) \in (H(\mathcal{A}_u) \times \mathcal{A}_u) + \delta_1\mathbb{B}$, then $(\theta, y)(t) \in \big(H(\mathcal{A}_u) \times \varphi(H(\mathcal{A}_u))\big) + \delta_2\mathbb{B}$, for all $t \geq 0$.* ■

The following proposition establishes a uniform convergence result for the control state x_u.

Proposition 16 *Let $\nu \in \mathbb{R}_{>0}$ and a compact set $K \in \mathbb{R}^{N_s+N_u}$ be given, and suppose that $\mathcal{A} + \nu\mathbb{B} \subset int(K)$. Let $\epsilon \in (0, \frac{\nu}{2})$. Suppose that Assumptions 21-25 and 28-30 hold Then, there exists $M \in \mathbb{R}_{>0}$, and $\delta^* \in \mathbb{R}_{>0}$ such that for each $\delta \in (0, \delta^*]$ there exists $a^* \in \mathbb{R}_{>0}$ such that for each $a \in (0, a^*)$ there exists $\tilde{e}^* \in \mathbb{R}_{>0}$ such that for each $\tilde{e} \in (0, \tilde{e}^*]$ there exists data $(\Delta T, \gamma^*, f_{ssi})$, and a pair $(\underline{\varepsilon}, \overline{\varepsilon}) \in \mathbb{R}^2_{>0}$ such that for each $\varepsilon \in (\underline{\varepsilon}, \overline{\varepsilon}]$ there exists a $T^* \in \mathbb{R}_{>0}$ such that each complete solution $x \in \mathcal{S}_{\tilde{\mathcal{H}}}(K)$ satisfies $x(t,j) \in ([0,1] \times [0,1] \times \mathbb{R}^m \times \mathbb{R}^p \times (\mathcal{A}_{x_u} + \epsilon\mathbb{B}) \times Q) \cap M\mathbb{B}$ for all $(t,j) \in dom(x)$ such that $t + j \geq T^*$.* ■

Proof of Proposition 16: The proof of Proposition 16 is based on Lemmas 25-27, given below, and the following construction: Let $K := K_\tau \times K_\gamma \times K_\xi \times K_\theta \times K_{u,z} \times K_u \times K_{\hat{y}} \times K_q \subset \mathbb{R}^{N_s+N_u}$ and ϵ be given. Let $\epsilon_1 \in (0, \epsilon)$, $k_{\theta,u} \in \mathbb{R}_{>0}$ such that $K_\theta \subset k_{\theta,u}\mathbb{B}$ and $H(K_u) \subset k_{\theta,u}\mathbb{B}$, and consider the sets

$$
\begin{aligned}
K'_\theta &:= [H(K_u) + \beta_\theta(2k_{\theta,u}, 0)\,\mathbb{B}] \cup K_\theta, \\
K'_y &:= \varphi(K'_\theta), \quad K'_\xi := (K'_y)^m \cup K_\xi, && \text{(H.3a)} \\
K'_{\hat{y}} &:= \{\zeta \in \mathbb{R}^{\bar{q}} : \zeta_{\bar{q}} \in K'_y \cup K'_J,\ \zeta_i \in K_{\hat{y}},\ i \neq \bar{q}\} && \text{(H.3b)} \\
K'_{u,z} &:= \left[\bigcup_{\delta \in [0,1]} G^L_\delta\left(K_{u,z}, K'_{\hat{y}} \times (K'_y \cup K'_J)\right)\right] \cup K_{u,z} \\
K'_{\hat{u}} &:= \{u \in \mathbb{R}^n : (u,z) \in K'_{u,z}\},\ K'_u := K'_{\hat{u}} + 1\mathbb{B}. \\
\overline{K}_\theta &:= H(K'_u + 1\mathbb{B}) + \beta_\theta\left(2M_{K'_{u\rho\mathbb{B}}}, 0\right)\mathbb{B}, \\
\overline{K}_y &:= \varphi(\overline{K}_\theta), \quad \overline{K}_\xi := (\overline{K}_y)^m \cup K'_\xi, && \text{(H.3c)} \\
\overline{K}_{\hat{y}} &:= \{\zeta \in \mathbb{R}^\sigma : \zeta_{\bar{q}} \in \overline{K}_y \cup \overline{K}_J,\ \zeta_i \in \overline{K}_{\hat{y}},\ i \neq \bar{q}\} && \text{(H.3d)}
\end{aligned}
$$

where $\beta_\theta(\cdot,\cdot)$ is a $\mathcal{KL}$ function given by the UGAS Assumption 22, K'_J in (H.3b) is defined as in Claim 1, $M_{K'_{u\mathbb{B}}} \in \mathbb{R}_{>0}$ is chosen sufficiently large to satisfy $K'_\theta \cup$

$(H(K'_u) + 1\mathbb{B}) \subset M_{K'_{u\mathbb{B}}}\mathbb{B}$, and $\overline{K}_J$ in (H.3d) is defined as in Claim 1 using (K'_u, K'_z) instead of (K_u, K_z). Let $K^0_u := K'_{u,z} \times K'_u \times (\overline{K}_{\hat{y}} \cup K'_{\hat{y}}) \times K_q \subset \mathbb{R}^{N_u}$. Using K^0_u and ϵ_1 let Theorem 5 generate $\delta^* \in (0,1)$, $a^*_\delta \in (0,1)$ and $\tilde{e}^*_{\delta,a} \in (0,1)$. Let $r_e \in (0,1)$ and $\tilde{e}_{\delta,a} \in (0, \tilde{e}^*_{\delta,a})$. By the ULAS result of Theorem 5 there exists a $M_u \in \mathbb{R}_{>0}$ such that the x_u-component of the solutions of (4.20) satisfies $x_u(j) \in M_u\mathbb{B}$ for all $j \geq 0$ and for all initial conditions in K^0_u. Let $M_{K^0_{u\mathbb{B}}} \in \mathbb{R}_{>0}$ be such that $H(M_u\mathbb{B}) + 1\mathbb{B} \subset M_{K^0_{u\mathbb{B}}}\mathbb{B}$. Define $K^0_\theta := \left(H(M_{K^0_{u\mathbb{B}}}) + \beta_\theta(2M_{K^0_{u\mathbb{B}}}, 0)\mathbb{B}\right) \cup \overline{K}_\theta$, $K^0_\xi := \varphi(K^0_\theta)^m \cup \overline{K}_\xi$, and $K^0_s := K_\tau \times K_\gamma \times K^0_\xi \times K^0_\theta$, which are all compact. Since $M_u\mathbb{B}$, K^0_s, and Q are compact, there exists an $M \in \mathbb{R}_{>0}$ such that $K^0_s \times M_u\mathbb{B} \times Q \subset M\mathbb{B}$. Using $\tilde{e}_{\delta,a}$ and the compact set $M\mathbb{B}$ let Proposition 11 generate the parameters $(\underline{\varepsilon}, \overline{\varepsilon}, \Delta T, \gamma^*) \in \mathbb{R}^3 \times \mathbb{Z}_{\geq 2m}$, and the continuous function $f_e(\cdot)$, and let $\varepsilon \in (\underline{\varepsilon}, \overline{\varepsilon})$. Using this construction we have the following lemmas:

Lemma 25 *Every complete solution $x \in \mathcal{S}_{\tilde{\mathcal{H}}}(K)$ satisfies $x(t,j) \in M\mathbb{B}$ for all $(t,j) \in dom(x)$.* ■

Proof: For any $q(0,0) \in Q$ every solution $x \in \mathcal{S}_{\tilde{\mathcal{H}}}(K)$ can stay at the mode $q(0,0)$ only for a finite amount of time. Indeed, note that solutions of (4.12) jump periodically. Whenever there is a jump, the jump map is characterized by (4.13). If $x_s \in D_s \cap \mathring{D}_e$ then x will jump according to the mapping $G_r \times G_q \times \ell$, which resets the states τ and γ, and updates q according to the mapping $\ell(\cdot)$. On the other hand, if $x_s \in D_s$ but $x_s \notin D_e$, the trajectories will evolve according to the triggering mechanism (4.6), which by Item 1) in Proposition 11 implies the existence of a $T_0 > 0$ such that for all $(t,j) \in \text{dom}(x)$ satisfying $t + j > T_0$ we have that $f_e(\xi(t,j)) < \varepsilon$. In turn, by Lemma 6, this implies the existence of a $T'_0 > 0$ such that every solution that was not in $\mathring{D}_e$ during jumps will now be in $\mathring{D}_e$ at some times $t_0 + j_0 < T'_0$. Since when $x_s \in D_e \backslash \mathring{D}_e$ both of the previously discussed updates are possible, we obtain the existence of a $T''_0 > 0$

such that for each $x \in \mathcal{S}_{\tilde{\mathcal{H}}}(K)$ there exists $(t_0, j_0) \in \mathrm{dom}(x)$ satisfying $t_0 + j_0 < T_0''$ such that $x(t_0, j_0) \in K_{q_0}$, where

$$K_{q_0} := \{0\} \times \{0\} \times K_\xi' \times K_\theta' \times K_{u,z}' \times K_u' \times K_{\hat{y}}' \times \{\ell(q_0)\}, \tag{H.4}$$

and where $q_0 := q(0,0)$. Moreover, by construction, we have that every solution satisfies $x(t,j) \in [0,1] \times [0,1] \times K_\xi' \times K_\theta' \times K_{u,z}' \times K_u' \times K_{\hat{y}}' \times Q =: \overline{K}_0$ for all $t + j \leq t_0 + j_0$.

Now, let us restart each solution from the set K_{q_0} given by (H.4). Again, using Proposition 11 there exists a $T_1 > 0$ such that every solution that starts at the set K_{q_0} will jump at some times (t_1, j_1) (different for each solution) satisfying $t_1 + j_1 < T_1$ using the mapping $G_r \times G_q \times \ell$. Moreover, the occurrence of an event will now imply that the state component x_s will be in the set (4.19), with $\mathbb{U} \cap \rho\mathbb{B}$ replaced by K_u', such that $x(t_1, j_1) \in K_{q_1}^{\tilde{e}}$, where

$$K_{q_1}^{\tilde{e}} := \{0\} \times \{0\} \times K_\xi^{\tilde{e}} \times K_\theta^{\tilde{e}} \times K_{u,z}' \times K_u' \times K_{\hat{y}} \times \{\ell(\ell(q_0))\},$$

and where the sets $K_\theta^{\tilde{e}}$ and $K_\xi^{\tilde{e}}$ are given by

$$K_\theta^{\tilde{e}} := H(K_u') + \tilde{e}\mathbb{B}, \quad K_\xi^{\tilde{e}} := (\varphi(H(K_u')) + \tilde{e}\mathbb{B})^m. \tag{H.5}$$

Moreover, for each solution $x \in \mathcal{S}_{\tilde{\mathcal{H}}}(K)$ and all $(t,j) \in \mathrm{dom}(x)$ satisfying $t + j \leq t_1 + j_1$ we have that $x(t,j) \in \big([0,1] \times [0,1]\overline{K}_\xi \times \overline{K}_\theta \times K_{u,z}' \times K_u' \times \overline{K}_{\hat{y}} \times Q\big) \cup \overline{K_0} := \overline{K}_1$, which follows by the construction of the dynamics (4.12) and the sets (H.3). This process can be iteratively repeated at most $2\bar{q} + 1$ times, leading to the existence of a $T' \in \mathbb{R}_{>0}$ such that for each $x \in \mathcal{S}_{\tilde{\mathcal{H}}}(K)$ there exists times $(t', j') \in \mathrm{dom}(x)$ satisfying $t' + j' < T'$ such that $q(t', j') = \underline{q}$ for the second time, and $q(t', j' + 1) = \underline{q} + 1$. Now, note that since $\hat{x}_{u,z}$ is updated only when there is a jump that updates q from $\underline{q}$ to $\underline{q}+1$,

only one jump of this type has occurred before time (t', j'). Also, after time (t_1, j_1), whenever there was a jump from one mode to another mode we have that $\theta \in K_\theta^{\tilde{e}}$ before flowing again. Using the definition of $M_{K'_{u\mathbb{B}}}$ and the fact that ξ correspond to measurements of $\varphi(\theta)$, and $\hat{y}$ correspond to measurements of $\varphi(\theta)$ at steady state (by item 2) in Propositon 11), we obtain that $x(t', j') \in \overline{K}_1$ for all $(t, j) \in \mathrm{dom}(x)$ satisfying $t + j \leq t' + j'$. Moreover, the second time that any solution hits the mode $\underline{q}$, and an event occurs, $\hat{y}$ and y will necessarily be given by (4.26), since $\hat{y}$ has been updated at the previous $(\bar{q} - \underline{q} - 1)$ events, each event describing a quasi-steady state condition. Therefore, starting from time (t_1, j_1) the updates of $\hat{x}_{u,z}$ will be characterized by Theorem 5 which gives a uniform bound $M_u\mathbb{B}$ for the state x_u for all $t + j > t_1 + j_1$. In turn, this uniform bound on x_u, and the quasi-steady state condition induced by the event set, gives the uniform bound K_θ^0 for the plant state θ for all $t + j > t_1 + j_1$. The construction of M establishes the result. ■

Lemma 26 *There exist a $T^* \in \mathbb{R}_{>0}$ such that for each solution $x \in \mathcal{S}_{\tilde{\mathcal{H}}}(K)$ and each pair $(t_1, j_1), (t_3, j_3) \in dom(x)$ such that $q(t_1, j_1) = q(t_3, j_3) = \underline{q}$ and such that there exists $(t_2, j_2) \in dom(x)$ satisfying $t_1 + j_1 < t_2 + j_2 < t_3 + j_3$ and $q(t_2, j_2) = \overline{q}$, the bound $(t_3 + j_3) - (t_1 + j_1) \leq T^*$ holds.* ■

Proof: Follows directly by the fact that $x(t, j) \in M\mathbb{B}$ for all $t + j \geq 0$ such that $(t, j) \in \mathrm{dom}(x)$, Proposition 11.1, Lemma 6, and the discussion in the proof of Lemma 25. ■

By the discussion in the last part of the proof of Lemma 25, whenever a solution $x \in \mathcal{S}_{\tilde{\mathcal{H}}}(K)$ hits the mode $\underline{q}$ for the second time, its evolution will be characterized by Theorem 5. Thus, Lemma 26 allows us to directly obtain the following uniform convergence result for the state x_u.

Lemma 27 *There exists a $T_c \in \mathbb{R}_{>0}$ such that for all $x \in \mathcal{S}_{\tilde{\mathcal{H}}}(K)$ and all $(t,j) \in dom(x)$ satisfying $t+j \geq T_c$, we have that $x_u(t,j) \in (\mathcal{A}_{\hat{x}_u} \times Q) + \epsilon\mathbb{B}$.* ■

H.6 Proof of Theorem 6

Let $\nu \in \mathbb{R}_{>0}$ be given and let $K \subset \mathbb{R}^{N_s+N_u}$ be a compact set satisfying $\mathcal{A} + \nu\mathbb{B} \subset \text{int}(K)$. Let $\delta_3 \in (0,\nu)$ and define $\delta_2 := \delta_3/\sqrt{m}$. Using these δ_2 and Lemma 24 generate δ_1. Let $\delta_0^b \in (0, \frac{\delta_1}{2})$. By upper semicontinuity of $H(\cdot)$ and compactness of $\mathcal{A}_u$ there exists a $\delta_0^a \in (0,\delta_0^b)$ such that $H\left(\mathcal{A}_u + \delta_0^a\mathbb{B}\right) \subset H(\mathcal{A}_u) + \delta_0^b\mathbb{B}$. Using this δ_0^a, by Proposition 16, there exists a δ^* such that $\forall\ \delta \in (0,\delta^*]\ \exists\ a^* \in (0,1)$ such that $\forall\ a \in (0,a^*)\ \exists\ \tilde{e}^* \in (0,\frac{\delta_1}{2})$ such that $\forall\ \tilde{e} \in (0,\tilde{e}^*)\ \exists$ data $(\Delta T, \gamma^*, f_e)$, and a pair $(\underline{\varepsilon}, \overline{\varepsilon})$ such that $\forall\ \varepsilon \in (\overline{\varepsilon}, \underline{\varepsilon}]\ \exists$ a T^* such that every complete $x \in \mathcal{S}_{\mathcal{H}}(K)$ satisfies $x(t,j) \in ([0,1]\times[0,1]\times\mathbb{R}^m \times \mathbb{R}^p \times (\mathcal{A}_{x_u} + \delta_0^a\mathbb{B}) \times Q) \cap M\mathbb{B}$ for all $(t,j) \in \text{dom}(x)$ such that $t+j \geq T^*$. Also, by Proposition 11.2, and the proof of Proposition 16, for all $t+j \geq T^*$ the condition $x(t,j) \in D_e \times D_u \times Q$ implies that $\theta(t,j) \in H(u(t,j)) + \tilde{e}\mathbb{B} \subset H(\mathcal{A}_u + \delta_0^a\mathbb{B}) + \tilde{e}\mathbb{B} \subset H(\mathcal{A}_u) + (\delta_0^b + \tilde{e})\mathbb{B} \subset H(\mathcal{A}_u) + \delta_1\mathbb{B}$. Since flows of θ happening after the input u has been updated can only happen after an event, for each $t+j \geq T^*$, the initial conditions of θ before starting to flow according to (6.2) will satisfy $\theta(t,j) \in H(\mathcal{A}_u) + \delta_1\mathbb{B}$. Since δ_1 was generated by δ_2 via Lemma 24, we obtain that $(\theta^\top, y)^\top(t,j) \in \big(H(\mathcal{A}_u) \times \varphi(H(\mathcal{A}_u))\big) + \delta_2\mathbb{B}$, $\forall\ (t,j) \in \text{dom}(x)$ such that $t+j \geq T^*$. Since each entry ξ_i of the vector $\xi \in \mathbb{R}^m$ corresponds to measurements of z gathered every ΔT seconds, we obtain that $\forall\ t+j \geq T^* + (\Delta T)m + (m-1) := T^{**}$ we have that $\xi_i(t,j) \in \varphi(H(\mathcal{A}_u)) + \delta_2\mathbb{B}\ \forall\ i \in \{1,\ldots,m\}$, which by the definition of δ_2 implies that $\xi(t,j) \in \varphi(H(\mathcal{A}_u))^m + \delta_3\mathbb{B}\ \forall\ t+j \geq T^*$. Then, every complete solution $x \in \mathcal{S}_{\tilde{\mathcal{H}}}(K)$ will satisfy $x(t,j) \in \mathcal{A} + \delta_3\mathbb{B}\ \forall\ (t,j) \in \text{dom}(x)$ such that $t+j \geq T^{**}$. The stability result follows by Lemma 22. ■

Appendix I

Proofs of Chapter 5

In this section we present the proofs of the results of Chapter 5. We start by proving Theorem 8.

I.1 Proof of Theorem 8

The proof of Theorem 8 follows two steps. First, we assume that $\bar{\mathbf{z}} = 0$, such that only the clocks τ_i need to be synchronized, and we establish synchronization for the network of clocks using a Lyapunov function and the invariance principle for hybrid systems. Second, we show that if $\bar{\mathbf{z}} > 0$, the synchronization of clocks is preserved, and a similar Lyapunov function can be constructed to show synchronization of the logic states.

Step 1: Consider the HDS (5.33) and let $\bar{\mathbf{z}} = 0$ such that the states z_i can be omitted and the stability properties of the system can be studied with respect to the set $\mathcal{A}_{\tau,\text{sync}}$ in (5.21). Since the flow set is compact there are no finite escape times. By assumption, solutions of system (5.31) converge asymptotically to the compact set $\mathcal{A}_{\mathcal{G}}$. Thus, to establish UGAS of the set $\mathcal{A}_{\tau,\text{sync}} \times \mathcal{A}_{\mathcal{G}}$ it suffices to study the convergence

and stability properties of the state τ with respect to the compact set $\mathcal{A}_{\tau,\text{sync}}$. Consider the Lyapunov function $V_\tau : [0,1]^N \to \mathbb{R}_{\geq 0}$ defined as the infimum of the lengths of all arcs that touch all agents τ_i, for all $i \in \mathcal{V}$, where the points 0 and 1 on the interval $[0,1]$ are identified to be the same, forming a circle with perimeter equal to 1. By construction, V_τ is positive definite with respect to $\mathcal{A}_{\tau,\text{sync}}$. Moreover, since all clocks flow at the same rate, the Lyapunov function is constant during flows. Also, since the jumps never increase the number of distinct points occupied by the agents, the Lyapunov function does not increase during jumps. Indeed, jumps occur only when one agent is at the end of the interval $[0,1]$, or when the graph $\mathcal{G}_c$ switches to a new configuration. In both cases the effect of the jumps on the state τ is to either leave the agent's location unchanged, or to move it to the beginning or end of the interval. Also, note that since the dynamics (5.31) generate solutions that can have at most N consecutive jumps, the existence of purely discrete or zeno solutions is ruled out. By assumption, there exists a hybrid time (t_0^*, j_0^*) with $t_0^* < T + \alpha$ and $j_0^* < J^*$, J being only a function of N and the parameters of (5.31), such that $q(t_0^*, j_0^*) \in Q_s$, i.e., $\mathcal{G}_\mathcal{C}$ is strongly connected. Moreover, since $\alpha > \frac{1}{\omega}$, the strong connectivity and configuration of the graph is preserved for at least $\frac{1}{\omega}$ seconds. Since by construction of V we must have $V_\tau(\tau) \leq \frac{N-1}{N} = 1 - \frac{1}{N}$ for all $\tau \in [0,1]^N$, and since the parameter r_i of every agent i satisfies $r_i \in (0, \frac{1}{N})$, there must exist a hybrid time $(t^*, j^*) > (t_0^*, j_0^*)$ in the domain of each solution, such that $\tau_i(t^*, j^*) = 1$ for some agent i, and $\tau_j > r_j$ for all $j \neq i$. Indeed, let τ_i be the first clock that satisfies $\tau_i = 1$ after the hybrid time (t_0^*, j_0^*). If τ_i does not correspond to the right extreme of of the arc V_τ, then there exists a τ_j satisfying $\tau_j < r_j$. Let τ_i be reset to 0, and let agent i' be the next agent that satisfies the condition $\tau_{i'} = 1$. Then, again, if $\tau_{i'}$ does not correspond to the right extreme of of the arc V, then there exists a τ_k satisfying $\tau_k < r_k$. This process can be repeated at most $N-1$ times, until eventually, after at most $\frac{1}{\omega}$ seconds of flow, agent i will satisfy again

the condition $\tau_i = 1$. Since $V_\tau < 1 - \frac{1}{N}$, it must be the case that $\tau_i = 1$, and $\tau_j > r_j$ for all agents j. Moreover since $t^* - t_0^* < \frac{1}{\omega}$, we have that $q(t^*, j^*) \in Q_s$ holds. From this point agent i will reset its clock to zero, forcing its neighbors to jump via (5.18a) to 1. Since $q(t^*, j^*) \in Q_s$ implies that the graph is strongly connected, this process will be repeated at most N times, generating at most N consecutive jumps before the clocks satisfy $\tau_i = 0$, for all $i \in \mathcal{V}$. In fact, suppose there is a group of agents, denoted P, that do not jump to the end of the interval while the rest of the agents do start at or jump to the end of the interval. Each element of P is connected to some element in the complement of P, and thus they will be forced to jump to the end of the interval when an appropriate member of the complement of P jumps to zero. From this point, the system can only flow synchronously, preserving the synchronization during the flows, and sequentially resetting τ_i to 0 whenever $\tau_i = 1$ for some agent i. This implies that no complete solution keeps $V_\tau(\tau)$ equal to a non-zero constant, and by [188, Thm. 7.6], τ is guaranteed to converge to $\mathcal{A}_{\tau,\text{sync}}$. The robustness properties of $\mathcal{A}_{\tau,\text{sync}}$ follow by Lemma 10. ■

Step 2: Let $\bar{\mathbf{z}} > 0$, and consider the compact set

$$\mathcal{A}_{\tau,z}^{\text{clocks}} := \mathcal{A}_{\tau,\text{sync}} \times Z^N \times \mathcal{A}_{\mathcal{G}}, \tag{I.1}$$

where $\mathcal{A}_{\tau,\text{sync}}$ is defined in (5.21), and note that $\mathcal{A}_{\tau,z} \times \mathcal{A}_{\mathcal{G}} \subset \mathcal{A}_{\tau,z}^{\text{clocks}}$. The compact set (I.1) corresponds to the case where only the clocks τ_i are synchronized, and the timer have converged to $\mathcal{A}_{\mathcal{G}}$. Note that when $\bar{\mathbf{z}} > 0$ the synchronization dynamics for τ are the same as in Step 1, except when $z_i = \bar{z}$ and $\tau_i = 1$ for some agent $i \in \mathcal{N}_{\mathcal{C}_{j,q}}$. In this latter case, if $i \in \mathcal{N}_{\mathcal{C}_{j,q}}$ and $z_j + \tau_j > r_j$, τ_j jumps to 1 and z_j jumps to $\bar{z}$. If $z_j + \tau_j < r_j$ (a condition that can happen only if $z_j = 0$), then τ_j jumps to 0 and z_j remains equal to 0, a point where agent j can only flow. Since no agent can jump out of the state $(0, 0)$, and agents always increase z_j whenever their jump, except when $z_j = \bar{\text{z}}$ such

that $z_j^+ = 0$, there must exist a time $(\tilde{t}, \tilde{j})$ where the HDS $\mathcal{H}_{x_{\tau,z}}$ must flow. Moreover, since τ_j still jumps either to 0 or 1, we have that the function V_τ constructed in Step 1 retains its main properties. Namely, it is constant during flows, non-increasing during jumps, and it satisfies $V_\tau(\tau) \leq 1 - \frac{1}{N}$. Since during flows the clocks evolve at a constant rate, we have again that no complete solution keeps V_τ at a value different to zero for all time, and synchronization of clocks is achieved in finite time. Using the fact that $|x_{\tau,z}|_{\mathcal{A}_{\tau,z}^{\text{clocks}}} = |\tau|_{\mathcal{A}_\tau^{\text{sync}}}$, we have that the set (I.1) is UGAS for the HDS $\mathcal{H}_{x_{\tau,z}}$.

Now consider the HDS with data (5.33b), (5.33c), and (5.33d), with the sets $C_{\tau,z}$ and $D_{\tau,z}$ intersected by the set $\mathcal{A}_\tau^{\text{sync}} \times Z^N$, i.e., with flow and jump set given by $C_{\tau,z} \cap (\mathcal{A}_\tau^{\text{sync}} \times Z^N)$, and $D_{\tau,z} \cap (\mathcal{A}_\tau^{\text{sync}} \times Z^N)$, respectively. Consider an interval $[0, \bar{\text{z}}+1]$, and let the points 0 and $\bar{\text{z}} + 1$ identify the same point in a circle with perimeter equal to $\bar{\text{z}} + 1$. Let $y_i = z_i + \tau_i$ be the position of the agent $i \in \mathcal{V}$ in this circle. Since $z_i \in Z$ is a nonnegative integer, and $\tau_i \in [0, 1]$, each non-integer position in the interval $[0, \bar{\text{z}} + 1]$ can be uniquely identified with a state (τ_i, z_i). Indeed, integer positions on $[0, \bar{\text{z}} + 1]$ correspond to the sets $\mathcal{A}_{\tau,z}^{\text{jump}_1}$ and $\mathcal{A}_{\tau,z}^{\text{jump}_2}$, which only contain the elements $\{(\mathbf{k}_N, \mathbf{0}_N), (\mathbf{0}_N, \mathbf{k}_N)\}$ for each $k \in \{0, \bar{\text{z}} + 1\}$. Thus, for each $k \in \{0, \bar{\text{z}} + 1\}$, the points $(\mathbf{k}_N, \mathbf{0}_N)$ and $(\mathbf{0}_N, \mathbf{k}_N)$ are identified with the same point in the circle of perimeter $\bar{\text{z}} + 1$. Based on this, consider the Lyapunov function $V_{\tau,z} : [0, 1]^N \times Z^N \to \mathbb{R}_{\geq}$ defined as the infimum of the length of all arcs that touch the position y_i of all agents in the circle. Then $V_{\tau,z}(\tau, z)$ is constant during flows. Moreover $V_{\tau,z}$ is positive definite with respect to $\mathcal{A}_{\tau,z}$. Additionally, during jumps, when $z_i < \bar{\text{z}}$ for all $i \in \mathcal{V}$, the position y_i of each agent $i \in \mathcal{V}$ is kept constant, and so the value of V doesn't change during these jumps. During jumps generated by some agent i satisfying $z_i = \bar{\text{z}}$ and $\tau_i = 1$, i.e., $z_i + \tau_i = \bar{\text{z}} + 1$, the position of the neighboring agents of i is either moved to the end of the interval, or kept constant at the initial of the circle. Therefore $V_{\tau,z}$ does not increase during jumps. Finally, note that since the data of the system is restricted to

the set $\mathcal{A}_{\tau,z}^{clock}$, the vector of clocks τ is synchronized, therefore $V_{\tau,z} \leq \bar{z}$ always hold by construction of $V_{\tau,z}$. To see this, we consider the two possible cases: 1) Each arc that touch agent's position y_i just at its endpoints has length less than or equal to 1, or 2) there exists an arc that touches agents just at its endpoints with length greater than 1. In the second case, since $\bar{z}+1$ arcs are enough to cover the circle, the complementary arc that touches all agents has length less than or equal to $\bar{z}+1-1=\bar{z}$. In the first case, we have that it is impossible to have such arcs with length less than 1 (since the clocks are synchronized). If the length is equal to 1, we have that at most $\bar{\text{z}}$ arcs of length 1 are needed to connect all agents. This establishes that $V_{\tau,z}(\tau,z) \leq \bar{z}$.

Finally, since the graph $\mathcal{G}_{\mathcal{C},q}$ is $(\alpha,T)-PSC$, there exists a hybrid time (t_0^*,j_0^*) with $t_0^* < T-\alpha$ and $j_0^* < J$, J being only a function of N and the parameters of (5.31), such that $q(t_0^*,j_0^*) \in Q_s$. Also, due to the fact that $\alpha > \frac{\text{card}(Z)}{\omega}$, the strong connectivity and time-invariance of the graph is preserved for at least $\frac{\text{card}(Z)}{\omega}$ seconds. Since the hybrid system with flow and jump set given by $C_{\tau,z} \cap (\mathcal{A}_\tau^{\text{sync}} \times Z^N) \times \mathcal{A}_\mathcal{G}$ and $D_{\tau,z} \cap (\mathcal{A}_\tau^{\text{sync}} \times Z^N) \times \mathcal{A}_\mathcal{G}$ is by construction synchronized in the clocks, there exists a hybrid time (t_1,j_1) such that $\tau_i(t_1,j_1)=1$ for all $i \in \mathcal{V}$ and with $t_1 - t_0^* \leq \frac{1}{\omega}$. Moreover, since whenever $z_i < \bar{\text{z}}$ agents always increase their mode z_i by 1, there must exist a time (t^*,j^*) after at most $\bar{\text{z}}-1$ intervals of flow of $\frac{1}{\omega}$ seconds, such that $\tau_i(t^*,j^*)=1$ and $z_i(t^*,j^*)=\bar{\text{z}}$ for some agent $i \in \mathcal{V}$. Based on the construction of the Lyapunov function this implies that $(z_i+\tau_i) > r_i$ for all $i \in \mathcal{V}$. At this point, since the graph is still strongly connected, the jump map will generate at most N consecutive jumps until all agents have converged to the beginning of the circle, i.e, $y_i=0$ for all $i \in \mathcal{V}$, which implies that $V_{\tau,z}=0$. This condition is preserved forward in time, which implies that no complete solution keeps $V_{\tau,z}(\tau,z)$ equal to a non-zero constant, and by [188, Thm. 7.6], we obtain UGAS of $\mathcal{A}_{\tau,z} \times \mathcal{A}_\mathcal{G}$ for the HDS with restricted jump and flow set. UGAS of the set $\mathcal{A}_{\tau,z} \times \mathcal{A}_\mathcal{G}$ for the original HDS $\mathcal{H}_{x_{\tau,z}}$ follows now by the UGAS

property of (I.1) established in the previous paragraph, and by the reduction principle [78, Corollary 7.24]. The robustness properties of $\mathcal{A}_{\tau,z}$ follow by Lemma 10. ■

I.2 Proof of Theorem 7

The proof of Theorem 7 follows four steps. First we intersect the data of the HDS $\mathcal{H}$ with the set $R^{3N} \times K$, where $K \subset \mathbb{R}^{n-3N}$ is compact, and by making use of Theorem 8, we will establish UGAS of the compact set $\mathcal{A}_{\tau,\alpha,z} \times K$. Second, we further intersect the data of this system with the set $\mathcal{A}_{\tau,\alpha,z} \times K$. For this synchronized system we show that if $\tilde{\rho}^* > 0$ is sufficiently small, whenever the i^{th} agent resets his clock and updates his controller, the values stored in s_i will correspond to an ε-perturbed version of the values of $[u^\top, h(\theta, u)^\top]^\top$ when $\tau_i = 1$. Moreover, the ε-perturbation shrinks to zero as $\tilde{\rho}^* \to 0^+$. Third, we show that for the liming case $\tilde{\rho}^* = 0$, every solution where each agent updates his controller only after every other agent has toggled α_i from 0 to 1, generates the same control and state updates as the centralized system (5.12). Since for any $\tilde{\rho}^* > 0$ every solution of the original system behaves in this way, this allows us to establish SGP-AS for the perturbed system with $\varepsilon > 0$. Finally, we use the reduction principle [241, Corollary 19] and Lemma 12 in order to establish a semiglobal practical stability result for the original system.

Step 1. By Assumption 32 and the construction of the flow map (5.24), system $\mathcal{H}$ has no finite scape times. Now, let $K \subset \mathbb{R}^{n-3N}$ be a compact set satisfying $\mathcal{A}_s^N \times \mathcal{A}_\xi \subset \text{int}(K)$, and define $\tilde{K} = \mathbb{R}^{3N} \times K$. Consider the HDS $\mathcal{H}_{\tilde{K}} = \{C_{\tilde{K}}, F, D_{\tilde{K}}, G_{\tilde{K}}\}$, where $C_{\tilde{K}} := C \cap \tilde{K}$, $D_{\tilde{K}} := D \cap \tilde{K}$, $G_{\tilde{K}} := G \cap \tilde{K}$, which restricts the states (s, θ, u) to the compact set K. Since the synchronization dynamics of (τ, z) are independent of the other states, and the graph is assumed to be time-invariant, by Theorem 8 we obtain directly UGAS of the set $\mathcal{A}_{\tau,\alpha,z} \times K$ for the HDS $\mathcal{H}_{\tilde{K}}$. In particular, the set

$\mathcal{A}_{\tau,\alpha,z} \times K$ is positively invariant, and every solution initialized in $C_{\tilde{K}} \cup D_{\tilde{K}}$ will converge to $\mathcal{A}_{\tau,\alpha,z} \times K$ in finite time.

Step 2. Let $K_{\text{sync}} := \mathcal{A}_{\tau,\alpha,z} \times K$, and consider the hybrid dynamical system $\mathcal{H}_{K_{\text{sync}}} := \{C_{K_{\text{sync}}}, F, D_{K_{\text{sync}}}, G_{K_{\text{sync}}}\}$, with data constructed as in Step 1, but with K_{sync} instead of $\tilde{K}$. This HDS corresponds to a system where the states (τ, z) are already synchronized. Let $\bar{\rho} = \max_{i \in \mathcal{V}} \rho_i$. By the construction of the jump map (5.28) based on (5.23), for each $(t_r, j_r) \in \text{dom}(x)$ such that $\tau_i(t_r, j_r) = 1$ and $\tau_i(t_r, j_r + 1) = 0$ for some agent $i \in \mathcal{V}$, the updates $u_i(t_r, j_r + 1)$ are generated by the mapping $G_{i,u,z}(s_i(t_r, j_r))$, with $s_i(t_r, j_r) = [s_{i,a}^\top, s_{i,b}^\top]^\top$, where $s_{i,a} = u(t_i', j_i')$, $s_{i,b} = h\big(\theta(t_i', j_i'), u(t_i', j_i')\big)$, $t_i' = t_r - \tilde{\rho}_i \omega^{-1}$, and $j_i' = \max\{k : (t_i', k) \in \text{dom}(x)\}$ i.e., the pair (t_i', j_i') is the hybrid time indicating the moment right after agent i sampled the value of the state θ and output vector y. Then, by (5.24), and omitting the discrete-time index, we have that $\theta(t_r) = \theta(t_i') + \int_{t_i'}^{t_r} \nu(\tau) d\tau$ for some measurable selection $\nu(t) \in P(\theta(t), u(t))$. Since by construction of $\mathcal{H}_{K_{\text{sync}}}$ the states θ and u are constrained to a compact set, by the local boundedness property of $P(\cdot, \cdot)$ there exists $M > 0$ such that $P(\theta, u) \subset M\mathbb{B}$ for all $(s, \theta, u) \in K$, which implies that $|\theta(t_r, j_r) - \theta(t_i', j_i')| \leq |\int_{t'}^{t_r} M d\tau| = \tilde{\rho}_i \omega^{-1} M$, and by definition of $\tilde{\rho}^*$ in Theorem 7 we have that $|\theta(t_r, j_r) - \theta(t_i', j_i')| \leq \tilde{\rho}^* \omega^{-1} M =: \delta$, for all $i \in \mathcal{V}$. Then, since u is kept constant during flows, we have that at time (t_r, j_r) the reset map (5.23c) satisfies $G_{z_i}(s_i(t_r, j_r)) \subset G_{z_i}(u(t_r, j_r), h(\theta(t_r, j_r) + \delta\mathbb{B}, u(t_r, j_r)))$, for all $i \in \mathcal{V}$. Since $G_{z_i}(\cdot, \cdot)$ is OSC and LB, it is also upper-semicontinuous. Therefore, by continuity of $h(\cdot, \cdot)$, upper semicontinuity of $G_{z_i}(\cdot, \cdot)$, and compactness of K, for each $\varepsilon > 0$ there exists $\delta > 0$ such that whenever an agent updates his controller, the update mapping satisfies $G_{i,u,z}(u, h(\theta + \delta\mathbb{B}, u)) \subset G_{i,u,z}(u, h(\theta, u)) + \varepsilon\mathbb{B} =: G_{\varepsilon,z_i}(u, \theta)$. Thus, $G_{K_{\text{sync}}} \subset G_{\varepsilon,K_{\text{sync}}}$, where $G_{\varepsilon,K_{\text{sync}}}$ is constructed as $G_{K_{\text{sync}}}$ but with G_{ε,z_i} instead of G_{z_i} in (5.23c). Since by construction of $\mathcal{H}_{K_{\text{sync}}}$ the clocks and logic modes are synchronized, the previous argument implies that for any $\varepsilon > 0$ there exists a $\tilde{\rho}^* > 0$ such

that whenever an agent jumps according to (5.23c), the states (θ, u) in system $\mathcal{H}_{K_{\text{sync}}}$ are updated as in the centralized system (5.12), plus an ε-perturbation on the jump map.

Step 3. Let $\varepsilon > 0$, and consider the inflated system $\mathcal{H}_{\varepsilon,K_{\text{sync}}}$ constructed as $\mathcal{H}_{K_{\text{sync}}}$ but with $G_{\varepsilon,K_{\text{sync}}}$ instead of $G_{K_{\text{sync}}}$. Then, the control updates of this system are the same as the centralized system (5.12), plus a small additive ε-perturbation on the jump map. By construction of $G_{\varepsilon,K_{\text{sync}}}$, as $\varepsilon \to 0^+$ we must also have that $\tilde{\rho}^* \to 0^+$, i.e., $\rho_i \to 1^-$ for all $i \in \mathcal{V}$, which means that agents should sample their neighbor's states and outputs closer and closer to the condition $\tau_j = 1$ for all $j \in \mathcal{N}_{\mathcal{C}_i}$. Note that increasing ρ_i shrinks the flow set $C_{i,1}$ in (5.22a), but for any $\rho_i < 1$ we have that $[\rho_i, 1] \neq \emptyset$, and the updates of u will always correspond to an ε-perturbation of the updates generated by the centralized system (5.12). In the limiting case, when $\varepsilon = 0$ such that $\rho_i = 1$ for all $i \in \mathcal{V}$, system $\mathcal{H}_{\varepsilon,K_{\text{sync}}}$ generates additional solutions where agents jump from $D_{i,0}$ to $D_{i,1}$ and then to $C_{i,0}$, without allowing the other agents to sample their states. However, again, for any $\tilde{\rho}^* > 0$ these extra solutions are precluded. Since when $\tilde{\rho}^* > 0$ the updates of (θ, u) in system $\mathcal{H}_{\varepsilon,K_{\text{sync}}}$ correspond to an ε-perturbed version of the centralized system (5.12), and every solution of $\mathcal{H}_{K_{\text{sync}}}$ is also a solution of $\mathcal{H}_{\varepsilon,K_{\text{sync}}}$, by Assumption 35 and Lemma 10, we have that every solution of system $\mathcal{H}_{K_{\text{sync}}}$ retains the SGP-AS property of the centralized system (5.12) in K. Namely, for any $\tilde{\epsilon} > 0$ there exists always $\tilde{\rho}^{**} > 0$ sufficiently small, such that for all $\tilde{\rho}^* \in (0, \tilde{\rho}^{**})$ every solution of $\mathcal{H}_{K_{\text{sync}}}$ will converge in finite-time to the set $\mathcal{A}_{\tau,\alpha,z} \times \left(\mathcal{A}_s^N \times \mathcal{A}_\xi\right) + \tilde{\epsilon}\mathbb{B}$.

Step 4. Using the result of the previous step, and Lemma 12, for each $\tilde{\epsilon} > 0$ such that $\left(\mathcal{A}_s^N \times \mathcal{A}_\xi\right) + \tilde{\epsilon}\mathbb{B} \subset K$, there exists an Ω-limit set $\Omega(K) \subset \mathcal{A} + \epsilon\mathbb{B}$ that is UGAS for system $\mathcal{H}_{K_{\text{sync}}}$. Since $\tilde{\epsilon}$ and K can always be chosen such that $\Omega(K) \subset \mathcal{A}_{\tau,\alpha,z} \times K$, and since by **Step 1** the set $\mathcal{A}_{\tau,\alpha,z} \times K$ is UGAS for system $\mathcal{H}_{\tilde{K}}$, by the Reduction Principle [78, Corollary 7.24] we obtain that $\Omega(K)$ is also UGAS for system $\mathcal{H}_{\tilde{K}}$. Finally, note

that by decreasing $\tilde{\rho}^*$ one can chose the set K and the $\tilde{\epsilon}$-neighborhood arbitrarily large and small, respectively. Moreover, as discussed in **Step 3**, decreasing $\tilde{\rho}^*$ does not affect the uniform bound on the states. This observations establishes the semi-global practical asymptotic stability result for system $\mathcal{H}$. ■

Appendix J

Stochastic Difference Inclusions

In this section we review some basic notions about stochastic difference inclusions, which are needed in Chapter 6.

J.1 Notation and Basic Definitions

$\mathbf{B}(\mathbb{R}^{\mathbf{m}})$ denotes the Borel field, i.e., the subsets of $\mathbb{R}^m$ generated from open subsets of $\mathbb{R}^m$ through complements and finite and countable unions. A set $F \subset \mathbb{R}^m$ is measurable if $F \in \mathbf{B}(\mathbb{R}^{\mathbf{m}})$. A mapping $M : \mathbb{R}^p \rightrightarrows \mathbb{R}^n$ is measurable [251, Def. 14.1] if for each open set $\mathcal{O} \subset \mathbb{R}^n$ the set $M^{-1}(\mathcal{O}) := \{v \in \mathbb{R}^p : M(v) \cap \mathcal{O} \neq \emptyset\}$ is measurable. When the values of M are closed, measurability is equivalent to $M^{-1}(\mathcal{O})$ being measurable for each closed set $\mathcal{O} \subset \mathbb{R}^n$ [251, Thm. 14.3].

J.2 Parameterized Stochastic Difference Inclusions with Inputs

We consider constrained stochastic discrete-time systems with inputs, given by

$$x^+ \in G_\delta(x, u, v) \qquad v \sim \mu(\cdot) \tag{J.1}$$

where $x \in \mathbb{R}^n$ is the current value of the state of the system at time $j \in \mathbb{Z}_{\geq 0}$, and x^+ represents the value of state x at the time $j+1$. The input $u \in \mathbb{R}^p$ is an explicit worst-case input, $G_\delta : \mathbb{R}^n \times \mathbb{R}^p \times \mathbb{R}^m \rightrightarrows \mathbb{R}^n$ is a set-valued mapping parameterized by a positive real number $\delta \in \mathbb{R}_{>0}$, and v is a random input taken from a sequence of independent, identically distributed (i.i.d) random variables $\{\mathbf{v}_k\}_{k=1}^{\infty}$. Note that for the particular case when $u = 0$, system (J.1) reduces to a standard stochastic difference inclusion without inputs, a class of systems previously studied in [252], [253], and [231], for example.

To define random solutions of systems of the form (J.1) we introduce a probability structure. Let $(\Omega, \mathcal{F}, \mathbb{P})$ be a probability space, where Ω denotes the set of all possible outcomes, $\mathcal{F}$ is the σ-field associated with Ω and $\mathbb{P}$ is the probability measure that assigns probability to events in $\mathcal{F}$. Since the sequence $\mathbf{v}_i : \Omega \mapsto \mathbb{R}^m$ is i.i.d it follows that $\mathbf{v}_i^{-1}(F) := \{\omega \in \Omega : \mathbf{v}_i(\omega) \in F\} \in \mathcal{F}$ for each $F \in \mathbf{B}(\mathbb{R}^m)$. We use $\mathcal{F}_i$ to denote the collection of sets $\{\omega \in \Omega : (\mathbf{v}_1(\omega), \ldots, \mathbf{v}_i(\omega)) \in F\}$, $F \in \mathbf{B}((\mathbb{R}^m)^i)$, which are the sub-$\sigma$-fields of $\mathcal{F}$ that form the minimal filtration of $\mathbf{v} := \{\mathbf{v_i}\}_{i=1}^{\infty}$. It follows from the i.i.d property that each random variable has the same probability measure $\mu : \mathbf{B}(\mathbb{R}^m) \mapsto [0, 1]$ defined as $\mu(F) := \mathbb{P}\{\omega \in \Omega : \mathbf{v}_i(\omega) \in F\}$, and for almost all $\omega \in \Omega$,

$$\begin{aligned}&\mathbb{E}[f(\mathbf{v}_0,\ldots,\mathbf{v}_i,\mathbf{v}_{i+1})|\mathcal{F}_i](\omega)\\&\qquad=\int_{\mathbb{R}^m} f(\mathbf{v}_0(\omega),\ldots,\mathbf{v}_i(\omega),v)\mu(dv),\end{aligned}\tag{J.2}$$

for each $i \in \mathbb{Z}_{\geq 0}$ and each measurable $f : (\mathbb{R}^m)^{i+2} \mapsto \mathbb{R}$.

We impose the following assumption on system (J.1).

Assumption 43 *There exists $\delta^* > 0$ such that for all $\delta \in (0, \delta^*)$ the mapping G_δ is locally bounded and $v \mapsto$ graph$(G_\delta(\cdot,\cdot,v)) := \{(x,u,y) \in \mathbb{R}^n \times \mathbb{R}^p \times \mathbb{R}^n : y \in G_\delta(x,u,v)\}$ is measurable with closed values.* □

By [251, Theorem 5.7(a)], Assumption 43 implies that $(x,u) \mapsto G_\delta(x,u,v)$ is outer-semicontinuous for each $v \in \mathbb{R}^m$. Moreover, by [251, Proposition 14.11(a) and Theorem 14.13(a)] measurability of $v \mapsto \text{graph}(G_\delta(\cdot,\cdot,v))$ implies that $v \mapsto G_\delta(x,u,v)$ is measurable for each $(x,u) \in \mathbb{R}^n \times \mathbb{R}^p$. Finally, note that the measurability condition of Assumption 43 holds if the domain of $v \mapsto \text{graph}(G(\cdot,\cdot,v))$ is countable or if G is OSC.

The type of inputs u allowed in (J.1) are worst-case inputs that satisfy a pointwise-in-time constraint of the form $u \in \lambda(x)\mathbb{B}$ where $\lambda : \mathbb{R}^n \to \mathbb{R}_{\geq 0}$ is a continuous function. Thus, we consider solutions generated by the system

$$x^+ \in G_\delta(x, \lambda(x)\mathbb{B}, v) \qquad v \sim \mu(\cdot) \tag{J.3}$$

The following Lemma is a trivial extension of [254, Proposition 1] for δ-parameterized set-valued mappings G_δ.

Lemma 28 *If $\lambda : \mathbb{R}^n \to \mathbb{R}_{\geq 0}$ is continuous and G_δ satisfies Assumption 43 then there exists $\delta^* > 0$ such that for all $\delta \in (0, \delta^*)$ the mapping $(x,v) \mapsto G_\delta(x, \lambda(x)\mathbb{B}, v)$ is locally bounded and $v \mapsto$ graph$(G_\delta(\cdot, \lambda(\cdot)\mathbb{B}, v))$ is measurable with closed values.* □

The graph of a sequence $\phi = \{\phi_i\}_{i=0}^{J-1}$ with $\phi_i \in \mathbb{R}^n$ is defined as the set $\text{graph}(\phi) = \bigcup_{i=0}^{J-1}(\{i\} \times \phi_i) \subset \mathbb{R}^{n+1}$. A sequence $(\phi, w) = \{(\phi_i, w_i)\}_{i=0}^{J-1}$ with $(\phi_i, w_i) \in \mathbb{R}^n \times \mathbb{R}^m$, is a *regular solution* of (J.3) starting at $x \in \mathbb{R}^n$ if $\phi_0 = x$ and $\phi_{i+1} \in G_\delta(\phi_i, \lambda(\phi_i), w_i)$ for all $i \in \{0, \ldots, J-2\}$. A mapping $\mathbf{x}$ from Ω to sequences is a *random solution* of (J.3) starting at $x \in \mathbb{R}^n$ if it satisfies the following two properties:

- (Pathwise feasibility) For each $\omega \in \Omega$, the sequence $\{(\mathbf{x}_i(\omega), \mathbf{v}_i(\omega))\}_{i=0}^{\mathbf{J}(\omega)-1}$ with arbitrarily $\mathbf{v}_0$ is a regular solution of (J.3) starting at x, where $\mathbf{J}(\omega)$ is the number of elements of the sequence $\mathbf{x}(w)$.

- (Causal measurability) For each $i \in \mathbb{Z}_{\geq 0}$, the mapping $\omega \mapsto \mathbf{x}_{i+1}(\omega)$ is $\mathcal{F}_i$-measurable where $\mathcal{F}_0 = \{\emptyset, \Omega\}$ and $(\mathcal{F}_1, \mathcal{F}_2, \ldots)$ is the minimal filtration of $\mathbf{v}$.

Remark 32 *Note that the causality condition prevents the value of the state up to the i^{th} jump from anticipating the value of the i^{th} or later random input. This causality condition plays an important role in the results of Chapter 6.* □

A random solution $\mathbf{x}$ is said to be maximal if it cannot be extended, i.e., there does not exist another random solution $\mathbf{y}$ from x such that $\text{dom } \mathbf{x}_i \subset \text{dom } \mathbf{y}_i$ for all $i \in \mathbb{Z}_{\geq 0}$, $\mathbf{y}_i(\omega) = \mathbf{x}_i(\omega)$ for all $\omega \in \text{dom } \mathbf{x}_i$ and all $i \in \mathbb{Z}_{\geq 0}$. We denote $\mathcal{S}_r(x)$ the set of maximal random solutions of (J.3) from $x \in \mathbf{R}^n$. In the case when $\mathbf{J}(\omega) = \infty$ for almost every $\omega \in \Omega$, we say that the random solution $\mathbf{x}$ is *almost surely complete*. Clearly, almost surely complete solutions are maximal, but not every maximal solution is almost surely complete. Maximal solutions of (J.1) can be guaranteed to be almost surely complete if, for example, $G_\delta(x, \lambda(x), v) \neq \emptyset$ for all $x \in D$, and $G_\delta(D \times \lambda(D) \times \mathcal{V}) \subset D$, where $\mathcal{V} := \cup_{\omega \in \Omega, i \in \mathbb{Z}_{\geq 0}} \mathbf{v}_i(\omega)$.

J.3 Some Stability Results for SDIs

In this section we introduce three novel stability definitions for SDIs of the form (J.3), as well as sufficient Lyapunov conditions that can be used to certify these stability notions .

J.3.1 Stability Notions and Sufficient Lyapunov Conditions for 0-Input Systems

We start by considering the SDI given by (J.3) for the case when $u = 0$, i.e., the 0-input case. The following definition aims to capture a global positive recurrence property (see also [255]) where the recurrence is established with respect to an open neighborhood of a compact set $\mathcal{A}$.

Definition 14 *For system* (J.1) *with* $u = 0$ *the compact set* $\mathcal{A} \subset \mathbb{R}^n$ *is said to be* uniformly globally practically positively recurrent (UGPPR) *if there exists* $\delta^* \in (0, 1]$ *and for each compact set* $K \subset \mathbb{R}^n$ *and* $\varepsilon > 0$ *and* $\delta \in (0, \delta^*]$ *there exists* $M_\delta > 0$ *such that*

$$\mathbb{E}\left[\inf\left\{k \in \mathbb{Z}_{\geq 0} : \mathbf{x}_k \in \mathcal{A} + \varepsilon\mathbb{B}^\circ\right\}\right] \leq M_\delta, \tag{J.4}$$

for all $\mathbf{x} \in \mathcal{S}_r(K)$. □

In essence, UGPPR requires that the sample paths of every random solution either stop or hit the set $\mathcal{A} + \varepsilon\mathbb{B}^o$ in finite time, where the upper bound of the hitting time is uniform over compact sets.

The following proposition establishes a sufficient Lyapunov condition for UGPPR in SDIs of the form (J.3) with $u = 0$, and satisfying Assumption 43.

Proposition 17 *Let $\mathcal{A} \subset \mathbb{R}^n$ be compact, and consider the system (J.1) under Assumption 43. If there exists an upper semicontinuous function $V : \mathbb{R}^n \mapsto \mathbb{R}_{\geq 0}$, $\alpha_1, \alpha_2 \in \mathcal{K}_\infty$, $\rho_1, \rho_2 \in \mathcal{K}$, and a $\delta^* \in (0,1)$ such that for all $\delta \in (0, \delta^*)$*

$$\alpha_1(|x|_{\mathcal{A}}) \leq V(x) \leq \alpha_2(|x|_{\mathcal{A}}), \quad \forall\ x \in \mathbb{R}^n \tag{J.5a}$$

$$\int_{\mathbb{R}^n} \max_{g \in G_\delta(x,0,v)} V(g)\mu(dv) - V(x) \leq -\rho_1(\delta) + \mathbb{I}_{C_\delta^c}(x), \tag{J.5b}$$

where $C_\delta := \{x \in \mathbb{R}^n : V(x) \geq \rho_2(\delta)\}$, then the set $\mathcal{A}$ is UGPPR.

Proof: Let $\varepsilon > 0$ and the compact set $K \subset \mathbb{R}^n$ be given. Let $R := \max_{x \in K \cap D} V(x)$. Pick $\delta \in (0, \delta^*]$ sufficiently small such that $V(x) < \rho_2(\delta)$ imply $|x|_{\mathcal{A}} < \varepsilon$. Let $\mathbf{T}_{\mathbf{x},C_\delta^c} : \Omega \to \mathbb{Z}_{\geq 0} \cup \{\infty\}$ and define $\mathbf{T}_{\mathbf{x},C_\delta^c} := \inf\{k \in \mathbb{Z}_{\geq 0} : \mathbf{x}_k(\omega) \in C_\delta^c\}$, and $\tau_n(\omega) := \min\{n, \mathbf{T}_{\mathbf{x},C_\delta^c}\}$. Then, for all $\mathbf{x} \in \mathcal{S}_r(K)$, we have that

$$\begin{aligned} V(\mathbf{x}_{\tau_n}) &= V(\mathbf{x}_0) + \sum_{i=1}^{\tau_n} (V(\mathbf{x}_i) - V(\mathbf{x}_{i-1})) \\ &= V(\mathbf{x}_0) + \sum_{i=1}^{n} (V(\mathbf{x}_i) - V(\mathbf{x}_{i-1}))\, \mathbb{I}(\mathbf{T}_{\mathbf{x},C_\delta^c} \geq i). \end{aligned}$$

Taking the expectation of $V(\mathbf{x}_{\tau_n})$ we get

$$\begin{aligned} \mathbb{E}[V(\mathbf{x}_{\tau_n})] &= \mathbb{E}[V(\mathbf{x}_0)] + \mathbb{E}\left[\sum_{i=1}^{\tau_n} (V(\mathbf{x}_i) - V(\mathbf{x_{i-1}}))\right] \\ &= V(x) + \mathbb{E}\left[\sum_{i=1}^{n} (V(\mathbf{x}_i) - V(\mathbf{x}_{i-1}))\, \mathbb{I}(\mathbf{T}_{\mathbf{x},C_\delta^c} \geq i)\right]. \end{aligned} \tag{J.6}$$

Also, note that since $\{\mathbf{T}_{\mathbf{x},C_\delta^c} \geq i\} \in \mathcal{F}_{i-1}$ we have that

$$\begin{aligned}
&\mathbb{E}\left[\sum_{i=1}^{n}\left(V(\mathbf{x}_i)-V(\mathbf{x}_{i-1})\right)\mathbb{I}(\mathbf{T}_{\mathbf{x},C_\delta^c}\geq i)\right]\\
&=\mathbb{E}\left[\sum_{i=1}^{n}\mathbb{E}\left[\left(V(\mathbf{x}_i)-V(\mathbf{x}_{i-1})\right)\mathbb{I}(\mathbf{T}_{\mathbf{x},C_\delta^c}\geq i)|\mathcal{F}_{i-1}\right]\right]\\
&=\mathbb{E}\left[\sum_{i=1}^{n}\mathbb{I}(\mathbf{T}_{\mathbf{x},C_\delta^c}\geq i)\mathbb{E}\left[\left(V(\mathbf{x}_i)-V(\mathbf{x}_{i-1})\right)|\mathcal{F}_{i-1}\right]\right]. \qquad \text{(J.7)}
\end{aligned}$$

By definition, for any $k \in \mathbb{Z}_{\geq 0}$ the following bound holds with probability one

$$\mathbb{E}\left[V(\mathbf{x}_k)|\mathcal{F}_{k-1}\right] \leq \int_{\mathbb{R}^m} \max_{g\in G(\mathbf{x}_{k-1},0,v)} V(g)\mu(dv), \qquad \text{(J.8)}$$

where using the fact that V is upper semicontinuous, and because of Assumption 1, the integral in (J.8) is well defined. Using (J.5b), (J.7) and (J.8) we get that for all $x \in C_\delta \cap D$

$$\begin{aligned}
&\mathbb{E}\left[\sum_{i=1}^{n}\left(V(\mathbf{x}_i)-V(\mathbf{x}_{i-1})\right)\mathbb{I}(\mathbf{T}_{\mathbf{x},C_\delta^c}\geq i)\right]\\
&\qquad\leq -\rho_1(\delta)\cdot\mathbb{E}\left[\sum_{i=1}^{n}\mathbb{I}(\mathbf{T}_{\mathbf{x},C_\delta^c}\geq i)\right]\\
&\qquad\leq -\rho_1(\delta)\cdot\mathbb{E}\left[\min\{\mathbf{T}_{\mathbf{x},C_\delta^c},n\}\right], \qquad \text{(J.9)}
\end{aligned}$$

and since $\mathbb{E}\left[V(\mathbf{x}_{\tau_n})\right] \geq 0$, by combining (J.6) and (J.9) we get that for all $x \in C_\delta$ and $\mathbf{x} \in \mathcal{S}_r(x)$, $\mathbb{E}\left[\min\{\mathbf{T}_{\mathbf{x},C_\delta^c},n\}\right] \leq V(x)/\rho_1(\delta)$. By the monotone convergence theorem, as $n \to \infty$ we have $\mathbb{E}\left[\mathbf{T}_{\mathbf{x},C_\delta^c}\right] \leq V(x)/\rho_1(\delta)$, but since δ was chosen such that $C_\delta^c \subset \mathcal{A}+\epsilon\mathbb{B}^o$, and R is an upper bound of $V(x)$ over the compact set K, we obtain that $\mathbb{E}\left[\mathbf{T}_{\mathbf{x},\mathcal{A}+\epsilon\mathbb{B}^o}\right] \leq K/\rho_1(\delta) =: M_\rho$, for all $\mathbf{x} \in \mathcal{S}_r(K \cap C_\delta)$. The result follows by noting that if $x \in C_\delta^c$ we obtain $\mathbb{E}\left[\mathbf{T}_{\mathbf{x},\mathcal{A}+\epsilon\mathbb{B}^o}\right] = 0$ since $\mathbf{x}_0(\omega) = x$. ■

A related but weaker notion of recurrence for parameterized stochastic systems is the notion of *uniform global practical recurrence* (UGPR).

Definition 15 *For system* (J.1) *with* $u = 0$ *the compact set* $\mathcal{A} \subset \mathbb{R}^n$ *is said to be* uniformly globally practically recurrent (UGPR) *if there exists* $\delta^* \in (0, 1]$ *and for each* $\delta \in (0, \delta^*]$*, each compact set* $K \subset \mathbb{R}^n$*, and each pair* $(\varepsilon, \rho) \in \mathbb{R}^2_{>0}$ *there exists* $T_\delta > 0$ *such that*

$$\mathbb{P}\left[\inf\left\{k \in \mathbb{Z}_{\geq 0} : \mathbf{x}_k \in \mathcal{A} + \varepsilon\mathbb{B}^\circ\right\} \leq T_\delta\right] \geq 1 - \rho$$

for all $\mathbf{x} \in \mathcal{S}_r(K)$. □

As it is the case for the standard notions of recurrence and positive recurrence, for a given $\delta > 0$ we have that UGPPR implies UGPR.

Lemma 29 *If* $\mathcal{A}$ *is UGPPR, then* $\mathcal{A}$ *is UGPR.* □

Proof: The proof parallels [256, Lemma 4.2]. Suppose the set $\mathcal{A}$ is UGPPR with $\delta^* \in \mathbb{R}_{>0}$. Let $K \subset \mathbb{R}^n$ and $(\varepsilon, \rho) \in \mathbb{R}^2_{>0}$ be given. Let M_δ such that (J.4) holds. Choose $T_\delta > 0$ such that $T_\delta > M_\delta/\rho$. Let $\mathbf{x} \in \mathcal{S}_r(K)$ and define $\mathbf{S} := \inf\{k \geq 0 : \mathbf{x}_k \in \mathcal{A} + \varepsilon\mathbb{B}^o\}$. Using Markov's inequality and inequality (J.4) we get

$$\mathbb{P}(\mathbf{S} > T_\delta) \leq \frac{\mathbb{E}[\mathbf{S}]}{T_\delta} < \rho. \tag{J.10}$$

This implies that $\mathbb{P}\left[\inf\left\{k \in \mathbb{Z}_{\geq 0} : \mathbf{x}_k \in \mathcal{A} + \varepsilon\mathbb{B}^\circ\right\} \leq T_\delta\right] \geq 1 - \rho$ holds for all $\mathbf{x} \in \mathcal{S}_r(K)$, which is the definition of UGPR. ■

Remark 33 (Global vs Semi-Global Results) *In the literature of stability theory for nonlinear dynamical systems e.g., [91], small persistent disturbances usually preclude global stability results, but rather induce "semi-global" properties, i.e., for each*

compact set of initial conditions one can always find a sufficiently small disturbance such that the convergence is guaranteed towards a neighborhood of the compact attractor $\mathcal{A}$. However, in stochastic systems it is usually difficult to establish this property, see for instance [243, Sec. 7.1]. In particular, semi-global results usually lead to solutions that can escape with probability one and in infinite time any given arbitrarily large compact subset of the state space. Because of this reason in this section we focus only on global results.

The following definition captures a mean-square exponential stability property with respect to a neighborhood of the compact attractor $\mathcal{A}$, where the neighborhood can be made arbitrarily small by decreasing the parameter δ.

Definition 16 *A compact set $\mathcal{A} \subset \mathbb{R}^n$ is said to be* mean-square practically exponentially stable *(MSP-ES) for the system (J.1) if there exist $\delta^* \in (0,1)$, positive real numbers β, $\lambda < \frac{1}{\delta^*}$, γ, and α, such that for all $\delta \in (0, \delta^*]$ and all $x_0 \in \mathbb{R}^n$ the following bound holds*

$$\mathbb{E}\left[|\mathbf{x}_k|_{\mathcal{A}}^2\right] \leq \beta(1-\delta\lambda)^k \|x_0\|_{\mathcal{A}}^2 + \gamma\delta^\alpha, \tag{J.11}$$

for all $k \in \mathbb{Z}_{\geq 0}$, and $\boldsymbol{x} \in \mathcal{S}_r(x_0)$. □

The following theorem provides a sufficient Lyapunov condition that certifies the notion of MSP-ES introduced in Definition 16.

Proposition 18 *Let $\mathcal{A} \subset \mathbb{R}^n$ be compact, and consider the system (J.1) under Assumption 43. If there exists an upper semicontinuous function $V : \mathbb{R}^n \mapsto \mathbb{R}_{\geq 0}$ and positive constants $(c_1, c_2, \lambda, \delta^*, K, \kappa) \in \mathbb{R}_{>0} \times \mathbb{R}_{>0} \times \mathbb{R}_{>0} \times (0,1) \times \mathbb{R}_{>0} \times \mathbb{R}_{>1}$, such that $\forall\ \delta \in (0, \delta^*)$*

$$c_1\|x\|_{\mathcal{A}}^2 \leq V(x) \leq c_2\|x\|_{\mathcal{A}}^2, \quad \forall\ \ x \in \mathbb{R}^n, \tag{J.12a}$$

$$\int_{\mathbb{R}^m} \max_{g \in G_\delta(x,0,v)} V(g)\mu(dv) \leq (1-\delta\lambda)V(x) + K\delta^\kappa, \ \forall x \in \mathbb{R}^n \tag{J.12b}$$

then, the set $\mathcal{A}$ is MSP-ES for (J.1). □

Proof: It follows from (7) and (J.12b), that for any $k \in \mathbb{Z}_{\geq 0}$ the following bound holds with probability one

$$\mathbb{E}\left[V(\mathbf{x}_k)|\mathcal{F}_{k-1}\right] \leq \int_{\mathbb{R}^m} \max_{g \in G(\mathbf{x}_{k-1},0,v)} V(g)\mu(dv) \tag{J.13}$$

$$\leq (1-\delta\lambda)V(\mathbf{x}_{k-1}) + K\delta^\kappa, \tag{J.14}$$

where using the fact that V is upper semicontinuous, and because of Assumption 1, the integral in (J.13) is well defined. Since we have that

$$\begin{aligned}\mathbb{E}\left[V(\mathbf{x}_k)\right] =& \mathbb{E}\left[\mathbb{E}\left[V(\mathbf{x}_k|\mathcal{F}_0)\right]\right] \\ =& \mathbb{E}\left[\mathbb{E}[\cdots \mathbb{E}\left[\mathbb{E}\left[V(\mathbf{x}_k)|\mathcal{F}_{k-1}\right]|\mathcal{F}_{k-2}\right]\cdots|\mathcal{F}_0]\right],\end{aligned}$$

we can apply (J.14) repeatedly to get

$$\begin{aligned}\mathbb{E}\left[V(\mathbf{x}_k)\right] &\leq (1-\delta\lambda)^k V(\mathbf{x}_0) + K\delta^\kappa \sum_{i=0}^{k-1}(1-\delta\lambda)^i \\ &\leq (1-\delta\lambda)^k V(\mathbf{x}_0) + K\delta^\kappa \frac{1}{\delta\lambda}.\end{aligned}$$

Using (J.12a) we have

$$\begin{aligned}c_1\mathbb{E}\left[\|\mathbf{x}_k\|_{\mathcal{A}}^2\right] &\leq (1-\delta\lambda)^k V(\mathbf{x}_0) + K\delta^\kappa \frac{1}{\delta\lambda} \\ &\leq (1-\delta\lambda)^k c_2\|\mathbf{x}_0\|_{\mathcal{A}}^2 + K\delta^\kappa \frac{1}{\delta\lambda},\end{aligned}$$

and then

$$\mathbb{E}\left[\|\mathbf{x}_k\|_{\mathcal{A}}^2\right] \leq \left(\frac{c_2}{c_1}\right)(1-\delta\lambda)^k\|\mathbf{x}_0\|_{\mathcal{A}}^2 + \delta^{\kappa-1}\frac{K}{c_1\lambda} \tag{J.15}$$

which implies MSP-ES with $\beta := c_2/c_1$, $\gamma = K/c_1\lambda$, and $\alpha = \kappa - 1 > 0$. ■

J.3.2 Stability Notions and Sufficient Lyapunov Conditions for SDIs with Inputs

We now consider SDIs of the form (J.3) for the general case when the input u is different from zero. The following stability notion aims to capture the effect of the size of the input on the convergence of the solutions of (J.3). It is aligned with the notions of input-to-state stability [257] and practical input-to-state stability studied in deterministic systems [91].

Definition 17 *The SDI* (J.3) *is said to be mean-square input-to-state practically stable (MSISpS) relative to the compact set* $\mathcal{A}$ *if:*

(a) The set $\mathcal{A}$ *is MSPES for* (J.3) *when* $\lambda(x) = 0$.

(b) There exists $\gamma \in \mathcal{K}_\infty$ *and* δ^* *such that for each* $\delta \in (0, \delta^*)$ *and* $c > 0$, *the set* $\mathcal{A} + \gamma(c)\mathbb{B}$ *is UGPPR for* (J.3) *when* $\lambda(x) = c$, *for all* $x \in D$.

By the definition of (J.3), when $\lambda(x) = 0$ we have that $u = 0$. Therefore, according to the definition (17), if the input of the system is set to zero, the notion of MSISpS coincides with the notion of MSPES. On the other hand, for the general case when $\lambda(x) \neq 0$, Definition (17) asks that for each $\varepsilon > 0$ the open set $\mathcal{A} + (\gamma(c) + \varepsilon)\mathbb{B}^o$ satisfies the property

$$\mathbb{E}\left[\inf\left\{k \in \mathbb{Z}_{\geq 0} : \mathbf{x}_k \in \mathcal{A} + (\gamma(c) + \varepsilon)\mathbb{B}^o\right\}\right] \leq M_\delta, \tag{J.16}$$

for all $\mathbf{x} \in \mathcal{S}_r(K)$ and some M_δ.

Using Propositions 17 and 18 we obtain directly the following theorem.

Theorem 14 *Let $\mathcal{A} \subset \mathbb{R}^n$ be compact, and consider the system (J.1) under Assumption 43. If, in addition to* (J.12a)*, the following condition holds:*

$$\int_{\mathbb{R}^n} V(x^+)\mu(dv) \leq \left(1 - \frac{1}{4}\delta\eta\right) V(x) + \delta^{\frac{3}{2}} K, \quad \forall \ \|x\|_{\mathcal{A}} \geq \frac{2\sqrt{\delta}}{\eta \underline{c}} |u|^2, \tag{J.17}$$

then the system is MSISpS.

Proof: Follows directly by applying Propositions 17 and 18, and using (J.12a). ■

Appendix K

Stochastic Hybrid Dynamical Systems and Proofs of Chapter 6

A stochastic hybrid dynamical system is characterized by the equation

$$\dot{x} \in F(x), \qquad x \in C \tag{K.1a}$$

$$x^+ \in G_\delta(x, v^+), \quad x \in D, \quad v \sim \mu(\cdot), \tag{K.1b}$$

where the set-valued mappings $F : \mathbb{R}^n \rightrightarrows \mathbb{R}^n$ and $G_\delta : \mathbb{R}^n \times \mathbb{R}^m \rightrightarrows \mathbb{R}^n$, called the flow map and the jump map, respectively, describe the evolution of the state x when it belongs to the flow set C or/and and the jump set D, respectively. The distribution function μ is derived from the probability space $(\Omega, \mathcal{F}, \mathbb{P})$ and a sequence of independent, identically distributed (i.i.d) input random variables $v_i : \Omega \to \mathbb{R}^m$ defined on $(\Omega, \mathcal{F}, \mathbb{P})$ for $i \in \mathbb{Z}_{\geq 1}$. Then, μ is defined as $\mu(A) := \mathbb{P}(\omega \in \Omega : \mathbf{v}_i(\omega) \in A)$ for every $A \in \mathbf{B}(\mathbb{R}^m)$. We denote by $\mathcal{F}_i$ the collection of sets $\{\omega : (\mathbf{v}_1(\omega), \ldots, \mathbf{v}_i(\omega)) \in A\}$, $A \in \mathbf{B}((\mathbb{R}^m)^i)$ which are the sub-σ fields of $\mathcal{F}$ that form the natural filtration of $\mathbf{v} = \{\mathbf{v}_i\}_{i=1}^{\infty}$. To define the solutions for the SHDS (K.1) we impose the following

conditions on the data of the system:

(C1) The sets C and D are closed.

(C2) F is OSC and LB relative to C, and $F(x)$ is convex and nonempty for every $x \in C$.

(C3) For each $\delta \in \mathbb{R}_{>0}$ the mapping G_δ is LB and the mapping $v \mapsto \text{graph}(G_\delta(\cdot, v)) := \{(x, y) \in \mathbb{R}^{2n} : y \in G_\delta(x, v)\}$ is measurable with closed values.

Solutions of (K.1) are defined on *hybrid time domains*. We recall [78, Chap. 2] that a compact hybrid time domain is a subset of $\mathbb{R}_{\geq 0} \times \mathbb{Z}_{\geq 0}$ of the form $\bigcup_{j=0}^{J}([t_j, t_{j+1}] \times \{j\})$ for some nonnegative integer J and some real numbers $0 = t_0 \leq t_1 \leq \ldots \leq t_{J+1}$. A hybrid time domain is a set $H \subset \mathbb{R}_{\geq 0} \times \mathbb{Z}_{\geq 0}$ such that, for each $(T, J) \in H$ the set $H \cap ([0, T] \times \{0, \ldots, J\})$ is a compact time domain. A *hybrid arc* is a mapping $\phi : H \to \mathbb{R}^n$ such that H is a hybrid time domain and, for each $j \in \mathbb{Z}_{\geq 0}$, $t \to \phi(t, j)$ is locally absolutely continuous. Given a measure space $(\Omega, \mathcal{F})$, a *stochastic hybrid arc* is a mapping $\mathbf{x}$ defined on Ω such that $\mathbf{x}(\omega)$ is a hybrid arc for each $\omega \in \Omega$ and the set-valued mapping from Ω to $\mathbb{R}^{n+2}$ defined by $\omega \mapsto \text{graph}(\mathbf{x}(\omega)) := \{(t, j, z) \in \mathbb{R}^{n+2} : \phi = \mathbf{x}(\omega), (t, j) \in \text{dom}(\phi), z = \phi(t, j)\}$ is $\mathcal{F}$-measurable. Define $\mathcal{F}_0 := \{\Omega, \emptyset\}$, and let $\{\mathcal{F}_i\}_{i=1}^{\infty}$ denote the minimal filtration associated to the random process $\{v_i\}_{i=1}^{\infty}$. An $(\{\mathcal{F}_j\}_{j=0}^{\infty})$-*adapted stochastic hybrid arc* is a stochastic hybrid arc such that the set-valued mapping $\omega \mapsto \text{graph}(\mathbf{x}(\omega)) \cap (\mathbb{R}_{\geq 0} \times \{0, \ldots, j\} \times \mathbb{R}^n)$ is $\mathcal{F}_j$ measurable for each $j \in \mathbb{Z}_{\geq 0}$. An adapted stochastic hybrid arc $\mathbf{x}$ is a *solution* to (K.1) from $x \in \mathbb{R}^n$, denoted by $\mathbf{x} \in \mathcal{S}_r(x)$, if with the definition $\phi_\omega := \mathbf{x}(\omega)$ for each $\omega \in \Omega$, we have that for each $\omega \in \Omega$:

1. $\phi_\omega(0, 0) = x$.

2. If $(t_1, j), (t_2, j) \in \mathrm{dom}(\phi_\omega)$ with $t_1 < t_2$ then, for almost every $t \in [t_1, t_2]$, $\phi_\omega(t, j) \in C$ and $\dot{\phi}_\omega \in F(\phi_\omega(t, j))$.

3. If $(t, j), (t, j{+}1) \in \mathrm{dom}(\phi_\omega)$, then $\phi_\omega(t, j) \in D$ and $\phi_\omega(t, j{+}1) \in G_\delta(\phi_\omega(t, j), \mathbf{v}_{j+1}(\omega))$.

We use the notation $\mathbf{x} \in \mathcal{S}_r(K)$, where $K \subset \mathbb{R}^n$, to indicate that $\mathbf{x}$ is a solution to the hybrid system (K.1) starting at some $x \in K$.

K.1 Proof of Lemma 9

Let $k \to (\alpha_i(k), \ell_i(k))$ be a complete solution of (6.12). It is immediate that

$$\ell_i(k+1) \geq \ell_i(k) - \rho + 1 - \alpha_i(k) \qquad \forall k \in \mathbb{Z}_{\geq 0},$$

and taking the summation from j_1 to $j_2 - 1$ we obtain

$$\ell_i(j_2) - \ell_i(j_1) \geq -\rho(j_2 - j_1) + \sum_{k=j_1}^{j_2-1} \Big(1 - \alpha_i(k)\Big). \tag{K.2}$$

Since the solution is complete, $\ell_i(k) \in [0, M]$ for all $k \in \mathbb{Z}_{\geq 0}$. Therefore,

$$\begin{aligned} M \geq \ell_i(j_2) &\geq \ell_i(j_1) - \rho(j_2 - j_1) + \sum_{k=j_1}^{j_2-1} \Big(1 - \alpha_i(k)\Big) \\ &\geq -\rho(j_2 - j_1) + \sum_{k=j_1}^{j_2-1} \Big(1 - \alpha_i(k)\Big). \end{aligned}$$

Rearranging this inequality gives the desired result. Now let $\alpha_i : \mathbb{Z}_{\geq 0} \to \{0, 1\}$ satisfy (6.13). Set $\ell_i(0) = 0$. Suppose there exists $\overline{k} \in \mathbb{Z}_{\geq 0}$ such that $\ell_i(\overline{k}{+}1) > M$. Then there exists $\underline{k} \in \mathbb{Z}_{\geq 0}$ such that $\ell_i(\underline{k}) = 0$, $\ell_i(k) \in [0, M]$ and $\ell_i(k+1) = \ell_i(k) + 1 - \rho - \alpha_i(k)$

for all $k \in \{\underline{k}, \ldots, \overline{k}\}$. Thus,

$$\begin{aligned}\ell_i(\overline{k}+1) &= \ell_i(\underline{k}) - \rho(\overline{k}-\underline{k}) + \sum_{k=\underline{k}}^{\overline{k}}(1-\alpha_i(k)) \\ &\leq -\rho(\overline{k}-\underline{k}) + M + \rho(\overline{k}-\underline{k}) = M \ ,\end{aligned}$$

which is a contradiction. ■

K.2 Proof of Theorem 9

System (6.15) satisfies Assumption 1, and since $G_\delta(x,v) \neq \emptyset$ for all $x \in D$, and by Lemma 9, we have that maximal solutions are almost surely complete.

To analyze the dynamics learning dynamics, we draw special attention to the dynamics of $\hat{u}$. To save on notation, we define

$$Q = \begin{bmatrix} Q_1 \\ \vdots \\ Q_n \end{bmatrix}, \quad L = \begin{bmatrix} L_1 \\ \vdots \\ L_n \end{bmatrix}. \tag{K.3}$$

Then, using (K.3) it follows that $\hat{u}^+$ has the form

$$\hat{u}^+ = \hat{u} + I(\delta_s)I(q)g(q,\hat{u},v), \tag{K.4}$$

which can be rewritten as

$$\begin{aligned}g(q,\hat{u},v) =& \Big[\Big(I(v)\otimes v^\top\Big)\Big(I\otimes I(q)I(\delta_p+\delta_m)\Big)\Big] \\ &\Big(Q2\hat{u}+L\Big) + \sqrt{\delta}|\delta_p-\delta_m|O(1).\end{aligned} \tag{K.5}$$

This implies that

$$\hat{u}^+ = \hat{u} + \delta \cdot O(\max\{1, |\hat{u}|\}). \tag{K.6}$$

Moreover, using Assumption 42 we obtain

$$\int_{\mathbb{R}^n} \left(I(v) \otimes v^T\right) \mu(dv) = \sum_{i=1}^{n} \left(I(e_i) \otimes e_i^T\right), \tag{K.7}$$

and thus, using (K.4), (K.41), (K.7), and the definition of u^* in (6.4) we have that

$$\begin{aligned} \int_{\mathbb{R}^n} g(q, \hat{u}, v)\mu(dv) =& I(q)I(\delta_p + \delta_m)2A(\hat{u} - u^*) \\ &+ \sqrt{\delta} \cdot |\delta_p - \delta_m| \cdot O(1). \end{aligned} \tag{K.8}$$

Using Assumption 40 of Section 6.1, let $w \in \mathbb{R}^n_{>0}$ be such that $I(w)A$ is symmetric and negative definite. Define

$$P := -I(w)A \tag{K.9a}$$

$$R(\hat{u}) := P(\hat{u} - u^*) \tag{K.9b}$$

$$V_1(\hat{u}) := R(\hat{u})^T P^{-1} R(\hat{u}) \tag{K.9c}$$

$$V_2(x) := R(\hat{u})^T \left((M+1)I - I(\ell)\right) R(\hat{u}) \tag{K.9d}$$

$$V(x) := V_1(\hat{u}) + \delta\mu V_2(x) \tag{K.9e}$$

$$\mu := 4 \min_{i \in \{1,\ldots,n\}} \frac{k_{s,i}(k_{p,i} + k_{s,i})}{w_i}. \tag{K.9f}$$

Due to these definitions, there exist positive real numbers $\underline{c}, \overline{c}$ such that, for all $\delta \in (0, 1)$

$$\underline{c}\|\hat{u}\|_{\mathcal{A}}^2 \leq V(x) \leq \overline{c}\|\hat{u}\|_{\mathcal{A}}^2 \qquad \forall x \in D, \tag{K.10}$$

where $\|\hat{u}\|_{\mathcal{A}} = \|\hat{u} - u^*\|$ since $q_i \in \{0, 1\}$ and $\ell_i \in [0, M]$, for all $i \in \{1, \ldots, n\}$. It follows from (6.12) that

$$I(\ell^+) \geq I(\ell) + (1 - \rho)I - I(q). \tag{K.11}$$

Therefore, using (K.6),

$$\begin{aligned}
V_2(x^+) &= R(\hat{u}^+)^\top \left((M+1)I - I(\ell^+)\right) R(\hat{u}^+) \\
&\leq R(\hat{u} + \delta O(\max\{1, |\hat{u}|\}))^\top \Big((M+1)I - I(\ell) \\
&\quad - (1-\rho)I + I(q)\Big) R(\hat{u} + \delta O(\max\{1, \|\hat{u}\|\})) \\
&\leq R(\hat{u})^\top \Big((M+1)I - I(\ell)\Big) R(\hat{u}) \\
&\quad - (1-\rho) R(\hat{u})^\top R(\hat{u}) + R(\hat{u})^\top I(q) R(\hat{u}) \\
&\quad + \delta O(\max 1, \|\hat{u}\|^2) \\
&\leq V_2(x) - (1-\rho) R(\hat{u})^\top R(\hat{u}) + R(\hat{u})^\top I(q) R(\hat{u}) \\
&\quad + \delta O(\max\{1, \|\hat{u}\|^2\}).
\end{aligned} \tag{K.12}$$

Also,

$$\begin{aligned}
V_1(\hat{u}^+) =& R(\hat{u} + I(\delta_s)g)^\top P^{-1} R(\hat{u} + I(\delta_s)g) \\
=& \left[P(\hat{u} - \hat{u}^* + I(\delta_s)g)\right]^\top P^{-1} \left[P(\hat{u} - u^* + I(\delta_s)g)\right] \\
=& \Big[\left[P(\hat{u} - u^*)\right]^\top + \left[PI(\delta_s)g\right]^\top\Big] P^{-1} \Big[\left[P(\hat{u} - u^*)\right] \\
&+ \left[PI(\delta_s)g\right]\Big] \\
=& R(\hat{u})^\top P^{-1} R(\hat{u}) + (\hat{u} - u^*)^\top PI(\delta_s)g + \\
&(I(\delta_s)g)^\top P(\hat{u} - u^*) + g^\top I(\delta_s) PI(\delta_s) g \\
=& V_1(\hat{u}) + 2(\hat{u-u^*})^\top PI(\delta_s)g + g^\top I(\delta_s) PI(\delta_s) g,
\end{aligned} \tag{K.13}$$

where for ease of notation we have omitted the arguments of g. Using (K.8) and (K.13) we get

$$\begin{aligned}\int_{\mathbb{R}^n} V_1(\hat{u}^+)\mu(dv) = V_1(\hat{u}) + 2(\hat{u}-u^*)^\top PI(\delta_s)\Big[I(\delta_p \\ + \delta_m)I(q)2A(\hat{u}-u^*) + \sqrt{\delta}\cdot|\delta_p-\delta_m|O(1)\Big] \\ + \int_{\mathbb{R}^n} g^\top I(\delta_s)PI(\delta_s)g\ \mu(dv).\end{aligned} \tag{K.14}$$

After a set of lengthy calculations we obtain

$$\begin{aligned}\int_{\mathbb{R}^n} g^\top I(\delta_s)PI(\delta_s)g\ \mu(dv) \leq & \delta^2 O\left(\max\{1,\|\hat{u}\|^2\}\right) \\ & + \delta^{5/2}O\left(\max\{1,\|\hat{u}\|\}\right) \\ & + \delta^3 O(1),\end{aligned}$$

which combined with (K.14) and (K.9f) implies

$$\begin{aligned}\int_{\mathbb{R}^n} V_1(\hat{u}^+)\mu(dv) \leq & V_1(\hat{u}) - \delta\mu R(\hat{u})^T I(q)R(\hat{u}) \\ & + \delta^{3/2}\cdot O\left(\max\left\{1,\|\hat{u}\|^2\right\}\right).\end{aligned} \tag{K.15}$$

Using (K.12) and (K.15) we have

$$\begin{aligned}\int_{\mathbb{R}^n} V(x^+)\mu(dv) &= \int_{\mathbb{R}^n}\left(V_1(\hat{u}^+)+\delta\mu V_2(x^+)\right)\mu(dv) \\ &\leq V_1(\hat{u}) + \delta\mu V_2(x) - \delta\mu(1-\rho) \\ & R(\hat{u})^T R(\hat{u}) + \delta^{3/2}O(\max\left\{1,\|\hat{u}\|^2\right\}).\end{aligned} \tag{K.16}$$

Let $\bar{P} := P^{-1} + (M+1)\delta\mu I$, and define

$$\eta := \mu(1-\rho)\lambda_{min}(\bar{P}^{-1}). \tag{K.17}$$

Equation (K.17) implies that $\mu(1-\rho)R(\hat{u})^\top R(\hat{u}) \geq \eta V(x)$, for all $\delta \in (0,1)$, and then using (K.10) we obtain

$$\begin{aligned}\int_{\mathbb{R}^n} V(x^+)\mu(dv) \leq & V(x) - \delta\eta V(x) + \delta^{\frac{3}{2}} O(\max\left\{1, \|\hat{u}\|^2\right\}) \\ \leq & V(x) - \delta\eta V(x) + \delta^{\frac{3}{2}} K + \delta^{\frac{3}{2}} K V(x) \end{aligned} \tag{K.18}$$

which gives the existence of $K > 0$, such that for δ sufficiently small we have that

$$\int_{\mathbb{R}^n} V(x^+)\mu(dv) \leq (1 - 0.5\delta\eta)V(x) + \delta^{\frac{3}{2}} K. \tag{K.19}$$

for all $x \in D$, which implies by that the compact set $\mathcal{A}$ is MSP-ES, with $\lambda = 0.5\eta$, and $\kappa = 3/2$. ■

K.3 Proof of Theorem 10

Focusing on the upper $s \times s$ block of A, denoted $A_{s\times s}$, it necessarily follows that there exists $w \in \mathbb{R}^s_{>0}$ such that $I_s(w)A_{s\times s}$ is symmetric and negative definite. Indeed,

$$\begin{bmatrix} I_s & 0 \end{bmatrix} \begin{bmatrix} I_a(w) & 0 \\ 0 & I_b(w) \end{bmatrix} A \begin{bmatrix} I_s \\ 0 \end{bmatrix} = I_a(w)A_{s\times s}. \tag{K.20}$$

Since the matrix on the left-hand side is symmetric and negative definite, it follows that $I_a(w)A_{s\times s}$ is symmetric and negative definite. We also note that in the case of a one-player sub-game, taken to be player i, if $(Q_i)_{ii} < 0$ then Assumption 40 holds for the sub-game. Thus, we can consider the analysis in the proof of Theorem 9 changing the payoff mapping to be a mapping $J : \mathbb{R}^{n+d} \to \mathbb{R}^n$ and partitioning the matrices Q_i so that the matrix A formed from the upper $s \times s$ blocks of Q_i satisfies Assumption

40. In general, we still have (K.41) which we can write with

$$u_a = \begin{bmatrix} u + I(\delta_p)I(q)v \\ u_p \end{bmatrix} u_b = \begin{bmatrix} u - I(\delta_m)I(q)v \\ u_m \end{bmatrix} \tag{K.21}$$

as

$$\begin{aligned} J_i(u_a) - J_i(u_b) = &\Big[(I(\delta_p + \delta_m)I(q)v)^T, (u_p \\ &- u_m)^T\Big] \left(Q_i \begin{bmatrix} 2u \\ 2u^* \end{bmatrix} + Q_i \begin{bmatrix} I(\delta_p - \delta_m)I(q)v \\ u_p + u_m - 2u^* \end{bmatrix} + L_i \right). \end{aligned}$$

In this case Eq. (K.41) can be written as,

$$\begin{aligned} g(q,u,v) =& I\left([v, \mathbf{0}]\right) \left[I \otimes \left([v^\top, \mathbf{1}^\top]M_b\right)\right] \left(2Q \begin{bmatrix} u \\ u^* \end{bmatrix} \right. \\ &\left. + QM_c + L_i \right), \end{aligned} \tag{K.22}$$

where $\mathbf{0} \in \mathbb{R}^s$, $\mathbf{1} \in \mathbb{R}^s$, and where the block matrices M_b and M_c are defined as

$$M_b := \begin{bmatrix} I(q)I(\delta_p + \delta_m), \mathbf{0} \\ \mathbf{0}, I(u_p - u_m) \end{bmatrix}, \tag{K.23}$$

$$M_c := \begin{bmatrix} I(\delta_p - \delta_m)I(q)v \\ u_p + u_m - 2u^* \end{bmatrix}. \tag{K.24}$$

Using the mixed product property of the Kronecker product we can rewrite (K.22) as

$$g(q,u,v) = \Big(I\left([v,\mathbf{0}]\right)\otimes[v^\top,\mathbf{1}^\top]\Big)\left[I\otimes M_b\right]\left(2Q\begin{bmatrix}u\\u^*\end{bmatrix}+ L\right)+\Big(I\left([v,\mathbf{0}]\right)\otimes[v^\top,\mathbf{1}^\top]\Big)\left[I\otimes M_b\right]2QM_c \tag{K.25}$$

In this case we have that (K.7) is now given by the block matrix

$$\int_{\mathbb{R}^n}\left(I\left([v,\mathbf{0}]\right)\otimes[v^\top,\mathbf{1}^\top]\right)\mu(dv)=\left[\sum_{i=1}^{n}\left(I(e_i)\otimes e_i^T\right)|\mathbf{0}_{s\times s}\right],$$

and we now obtain that

$$\begin{aligned}&\int_{\mathbb{R}^n} g(q,u,v)\mu(dv) =\\ &= I\left([q^\top,\mathbf{0}^\top]\right)I\left([(\delta_p+\delta_m)^\top,\mathbf{0}^\top]\right)\left(2A\begin{bmatrix}\left[u\right]_{n-r\times 1}\\ \left[u^*\right]_{r\times 1}\end{bmatrix}+B\right)\\ &+2\int_{\mathbb{R}^n}\Big(I\left([v,\mathbf{0}]\right)\otimes[v^\top,\mathbf{1}^\top]\Big)\left[I\otimes M_b\right]QM_c\mu(dv)\end{aligned} \tag{K.26}$$

For each of the n players we partition each matrix Q_i as

$$Q^i=\left[\begin{array}{c|c}Q^i_s & Q^{i^\top}_{ns}\\ \hline Q^i_{ns} & Q^i_{nn}\end{array}\right] \tag{K.27}$$

Using this partitioning we get that

$$[I \otimes M_b]\, Q = \left[\begin{array}{c|c} I(q\delta^+)Q_s^1 & I(q\delta^+)Q_{ns}^{1^\top} \\ \hline I(u_{pm}^-)Q_{ns}^1 & I(u_{pm}^-)Q_{nn}^1 \\ \hline I(q\delta^+)Q_s^2 & I(q\delta^+)Q_{ns}^{2^\top} \\ \hline I(u_{pm}^-)Q_{ns}^2 & I(u_{pm}^-)Q_{nn}^2 \\ \hline \vdots & \vdots \\ \hline I(q\delta^+)Q_s^n & I(q\delta^+)Q_{ns}^{n^\top} \\ \hline I(u_{pm}^-)Q_{ns}^n & I(u_{pm}^-)Q_{nn}^n \end{array}\right] \tag{K.28}$$

such that $[I \otimes M_b]\, QM_c$ is given by

$$[I \otimes M_b]\, QM_c = \left[\begin{array}{c} I(q\delta^+)Q_s^1 I(q\delta^-)v + I(q\delta^+)Q_{ns}^{1^\top} u_{pm}^+ \\ \hline I(u_{pm}^-)Q_{ns}^1 I(q\delta^-)v + I(u_{pm}^-)Q_{nn}^1 u_{pm}^+ \\ \hline I(q\delta^+)Q_s^2 I(q\delta^-)v + I(q\delta^+)Q_{ns}^{2^\top} u_{pm}^+ \\ \hline I(u_{pm}^-)Q_{ns}^2 I(q\delta^-)v + I(u_{pm}^-)Q_{nn}^2 u_{pm}^+ \\ \hline \vdots \\ \hline I(q\delta^+)Q_s^n I(q\delta^-)v + I(q\delta^+)Q_{ns}^{n^\top} u_{pm}^+ \\ \hline I(u_{pm}^-)Q_{ns}^n I(q\delta^-)v + I(u_{pm}^-)Q_{nn}^n u_{pm}^+ \end{array}\right]$$

and then the argument of the integral in the second term of Eq. (K.26) can be written as

$$
\begin{aligned}
=&I(v)\begin{bmatrix}
v^\top\left[I(q\delta^+)Q_s^1I(q\delta^-)v+I(q\delta^+)Q_{ns}^{1^\top}u_{pm}^+\right]+\\
\mathbf{1}^\top[I(u_{pm}^-)Q_{ns}^1I(q\delta^-)v+I(u_{pm}^-)Q_{nn}^1u_{pm}^+]\\
\hline
v^\top\left[I(q\delta^+)Q_s^2I(q\delta^-)v+I(q\delta^+)Q_{ns}^{2^\top}u_{pm}^+\right]+\\
\mathbf{1}^\top\left[I(u_{pm}^-)Q_{ns}^2I(q\delta^-)v+I(u_{pm}^-)Q_{nn}^2u_{pm}^+\right]\\
\hline
\vdots\\
\hline
v^\top\left[I(q\delta^+)Q_s^{n-r}I(q\delta^-)v+I(q\delta^+)Q_{ns}^{n-r^\top}u_{pm}^+\right]+\\
\mathbf{1}^\top\left[I(u_{pm}^-)Q_{ns}^{n-r}I(q\delta^-)v+I(u_{pm}^-)Q_{nn}^{n-r}u_{pm}^+\right]\\
\hline
\mathbf{0}_{r\times1}
\end{bmatrix}\\
=&\begin{bmatrix}
v_1\left(v^\top\left[I(q\delta^+)Q_s^1I(q\delta^-)v+I(q\delta^+)Q_{ns}^{1^\top}u_{pm}^+\right]+\right.\\
\left.\mathbf{1}^\top[I(u_{pm}^-)Q_{ns}^1I(q\delta^-)v+I(u_{pm}^-)Q_{nn}^1u_{pm}^+]\right)\\
\hline
v_2\left(v^\top\left[I(q\delta^+)Q_s^2I(q\delta^-)v+I(q\delta^+)Q_{ns}^{2^\top}u_{pm}^+\right]+\right.\\
\left.\mathbf{1}^\top\left[I(u_{pm}^-)Q_{ns}^2I(q\delta^-)v+I(u_{pm}^-)Q_{nn}^2u_{pm}^+\right]\right)\\
\hline
\vdots\\
\hline
v_{n-r}\left(v^\top\left[I(q\delta^+)Q_s^{n-r}I(q\delta^-)v+I(q\delta^+)Q_{ns}^{n-r^\top}u_{pm}^+\right]+\right.\\
\left.\mathbf{1}^\top\left[I(u_{pm}^-)Q_{ns}^{n-r}I(q\delta^-)v+I(u_{pm}^-)Q_{nn}^{n-r}u_{pm}^+\right]\right)\\
\hline
\mathbf{0}_{r\times1}
\end{bmatrix}
\end{aligned}
\tag{K.29}
$$

where each block in (K.29) corresponds to a scalar associated to each player. Defining $M_{i,1}=I(q\delta^+)Q_s^iI(q\delta^-)$, $M_{i,2}=I(q\delta^+)Q_{ns}^{1^\top}u_{pm}^+$, $M_{i,3}=I(u_{pm}^-)Q_{ns}^{n-r}I(q\delta^-)$, and $M_{i,4}=$

$I(u_{pm}^{-})Q_{nn}^{n-r}u_{pm}^{+}$, each block associated to each player can be written as

$$v_i(v^\top M_{i,1}v) + v_i(v^\top M_{i,2}) + v_i(\mathbf{1}^\top M_{i,3}v) + v_i(\mathbf{1}^\top M_{i,4}) \tag{K.30}$$

and due to the zero-mean property of v we have that

$$\int_{\mathbb{R}^n} v_i(\mathbf{1}^\top M_{i,4})\mu(dv) = 0. \tag{K.31}$$

Also we have that

$$\int_{\mathbb{R}^n} v_i(v^\top M_{i,1}v)\mu(dv) = \sqrt{\delta}|\delta_p - \delta_m|O(1). \tag{K.32}$$

Similarly we have that

$$\begin{aligned} v_i(v^\top M_{i,2}) &= v_i\left(u_{pm}^{+\top}Q_{ns}^{i}I(q\delta^{+})v_s\right)^\top \\ &= v_i\Big(u_{pm}^{+\top}\big(Q_{ns,col_1}^{i}\delta_1^{+}q_1v_1 + \dots \\ &\quad + Q_{ns,col_j}^{i}\delta_j^{+}q_jv_j + \\ &\quad \dots + Q_{ns,col_{n-r}}^{1}\delta_{n-r}^{+}q_{n-r}v_{n-r}\big)\Big)^\top \end{aligned} \tag{K.33}$$

and using the fact that $\mathbb{E}[vv^\top] = I$ we obtain that

$$\begin{aligned} \int_{\mathbb{R}^n} v_i(v^\top M_{i,2}\mu(dv) &= \left(u_{pm}^{+\top}Q_{ns,col_i}^{i}\delta_i^{+}q_i\right)^\top \\ &= \delta_i^{+}q_iQ_{ns,col_i}^{i\top}u_{pm}^{+} \\ &= \delta_i^{+}q_iu_{pm}^{+\top}Q_{ns,col_i}^{i} \end{aligned} \tag{K.34}$$

The same reasoning can be applied to $M_{i,3}$, obtaining

$$\int_{\mathbb{R}^n} v_i(v^\top M_{i,3}\mu(dv) = \delta_i^- q_i u_{pm}^{-\top} Q^i_{ns,col_i}. \tag{K.35}$$

Therefore, for each i^{th} player, the second term in (K.26) is given by

$$\begin{aligned}
&= 2\delta_i^+ q_i u_{pm}^{+\top} Q^{i\top}_{ns,col_i} + 2\delta_i^- q_i u_{pm}^{-\top} Q^i_{ns,col_i} \\
&= 2q_i \left[\delta_i^+ u_{pm}^+ + \delta_i^- u_{pm}^-\right]^\top Q^i_{ns,col_i} \\
&= 2q_i \Big[(\delta_{p,i} + \delta_{m,i})(u_{p,i} + u_{m,i} - 2u_i^*) \\
&\quad + (\delta_{p,i} - \delta_{m,i})(u_{p,i} - u_{m,i})\Big]^\top Q^i_{ns,col_i} \\
&= 2q_i \Big[\delta_{p,i} d_p + \delta_{m,i} d_m\Big]^\top Q^i_{ns,col_i} \\
&= 2q_i \delta_{p,i} \left(Q^i_{ns,col_i}\right)^\top d_p + 2q_i \delta_{m,i} \left(Q^i_{ns,col_i}\right)^\top d_m
\end{aligned} \tag{K.36}$$

Finally, using the symmetry of each matrix Q we have that (K.36) can be written as

$$= 2q_i \delta_{p,i} Q^i_{ns,row_i} d_p + 2q_i \delta_{m,i} Q^i_{ns,row_i} d_m, \forall\ i \in \{1, \ldots, n\} \tag{K.37}$$

Now, recall that the matrix A is given by the matrix whose i^{th} row corresponds to the i^{th} row of Q_i. Therefore we can also partition A as

$$A = \left[\begin{array}{c|c} A_s & A^r_{ns} \\ \hline A^L_{ns} & A_{nn} \end{array}\right] \tag{K.38}$$

where the upper block contains the entries of the matrices Q_i associated to players that are still aiming to converge to the Nash equilibrium. Using (K.38), (K.32), and (6.4)

we obtain that (K.26) is given by

$$\begin{aligned}
&\int_{\mathbb{R}^n} g(q,u,v)\mu(dv) = \\
&I\left([q^\top, \mathbf{0}^\top]\right) I\left([(\delta_p+\delta_m)^\top, \mathbf{0}^\top]\right) \left(2A \begin{bmatrix} \left[u-u^*\right]_{n-r\times 1} \\ \left[\mathbf{0}\right]_{r\times 1} \end{bmatrix} \right) \\
&+ \begin{bmatrix} 2I(q)I(\delta_p)A_{ns}^r d_p + 2I(q)I(\delta_m)A_{ns}^r d_m + \sqrt{\delta}|\delta_p-\delta_m|O(1) \\ \mathbf{0} \end{bmatrix}
\end{aligned} \tag{K.39}$$

and therefore we obtain that the dynamics of the agents who are still trying to achieve a Nash equilibrium are given by

$$\begin{aligned}
u^+ &= u + I(\delta_s)I(q)I(\delta_p+\delta_m)2A(u-u^*) \\
&\quad + \delta_s\sqrt{\delta}|\delta_p-\delta_m|O(1) + 2I(q)\delta\gamma_1 d_p + I(q)\delta\gamma_2 d_m, \\
&= u + \delta O(\max\{1,|u|,|d_p|,|d_m|\})
\end{aligned} \tag{K.40}$$

where $\gamma_1 := I(k_s)I(k_p)A_{ns}^r$, and $\gamma_2 := I(k_s)I(k_m)A_{ns}^r$.

Using the same quadratic Lyapunov function $V(x)$ as in [231], and following a similar analysis we now obtain the following inequality

$$\begin{aligned}
\int_{\mathbb{R}^n} V(x^+)\mu(dv) &\leq V(x) - \delta\eta V(x) \\
&\quad + \delta^{\frac{3}{2}} O\left(\max\left\{1, \|u\|^2, |d_p|^2, |d_m|^2\right\}\right), \\
&\leq V(x) - \delta\eta V(x) + \delta^{\frac{3}{2}}K + \delta\delta^{\frac{1}{2}}KV(x) \\
&\quad + \delta^{\frac{3}{2}}\left(d_p^2 + d_m^2\right),
\end{aligned}$$

selecting $\delta \in (0,1)$ such that $\delta^{\frac{1}{2}} K \leq 0.25\eta$ we obtain that

$$\begin{aligned}\int_{\mathbb{R}^n} V(x^+)\mu(dv) &\leq V(x) - \delta\eta V(x) + \delta^{\frac{3}{2}} K + \delta\frac{1}{4}\eta V(x) \\ &\quad + \delta^{\frac{3}{2}}\left(d_p^2 + d_m^2\right) \\ &\leq \left(1 - \frac{1}{4}\delta\eta\right) V(x) + \delta^{\frac{3}{2}} K - \frac{1}{2}\delta\eta V(x) \\ &\quad + \delta^{\frac{3}{2}}\left(d_p^2 + d_m^2\right)\end{aligned}$$

Using the fact that $V(x)$ is quadratic we obtain

$$\begin{aligned}\int_{\mathbb{R}^n} V(x^+)\mu(dv) &\leq V(x) - \delta\eta V(x) + \delta^{\frac{3}{2}} K + \delta\frac{1}{4}\eta V(x) \\ &\quad + \delta^{\frac{3}{2}}\left(d_p^2 + d_m^2\right) \\ &\leq \left(1 - \frac{1}{4}\delta\eta\right) V(x) + \delta^{\frac{3}{2}} K - \frac{1}{2}\delta\eta\underline{c}\|x\|_{\mathcal{A}} \\ &\quad + \delta^{\frac{3}{2}}\left(d_p^2 + d_m^2\right)\end{aligned}$$

which implies that

$$\begin{aligned}\int_{\mathbb{R}^n} V(x^+)\mu(dv) \leq \left(1 - \frac{1}{4}\delta\eta\right) V(x) + \delta^{\frac{3}{2}} K, \\ \forall\ \|x\|_{\mathcal{A}} \geq \frac{2\sqrt{\delta}}{\eta\underline{c}}|d|^2,\end{aligned}$$

which establishes MSISpS with respect to the input $d = [d_p, d_m]^\top$ and the parameter δ. ■

K.4 Proof of Theorem 11

The proof starts by noticing that for any initial condition $(\tau_c(0,0), z_c(0,0)) \in [0,1] \times Z$, the evolution of τ_c and z_c is independent of the other states. Moreover, by the automaton-like behavior induced by the SHDS (6.19), for any $\Delta T > 0$ the state z_c will hit in order every mode in Z infinitely often, and since the function f_τ in (6.20) resets τ_c whenever there is a jump from the modes 2 and 3, there exists a time (t^*, j^*) such that for all (t, j) in the domain of a solution satisfying $t + j \geq t^* + j^*$ we have that $z_c(t, j) \in \{4, 1\}$ implies that $\tau_c(t, j) = 0$. This establishes the uniform attractivity and invariance of the set $\mathcal{A}_{\tau,q}$. Now, let $K_\theta \subset \mathbb{R}^p$ and $K_u = [-\varepsilon_1, \varepsilon_1] \times \ldots \times [-\varepsilon_n, \varepsilon_n]$. By Proposition 13, for each $\rho > 0$ there exists ΔT, such that (6.22) holds. Since $H(\cdot)$ in M_{K_u} is OSC and LB, then $H(\cdot)$ is upper-semicontinuous on compact sets, which implies that for each $\epsilon_1 > 0$ there exists $\rho > 0$ such that $H(K_u + \rho\mathbb{B}) \subset H(K_u) + \epsilon_1\mathbb{B}$. Moreover, since $\varphi(\cdot)$ is continuous, for each $\epsilon_0 > 0$ there exists an $\epsilon_1 > 0$ such that $\varphi_i(H(K_u) + \epsilon_1\mathbb{B}, K_u) \subset \varphi_i(H(K_u), K_u) + \epsilon_0\mathbb{B} = J_i(K_u) + \epsilon_0\mathbb{B}$. Now note that the state $\hat{u}$ is updated only at the mode 4, and via the dynamics (6.8). Assuming that $s = v$, and $\hat{y}_i = (J_i(u_a), J_i(u_b))^\top$, and based on [231], this dynamics can be written as

$$\hat{u}^+ = \hat{u} + \Big[\Big(I(v) \otimes v^\top\Big)\Big(I \otimes I(q)I(\delta_p + \delta_m)\Big)\Big] \times \Big(2Q\hat{u} + L\Big) + \sqrt{\delta}|\delta_p - \delta_m|O(1), \tag{K.41}$$

where $\otimes$ is the Kronecker product, Q is a block matrix with each row-block i corresponding to Q_i, and L is a block matrix with each row-block corresponding to L_i. Therefore, by selecting $\epsilon_0 < \sqrt{\delta}|\delta_p - \delta_m|$ there exists a $\Delta T > 0$ such that whenever the system hits the mode 4 after hitting the modes 1, 2, and 3 in order, and $u \in K_u$, the update mapping for the state $\hat{u}_i$, given in (6.21d), will generate solutions that are also

solutions of (K.41). This implies that for ΔT sufficiently large, the stability properties of the dynamics $\hat{x}$ are preserved from this point. Now, to analyze the behavior of the dynamics in the transient of the automaton, note that for each random solution $\mathbf{x}_c$ of (6.19) with initial condition $x_c(0,0) \in C_c \cup D_c$ there exists (t^*, j^*) such that z has hit every mode in Z and $q(t^*, j^*) = 4$. Moreover, since the time domains of the solutions depend only on ΔT, $z_c(0,0)$, and $\tau_c(0,0)$, and the compactness of $[0,1] \times Z$, there exists a T^*, such that $t^* + j^* \leq T^*$ for all solutions of system (6.19). Using LB of G_δ^z, the absence of finite escape times in (6.19b), and the boundedness of the random variables, given the initial condition there exists a $\rho_{\delta,\hat{x}(0,0)}$ such that for each solution starting at $\hat{\mathbf{x}}(0,0)$ we have that $\hat{x}(t^*, j^*) \in \mathcal{A}_{\hat{x}} + \rho_{\delta,\hat{x}(0,0)}\mathbb{B}$. Then, we have that for all $j \geq j^*$ such that $z = 4$ the state $\hat{x}$ satisfies during jumps the bound

$$\mathbb{E}[|\hat{\mathbf{x}}(t,j)|^2_{\mathcal{A}_{\hat{x}}} | \mathcal{F}_{j^*}] \leq \sigma(1-\delta\lambda)^{j-j^*} |\hat{x}(t^*, j^*)|^2_{\mathcal{A}_{\hat{x}}} + \gamma\delta^\alpha. \tag{K.42}$$

Since $\hat{\mathbf{x}}(t^*, j^*) \in \mathcal{A}_{\hat{x}} + \rho_{\delta,\hat{x}(0,0)}\mathbb{B}$ for all $\omega \in \Omega$, taking the expectation at both sides of (K.42) we obtain that during jumps at the mode 4 we have

$$\mathbb{E}\left[\|\hat{\mathbf{x}}(t,j)\|^2_{\mathcal{A}_{\hat{x}}}\right] \leq \sigma(1-\delta\lambda)^{j-j^*} \rho_{\delta,\hat{x}(0,0)} + \gamma\delta^\alpha, \tag{K.43}$$

and note that since $\hat{\mathbf{x}}$ is kept constant during flows, and $t < \Delta T + j\Delta T$ always hold, equation (K.43) can be written as (6.27), where $\underline{\mathbf{j}}(t)$ is the smallest integer j such that (t,j) is in the domain of the solution. This establishes the inequality (6.27). Equation (6.26) follows by Proposition 13, the fact that δ is chosen sufficiently small, and that the $\mathcal{KL}$ bound holds for all $\omega \in \Omega$. ■

K.4.1 Proof of Theorem 12

Note that the synchronization and coordination dynamics evolve independently of the dynamics of the plant and the stochastic dynamics generated by $G^z_{\delta,i}$. Indeed, by Proposition 14, there exists a hybrid time (t^*, j^*) such that for any initial condition of τ and z in $[0,1]^n \times Z^n$, and all $t + j > t^* + j^*$ satisfying $(t, j) \in \mathrm{dom}(\mathbf{x})$ we have that $(\tau(t, j), z(t, j)) \in \mathcal{A}_{sync}$. From this point the distributed dynamics (6.35) behave as the centralized dynamics (6.19), with the only difference that agents now jump sequentially instead of simultaneously, and note that since $G^z_{\delta,i}$ only depends on the states of agent i, this sequential jumps do not affect the updates of the agents. Therefore, from this point the analysis follows the same steps as in the proof of Theorem 11.

Bibliography

[1] P. A. Ioannou and J. Sun, *Robust Adaptive Control*. Dover Publications Inc., Mineola, NY., 2012.

[2] S. Sastry and M. Bodson, *Adaptive Control: Stability, Convergence, and Robustness*. Prentice-Hall, Englewood Cliffs, NJ, 1989.

[3] M. Krstić, I. Kanellakopoulos, and P. V. Kokotović, *Nonlinear and adaptive control design*. John Wiley & Sons, New York, NY, 1995.

[4] R. S. Sutton and A. G. Barto, *Reinforcement Learning: An Introduction*. MIT Press, Cambridge, MA, 1998.

[5] K. S. Narendra and A. M. Annaswamy, *Stable Adaptive Systems*. Courier Corporation, 2012.

[6] J. A. Farrell and M. M. Polycarpou, *Adaptive Approximation Based Control: Unifying Neural, Fuzzy and Traditional Adaptive Approximation Approaches*. John Wiley & Sons, Hoboken, New Jersey, 2006.

[7] B. D. Anderson, R. R. Bitmead, C. R. Johnson, P. V. Kokotovic, R. L. Kosut, I. Mareels, and et al., *Stability of adaptive systems*. MIT Press, Cambridge, MA, 1986.

[8] K. J. Astrom and B. Wittenmark, *Adaptive Control*. Addison-Wesley Publishing Company, 1989.

[9] A. Astolfi, D. Karagiannis, and R. Ortega, *Nonlinear and Adaptive Control with Applications*. Springer, 2008.

[10] C. Cao and N. Hovakimyan, *L1 Adaptive Control Theory: Guaranteed Robustness with Fast Adaptation*. SIAM Series: Advances in Design and Control, Philadelphia, PA, 2010.

[11] F. L. Lewis and D. Liu, *Reinforcement Learning and Approximate Dynamic Programming for Feedback Control*. John Wiley/IEEE Press, Computational Intelligence Series, Hoboken, New Jersey, 2012.

[12] E. Mosca, *Optimal, Predictive, and Adaptive Control*. Prentice Hall, 1995.

[13] M. Guay, V. Adetola, and D. DeHaan, *Robust and Adaptive Model Predictive Control of Nonlinear Systems*. The Institution of Engineering and Technology, London, UK, 2015.

[14] G. Tao, *Multivariable adaptive control: A survey*, *Automatica* **50** (2014) 2737–2764.

[15] M. Wooldridge, *Introduction to MultiAgent Systems*. John Wiley & Sons, United Kingdom, 2009.

[16] J. P. Hespanha, P. Naghshtabrizi, and Y. Xu, *A survey of recent results in networked control systems*, *Proceedings of the IEEE* **95** (2007), no. 1 138–162.

[17] J. S. Shamma and G. Arslan, *Dimensions of cooperative control*, in *Cooperative Control of Distributed Multi-Agent Systems* (J. S. Shamma, ed.), pp. 3–17. John Wiley & Sons, Englang, 2007.

[18] H. F. Wang, *Multi-agent coordination for the secondary voltage control in power-systems contingencies*, *IEE Proceedings - Generation, Transmission and Distribution* **148** (2001) 61–66.

[19] A. Pantoja and N. Quijano, *A population dynamics approach for the dispatch of distributed generators*, *IEEE Transactions on Industrial Electronics* **58** (2011), no. 10 4559–4567.

[20] F. Dorfler, J. Simpson-Porco, and F. Bullo, *Breaking the hierarchy: Distributed control & economic optimality in microgrids*, *IEEE Transactions on Control of Network Systems* **3** (2016), no. 3 241–253.

[21] F. Bullo and J. Cortés, *Distributed Control of Robotic Networks*. Princeton University Press, Princeton, New Jersey, 2009.

[22] J. Liu and J. Wu, *Multiagent Robotic Systems*. CRC Press, Boca Raton, Florida, 2001.

[23] A. Martinoli, F. Mondada, N. Correll, G. Mermoud, M. Egerstedt, M. Hsieh, L. Parker, and K. Stoy, *Distributed Autonomous Robotic Systems*. Springer-Verlag Berlin Heidelberg, 2013.

[24] J. Barreiro-Gomez, N. Quijano, and C. Ocampo-Martinez, *Constrained distributed optimization: A population dynamics approach*, *Automatica* **69** (2016) 101–116.

[25] A. Núñez, C. Ocampo-Martinez, J. M. Maestre-Torreblanca, and B. D. Schutter, *Time-varying scheme for non-centralized model predictive control of large-scale systems*, *Mathematical Problems in Engineering, Special Issue on Advanced Control of Complex Dynamical Systems with Applications* (2015) 1–17.

[26] M. Tlig and N. Bhouri, *A multi-agent system for urbam traffic and busses regularity control*, *Procedia - Social and Behavioral Sciences* **20** (2011) 896–905.

[27] P. G. Balaji and D. Srinivasan, *Multi-agent system in urban traffic signal control*, *IEEE Computational Intelligence Magazine* **5** (2010) 43–51.

[28] D. Srinivasan, M. C. Choy, and R. L. Cheu, *Neural networks for real-time traffic signal control*, *IEEE Transactions on Intelligent Transportation Systems* **7** (2006) 261–272.

[29] R. Vidal, O. Shakernia, H. J. Kim, D. H. Shim, and S. Sastry, *Probabilistic pursuit-evasion games: theory, implementation, and experimental evaluation*, *IEEE Transactions on Robotics and Automation* **18** (2002) 662–669.

[30] J. Thunberg, W. Song, E. Montijano, Y. Hong, and X. Hu, *Distributed attitude synchronization control of multi-agent systems with switching topologies*, *IEEE Transactions on Robotics and Automation* **18** (2002) 662–669.

[31] C. Song, L. Liu, G. Feng, and S. Xu, *Coverage control for heterogeneous mobile sensor networks on a circle*, *Automatica* **63** (2016) 349–358.

[32] R. Olfati-Saber, J. Fax, and R. Murray, *Consensus and cooperation in networked multi-agent systems*, *Proceedings of the IEEE* **95** (2007), no. 1 215–233.

[33] J. Cortes, S. Martinez, T. Karatas, and F. Bullo, *Coverage control for mobile sensing networks*, *In proc. of IEEE International Conference on Robotics and Automation* **2** (2002) 1327–1332.

[34] D. Fitoussi and M. Tennenholtz, *Choosing social laws for multi-agent systems: Minimality and simplicity*, *Artificial Intelligence* **119** (2000) 61–101.

[35] P. Jia, A. MirTabatabaei, N. E. Friedkin, and F. Bullo, *Opinion dynamics and the evolution of social power in influence networks*, *SIAM Review* **57** (2015), no. 3 367–397.

[36] B. Altin and K. Barton, *L1 adaptive control in an iterative learning control framework: Stability, robustness and design trade-offs*, *In proc. of American Control Conference, Washington, DC, USA* (2013) 6697–6702.

[37] C. Chien, *A sampled-data iterative learning control using fuzzy network design*, *International Journal of Control* **73** (2000) 902–913.

[38] M. Benosman, *Learning-Based Adaptive Control: An Extremum Seeking Approach - Theory and Applications*. Butterworth-Heinemann, Cambridge, MA, 2016.

[39] M. Benosman, *Multi-parametric extremum seeking-based auto-tuning for robust input-output linearization control*, *In proc. of 53rd IEEE Conference on Decision and Control, Los Angeles, CA* (2014) 2685–2690.

[40] M. Benosman and G. Atinc, *Nonlinear adaptive control of electromagnetic actuators.*, *In SIAM Conference on Control and Applications* (2013) 29–36.

[41] M. Benosman and G. Atinc, *Nonlinear learning-based adaptive control for electromagnetic actuators*, *In proc. of IEEE European Control Conference, Zurich* (2013) 2904–2909.

[42] M. Benosman and G. Atinc, *Nonlinear adaptive control of electromagnetic actuators*, *IET Control Theory Appl.* (2015) 258–269.

[43] M. Benosman and M. Xia, *Extremum seeking-based indirect adaptive control for nonlinear systems with time-varying uncertainties*, *In proc. of European Control Conference, Linz, Auztria* (2015) 2780–2785.

[44] M. Guay and T. Zhang, *Adaptive extremum seeking control of nonlinear dynamic systems with parametric uncertainties*, *Automatica* **39** (2003) 1283–1293.

[45] C. Zhang and R. O. nez, *Extremum-Seeking Control and Applications: A Numerical Optimization-Based Approach*. Springer, New York, 2012.

[46] S. Z. Khong, D. Nešić, and M. Krstić, *Iterative learning control based on extremum seeking*, *Automatica* **66** (2016) 238–245.

[47] P. Frihauf, M. Krstic, and T. Basar, *Finite-horizon LQ control for unknown discrete-time linear systems via extremum seeking*, *European Journal of Control* **19** (2013) 399–407.

[48] A. Subbaraman and M. Benosman, *Extremum seeking-based iterative learning model predictive control (esilc-mpc)*, in *12th IFAC Workshop on Adaptation and Learning in Control and Signal*, pp. 193–198, 2016.

[49] S. Bruggemann, C. Possieri, J. I. Poveda, and A. R. Teel, *Robust constrained model predictive control with persistent model adaptation*, *IEEE 55th Conference on Decision and Control* (2016) 2364–2369.

[50] B. Gruenwald and T. Yucelen, *On transient performance improvement of adaptive control architectures*, *International Journal of Control* **11** (2015) 2305–2315.

[51] F. L. Lewis, D. Vrabie, and K. G. Vamvoudakis, *Reinforcement learning and feedback control: using natural decision methods to design optimal adaptive controllers*, *IEEE Control Systems Magazine* **32** (2012) 76–105.

[52] C. Wang and D. J. Hill, *Deterministic Learning Theory for Identification, Recognition, and Control*. CRC Press, Boca Raton, FL, 2010.

[53] C. Wang, D. J. Hill, S. S. Ge, and G. Chen, *An ISS-modular approach for adaptive neural control of pure-feedback systems*, *Automatica* **42** (2006) 723–731.

[54] K. J. Hunt, D. Sbarbaro, R. ZBikowski, and P. J. Gawthrop, *Neural networks for control systems: A survey*, *Automatica* **28** (1992), no. 6 1083–1112.

[55] J. I. Poveda, K. G. Vamvoudakis, and M. Benosman, *A neuro-adaptive architecture for extremum seeking control using hybrid learning dynamics*, *In proc. of American Control Conferece. Boston, MA.* (2017) 542–547.

[56] Z.-P. Jiang and Y. Jiang, *Robust adaptive dynamic programming for linear and nonlinear systems: An overview*, *European Journal of Control* **19** (2013), no. 5.

[57] L. Koszaka, R. Rudek, and I. Pozniak-Koszalka, *An idea of using reinforcement learning in adaptive control systems*, *International Conference on Networking, International Conference on Systems, and International Conference on Mobile Communications and Learning Technologies* (2006) 190.

[58] D. Vrabie, K. G. Vamvoudakis, and F. L. Lewis, *Optimal Adaptive Control and Differential Games by Reinforcement Learning Principles*. IET Press, 2012.

[59] M. I. Abouheaf and M. S. Mahmoud, *Microgrids*, ch. Online Adaptive Learning Control Schemes for Microgrids. Elsevier, 2017.

[60] R. Modares, F. Lewis, T. Yucelen, and G. Chowdhary, *Adaptive optimal control of partially-unknown constrained-input systems using policy iteration with experience replay, AIAA Guidance, Navigation and Control Conference, Boston, MA, doi:10.2514/6.2013-4519* (2013).

[61] J. T. Spooner, M. Maggiore, R. O. nez, and K. M. Passino, *Stable adaptive control and estimation for nonlinear systems*. Wiley-Interscience, New York, 2002.

[62] H. Hjalmarsson, *From experiment design to closed-loop control*, *Automatica* **41** (2005), no. 3 393–438.

[63] H. Hjalmarsson, *Iterative feedback tuning: An overview*, *Int. J. Adapt. Control Signal Process* **16** (2002), no. 5 373–395.

[64] M. Benosman, *Multi-parametric extremum seeking-based auto-tuning for robust input-output linearization control*, *Int. Journal of Robust and Nonlinear Control* **26** (2016), no. 18.

[65] R. Olfati-Saber and R. Murray, *Consensus problems in networks of agents with switching topology and time-delays*, *IEEE Transactions on Automatic Control* **49** (2004) 1520–1533.

[66] A. Jadbabaie, J. Lin, and A. S. Morse, *Coordination of groups of mobile autonomous agents using nearest neighbor rules*, *IEEE Transactions on Automatic Control* **48** (2003), no. 6 988–1001.

[67] F. Dorfler and F. Bullo, *Synchronization in complex networks of phase oscillators: A survey*, *Automatica* **50** (2014), no. 6 1539–1564.

[68] H. L. Trentelman, K. Takaba, and N. Monshizadeh, *Robust synchronization of uncertain linear multi-agent systems*, *IEEE Transactions on Automatic Control* **58** (2013), no. 6 1511–1523.

[69] H. G. Tanner, G. J. Pappas, and V. Kumar, *Leader-to-formation stability*, *IEEE Transactions on Robotics and Automation* **20** (2004), no. 3 443–455.

[70] M. Egerstedt and X. Hu, *Formation constrained multi-agent control*, *IEEE Transactions on Robotics and Automation* **17** (2001), no. 6 947–951.

[71] R. Olfati-Saber, *Flocking for multi-agent dynamic systems: algorithms and theory*, *IEEE Transactions on Automatic Control* **51** (2006), no. 3 401–420.

[72] H. Tanner, A. Jadbabie, and G. J. Pappas, *Flocking in fixed and switching networks*, *IEEE Transactions on Automatic Control* **52** (2007), no. 5 863–868.

[73] C. D. Godsil and G. Royle, *Algebraic graph theory*. Springer, 2001.

[74] S. Mannor and J. S. Shamma, *Multi-agent learning for engineers*, *Artificial Intelligence* **171** (2007), no. 7 417–422.

[75] J. R. Marden, G. Arslan, and J. S. Shamma, *Cooperative control and potential games*, *IEEE Transactions on Systems, Man, and Cybernetics - Part B: Cybernetics* **39** (2009), no. 6 1393–1407.

[76] G. Obando, J. Poveda, and N. Quijano, *Replicator dynamics under perturbation and time delays*, *Mathematics of Controls, Signals and Systems* **28** (2016), no. 3 1–32.

[77] E. D. Sontag and H. J. Sussmann, *Mathematical theory of neural networks*, *Technical Report* (1997).

[78] R. Goebel and R. G. S. an A. R. Teel, *Hybrid Dynamical Systems: Modeling, Stability, and Robustness*. Princeton University Press, 2012.

[79] C. G. Cassandras and S. Lafortune, *Introduction to Discrete Event Systems*. Springer, 2008.

[80] D. Liberzon, *Switching in Systems and Control*. Birkhauser, Boston, MA., 2003.

[81] E. D. Sontag, *Interconnected Automata and Linear Systems: A Theoretical Framework in Discrete-Time*, pp. 436–448. Springer, 1996.

[82] J. Poveda, N. Ochoa-Lleras, and C. Rodriguez, *Guidance of an autonomous glider based on proportional navigation and virtual targets: A hybrid dynamical systems approach*, *AIAA Guidance, Navigation, and Control Conference. Minneapolis, Minnesota.* (2012).

[83] M. Leblanc, *Sur l'electrification des chemins de fer au moyen de courants alternatifs de frquence elevee*, *Rev. Gen. Electr.* (1922).

[84] I. S. Morosanov, *Method of extremum control*, *Automatic and Remote Control* **18** (1957) 1077–1092.

[85] S. M. Meerkov, *Asymptotic methods for investigating quasi-stationary states in continuous systems of automatic optimization*, *Automatic and Remote Control* **11** (1967) 1726–1743.

[86] D. DeHaan and M. Guay, *Extremum-seeking control of state-constrained nonlinear systems*, *Automatica* **41** (2005) 1567–1574.

[87] A. R. Teel and D. Popović, *Solving smooth and nonsmooth multivariable extremum seeking problems by the methods of nonlinear programming*, *Proc. of the American Control Conference* (2001) 2394–2399.

[88] M. Krstić and H.-H. Wang, *Stability of extremum seeking feedback for general nonlinear dynamic systems*, *Automatica* **36** (2000), no. 4 595–601.

[89] H. K. Khalil, *Nonlinear Systems*. Prentice Hall, Upper Saddle River, NJ, 2002.

[90] Y. Tan, D. Nešić, and I. Mareels, *On non-local stability properties of extremum seeking controllers*, *Automatica* **42** (2006), no. 6 889–903.

[91] A. R. Teel, L. Moreau, and D. Nešić, *A Unified Framework for Input-to-State Stability in Systems With Two Time Scales*, *IEEE Trans. Autom. Control.* **48** (2003) 1526–1544.

[92] H. Dürr, M. Stanković, C. Ebenbauer, and K. H. Johansson, *Lie bracket approximation of extremum seeking systems*, *Automatica* **49** (2013) 1538–1552.

[93] M. Haring, N. Wouw, and D. Nešić, *Extremum-seeking control for nonlinear systems with periodic steady-state outputs*, *Automatica* **49** (2013) 1883–1891.

[94] J. Cochran and M. Krstić, *Nonholonomic source seeking with tuning of angular velocity*, *IEEE Trans. on Autom. Control* **54** (2009) 717–731.

[95] D. Nešić, A. Mohammadi, and C. Manzie, *A framework for extremum seeking control of systems with parameter uncertainties*, *IEEE Trans. Autom. Control* **58** (2013) 435–448.

[96] D. Nešić, Y. Tan, W. Moase, and C. Manzie, *A unifying approach to extremum seeking: Adaptive schemes based on estimation of derivatives*, *49th IEEE Conf. Decision Control* (2010) 4625–4630.

[97] N. Ghods and M. Krstić, *Multiagent deployment over a source*, *IEEE Trans. Control Syst. Tech.* **20** (2012) 277–285.

[98] W. H. Moase and C. Manzie, *Fast extremum-seeking for Wiener-Hammerstein plants*, *Automatica* **48** (2012) 2433–2443.

[99] A. Ghaffari, M. Krstić, and D. Nešić, *Multivariable newton-based extremum seeking*, *Automatica* **48** (2012) 1759–1767.

[100] G. Mills and M. Krstić, *Constrained extremum seeking in 1-dimension*, *In Proc. of 53rd IEEE Conf. Decision Control* (2014) 2654–2659.

[101] J. I. Poveda and N. Quijano, *Shahshahani gradient-like extremum seeking*, *Automatica* **58** (2015) 51–59.

[102] J. I. Poveda, R. Kutadinata, C. Manzie, D. Nešíc, A. R. Teel, and C. Liao, *Hybrid extremum seeking for black-box optimization in hybrid plants: An analytical framework*, *in Proc. 57th IEEE Conferece on Decision and Control, to appear.* (2018).

[103] H. Yu and U. Ozguner, *Extremum-seeking control strategy for ABS system with time delay*, *In Proc. of American Control Conference* (2002) 3753–3758.

[104] P. Binetti, K. B. Ariyur, M. Krstić, and F. Bernelli, *Formation flight optimization using extremum seeking feedback*, *AIAA J. Guid. Control Dyn* **26** (2003) 132–142.

[105] P. Frihauf, M. Krstic, and T. Basar, *Nash equilibrium seeking in noncooperative games*, *IEEE Transactions on Automatic Control* **57** (May, 2012) 1192–1207.

[106] R. Kutadinata, W. H. Moase, and C. Manzie, *Dither re-use in nash equilibrium seeking*, *IEEE Trans. Autom. Control* **60** (2015) 1433–1438.

[107] J. Poveda and N. Quijano, *Distributed extremum seeking for real-time resource allocation*, *in Proc. of American Control Conference* (2013) 2772–2777.

[108] J. Poveda and N. Quijano, *Dynamic bandwidth allocation in wireless networks using a Shahshahani gradient based extremum seeking control*, *6th Int. Con. On Network Games, Control and Optimization (NetGCoop)* (2012) 44–50.

[109] J. Poveda and N. Quijano, *A shahshahani gradient based extremum seeking scheme*, *in Proc. of Conference on Decision and Control (CDC)* (2012) 5104–5109.

[110] J. Cochran, E. Kanso, S. D. Kelly, H. Xiong, and M. Krstić, *Source seeking for two nonholonomic models of fish locomotion*, *IEEE Trans. on Robotics* **25** (2009) 1166–1176.

[111] A. Ghaffari, M. Krstić, and S. Seshagiri, *Power optimization and control in wind energy conversion systems using extremum seeking*, *IEEE Trans. Control Syst. Tech.* **22** (2014) 1684–1695.

[112] X. T. Zhang, D. M. Dawson, W. E. Dixon, and B. Xian, *Extremum-seeking nonlinear controllers for a human exercise machine*, *IEEE Trans. Mechatronics* **11** (2006) 233–240.

[113] P. N. Brown and J. R. Marden, *Studies on robust social influence mechanisms*, *IEEE Control Systems Magazine* **37** (2017), no. 1 98–115.

[114] F. Farokhi and K. H. Johansson, *A picewise-constant congestion taxing policty for repeated routing games*, *Transporation Research Part B* **78** (2015) 123–143.

[115] A. Kleiner, B. Nebel, and V. A. Ziparo, *A mechanism for dynamic ride sharing based on parallel auctions*, *Proc. 22nd Int. Join Conference on Artificial Intelligence* (2011) 266–272.

[116] M. Esmaeili, M. B. Aryabezhad, and P. Zeephongsekul, *A game theory approach in seeler-buyer supply chain*, *European Journal of Operations Research* **195** (2009), no. 2 442–448.

[117] N. Quijano, C. Ocampo-Martinez, J. Barreiro-Gomez, G. Obando, A. Pantoja, and E. Mojica-Nava, *The role of population games and evolutionary dynamics in distributed control systems: The advantages of evolutionary game theory*, *IEEE Control Systems Magazine* **37** (2017), no. 1 70–97.

[118] W. H. Sandholm, *Negative externalities and evolutionary implementation*, *The Review of Economic Studies* **72** (2005), no. 3 885–915.

[119] U. Bhaskar, K. Ligett, and L. J. Schulman, *Achieving target equilibria in network routing games without knowing the latency functions*, *IEEE Annual Symposium on Foundations of Computer Science* (2014) 31–40.

[120] G. Zhang, X. Ma, and Y. Wang, *Self-adaptive tolling strategy for enhanced high-occupancy toll lane operations*, *IEEE Transactions on Intelligent Transportation Systems* **15** (2014), no. 1 306–317.

[121] W. Sandholm, *Evolutionary implementation and congestion pricing*, *Review of Economic Studies* **69** (2002), no. 667-689.

[122] M. Beckman, C. McGuire, and C. B. Winsten, *Studies in the economics of transportation*. Yale University Press, 1956.

[123] J. I. Poveda, P. N. Brown, J. R. Marden, and A. R. Teel, *A class of neural-based dynamics for online learning of incentive mechanisms in congestion games with stochastic switching graphs*, in *Southern California Machine Learning Symposium, Poster Presentation*, (Caltech), Nov,, 2016.

[124] G. Karakostas and S. Kolliopoulos, *Edge pricing of multicommodity networks for heterogeneous selfish users*, *Proc. of 45th Annual IEEE Symposium on Fundations of Computer Science* (2004) 268–276.

[125] L. Fleischer, K. Jain, and M. Mahdian, *Tolls for heterogeneous selfish users in multicommodity networks and generalized congestion games*, *Proc. of 45th Annu. IEEE Symp. Foundation Computer Science, Rome, Italy* (2004) 277–285.

[126] I. C. Konstantakopoulos, L. J. Ratliff, M. Jin, C. Spanos, and S. S. Sastry, *Smart building energy efficiency via social game: a robust utility learning framework for closing–the–loop*, *Science of Smart City Operations and Platforms Engineering* (2016).

[127] P. Tabuada, *Event-triggered real-time scheduling of stabilizing control tasks*, *IEEE Trans. on Automatic Control* **52** (2007) 1680–1685.

[128] W. P. M. H. Heemels, M. C. F. Donkers, and A. R. Teel, *Periodic event-triggered control for linear systems*, *IEEE Trans. on Automatic Control* **58** (2013) 847–861.

[129] S. Kia, J. Cortés, and S. Martínez, *Distributed convex optimization via continuous-time coordination algorithms with discrete-time communication*, *Automatica* **55** (2014) 254–264.

[130] K. Vamvoudakis, *Event-triggered optimal adaptive control algorithm for continuous-time nonlinear systems*, *IEEE Journal of Automatica SINICA* **1** (2014) 282–293.

[131] A. Cortés and S. Martínez, *Self-triggered best response dynamics for continuous games*, *IEEE Trans. on Automatic Control* **60** (2015) 1115–1120.

[132] A. Sahoo, H. Xu, and S. Jagannathan, *Adaptive neural network-based event-triggered control of single-input single-output nonlinear discrete-time systems*, *IEEE Trans. Neural Networks and Learning Syst.* **27** (2016) 151–164.

[133] D. Popović, *Topics in Extremum Seeking, PhD Thesis*. University of California, Santa Barbara, CA, USA, 2004.

[134] D. Nešić, T. Nguyen, Y. Tan, and C. Manzie, *A non-gradient approach to global extremum seeking: An adaptation of the shubert algorithm*, *Automatica* **49** (2013) 809–815.

[135] S. Z. Khong, D. Nešić, Y. Tan, and C. Manzie, *Unified framework for sampled-data extremum seeking control: Global optimisation and multi-unit systems.*, *Automatica* **49** (2013) 2720–2733.

[136] J. Barreiro-Gomez, C. Ocampo-Martinez, F. Bianchi, and N. Quijano, *Model-free control for wind farms using gradient estimation-based algorithm*, *in Proc. of European Control Conference* (2015) 1516–1521.

[137] S. Z. Khong, Y. Tan, C. Manzie, and D. Nesic, *Multi-agent source seeking via discrete-time extremum seeking control*, *Automatica* **50** (2014), no. 9 2312–2320.

[138] S. Z. Khong, D. Nešić, C. Manzie, and Y. Tan, *Multidimensional global extremum seeking via the DIRECT*, *Automatica* **49** (2013) 1970–1978.

[139] D. V. Dimarogonas, E. Frazzoli, and K. H. Johansson, *Distributed event-triggered control for multi-agent systems*, *IEEE Transactions on Automatic and Control* **57** (2012), no. 5 1291–1297.

[140] C. D. Persis and P. Frasca, *Robust self-triggered coordination with ternary controllers*, *IEEE Transactions on Automatic and Control* **58** (2013), no. 12 3024–3038.

[141] C. D. Persis and R. Postoyan, *A lyapunov redesign of coordination algorithms for cyber-physical systems*, *IEEE Transactions on Automatic and Control* **62** (2017), no. 2 808–823.

[142] T. Chen and B. Francis, *Optimal Sampled-Data Control Systems*. Springer-Verlag, 1995.

[143] Y. Cao and W. Ren, *Multi-vehicle coordination for double-integrator dynamics under fixed undirected/directed interaction in a sampled-data setting*, *International Journal of Robust and Nonlinear Control* **20** (2010) 987–1000.

[144] F. Xiao and L. Wang, *Asynchronous consensus in continuous-time multi-agent systems with switching topology and time-varying delays*, *IEEE Trans. on Automatic Control* **53** (2008), no. 8 1804–1816.

[145] J. Wang, J. Feng, C. Xu, M. Z. Q. Chen, Y. Zhao, and J. Feng, *The synchronization of instantaneously coupled harmonic oscillators using sampled data with measurement noise*, *Automatica* **66** (2016) 155–162.

[146] J. I. Poveda, M. Benosman, and A. R. Teel, *Hybrid online learning control in networked multiagent systems: A survey*, *International Journal of Adaptive Control and Signal Processing* (2018) 1–34.

[147] D. Nešić, A. R. Teel, and P. V. Kokotović, *Sufficient conditions for stabilization of sampled-data nonlinear systems via discrete-time approximations*, *Systems & Control Letters* **38** (1999) 259–270.

[148] D. Nešić and A. R. Teel, *A framework for stabilization of nonlinear sampled-data systems based on their approximate discrete-time models*, *IEEE Trans. on Automatic Control* **49** (2004), no. 7 1103–1121.

[149] D. Nešić and D. Liberzon, *A unified framework for design and analysis of networked and quantized control systems*, *IEEE Trans. Autom. Control.* **54** (2009), no. 4 732–746.

[150] D. Nešić, A. R. Teel, and D. Carnevale, *Explicit computation of the sampling period in emulation of controllers for nonlinear sampled-data systems*, *IEEE Transactions on Automatic and Control* **54** (2009), no. 3 619–624.

[151] R. Postoyan, P. Tabuada, D. Nešić, and A. Anta, *A framework for the event-trigered stabilization of nonlinear systems*, *IEEE Trans. Autom. Control.* **60** (2015), no. 4 982–996.

[152] W. P. M. H. Heemels, A. R. Teel, N. Wouw, and D. Nešić, *Networked control systems with communication constraints: Tradeoffs between transmission intervals, delays and performance*, *IEEE Trans. Autom. Control.* **55** (2010), no. 8 1781–1795.

[153] A. R. Teel, *Robust hybrid control systems: An overview of some recent results*, in *Lecture Notes in Control and Information Sciences*, vol. 353, pp. 279–302. Springer, 2007.

[154] J. I. Poveda and A. R. Teel, *Distributed robust stochastic learning in asynchronous networks of sampled-data systems*, *IEEE Conference on Decision and Control* (2016) 401–406.

[155] J. I. Poveda and A. R. Teel, *A robust event-triggered approach for fast sampled-data extremization and learning*, *IEEE Transactions on Automatic Control* **62** (2017), no. 10 4949–4964.

[156] S. E. Tuna, R. G., M. J. Messina, and A. R. Teel, *Hybrid MPC: Open-minded but not easily swayed*, in *Lecture Notes in Control and Information Sciences*, pp. 17–34. Springer, 2007.

[157] E. Sontag, *Stability and stabilization: Discontinuities and the effect of disturbances*, in *Nonlinear Analysis, Differential Equations and Control*, vol. 528 of *NATO Science Series*, pp. 551–598. 1999.

[158] F. Nunez, Y. Wang, A. Teel, and F. J. D. III, *Synchronization of pulse-coupled oscillators to a global pacemaker*, *Systems & Control Letters* **88** (2016) 75–80.

[159] A. V. Proskurnikov and M. Cao, *Synchronization of pulse-coupled oscillators and clocks under minimal connectivity assumptions*, *IEEE Transactions on Automatic and Control* **62** (2017), no. 11 5873–5879.

[160] S. Phillips and R. G. Sanfelice, *Robust asymptotic stability of desynchronization in impulse-coupled oscillators*, *IEEE Transactions on Control of Network Systems* **3** (2016), no. 2 127–136.

[161] J. I. Poveda and A. R. Teel, *A hybrid systems approach for distributed nonsmooth optimization in asynchronous multi-agent sampled-data systems*, *10th IFAC Symposium on Nonlinear Control Systems* **49** (2016), no. 18 152–157.

[162] S. S. Stanković, M. S. Stanković, and D. M. Stipanović, *Decentralized parameter estimation by consensus based stochastic approximation*, *IEEE Transactions on Automatic and Control* **56** (2011), no. 3 531–543.

[163] T. Başar and G. J. Olsder, *Dynamic Noncooperative Game Theory*. Academic Press, San Diego, CA, 1995.

[164] N. Li and J. Marden, *Designing games for distributed optimization*, *Proc. of 50th IEEE Conference on Decision and Control* (2011) 2434–2440.

[165] G. Arslan and J. S. Shamma, *Anticipatory learning in general evolutionary games*, *45th IEEE Conference on Decision and Control* (2006) 6289–6294.

[166] J. Poveda and N. Quijano, *Extremum seeking for multi-population games*, *Proc. 52nd IEEE Conference on Decision and Control* (2013) 829–851.

[167] M. Baradaran, J. I. Poveda, and A. R. Teel, *Stochastic hybrid inclusions applied to non-convex optimization and distributed learning*, *IEEE 57th Conference on Decision and Control, to appear.* (2018).

[168] J. R. Marden, H. P. Young, G. Arslan, and J. S. Shamma, *Payoff-based dynamics for multiplayer weakly acyclic games*, *SIAM J. Control. Optim.* **48** (2009), no. 1 373–396.

[169] M. Stanković, K. H. Johansson, and D. M. Stipanović, *Distributed seeking of nash equilibria with applications to mobile sensor networks*, *IEEE Transactions on Automatic Control* **57** (2012), no. 4 904–919.

[170] J. C. Spall, *Multivariable stochastic approximation using a simultaneous perturbation gradient approximation*, *IEEE Transactions on Automatic and Control* **37** (1992), no. 3 332–341.

[171] S. Liu and M. Krstic, *Stochastic Nash equilibrium seeking for games with general nonlinear payoffs*, *SIAM J. Control Optim.* **49** (2011), no. 4 1659–1679.

[172] S. Amin, G. A. Schwartz, and S. S. Sastry, *Security of interdependent and identical networked cotrol systems*, *Automatica* **49** (2013) 186–192.

[173] X. Jin, W. M. Haddad, and T. Yucelen, *An adaptive control architecture for mitigating sensor and actuator attacks in cyber-physical systems*, *IEEE Transactions on Automatic and Control* **62** (2017), no. 11 6058–6064.

[174] M. Xue, W. Wang, and S. Roy, *Security concepts for the dynamics of autonomous vehicle networks*, *Automatica* **50** (2014), no. 3 852–857.

[175] F. Miao, Q. Zhu, M. Pajic, and G. J. Pappas, *A hybrid stochastic game for secure control of cyber-physical systems*, *Automatica* **93** (2018) 5563.

[176] D. Shi, Z. Guo, K. H. Johansson, and L. Shi, *Causality countermeasures for anomaly detection in cyber-physical systems*, *IEEE Trans. on Automatic Control* **63** (2018), no. 2 386–401.

[177] S. M. Dibaji and H. Ishii, *Resilient consensus of second-order agent networks: Asynchronous update rules with delays*, *Automatica* **81** (2017) 123–132.

[178] A. D'Innocenzo, F. Smarra, and M. D. D. Bedetto, *Resilient stabilization of multi-hop control networks subject to malicious attacks*, *Automatica* (2016) 1–9.

[179] Y. V. Orlov, *Discontinuous Systems, Lyapunov Analysis and Robust Synthesis under Uncertainty Conditions*. Springer, 2009.

[180] D. Shevitz and B. Paden, *Lyapunov stability theory of nonsmooth systems*, *IEEE Trans. Autom. Control* **39** (1994) 1910–1914.

[181] C. Cai, A. R. Teel, and R. Goebel, *Smooth Lyapunov functions for hybrid systems. part II: (pre)asymptotically stable compact sets*, *IEEE Transactions on Automatic Control* **53** (2008), no. 3 734–748.

[182] A. Bhaya and E. Kaszkurewicz, *Control perspectives on numerical algorithms and matrix problems*. SIAM, 2006.

[183] W. Sandholm, *Population Games and Evolutionary Dynamics*. The MIT Press, 2010.

[184] J. Hespanha and A. Morse, *Stability of switched systems with average dwell-time*, *38th IEEE Conf. Decision Control* **3** (1999) 2655–2660.

[185] A. Morse, *Supervisory control of families of linear set-point controllers-part I: Eact matching*, *IEEE Trans. Autom. Control* **41** (1996) 1413–1431.

[186] D. M. de la Peña and P. D. Christofides, *Stability of nonlinear asynchronous systems*, *Syst. Control Lett.* **57** (2008) 465–473.

[187] G. Yang and D. Liberzon, *Input-to-state stability for switched systems with unstable subsystems: A hybrid Lyapunov construction*, *53rd IEEE Conf. Decision Control* (2014) 6240–6245.

[188] R. G. Sanfelice, R. Goebel, and A. R. Teel, *Invariance principles for hybrid systems with connections to detectability and asymptotic stability*, *IEEE Trans. Autom. Control* **52** (2007) 2282–2297.

[189] C. G. Mayhew, *Hybrid Control for Topologically Constrained Systems, Ph.D Dissertation*. University of California, Santa Barbara, 2010.

[190] T. Strizic, J. I. Poveda, and A. R. Teel, *Hybrid gradient descent for robust global optimization on the circle*, *Under Review.* (2017).

[191] R. Sanfelice, *Robust Hybrid Control Systems*. Ph.D. Dissertation, University of California, Santa Barbara, CA, USA, 2007.

[192] R. G. Sanfelice, M. J. Messina, S. E. Tuna, and A. R. Teel, *Robust hybrid controllers for contrinuous-time systems with applications to obstacle avoidance and regulation to disconnected set of points*, *In Proc. of American Control Conference* (2006) 3352–3357.

[193] J. Cortés, *Finite-time convergent gradient flows with applications to network consensus*, *Automatica* **42** (2006) 1993–2000.

[194] J. B. Rosen, *Existence and uniqueness of equilibrium points for concave n-person games*, *Econometrica* **33** (1965) 520–534.

[195] N. Ghods and M. Krstic, *Multi-agent deployment around a source in one dimension by extremum seeking*, *2010 American Control Conference* (2010) 4794–4799.

[196] J. I. Poveda, M. Benosman, R. G. Sanfelice, and A. R. Teel, *A hybrid adaptive feedback law for robust obstacle avoidance and coordination in multiple vehicle systems*, *In proc. of American Control Conferece* (2018).

[197] M. Ye and G. Hu, *Distributed extremum seeking for constrained network optimization and its application to energy consumption control in smart grid*, *IEEE Transactions on Control Systems Technology, DOI:10.1109/TCST.2016.2517574* (2016).

[198] K. Ma, G. Hu, and C. J. Spanos, *Distributed energy consumption control via real-time pricing feedback in smart grid*, *IEEE Transactions on Control System Technology* **22** (2014), no. 5 1907–1914.

[199] P. Lin, W. Ren, and J. A. Farrell, *Distributed continuous-time optimization: nonuniform gradient gains, finite-time convergence, and convex constraint set*, *IEEE Transactions on Automatic Control, 10.1109/TAC.2016.2604324* (2016).

[200] J. I. Poveda, M. Benosman, and A. R. Teel, *Distributed extremum seeking in multi-agent systems with arbitrary switching graphs*, *IFAC World Congress* **50** (2016), no. 1 735–740.

[201] R. Kutadinata, W. Moase, C. Manzie, L. Zhang, and T. Garoni, *Enhancing the performance of existing urban traffic light control through extremum-seeking*, *Transportation Research Part C: Emerging Technologies* **62** (2016) 1–20.

[202] J. P. Hespanha, D. Liberzon, and A. R. Teel, *On input-to-state stability of impulsive systems*, *44th IEEE Conference on Decision and Control* (2005) 3992–3997.

[203] R. J. Kutadinata, W. Moase, and C. Manzie, *Extremum-seeking in singularly perturbed hybrid systems*, *IEEE Transactions on Automatic and Control* **62** (2017), no. 6 3014–3020.

[204] A. R. Teel and D. Nešić, *Lyapunov functions for $\mathcal{L}2$ and input-to-stat stability in a class of quantized control systems*, *50th IEEE Conference on Decision and Control* (2011) 4542–4547.

[205] J. Xu and Y. C. Soh, *A distributed simultaneous perturbation approach for large-scale dynamic optimization problems*, *Automatica* **72** (2016) 194–204.

[206] J. I. Poveda and A. R. Teel, *A framework for a class of hybrid extremum seeking controllers with dynamic inclusions*, *Automatica* **76** (2017) 113–126.

[207] A. Scheinker and D. Scheinker, *Bounded extremum seeking with discontinuous dithers*, *Automatica* **69** (2016) 250–257.

[208] Y. Tan, D. Nesić, and I. Mareels, *On the choice of dither in extremum seeking systems: A case study*, *Automatica* **44** (2008) 14446–1450.

[209] K. G. Vamvoudakis and F. L. Lewis, *Online actor-critic algorithm to solve the continuous-time infinite horizon optimal control problem*, *Automatica* **46** (2010), no. 5 878–888.

[210] K. Hornik, S. Stinchcombe, and H. White, *Universal approximation of an unknown mapping and its derivatives using multilayer feedforward networks*, *Neural Networks* **3** (1990) 551–560.

[211] B. A. Finlayson, *The method of weighted residuals and variational principles*. New York: Academic Press., 19990.

[212] M. Abu-Khalaf and F. L. Lewis, *Nearly optimal control laws for nonlinear systems with saturating actuators using a nwural network hjb approach*, *Automatica* **41** (2005), no. 5 779–791.

[213] P. Ioannou and B. Fidan, *Advances in design and control, Adaptive Control Tutorial*. SIAM, 2006.

[214] E. W. Sandberg, *Notes on uniform approximation of time-varying systems on finite time intervals*, *IEEE Transactions on Circuits and Systems-1: Fundamental Theory and Applications* **45** (1998), no. 8 863–865.

[215] J. I. Poveda, P. N. Brown, J. R. Marden, and A. R. Teel, *A class of distributed adaptive pricing mechanisms for societal systems with limited information*, *56th IEEE Conference on Decision and Control* (2017) 1490–1495.

[216] J. Wardrop, *Some theoretical aspects of road traffic research*, *Proc. Inst. Civil Eng. Part II* **1** (1952), no. 36 352–362.

[217] J. Hofbauer and K. Sigmund, *Evolutionary Games and Population Dynamics*. Cambridge University Press, Cambridge, UK, 1998.

[218] B. Gharesifard and J. Cortés, *Distributed continuous-time convex optimization on weight-balanced digraphs*, *IEEE Transactions on Automatic and Control* **59** (2014), no. 3 781–786.

[219] A. Cherukuri, B. Gharesifard, and J. Cortés, *Saddle-point dynamics: Conditions for asymptotic stability of saddle points*, *SIAM J. Control and Optimization* **55** (2017), no. 1 486–511.

[220] U. Lee and M. Mesbahi, *Constrained consensus avia logarithmic barrier functions*, *50th IEEE Conference on Decision and Control* (2011) 3608–3613.

[221] J. Calfee and C. Winston, *The value of automobile travel time: implications for congestion policty*, *Journal of Public Economics* **69** (1998) 83–102.

[222] M. A. Mabrok and J. S. Shamma, *Passivity analysis of higher order evolutionary dynamics and population games*, *arXiv:1609.04952v1* (2016).

[223] M. J. Fox and J. S. Shamma, *Population games, stable games, and passivity*, *Games* **4** (2013), no. 4 561–583.

[224] R. G. Sanfelice and A. R. Teel, *On singular perturbations due to fast actuators in hybrid control systems*, *Automatica* (2011) 692–701.

[225] F. H. Clarke, *Optimization and Nonsmooth Analysis*. SIAM, Philadelphia, 1990.

[226] P. Holoborodko, *Smooth noise robust differentiators*, *http://www.holoborodko.com/pavel/numerical-methods/numerical-derivative/smooth-low-noise-differentiators/* (2008).

[227] S. Cao and R. R. Rhinehart, *An efficient method for on-line identification of steady state*, *J. Proc. Control.* **5** (1995) 363–374.

[228] T. Jiang, B. Chen, X. He, and P. Stuart, *Application of steady-state detection method based on wavelet transform*, *Computers and Chemical Engineering* **27** (2003) 569–578.

[229] M. Mansour and J. E. Ellis, *Comparison of methods for estimating real process derivatives in on-line optimization*, *Applied Mathematical Modelling* **27** (2003) 275–291.

[230] E. Cruz-Zavala, J. A. Moreno, and L. M. Fridman, *Uniform robust exact differentiator*, *IEEE Trans. on Automatic Control* **56** (2011) 2727–2733.

[231] J. I. Poveda, A. R. Teel, and D. Nešić, *Flexible Nash seeking using stochastic difference inclusions*, *In Proc. of American Control Conference* (2015) 2236–2241.

[232] S. Bhatnagar, H. L. Prasad, and L. A. Prashanth, *Stochastic Recursive Algorithms for Optimization*. Springer-Verlag, London, 2013.

[233] A. R. Teel, *Lyapunov methods in non smooth optimization, part ii: persistently exciting finite differences*, *In proc. of IEEE Conference on Decision and Control* (2000) 118–123.

[234] S. T. Glad, *Computing the settling time for nonlinear step responses*, *7th IFAC Symposium on Nonlinear Control Systems* **40** (2007) 119–122.

[235] D. E. Seborg, T. F. Edgar, D. A. Mellichamp, and F. J. Doyle, *Process Dynamics and Control*. Wiley, New Jersey, 2010.

[236] S. Bittanti and P. Colaneri, *Periodic Systems - Filtering and Control*. Springer, 2009.

[237] M. Mesbahi and M. Egerstedt, *Graph Theoretic Methods in Multiagent Networks*. Princeton University Press, 2010.

[238] F. Bullo, *Lectures on Network Systems*. Version 0.96, 2018. With contributions by J. Cortes, F. Dorfler, and S. Martinez.

[239] A. R. Teel, *Nonlinear systems: discrete-time stability and control*. Lecture Notes, University of California, Santa Barbara, 2004.

[240] A. R. Teel and J. I. Poveda, *A hybrid systems approach to global synchronization and coordination of multi-agent sampled-data systems*, *In proc. of Analy. and Design of Hybrid Syst.* (2015) 123–128.

[241] R. Goebel, R. G. Sanfelice, and A. R. Teel, *Hybrid dynamical systems*, *IEEE Control Systems Magazine* **29** (2009), no. 2 28–93.

[242] R. J. Kutadinata, W. H. Moase, and C. Manzie, *Non-local stability of a nash equilibrium seeking scheme with dither re-use*, *in Proc. of Conference on Decision and Control* (2012) 6077–6082.

[243] S. Grammatico, A. Subbaraman, and A. R. Teel, *Discrete-time stochastic control systems: A continuous lyapunov function implies robustness to strictly causal perturbations*, *Automatica* **49** (2013), no. 10 2939–2952.

[244] Q. Zhu, H. Tembine, and T. Basar, *Hybrid learning in stochastic games and its applications in network security*, *Reinforcement Learning and Approximate Dynamic Programming for Feedback Control, IEEE Press/Wiley, ch14* (2013) 305–329.

[245] A. Cortes and S. Martinez, *Hierarchical management of demand response events with on/off loads*, *to appear in Proc. of American Contr. Conf.* (2016).

[246] C. Cai, R. Goebel, R. Sanfelice, and A. R. Teel, *Hybrid systems: Limit sets and zero dynamics with a view toward output regulation*, *Analysis and Design of Nonlinear control systems* (2008) 241–261.

[247] C. M. Kellett and A. R. Teel, *On the robustness of $\mathcal{KL}$-Stability for difference inclusions: Smooth discrete-time lyapunov functions*, *SIAM J. Control Optim.* **44** (2005) 777–800.

[248] W. Wang, A. R. Teel, and D. Nešić, *Analysis for a class of singularly perturbed hybrid system via averaging*, *Automatica* **48** (2012) 1057–1068.

[249] W. Wang, A. R. Teel, and D. Nešić, *Averaging in singularly perturbed hybrid systems with hybrid boundary layer systems*, *51st IEEE Conference on Decision and Control* (2012) 6855–6860.

[250] A. R. Teel and L. Praly, *A smooth lyapunov function from a class-kl estimate involving two positive semidefinite functions*, *ESAIM: Control, Optimisation and Calculus of Variations* (2000) 313–367.

[251] R. T. Rockafellar and R. J. Wets, *Variational Analysis*. Springer, 1998.

[252] A. R. Teel, J. P. Hespanha, and A. Subbaraman, *A converse Lyapunov theorem and robustness for asymptotic stability in probability*, *IEEE Transactions on Automatic Control* (2014) 2426–2441.

[253] A. Subbaraman and A. R. Teel, *A converse Lyapunov theorem for strong global recurrence*, *Automatica* **49** (2013), no. 10 2963–2974.

[254] A. R. Teel, J. Hespanha, and A. Subbaraman, *Equivalent characterizations of input-to-state stability for stochastic discrete-time systems*, *IEEE Transactions on Automatic Control* **59** (2014), no. 2 516–522.

[255] A. Subbaraman and A. R. Teel, *On the equivalence between global recurrence and the existence of a smooth lyapunov function for hybrid systems*, *Systems & Control Letters* **88** (2016) 54–61.

[256] A. R. Teel, A. Subbaraman, and A. Sferlazza, *Stability analysis for stochastic hybrid systems: a survey*, *Automatica* **50** (2014), no. 10 2435–2456.

[257] E. D. Sontag, *Smooth stabilization implies coprime factorization*, *IEEE Transactions on Automatic Control* **34** (1989) 435–443.